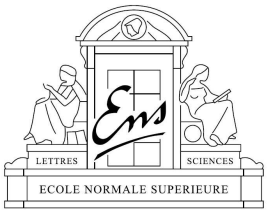

UNIVERSITÉ PIERRE ET MARIE CURIE - PARIS VI

et

INSTITUT DE PHYSIQUE THÉORIQUE - CEA/SACLAY

École Doctorale de Physique de la Région Parisienne - ED 107

Thèse de doctorat

Spécialité : **Physique Théorique**

Indecomposability in field theory and applications to disordered systems and geometrical problems

---

présentée par Romain Vasseur

pour obtenir le grade de Docteur de l'Université Pierre et Marie Curie

Thèse préparée sous la direction de Hubert Saleur et de Jesper Jacobsen

Soutenue le 27 Septembre 2013 devant le jury composé de :

Denis Bernard	Examinateur	École Normale Supérieure
John Cardy	Rapporteur	Oxford University
Matthias Gaberdiel	Rapporteur	ETH Zürich
Jesper Jacobsen	Membre invité (co-directeur)	École Normale Supérieure
Nicholas Read	Examinateur	Yale University
Hubert Saleur	Directeur de thèse	CEA Saclay
Jean-Bernard Zuber	Président du jury	Université Pierre et Marie Curie

Indecomposabilité dans les théories des champs et applications aux systèmes désordonnés et aux problèmes géométriques

Résumé :

Les théories des champs conformes logarithmiques (LCFTs) sont cruciales pour décrire le comportement critique de systèmes physiques variés : les transitions de phase dans les systèmes électroniques désordonnés sans interaction (comme par exemple la transition entre plateaux dans l'effet Hall quantique entier), les points critiques désordonnés dans les systèmes statistiques classiques (comme le modèle d'Ising avec liens aléatoires), ou encore les modèles géométriques critiques (comme la percolation ou les marches aléatoires auto-évitantes). Les LCFTs décrivent des théories non unitaires, qui ne seraient probablement pas pertinentes dans le contexte de la physique des particules, mais qui apparaissent naturellement en matière condensée et en physique statistique. Sans cette condition d'unitarité, toute la puissance algébrique qui a fait le succès des théories conformes est fortement compromise à cause de "l'indécomposabilité" de la théorie des représentations sous-jacente. Ceci a pour conséquence de modifier les fonctions de corrélation algébriques par des corrections logarithmiques, et réduit sévèrement l'espoir d'une classification générale.

Le but de cette thèse est d'analyser ces théories logarithmiques en étudiant leur régularisation sur réseau, l'idée principale étant que la plupart des difficultés algébriques causées par l'indécomposabilité sont déjà présentes dans des systèmes de taille finie. Notre approche consiste à considérer des modèles statistiques critiques avec matrice de transfert non diagonalisable (ou des chaînes de spins critiques avec Hamiltonien non diagonalisable) et d'analyser leur limite thermodynamique à l'aide de différentes méthodes numériques, algébriques et analytiques. On explique en particulier comment mesurer numériquement les paramètres universels qui caractérisent les représentations indécomposables qui apparaissent à la limite continue. L'analyse détaillée d'une vaste classe de modèles sur réseau nous permet également de conjecturer une classification de toutes les LCFTs chirales pertinentes physiquement, pour lesquelles la seule symétrie est donnée par l'algèbre de Virasoro. Cette approche est aussi partiellement étendue aux théories non chirales, avec une attention particulière portée au problème bien connu de la formulation d'une théorie des champs cohérente qui décrirait la percolation en deux dimensions. On montre que les modèles sur réseaux périodiques ou avec bords peuvent être reliés algébriquement seulement dans le cas des modèles minimaux, impliquant des conséquences intéressantes pour les théories des champs sous-jacentes. Un certain nombre d'applications aux systèmes désordonnés et aux modèles géométriques sont également abordées, avec en particulier une discussion détaillée des observables avec comportement logarithmique au point critique dans le modèle de Potts en dimension arbitraire.

Mots clefs : Théories des Champs Conformes Logarithmiques, Représentations indecomposables, Modèles sur réseau, Systèmes désordonnés, Problèmes géométriques.

Indecomposability in field theory and applications to disordered systems and geometrical problems

Abstract:

Logarithmic Conformal Field Theories (LCFTs) are crucial for describing the critical behavior of a variety of physical systems. These include phase transitions in disordered non-interacting electronic systems (such as the transition between plateaus in the integer quantum Hall effect), disordered critical points in classical statistical models (such as the random bond Ising model), or critical geometrical models (such as polymers and percolation). LCFTs appear when one has to give up the unitarity condition, which is natural in particle physics applications, but not in statistical mechanics and condensed matter physics. Without unitarity, the powerful algebraic approach of conformal invariance encounters formidable technical difficulties due to 'indecomposability'. This in turn yields logarithmic corrections to the power-law correlations at the critical point, and prevents the use of general classification techniques that have proven so powerful in the unitary case.

The goal of this thesis is to understand LCFTs by studying their lattice regularizations, the crucial point being that most algebraic complications due to indecomposability occur in finite size systems as well. Our approach is thus to consider critical statistical models with non-diagonalizable transfer matrices, or gapless quantum spin chains with non-diagonalizable hamiltonians, and to study their scaling limit by utilizing a variety of algebraic, numerical and integrable techniques. We show how to measure numerically universal parameters that characterize the indecomposable representations of the Virasoro algebra which emerge in the thermodynamic limit. An extensive understanding of a wide class of lattice models allows us to conjecture a tentative classification of all possible (chiral) LCFTs with Virasoro symmetry only. This approach is partially extended to the bulk case, for which we discuss how the long-standing bulk CFT formulation of percolation can be tackled along these lines. We also argue that boundary and periodic lattice models can be related algebraically only in the case of minimal models, and we work out the consequences for the underlying boundary and bulk field theories. Several concrete applications to disordered systems and geometrical problems are discussed, and we uncover a large class of geometrical observables in the Potts model that behave logarithmically at the critical point.

Key words: Logarithmic Conformal Field Theory, Indecomposable representations, Temperley-Lieb algebra, Lattice models, Disordered systems, Geometrical problems.

Remerciements

Je voudrais commencer par remercier John Cardy et Matthias Gaberdiel, qui ont accepté la pénible tache de rapporteur, ainsi que les examinateurs, Denis Bernard, Nicholas Read et Jean-Bernard Zuber. Merci pour votre aide et vos conseils pour améliorer mon manuscrit. Je suis très conscient du travail qu'être membre d'un comité de thèse représente, et je vous suis extrêmement reconnaissant d'avoir accepté de braver des heures de transport pour venir assister à ma soutenance.

Je remercie aussi Hubert et Jesper, qui en plus de leur qualités scientifiques indiscutables, m'ont beaucoup appris et aidé dans bien des domaines, en particulier dans mes moments de doute, ou pendant la période difficile des recherches de postdocs. Merci également de m'avoir soutenu durant mon changement de thématique après ma première moitié de thèse, même si cela représentait un certain nombre de risques et de difficultés pour vous aussi. Je sais que j'ai pu râler à certains moments, mais je suis vraiment ravi d'avoir fait ma thèse avec vous deux, vous avez toujours été disponibles et à l'écoute en cas de problème : travailler avec vous durant ces trois années a toujours été un plaisir. Je tiens également à remercier tout particulièrement Azat Gainutdinov qui a été postdoc à Saclay durant toute ma thèse : j'ai beaucoup apprécié travailler avec toi sur tous ces projets, ça a été très stimulant et bénéfique pour moi.

J'ai eu la chance d'avoir des bureaux dans deux laboratoires, au LPTENS et à l'IPhT au CEA, ce qui me semble être un luxe à l'heure ou l'espace disponible pour les thésards est chaque année plus restreint. Merci à tous les gens qui font la vie de ces laboratoires, je pense notamment à tous les membres du staff administratif, mais aussi au personnel informatique et à tous les chercheurs avec qui j'ai eu l'opportunité de discuter. Merci à Olivier Golinelli et à Stéphane Nonnenmacher pour leurs conseils. Je tiens également à remercier tous les thésards et les postdocs qui ont croisé mon chemin à Saclay (dans le désordre Piotr – sans toi Alexandre m'aurait encore plus empêché de travailler – et Julien – sans toi, j'aurais sans doute oublié des noms dans cette liste – les anciens du M2, et aussi Thiago, Jean-Marie, Benoit, Rémi, Bruno, Richard, Guillaume, Hélène, Alexander, Hanna, Antoine, Jérôme et tous les thésards/postdocs qui continuent de manger ensemble le midi, ainsi que Katya, Nicolas et Thomas qui ont partagé mon bureau), à l'ENS ou à Jussieu (Michele, Tristan, Fabien, Sébastien, Alexander, Julius et à tous ceux qui ont participé de près ou de loin au séminaire jeunes cond-mat, qui je l'espère continuera pendant de nombreuses années), ou au hasard

d'une conférence (je pense surtout à Jacopo et Loic récemment). Il m'est impossible de citer tous les noms ici, mais je souhaite remercier tout particulièrement Alexandre bien sûr, pour toutes nos discussions scientifiques ou non, et Swann pour les sandwiches Libanais du mercredi et sa compagnie durant le M2 (je me rappellerai toujours du "that's my spot" avec Pilou). Scu : malgré les nombreuses heures pendant lesquelles tu m'as empêché de travailler, je reste persuadé qu'un certain nombre de résultats de cette thèse auraient sans doute mis plus de temps à prendre forme sans nos innombrables discussions ! Enfin, je souhaite aussi remercier les thésards anciens ou actuels de Jesper et Hubert : Eric (merci pour tes commentaires sur ce manuscrit !) et Roberto qui ont été thésards en même temps que moi, mais aussi Jérôme, Constantin et Yacine pour les discussions scientifiques ou non que nous avons pu avoir.

Il va sans dire que Cédric, Wahb et Alexandre tiennent une place très particulière dans ces remerciements : sans toutes nos soirées restau/pizzas/fondues/sushis/coktails depuis l'ENS Lyon, et sans nos vacances à New York et dans l'ouest américain pour notre mariage avec Mandy, ces années de thèse auraient sans doute été moins sympathiques (mais probablement plus bénéfiques pour ma ligne). Je suis très content que nous ayons suivi des parcours similaires durant toutes ces années, votre présence va sans aucun doute me manquer l'année prochaine.

Je remercie ma mère et Philippe pour leur soutien sans faille durant ma thèse, mais aussi avant en prépa et à l'ENS, je ne sais pas ce qu'on aurait fait sans vous. Merci pour tous ces moments réconfortants autour d'une bonne pizza ! Merci aussi à Anne, Dom, Francine et Joel pour avoir fait le déplacement pour ma soutenance, je suis ravi que vous soyez là. Je profite aussi de ces quelques lignes pour penser à Sara et Raphael qui n'ont pas beaucoup vu leur frère durant l'écriture de cette thèse, et aussi à Laure.

Enfin, mes derniers remerciements vont tout naturellement à ma femme Mandy, qui a vécu ses années de thèses avec moi et qui me suit depuis toutes ces années d'études. Inutile d'en écrire des pages, je n'en serais pas là sans toi, et j'ai hâte de profiter de notre nouvelle vie en Californie avec Newton !

Note to the reader

This manuscript contains a review of my doctoral work on Logarithmic Conformal Field Theory that corresponds more or less to the first two years of my PhD thesis. More recently, I have been involved in various projects related to quantum quenches and entanglement in quantum impurity problems, which would have arguably deserved one or two chapters in this thesis manuscript. However, for the sake of consistency and brevity, I have decided not to include here this part of my work. I refer the interested reader to the original papers on that topic that are included at the end of this thesis.

Before embarking on our journey through the various aspects of Logarithmic Conformal Field Theories, I would like to warn the reader that I have chosen to address this admittedly very technical topic in a rather loose way, without paying too much attention to precise mathematical definitions. The words 'modules' and 'representations' are used interchangeably, very technical mathematical concepts such as 'tiltings' or 'projectives' are defined and used in a 'physical way' *etc.* I hope that the reader fond of mathematical rigor will forgive me for that pedagogical choice.

Contents

Chapter 1

Introduction: logarithmic correlations in condensed matter physics

This thesis manuscript aims at providing a rather self-contained introduction to the field of Logarithmic Conformal Field Theory (LCFT), with of course a particular emphasis on the work of the author. The techniques of Conformal Field Theory (CFT) have proven very efficient over the past decades at describing critical phenomena. In a typical critical physical system, the correlations within the sample do not decay exponentially with a characteristic correlation length ξ, but rather algebraically with a set of universal critical exponents that may be the same for very different physical problems, depending on the symmetries and the dimensionality of the system rather than on microscopic details. In the well-known example of the ferromagnetic/antiferromagnetic transition, described in its simplest version by the Ising model (see Fig. 1.1), the correlation length diverges as $\xi \sim |T - T_c|^{-\nu}$ when the temperature approaches the so-called Curie temperature T_c, with a critical exponent ν ($\nu = 1$ in $d = 2$ dimensions, and $\nu = \frac{1}{2}$ in mean-field theory). At the critical point $T = T_c$, the two-point function of the spin operator $S(r)$ scales as

$$\langle S(\vec{r}_1) S(\vec{r}_2) \rangle \sim |\vec{r}_1 - \vec{r}_2|^{2-d-\eta} , \tag{1.1}$$

where η is yet another critical exponent, with $\eta = \frac{1}{4}$ in two dimensions, as computed by Wu and Chen [1, 2], more than twenty years after the exact calculation of the free energy by Onsager [3]. The power-law behavior of eq. (1.1) can actually be traced back to the expected scale invariance at the critical point. As it turns out, the symmetry of the critical point is much larger and contains all transformations preserving local scale invariance; these are called conformal transformations, and they include for example rotation and translation symmetries. Quantum Field Theories with such conformal symmetry describe Renormalization Group fixed points, and are called Conformal Field Theories. CFTs are very constrained by symmetry, especially in two dimensions (2D) where the Lie algebra of conformal transformations becomes infinite, giving rise to the

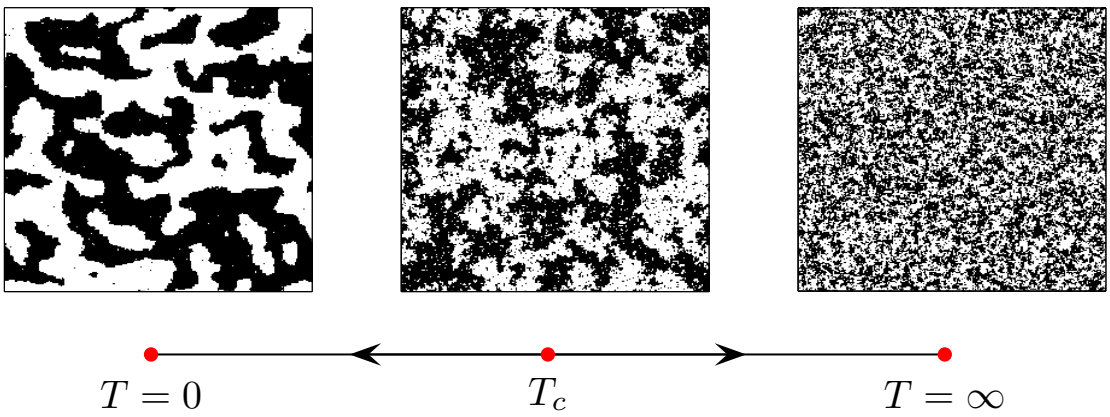

Figure 1.1: Phase diagram of the two-dimensional Ising model. The system flows, in the sense of the renormalization group, to a massive disordered phase for $T > T_c$. At the critical point $T = T_c$, the low energy behavior of the Ising model is described by a Conformal Field Theory with central charge $c = \frac{1}{2}$.

celebrated Virasoro algebra

$$[L_n, L_m] = (n-m)L_{n+m} + \frac{c}{12} n(n^2-1)\delta_{n+m,0}, \tag{1.2}$$

where $c \in \mathbb{R}$ (or $c \in \mathbb{C}$ *a priori*) is the central charge. Since the seminal paper [4], many exact results for critical systems have been obtained using conformal invariance techniques. Among the most famous examples are the unitary minimal models $\mathcal{M}(p, p+1)$, with central charge [5, 6]

$$c = 1 - \frac{6}{p(p+1)}, \quad \text{with } p \geq 3 \text{ integer}, \tag{1.3}$$

obtained from the classification of *irreducible* representations of the Virasoro algebra (1.2). In that series, $p = 3$ corresponds to the Ising model, $p = 4$ to the tricritical Ising model, $p = 5$ to the 3-state Potts model, *etc.* It is also worth pointing out that as p increases, more and more relevant operators are allowed and the corresponding critical points are obtained through fine tuning of more and more parameters, so that only small values of p are actually interesting for practical applications. CFTs were also found to have a very broad range of applications in condensed matter and quantum impurity physics (related to Boundary CFTs [7]), from the Kondo effect [8], the Fermi Edge singularity [9] or the wave functions describing Fractional Quantum Hall states [10] to, more recently, entanglement entropy [11], quantum quenches [12, 13] or non-equilibrium heat current [14] calculations in 1D quantum spin chains.

Despite its success, many interesting physical applications of CFT actually involve much more complicated field theories whose understanding is not complete. These include for instance quantum critical points in disordered systems of non-interacting fermions – an example being the long sought-after theory of the transition between

plateaus in the Integer Quantum Hall Effect (IQHE) [15] (see *e.g.* [16] for a review from a CFT perspective and references therein), two-dimensional geometrical problems such as self-avoiding walks and percolation [17], or critical systems with quenched disorder in general [18, 19]. Those arguably interesting physical problems turn out to be described by daunting CFTs that show unusual features such as non-unitarity, which means one has to deal with non-Hermitian Hamiltonians and negative norm-square states, or non-rationality, which implies that the scaling operators in the theories cannot be simply described by a finite set of primary operators – all remaining operators being roughly derivatives (descendants) of these few primary fields. As we shall discuss shortly, non-unitarity opens the door to *indecomposability*, a crucial feature that ultimately lead to logarithmic corrections to algebraic correlations such as (1.1)

$$\langle \tilde{S}(\vec{r}_1)\tilde{S}(\vec{r}_2)\rangle \sim |\vec{r}_1 - \vec{r}_2|^{-2\Delta}\,(\alpha + \beta \log|\vec{r}_1 - \vec{r}_2|), \tag{1.4}$$

where Δ is the scaling dimension of the field $\tilde{S}$. It is important to emphasize the fact the logarithmic corrections in (1.4) appear *at* the critical point; in particular, those *are not* sub-leading corrections produced by marginally irrelevant operators as in the ϕ^4 field theory in $d = 4$ dimensions [20] or in the XY model at the Kosterlitz-Thouless point [21]. The existence of logarithmic fields like $\tilde{S}(\vec{r})$ requires the generalization of the usual scale invariance principle of a Quantum Field Theory, which translates into complicated *indecomposable* representations from the point of view of the Virasoro algebra. This shall be explained in more detail in the following.

The remainder of this introduction will be devoted to some examples of physical systems expected to have logarithmic correlations. We will also give some motivations for the lattice methods that shall be used extensively throughout this thesis.

1.1 Non-unitarity and LCFTs in statistical mechanics and condensed matter

Whereas non-unitarity can probably be considered as non-physical in the context of particle physics and traditional Quantum Mechanics, it turns out to be a quite natural feature in statistical mechanics, geometrical problems and condensed matter physics. For instance, the description of statistical properties of geometrical problems such as percolation (see Fig. 1.2) or self-avoiding walks (SAWs, also known as dilute polymers) involves features that are more complicated than those of the minimal models (1.3). One might reasonably think that this is in fact due to the non-local nature of these geometrical problems. Indeed, the main difference between, say the Ising model and percolation, is the intrinsic non-locality of the physical observables in percolation, where one is interested in connectivity probabilities of percolation clusters rather than in local spin or energy observables. However, this point of view is somehow misleading, as genuine non-locality would obviously spoil the Field Theory description of the problem. In fact, those geometrical problems are only superficially non-local, as the non-locality can be traded for non-unitarity and complex Boltzmann weights [22], by reformulating them in terms of vertex models. Giving a weight $n = 2\cos\gamma$ to a loop on the honeycomb

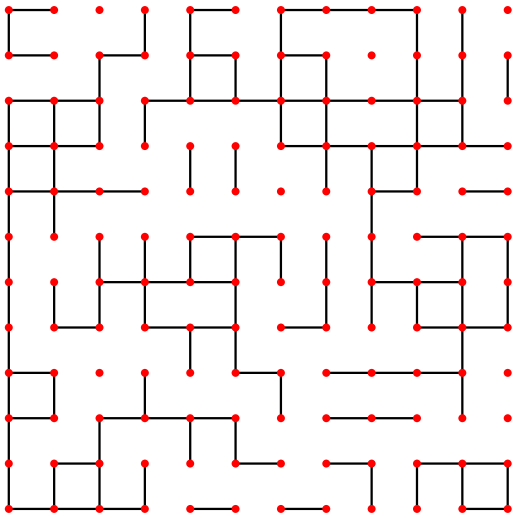

Figure 1.2: Two-dimensional percolation configuration on the square lattice. Bonds are occupied with probability p, and at the critical point $p = p_c = \frac{1}{2}$, the scaling properties of percolation clusters are described by a $c = 0$ (L)CFT.

lattice can for example be done by orienting the loops, and giving an elementary complex weight $\mathrm{e}^{\pm i\gamma/6}$ to each left/right turn. Summing over both loop orientations thus gives each loop a fugacity $2\cos(6 \times \gamma/6) = n$ as requested, since the number of left and right turns in a closed loop can only differ by 6. One therefore recovers locality at the price of giving up the natural probabilistic interpretation of the models. From the 2D CFT perspective, the scaling properties of percolation and SAWs can be described by correlation functions and critical exponents given by a CFT with central charge $c = 0$. As we shall see later on, such $c = 0$ must be non-unitary, and actually logarithmic, in order to be non-trivial. The only unitary CFT with $c = 0$ indeed has a unique observable, the identity operator with scaling dimension $\Delta = 0$ [6]. It is also worth mentioning that even the Ising model can be considered as a LCFT, provided that one includes (apparently) non-local observables in the theory, such as fields measuring the probability that two spins belong to the same spin cluster for example. In that sense, logarithmic CFTs can actually be thought of as extensions of the minimal models outside the minimal Kac table, thus including more operators in the theory.

A few important remarks should be emphasized at this point.

- In the case of percolation or SAWs, the logarithmic nature of the LCFTs did not deter physicists from using conformal invariance to compute interesting physical quantities such as critical exponents [23, 24] and crossing probabilities [25]. However, the full CFT description of such geometrical problems remains sadly unknown [26], as are almost all bulk correlation functions.
- Although we have insisted on the fact that one of the main aspects of a LCFT is non-unitarity, there exist some very simple non-unitary CFTs which can be tackled quite easily. Minimal models can indeed be extended to non-unitary theories, a well-known example being the Yang-Lee singularity CFT $\mathcal{M}(2, 5)$ with

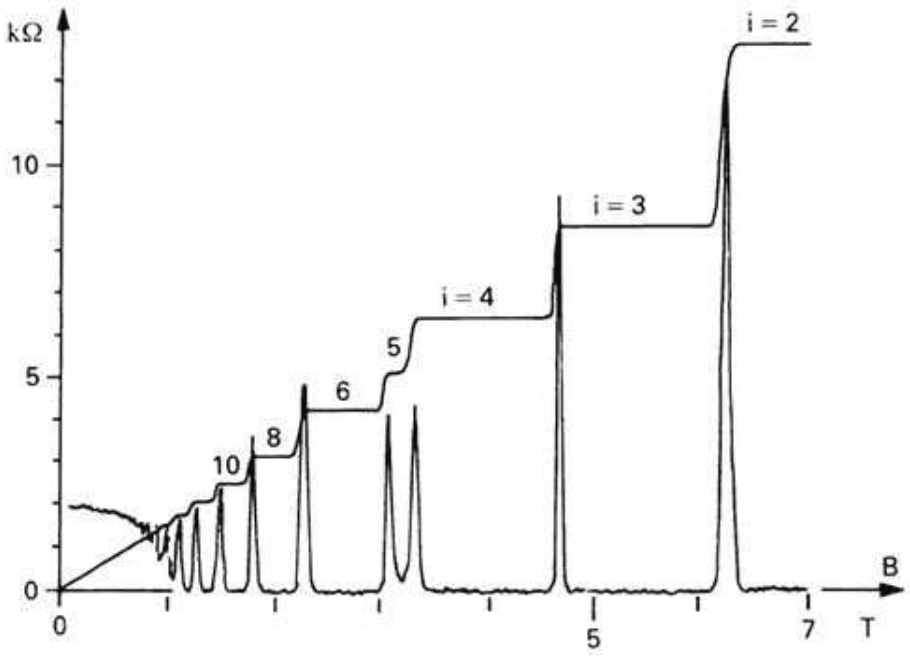

Figure 1.3: Plateaus for the Hall resistance and peaks of the Ohmic resistance in the integer quantum Hall effect. Neighboring values of i are separated by a quantum critical point, whose properties are described by a $c = 0$ 2D (L)CFT. (figure taken from `http://www.nobelprize.org/nobel_prizes/physics/laureates/1998/press.html`).

central charge $c = -\frac{22}{5}$, describing the Ising model above its critical temperature in a non-zero, purely imaginary magnetic field [27]. Therefore, although a LCFT *must* be non-unitary, non-unitary CFTs do not have to be logarithmic and can be described thanks to a finite number of irreducible Virasoro representations just like unitary minimal models.

- The key feature of a LCFT is rather *indecomposability*, which means, from the point of view of Virasoro representation theory, that one has to deal with complicated reducible representations that cannot be decomposed into a direct sum of irreducible representations. In physical terms, this will imply the non-diagonalizability of the scale transformation generator – the Hamiltonian in a 2D CFT. This is allowed because the scale transformation generator does not have to be Hermitian in a non-unitary theory. We will come back to this in the next chapter.

Disordered systems provide another class of physical systems whose critical points are expected to be described by LCFTs. Of course, impurities and random disorder break conformal invariance in general, but upon averaging over disorder configurations, it is reasonable to expect that conformal invariance could be restored for specific values of the disorder strength and other physical parameters such as the temperature. We will call disordered or random critical points the resulting conformally invariant RG fixed points. The main issue when facing a problem with quenched disorder is to

average correlation functions such as

$$\langle \mathcal{O} \rangle = \frac{1}{Z[\{h(\vec{r})\}]} \mathrm{Tr}_\phi \left(\mathcal{O} \mathrm{e}^{-H[\phi,\{h(\vec{r})\}]} \right), \tag{1.5}$$

over some quenched disordered variable $h(\vec{r})$. One solution to get rid of the partition function in the numerator of (1.5) is to consider $n \in \mathbb{Z}$ copies (replicas) of the system, and then to take a formal $n \to 0$ limit to recover physical results. Another alternative in the case of non-interacting system is to find other degrees of freedom ψ such that $Z^{-1} = \mathrm{Tr}_\psi \mathrm{e}^{-H[\psi]}$. This is the essence of the supersymmetry (SUSY) approach to disordered systems [28], where in practical applications, ϕ and ψ are bosonic and fermionic degrees of freedom, respectively. In both approaches, one ends up computing averaged observables using an effective field theory with trivial partition function, thus implying [29] the vanishing of the central charge $c = 0$ for disordered fixed points [18, 19]. Among the examples of problems described by $c = 0$ LCFT is the transition between plateaus in the IQHE mentioned above [16] (see Fig. 1.3), or for instance, the so-called Nishimori point in the two-dimensional random-bond Ising model (see *e.g.* [30]). Other examples include the Spin Quantum Hall Transition – related to classical percolation [31], or Dirac fermions in a random SU(N) gauge potential [32–34].

Of course, physical applications of LCFTs are not restricted to condensed matter physics. For example, let us also mention Abelian sandpile models [35, 36], 2D turbulence [37, 38], or the AdS/CFT correspondence where LCFTs describe the massless limit of non-linear sigma models with non-compact target spaces [39, 40]. LCFTs also appear as duals of 'logarithmic gravity' theories in the AdS/LCFT correspondence [41, 42], and they also play an important role in 4D gauge theories [43].

Given the broad range of applications of LCFTs, it seems quite natural to try to push further our understanding of such quantum field theories, in the hope that someday we will be able to classify and handle them as well as we do minimal CFTs. In this thesis, we will mostly focus on lattice models and point out how they can help in getting LCFTs under control. However, before we turn to this *lattice regularization approach* (or *lattice approach*), let us make a short historical detour to understand how and why physicists got interested in LCFTs in the first place.

1.2 A little bit of history

It is of course not the purpose of this short paragraph to provide a detailed account of all the contributions to the LCFT field, but rather to point out that the key ideas of Logarithmic CFTs came out of rather different communities, ranging from pure mathematics and string theory to condensed matter. The first observation of logarithmic terms and indecomposability in CFTs probably goes back to the work of Rozansky and Saleur [44] in 1992, who studied the Wess-Zumino-Witten (WZW) model on the supergroup GL(1|1). This was followed shortly after by the pioneering paper of Gurarie [45] in 1993, who first introduced the concept of logarithmic operators and explained how these were compatible with conformal invariance. Although it would be

fair to say that LCFTs remained mostly unknown to most theoretical physicists at the time, several key papers contributed to the birth of the LCFT field a few years later, in 1996. First, logarithmic operators were shown by Caux, Kogan and Tsvelik to appear in the problem of Dirac Fermions in a random gauge potential [32]. At the same time, Gaberdiel and Kaush [46, 47], and Flohr [48], studied indecomposable fusion rules and logarithmic operators with motivations rather far from condensed matter physics and disordered systems. The same year again, the mathematician Rohsiepe uploaded on arXiv his preliminary work on Virasoro staggered modules [49], which were realized to be of crucial importance to LCFTs many years later. A few years afterwards, Gurarie introduced his b-number for $c = 0$ CFTs [50], which turned out to be closely related to the apparently very different indecomposability parameters studied a bit earlier in [46]. At the time, the number b was thought to be a sort of new "central charge", that would allow one to distinguish between different $c = 0$ CFTs. Right about the same time, Kausch introduced the theory of symplectic fermions [51, 52], which remains even now one of the few exactly solvable logarithmic theories, for which everything is under control. Cardy then showed that logarithmic corrections in disordered systems and in polymers could be understood in terms of limits within a replica approach [18, 53], thus providing a simple physical mechanism for the appearance of logarithmic correlations in disordered systems in general. Disordered systems and $c = 0$ CFTs were also studied by Gurarie and Ludwig [19, 54], who computed for the first time the allowed values for b in the boundary versions of polymers and percolation.

It is now well-accepted that LCFTs are not characterized by a single parameter b, but rather by a complex structure of indecomposable Virasoro representations, with an infinite set of indecomposability parameters akin to b characterizing their structure. Over the past few years, two lines of thought have been considered. The first one is to deal directly with complicated indecomposable Virasoro representations (see *e.g.* [55–60]). The second approach is somewhat more concrete, and consists in studying thoroughly lattice models whose continuum limit is described by LCFTs. This is this 'lattice approach' that we shall analyze in details in the following.

1.3 Why lattice models?

Most of our understanding of ordinary (non-logarithmic, rational) CFTs came from the classification of irreducible representations of the Virasoro algebra. The null-vector conditions in Virasoro representation theory strongly constrain the operator content of minimal CFTs, and they also allow one to compute correlation functions through differential equations *etc* [4–6, 61]. LCFTs, on the other hand, though still constrained by representation theory – at least compared to completely irrationnal CFTs with generic central charge, remain very poorly understood mainly because the involved (indecomposable) modules of the Virasoro algebra have a very complicated structure. It is actually believed that it is impossible to classify such indecomposable modules; this is why the representation theory of Virasoro is said to be *wild* [62], which roughly means that it is as complicated as it can be. It might therefore be hopeless to try to solve LCFTs by classifying Virasoro representations, although several partial results

have emerged in that direction recently [1].

Although it might appear almost as a bit of a heresy in the CFT world, LCFTs seem so complicated that another possibility is to turn to specific examples, from which one might hope to extract generic features. WZW models with super target spaces do provide 'simple' examples of LCFTs [63–65], but although some interesting lessons can be learned from them, all the known examples seem to be very closely related [66], and their features far from being generic.

Another approach that has proven very helpful consists in considering lattice models as lattice regularizations of LCFTs, that is, lattice models whose continuum limit is described by LCFTs. This may seem completely hopeless at first sight, as lattice models are in principle much more complicated than field theories. In particular, conformal invariance obviously holds only in the continuum limit. However, it was realized over the years that many features of the continuum limit already appear on small lattice systems, albeit in some finite dimensional forms. This was first observed quite a while ago using quantum groups by Pasquier and Saleur [67], although it was formalized as an efficient tool to study LCFTs only a few years ago by Read and Saleur [68, 69], and independently with less algebraic emphasis, by Pearce, Rasmussen and Zuber [70]. The point is that most of the algebraic features that make LCFTs so complicated, such as indecomposability, are already present in finite lattice systems. In general, we would like to get a handle on LCFTs that describe fixed points of interacting, non-unitary, field theories with well defined local actions. If such LCFTs do exist, it is reasonable to expect that they can be realized as continuum limit (or scaling limit) of lattice models, such as quantum spin chains with local interactions. The Hamiltonian densities form a lattice algebra whose representation theory is well under control, and as the continuum limit is taken, one expects conformal symmetry to emerge, and this lattice algebra to tend to Virasoro in some sense that remains to be made more precise. As we shall argue, Virasoro indecomposable modules and their fusion rules can be seen as scaling limits of lattice representations, and much crucial physical information, including indecomposability parameters or b-numbers generalizing Gurarie's [50], can be recovered from the lattice. The lattice approach that we shall describe in this thesis mostly relies on the original work of Read and Saleur [68, 69], but we will try to connect our results to other approaches whenever possible.

Yet another good reason to study lattice models in the LCFTs context is that after all, at least for a condensed matter/statistical physicist, LCFTs can be considered as physical only if they do describe the low energy limit of some microscopic model of physical relevance. It might of course be important to construct $c = 0$ theories from a purely abstract point of view, but arguably, the ultimate goal is to get under control the CFTs describing physical systems such as percolation or disordered systems. It is therefore quite natural to try to stay as concrete as possible from the very beginning. Many other interesting questions then emerge; for example, if correlation functions

1. In particular, Kytölä and Ridout have recently managed to classify rigorously a special class of Virasoro representations called *staggered modules* [59], following the pioneering work of Rohsiepe [49]. These modules seem to play a special role in the physics of boundary LCFTs, and it is for example quite satisfying to see that the b-number of Gurarie [50] can actually be computed from a purely algebraic viewpoint [57]. We shall come back to these staggered modules in Chapter 2.

such as (1.4) do appear in physical systems, then what do they describe precisely? What kind of physical observables are logarithms related to? Can we understand indecomposability more physically? We will see that studying directly concrete lattice models provides reasonably-satisfying partial answers to these questions.

1.4 Organization of the manuscript

The outline of the remainder of this thesis is as follows:

- Chapter 2 contains an introduction to Logarithmic CFTs and indecomposability, assuming that the reader has a basic knowledge of CFTs only. All the relevant algebraic concepts (indecomposable representations, staggered modules for Virasoro *etc.*) are introduced using concrete examples. This chapter does not contain any new result *per se* – although it does reproduce some of the operator product expansion arguments presented in [71, 72], but hopefully it provides a self-contained review of the field with examples worked out in details, that will take the reader from logarithmic correlations to complicated indecomposable Virasoro representations.
- Chapter 3 is a review of how lattice models can provide regularizations of Logarithmic CFTs, using the ideas of Read and Saleur [68, 69] – relying quite heavily on the recent review [73]. We explain how to measure indecomposability parameters [71] and how to compute fusion rules [72] directly from the lattice.
- In chapter 4, we push further the ideas of the previous chapter to attempt a classification of Virasoro indecomposable representations relevant for physical applications [74]. We also study non-chiral (bulk) LCFTs, that are obtained as scaling limits of periodic lattice models, mostly from the point of view of indecomposability parameters [75]. Some (yet) unpublished results on the relation between open and periodic lattice models [76] and periodic percolation are also discussed.
- In the last chapter 5, we first discuss why LCFTs are relevant to describe critical points in quenched disordered systems using supersymmetry or the replica trick [18]. We also adapt the ideas of Cardy [18, 77] to obtain geometrical observables in the Potts model – and in particular in percolation – that behave logarithmically at the critical point. The $O(n)$ model, dilute polymers and spanning trees are also discussed from the perspective of LCFTs. This chapter is based on the papers [78, 79].

Chapter 2

A short introduction to Logarithmic Conformal Field Theory

In this chapter, we will review the main ingredients of Logarithmic CFTs. Although conformal invariance yields several general results, *e.g.* the form of two and three-point correlators [80], in any dimension, most of the successes of CFTs are restricted to $d = 2$ dimensions (see *e.g.* [61, 81]), where the conformal group becomes infinite dimensional. We will henceforth restrict ourselves to two dimensions, mainly to fix some notations that will be used throughout this thesis. However, note that in principle, LCFTs exist in any dimension, and some of the results of this section can actually be readily generalized to higher dimensions. We shall come back to higher dimensional LCFTs in Chapter 5.

We will begin this chapter by coming back to CFT basics, and analyze how scale invariance can be made compatible with logarithmic correlations. We will show that logarithms are related to Jordan cells in the scale transformation generator, and we shall discuss the general form of the logarithmic correlators [45]. At this point, we will introduce the indecomposability parameters or b-numbers that characterize the logarithmic structure of a LCFT. The second section of this chapter is a review of the '$c \to 0$ catastrophe' [50, 54], and contains a discussion of a general pattern to explain how LCFTs can be thought of as limits of ordinary (non-logarithmic but irrational) CFTs [1]. Within this approach, logarithms can be shown to arise as limits of power-law correlations, thus yielding simple formula for the indecomposability parameters [71]. In order to relate these results to more formal algebra, we define and give simple examples of indecomposable representations in the case of the Lie superalgebra $\mathfrak{gl}(1|1)$. The symplectic fermions theory [51, 52] will then provide a concrete example to illustrate all these new concepts: logarithms, indecomposable representations, indecomposability parameters, *etc.* Finally, the end of this chapter will be devoted to the ubiquitous Virasoro staggered modules – a class of indecomposable Virasoro modules especially important to LCFTs. This will also give us a chance to define indecomposability parameters in a purely algebraic language, as a number characterizing a Virasoro representation.

1. This idea will be used extensively in Chapter 5.

In this chapter, the emphasis will be on (L)CFTs rather than on lattice models. We will therefore try not to think of CFTs as describing properties of statistical models for a while, but rather consider them as abstract field theories that satisfy conformal invariance. We will go back to lattice models and show how all the results of this chapter are related to interesting physical problems in the next chapters.

2.1 Logarithmic operators, scale invariance and indecomposability parameters

In this first section, we define Logarithmic operators and show that logarithmic correlations do not break conformal invariance. We derive the general form of two-point functions in the case of a rank-two Jordan cell in the scale transformation generator, and discuss the case of higher-rank Jordan cells. Furthermore, we introduce indecomposability parameters, also called logarithmic couplings or b-numbers.

2.1.1 Conformal invariance in 2D, primary operators and Ward identity

We start with some general well-known results on ordinary (non logarithmic) CFTs. More details can be found in [61] or in the seminal paper [4].

Conformal transformations

A conformal transformation is defined as an invertible mapping $\vec{x} \mapsto \vec{\tilde{x}}$ which preserves the form of the metric tensor $g_{\mu\nu}(\vec{x})$, up to a local scale $\Lambda(\vec{x})$

$$g_{\mu\nu}(\vec{\tilde{x}}) = \Lambda(\vec{x}) g_{\mu\nu}(\vec{x}). \tag{2.1}$$

These transformations form the conformal group, which contains the Poincaré group as a subgroup ($\Lambda(\vec{x}) = 1$), as well as scale transformations ($\Lambda(\vec{x}) = \Lambda$). Conformal invariance can be thought of as a local version of scale invariance. In generic dimension d, the conformal group can be shown to be isomorphic to $SO(d+1,1)$, and the covariance of the correlation functions under this finite dimensional Lie group already enforces the form of two and three-point correlators [80]. However, in two dimensions [2], eq. (2.1) reduces to the Cauchy-Riemann equations and any analytical mapping $w(z)$ ($\bar{\partial} w = 0$) is conformal, *i.e.* preserves angles in 2D (see Fig. 2.1). Strictly speaking, these conformal transformations do not have to be well-defined everywhere and invertible, which leads to the distinction between *local* and *global* conformal transformations. The subset of global invertible transformations form the group of global conformal transformations $SL(2,\mathbb{C})/\mathbb{Z}_2 \simeq SO(3,1)$.

2. We will use complex coordinates $z = x^0 + ix^1$ and $\bar{z} = x^0 - ix^1$, with $\partial = \frac{1}{2}(\partial_0 - i\partial_1)$ and $\bar{\partial} = \frac{1}{2}(\partial_0 + i\partial_1)$.

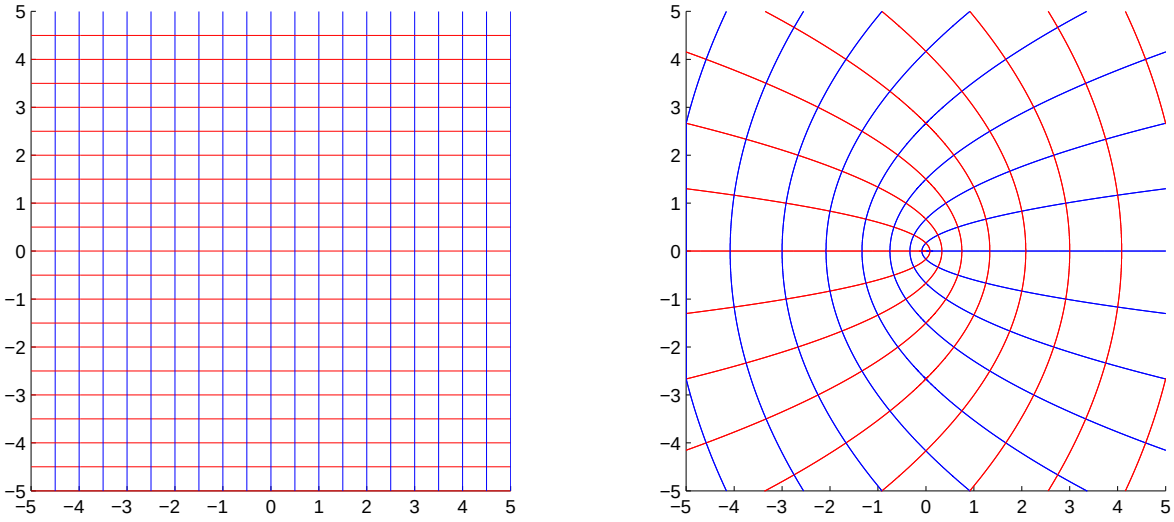

Figure 2.1: A rectangular grid (left) and its image under the conformal transformation $f(z) = \frac{z^2}{3}$ (right). An important point is that $f(z)$ preserves angles as can clearly be seen on these pictures.

Primary operators

CFTs are quantum field theories with conformal transformations as symmetry. The fundamental fields of a CFT are the so-called primary operators $\phi_{h,\bar{h}}(z,\bar{z})$ which transform covariantly under a conformal map $z \mapsto w(z)$, $\bar{z} \mapsto \bar{w}(\bar{z})$

$$\tilde{\phi}_{h,\bar{h}}(w,\bar{w}) = \left(\frac{dw}{dz}\right)^{-h} \left(\frac{d\bar{w}}{d\bar{z}}\right)^{-\bar{h}} \phi_{h,\bar{h}}(z,\bar{z}), \tag{2.2}$$

where $h, \bar{h}$ are the conformal weights of the field ϕ. In order to recover some more physically transparent quantities, we define

$$\Delta = h + \bar{h}, \tag{2.3a}$$
$$s = h - \bar{h}. \tag{2.3b}$$

Δ is the usual scaling dimension that controls how ψ transforms under a scale transformation $\vec{x} \mapsto \Lambda\vec{x}$

$$\tilde{\phi}(\Lambda\vec{x}) = \Lambda^{-\Delta}\phi(\vec{x}), \tag{2.4}$$

whereas s is the conformal spin which appears naturally when rotating the system with an angle θ

$$\tilde{\phi}(\mathcal{R}_\theta\vec{x}) = \mathrm{e}^{i\theta s}\phi(\vec{x}). \tag{2.5}$$

Note that if ϕ transforms as (2.2) (*i.e.* is primary), its derivatives will not be primary and will have more complicated transformation laws under conformal transformations.

Stress-energy tensor and Ward identity

A fundamental object in a CFT is the stress-energy tensor $T^{\mu\nu}$, defined through the variation of the action S under an arbitrary transformation of the coordinates $x^\mu \mapsto x^\mu + \epsilon^\mu$

$$\delta S = \frac{1}{2\pi} \int \mathrm{d}^2x \; T^{\mu\nu} \; \partial_\mu \epsilon_\nu. \tag{2.6}$$

The stress-energy tensor measures the reaction of the system with respect to a change in geometry. It can be chosen to be symmetric, and invariance with respect to rotations and translations implies, in complex coordinates, that $\partial\bar{T} = \bar{\partial}T = 0$ with $T(z) = T_{zz}$ and $\bar{T}(\bar{z}) = T_{\bar{z}\bar{z}}$. Scale invariance makes the stress-energy tensor traceless, so that $T_{z\bar{z}} = T_{\bar{z}z} = \frac{1}{4}T^\mu_\mu = 0$. In an ordinary CFT, the holomorphic and antiholomorphic dependence decouple, and the whole theory can be constructed as sum of tensor products of chiral and anti-chiral sectors [3]. We will thus forget about the antiholomorphic sector for now, and focus on infinitesimal holomorphic conformal transformations $z \mapsto w(z) = z + \epsilon(z)$. Using (2.2), a primary field ϕ_h with holomorphic conformal weight h transforms as

$$\delta\phi_h = \epsilon\partial\phi_h + h\phi_h\partial\epsilon. \tag{2.7}$$

The variation of correlation functions involving ϕ_h under this infinitesimal conformal transformation can also be expressed in terms of a contour integral involving the stress-energy tensor $T(z)$

$$\delta\phi_h = \oint_z \frac{\mathrm{d}\xi}{2\pi i}\epsilon(\xi)T(\xi)\phi_h(z), \tag{2.8}$$

where this equality should be understood as holding when inserted in a correlator. From (2.7) and (2.8), one obtains the following *Operator Product Expansion* (OPE) – called conformal Ward identity,

$$T(z)\phi_h(w) \sim \frac{h}{(z-w)^2}\phi_h(w) + \frac{1}{z-w}\partial\phi_h(w), \tag{2.9}$$

where we dropped less singular contributions. Let us also define the Virasoro modes L_n as the Laurent series

$$T(z) = \sum_{n\in\mathbb{Z}} \frac{L_n}{z^{n+2}}. \tag{2.10}$$

3. This will not hold anymore for a LCFT, where the holomorphic and antiholomorphic sectors can be glued in a highly non-trivial fashion.

We also define the antiholomorphic modes $\bar{L}_n$ from $\bar{T}(\bar{z})$ in the same way. The Virasoro modes L_n and $\bar{L}_n$ satisfy the commutation relations of the Virasoro algebra (1.2), with $\left[L_n, \bar{L}_m\right] = 0$. The Virasoro algebra structure is encoded in the following OPE

$$T(z)T(w) \sim \frac{c/2}{(z-w)^4} + \frac{2}{(z-w)^2}T(w) + \frac{1}{z-w}\partial T(w), \tag{2.11}$$

where we recall that c is the central charge of the theory. The stress-energy tensor provides an example of quasiprimary field, which satisfies (2.2) only for global conformal transformations.

Within the usual radial quantization framework, the vacuum state $|0\rangle$ is defined such that $L_n|0\rangle = 0$ for all $n \geq -1$. This implies that the vacuum must be invariant under global conformal transformations, spanned by L_{-1}, L_0 and L_1. The Ward identity (2.9) then implies that the asymptotic state $|\phi_h\rangle = \lim_{z\to 0}\phi_h(z)|0\rangle$ is an eigenstate of L_0 with eigenvalue h, and $L_n|\phi_h\rangle = 0$ for $n > 0$. The operator L_0 in the chiral theory, or rather $L_0 + \bar{L}_0$ in the full theory, generates the scale transformations (or dilatations) $\vec{x} \mapsto \Lambda\vec{x}$, which are nothing but time translations in radial quantization. Hence, L_0 (or $L_0 + \bar{L}_0$) plays the role of the Hamiltonian of the system.

2.1.2 Logarithmic operators and two-point functions

Let us now turn to the definition of logarithmic operators [45] (see also the recent review [82] and references therein), and compute their two-point correlation functions.

Logarithmic operators

For the sake of the argument, we shall focus on the holomorphic sector only. We will come back to non-chiral correlation functions later. Let ϕ be a primary field with conformal weight h. The associated state $|\phi\rangle$ is thus an eigenstate of the Hamiltonian L_0 – the scale transformations generator: $L_0|\phi\rangle = h|\phi\rangle$. It satisfies $L_1|\phi\rangle = L_2|\phi\rangle = 0$. Let us now imagine that there exists a field ψ which satisfies

$$T(z)\psi(w) \sim \cdots + \frac{h\psi + \phi}{(z-w)^2} + \frac{1}{z-w}\partial\psi, \tag{2.12}$$

so that $L_0|\psi\rangle = h|\psi\rangle + |\phi\rangle$, and $L_{n>0}|\psi\rangle \neq 0$ in general. We will nevertheless assume that $L_1|\psi\rangle = 0$. The field $\psi(z)$ is called *logarithmic partner* of ϕ. Concrete examples of such fields will be given later. In the basis $(|\phi\rangle, |\psi\rangle)$, Hamiltonian reads

$$L_0 \;=\; \begin{pmatrix} h & 1 \\ 0 & h \end{pmatrix}. \tag{2.13}$$

It has a rank-two Jordan cell and is therefore *non-diagonalizable*. We will say that the two fields ϕ and ψ are mixed by L_0 into a rank-two Jordan cell. Under global

infinitesimal conformal transformations $w(z) = z + \epsilon(z)$ [4], they transform as

$$\delta\phi = \epsilon\partial\phi + h\phi\partial\epsilon, \tag{2.14a}$$
$$\delta\psi = \epsilon\partial\psi + (h\psi + \phi)\partial\epsilon. \tag{2.14b}$$

Let us emphasize again that these equations hold if $\epsilon(z) = a + bz + cz^2$, that is, if $w(z) = z + \epsilon(z)$ is a global conformal transformation. In general, the transformation laws are more complicated and involve higher derivatives of $\epsilon(z)$; in particular, recall that ψ does not transform as (2.14) for an arbitrary conformal transformation.

After a finite scale transformation $z \mapsto \Lambda z$, one has

$$\begin{pmatrix} \tilde{\psi}(\Lambda z) \\ \tilde{\phi}(\Lambda z) \end{pmatrix} = \Lambda^{-\begin{pmatrix} h & 1 \\ 0 & h \end{pmatrix}} \begin{pmatrix} \psi(z) \\ \phi(z) \end{pmatrix} = \begin{pmatrix} \Lambda^{-h}(\psi(z) - \phi(z)\log\Lambda) \\ \Lambda^{-h}\phi(z) \end{pmatrix}. \tag{2.15}$$

Physically, this means that after a scale transformation, or after a Renormalization Group (RG) transformation, the field $\psi(z)$ will be mixed with the scaling field $\phi(z)$, and there is of course no way to change the field basis to get rid of this mixing. Non-diagonalizable RG flows are allowed because of the non-unitarity of the theory, and although it might seem quite exotic at first sight, we will see in the next chapters that such logarithmic fields are quite common is physics.

Note that because the Hamiltonian is non-diagonalizable, it is also non hermitian so we can see at this point that if such logarithmic partner fields do exist, the CFT cannot be unitary. Nevertheless, it is worth pointing out that one still has $L_0^\dagger = L_0$ for the usual Virasoro bilinear form $L_n^\dagger = L_{-n}$, by definition, but the bilinear form $\dagger$ is no longer positive definite. For instance, we will show in the next paragraph that conformal invariance leads to $\langle\phi|\phi\rangle = 0$.

Logarithmic two-point functions

Now that we know how these logarithmic fields transform under global conformal transformations, we would like to compute their two-point correlation functions – three-point functions could also be considered but we will restrict to two-point function for the sake of simplicity. Just like in ordinary CFT, global conformal invariance fixes the form of two and three-point correlators in any dimension [80], but we will restrict to two dimensions for now, postponing our discussion of higher dimensional LCFTs to Chap. 5.

First of all, because of translation invariance ($\epsilon = a$), the correlators $\langle\phi(z)\phi(w)\rangle$, $\langle\phi(z)\psi(w)\rangle$ and $\langle\psi(z)\psi(w)\rangle$ depend only on $u = z-w$. We will denote by $f(u)$, $g(u)$ and $h(u)$ the corresponding functions, that is, $\langle\phi(z)\phi(w)\rangle = f(z-w)$, $\langle\phi(z)\psi(w)\rangle = g(z-w)$ and $\langle\psi(z)\psi(w)\rangle = h(z-w)$. Note that we already anticipated that $\langle\phi(z)\psi(w)\rangle = \langle\psi(z)\phi(w)\rangle$ for the sake of simplicity. Scale invariance ($\epsilon = az$) then implies the

4. Translations correspond to the choice $\epsilon(z) = a$, dilatations to $\epsilon(z) = az$, and special conformal transformations to $\epsilon(z) = az^2$, with $a \in \mathbb{C}$.

following differential equations

$$u\frac{df}{du} + 2hf = 0, \tag{2.16a}$$

$$u\frac{dg}{du} + 2hg + f = 0, \tag{2.16b}$$

$$u\frac{dk}{du} + 2hk + 2g = 0. \tag{2.16c}$$

Similarly, it is straightforward to show that special conformal transformations yield equations that are compatible with (2.16) if and only if $f(u) = 0$. The remaining equations can readily be solved, and one ends up with

$$\langle\phi(z)\phi(0)\rangle = 0, \tag{2.17a}$$

$$\langle\phi(z)\psi(0)\rangle = \frac{b}{z^{2h}}, \tag{2.17b}$$

$$\langle\psi(z)\psi(0)\rangle = \frac{\theta - 2b\log z}{z^{2h}}, \tag{2.17c}$$

where θ and b are some constants. Let us assume for the sake of the argument that the normalization of ϕ can be fixed in some way, then the normalization of ψ is given [5] by the equation $L_0\psi = h\psi + \phi$. In that case, while the constant θ is arbitrary and can be canceled by a choice $\psi \to \psi - \frac{\theta}{2b}\phi$, the parameter b is a fundamental number that characterizes the structure of the Jordan cell. It is unique and well-defined once a given normalization of the field ϕ has been chosen [6]. We also emphasize that the logarithmic term in the correlation function $\langle\psi(z)\psi(0)\rangle$ is perfectly consistent with scale and conformal invariance, but it implies that L_0 is non-diagonalizable because $\log\Lambda z = \log\Lambda + \log z$. It is also important to remark that $\phi(z)$ must be a null-field by conformal invariance, that is to say, introducing the usual Virasoro bilinear form, $\langle\phi|\phi\rangle = 0$ [7]. However, $\phi(z)$ *does not* decouple as the correlator $\langle\phi(z)\psi(0)\rangle$ does not vanish. This is crucially different from what we are used to with ordinary CFTs. Finally, let us point out that logarithmic partners are unique: this can be argued using conformal invariance, or more simply by remarking that if $L_0|\psi_1\rangle = h|\psi_1\rangle + |\phi\rangle$ and $L_0|\psi_2\rangle = h|\psi_2\rangle + |\phi\rangle$, then the combination $|\psi_1\rangle - |\psi_2\rangle$ decouples and there remains only one true logarithmic partner $(|\psi_1\rangle + |\psi_2\rangle)/2$. However, higher-rank Jordan cells are allowed (see next paragraph).

Note that similar equations can be obtained in the non-chiral case, but the important point is that $L_0 - \bar{L}_0$ has to remain diagonalizable so that the theory remains local [83]. Therefore, if L_0 is non-diagonalizable, then so is $\bar{L}_0$. Two-point correlation functions are readily obtained by replacing $\log z \to \log|z|^2$, and $z^{2h} \to z^{2h}\bar{z}^{2\bar{h}}$.

5. Note however that there still remains a degree of freedom $\psi \to \psi + \alpha\phi$ in the definition of ψ.

6. Anticipating a little bit, in most (but not all) cases of interest, ϕ is a descendant of another primary field. The normalization is then be given by the way ϕ is related to this 'parent' primary field, see eq. (2.21).

7. Note also that $\langle\psi|\psi\rangle = \infty$.

Generalization to higher-rank Jordan cells

Of course, more logarithmic partners can be considered. As a simple example, let us consider the case of a rank 3 Jordan cell so that L_0 expressed in the basis $\big(\phi(z), \psi_1(z), \psi_2(z)\big)$ reads

$$L_0 = \begin{pmatrix} h & 1 & 0 \\ 0 & h & 1 \\ 0 & 0 & h \end{pmatrix}. \tag{2.18}$$

One can then show that global conformal invariance enforces

$$\begin{aligned} \langle \phi(z)\phi(0)\rangle &= \langle \psi_1(z)\phi(0)\rangle = 0, && \text{(2.19a)} \\ \langle \psi_1(z)\psi_1(0)\rangle &= \langle \psi_2(z)\phi(0)\rangle = \frac{b}{z^{2h}}, && \text{(2.19b)} \\ \langle \psi_2(z)\psi_1(0)\rangle &= \frac{\theta_1 - 2b\log z}{z^{2h}}, && \text{(2.19c)} \\ \langle \psi_2(z)\psi_2(0)\rangle &= \frac{\theta_2 - 2\theta_1\log z + 2b\log^2 z}{z^{2h}}. && \text{(2.19d)} \end{aligned}$$

Note that there still is a unique 'b number' that characterizes these correlation functions, assuming that a given normalization of the null field ϕ has been chosen. The other coefficients θ_1, θ_2 are non-universal, and depend on the UV cutoff. This can be generalized to Jordan cells of any rank k [84], with logarithmic terms $\log^{k-1} z$ in two-point correlation functions.

2.1.3 Indecomposability parameters

The parameter b in eq.(2.17) is a fundamental, universal number that characterizes the structure of the Jordan cell and appears as an amplitude of the logarithmic term. It is uniquely defined once a normalization for the field ϕ has been chosen (in almost all the cases encountered in this thesis, this normalization will be given by eq. (2.21), see below). In the case of a rank-2 Jordan cell, there is a unique such b-number, also called indecomposability parameter or logarithmic coupling. More formally, we have

$$b \equiv \lim_{z\to\infty} z^{2h}\langle \phi(z)\psi(0)\rangle. \tag{2.20}$$

In fact, there is another more algebraic, closely related parameter that also goes by these names in the literature. To avoid any confusion, we will refer to the coefficient b appearing in correlation functions as *physical* indecomposability parameter, and we will denote by β *algebraic* indecomposability parameters.

In order to introduce β, let us remark that in most cases that we will encounter in this thesis (but not all), the null field $\phi(z)$ is actually a descendant of a primary field

$\xi(z)$, with conformal weight $h_\xi \leq h = h_\phi = h_\psi$. This means that we can write

$$\phi(z) = A\xi(z), \quad A = L_{-n} + \alpha_{(1)} L_{-n+1} L_{-1} + \cdots + \alpha_{(P(n)-1)} L_{-1}^n, \tag{2.21}$$

where $n = h - h_\xi$ and $P(n)$ is the number of partitions of the integer n. A belongs to the universal cover of the Virasoro algebra, that is, it consists of words of the Virasoro generators L_n. The $\alpha_{(i)}$ coefficients are uniquely fixed by the null-vector condition $L_{+1}\phi = L_{+2}\phi = 0$. In that case, we define the *algebraic* indecomposability using Virasoro bilinear form

$$\beta \equiv \langle \phi | \psi \rangle \,, \tag{2.22}$$

where we normalized $\xi(z)$ such that $\langle \xi | \xi \rangle = 1$. Note that it is also possible to define β through the equation

$$A^\dagger \psi(z) = \beta \xi(z). \tag{2.23}$$

It is important to notice at this point that the choice that we adopted for the normalization of the operator A is crucial for the value of β. Different choices have been used in the literature, and some of them may yield simpler expressions for β. Unless otherwise indicated, we will always use the convention given by eq. (2.21). As an example, we will see in the next section that the stress-energy tensor $\phi(z) = T(z) = L_{-2} I$ ($A = L_{-2}$ here) has a logarithmic partner $\psi(z) = t(z)$ for non-trivial $c = 0$ theories. To summarize this general structure, we will use the following diagram

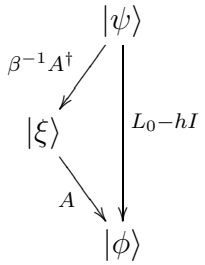

(2.24)

where the arrows are only here to indicate the action of the Virasoro generators L_0, A and $A^\dagger$. They will acquire a more precise meaning in the following sections.

Because of (2.17b), it might be tempting to claim that $b \equiv \lim_{z\to\infty} z^{2h} \langle \phi(z)\psi(0) \rangle$ is equal to $\beta \equiv \langle \phi | \psi \rangle$. However, one has to be careful since once the adjoint operator is defined for the state $|\xi\rangle$, then the adjoint for its descendant $|\phi\rangle = A\,|\xi\rangle$ is fixed, and generally it will not coincide with the naive definition $\lim_{z\to\infty} z^{2h}\, \langle 0|\, \phi(z)$ [58, 72]. We will remember that in general, $b \neq \beta$.

Indecomposability parameters also play a crucial role in the representation theory of the Virasoro algebra, and we will come back to this in section 2.5. After these formal definitions, it is now time to turn to more concrete examples.

2.2 $c \to 0$ catastrophe, differential equations and generalizations

In a Quantum Field Theory, Operator Product Expansions (OPEs) are fundamental as they encode the structure of the correlation functions. In 2D, conformal invariance strongly constrains the structure of OPEs. It may happen that OPE coefficients (either the structure constants or the coefficients in front of the descendants) become ill-defined when the central charge approaches a 'logarithmic' value ($c = 0$ typically). One possibility to solve this 'catastrophe' is to look for other fields in the OPE that will 'collide' with the diverging term in order to cancel out the divergence. This is the essence of the so-called '$c \to 0$ catastrophe' [18, 19, 50, 54, 85, 86], which predicts the existence of a logarithmic partner $t(z)$ for the stress energy tensor $T(z)$ in $c = 0$ CFTs.

2.2.1 $c \to 0$ catastrophe

Conformal Field Theories with central charge $c \to 0$ are arguably the most important examples of LCFTs as far as physical applications are concerned. One important feature of such LCFTs is that the stress energy tensor $T(z)$ has a logarithmic partner $t(z)$. We review here the argument leading to this conclusion.

Kac operators

Now that we are turning to more explicit examples, we need to introduce some additional notations to parametrize the central charge and the Kac table. We will use the following parametrization for the central charge

$$c = 1 - \frac{6}{p(p+1)}, \tag{2.25}$$

with $p \in \mathbb{R}$, so that the Kac formula at central charge c reads

$$h_{r,s} = \frac{((p+1)r - ps)^2 - 1}{4p(p+1)}. \tag{2.26}$$

We will call Kac operators the fields $\Phi_{r,s}$ (r, s positive integers) with conformal weights $h_{r,s}$ [8] that are degenerate [9] at level rs. An example of Kac operator is given by the identity $1 = I = \Phi_{1,1}$, which satisfies a trivial differential equation at level 1 $L_{-1}I = \partial I = 0$.

8. Recall that unless mentioned explicitly, we restrict our study to the case of chiral LCFTs, with only one copy of the Virasoro algebra. In the language of lattice models, this will correspond to open boundary conditions.

9. In the language of Virasoro representation theory (see section 2.5), Kac operators are associated with what we shall call Kac modules $\mathcal{K}_{r,s} \equiv \mathcal{V}_{h_{r,s}}/\mathcal{V}_{h_{r,-s}}$, where $\mathcal{V}_h$ is the Verma module of conformal weight h.

$c \to 0$ catastrophe and b-number

In this section, we will focus on Kac operators $\Phi_{1+2j,1}$ ($j \in \mathbb{N}/2$) lying on the first column of the Kac table. The structure of the OPEs of these Kac operators is encoded in the following *fusion rules* [4]

$$\Phi_{1+2j_1,1} \times_f \Phi_{1+2j_2,1} = \sum_{j=|j_1-j_2|}^{j_1+j_2} \Phi_{1+2j,1}, \tag{2.27}$$

where as usual, we dropped all the numerical coefficients, as well as the descendants. The operators $\Phi_{1+2j,1}$ form a close algebra under fusion, and as we shall see in the next chapters, this choice corresponds to 'dilute' loop models on the lattice. Note also that these fusion rules have a $SU(2)$ structure, and we will also come back to this crucial point in the next chapters. These fusion rules hold only when the central charge is *generic*, in particular when it is irrational. When c takes specific values, typically $c = 0$, 'mixing' will occur between the different Kac operators and logarithmic corrections will appear in correlation functions. These logarithmic operators correspond to fields that are quotiented out in minimal models.

To see this more explicitly, let us consider the OPE of $\Phi_{2,1}$ with itself at $c \neq 0$. Conformal invariance then enforces

$$\begin{aligned}\Phi_{2,1}(z)\Phi_{2,1}(0) \sim \frac{C^{\Phi_{1,1}}_{\Phi_{2,1}\Phi_{2,1}}}{z^{2h_{2,1}}} \left(1 + \frac{2h_{2,1}}{c} z^2 T(0) + \frac{h_{2,1}}{c} z^3 \partial T(0) + \dots\right) \\ + \frac{C^{\Phi_{3,1}}_{\Phi_{2,1}\Phi_{2,1}}}{z^{2h_{2,1}-h_{3,1}}} \left(\Phi_{3,1}(0) + \frac{z}{2}\partial\Phi_{3,1}(0) + \dots\right).\end{aligned} \tag{2.28}$$

If we try to take naively the limit $c \to 0$, we immediately face a problem as the term $\frac{2h_{2,1}}{c} z^2 T(0)$ in the identity channel is ill-defined ($h_{2,1} = \frac{5}{8} \neq 0$ at $c = 0$). Other descendants in the identity sector, such as ∂T, will also show similar divergences. This problem is of course not specific to the fusion of the field $\Phi_{2,1}$ with itself as it will occur systematically in the identity channel. One possibility to fix this problem would be that $C^{\Phi_{1,1}}_{\Phi_{2,1}\Phi_{2,1}}$ vanishes at $c = 0$. This actually happens in the bulk (non-chiral) case for Kac operators [53, 75, 77] (regarding bulk LCFTs, see also section 4.2 in this thesis), but unless there is no other choice, it is customary to set $C^{\Phi_{1,1}}_{\Phi_{2,1}\Phi_{2,1}} = 1$.

To kill the divergent terms, we introduce a new field $t(z)$

$$t(z) = \frac{2b(c)}{c} \left(C^{\Phi_{3,1}}_{\Phi_{2,1}\Phi_{2,1}} \frac{c}{2h_{2,1}} \Phi_{3,1}(z) + T(z)\right), \tag{2.29}$$

with $b(c) = -\frac{c/2}{h_{3,1}-2}$. In terms of this field (admitting for the moment that it is meaningful in the $c \to 0$ limit), it is straightforward to check that the OPE is well-defined

at $c = 0$, but that it becomes logarithmic

$$\Phi_{2,1}(z)\Phi_{2,1}(0) \sim \frac{1}{z^{5/4}} \left(1 + \frac{h_{2,1} z^2}{b} (t(0) + \log z \; T(0)) + \frac{h_{2,1} z^3}{2b} (\partial t(0) + \log z \; \partial T(0)) + \dots \right), \tag{2.30}$$

with $b = \lim_{c \to 0} b(c) = 5/6$ and $h_{2,1} = \frac{5}{8}$.

It is important to notice that although the field $t(z)$ is built out of two divergent quantities, one can check that it is perfectly well-defined when inserted in correlation functions, as long as the limit process is properly respected. As $c \to 0$, the eigenvectors $T(z)$ and $\Phi_{3,1}$ of L_0 become degenerate with the same conformal weight $h_{3,1} = 2$. The generically primary field $\Phi_{3,1}$ is ill-defined in the limit, but if one considers the appropriate combination with $T(z)$, one can construct a new well-defined field $t(z)$ given by (2.29) that will be mixed into a Jordan cell with $T(z)$ at $c = 0$. It is indeed straightforward to check that $L_0 \, |t\rangle = 2 \, |t\rangle + |T\rangle$ in radial quantization, as well as

$$\langle T(z)T(0) \rangle = 0 \tag{2.31a}$$

$$\langle T(z)t(0) \rangle = \frac{b}{z^4} \tag{2.31b}$$

$$\langle t(z)t(0) \rangle = \frac{\theta - 2b \log z}{z^4}, \tag{2.31c}$$

as expected for a logarithmic partner [10].

Another important remark is that despite the fact that the definition of $t(z)$ in (2.29) seems to depend on the particular fusion that one considers in the first place (here $\Phi_{2,1}$), all the physical properties of this field, including the OPEs and the correlation functions, do not depend on this feature. In particular, we expect the coefficient $C^{\Phi_{3,1}}_{\Phi_{2,1}\Phi_{2,1}}$ to be irrelevant for our matters, and if we were to define $t(z)$ to cancel the divergence in another fusion (say $\Phi_{5,1} \times_f \Phi_{5,1}$), we would find a field $t(z)$ with the same properties. It is thus natural to conjecture that in the limit $c \to 0$, these different definitions coincide, up to a rescaling.

We have thus identified explicitly a logarithmic field at $c = 0$ that arises as a mixing of $T(z) = L_{-2} I$ and $\Phi_{3,1}$. This limit argument also allowed us to compute the value of the physical indecomposability parameter

$$b_{\text{polymers}} = - \lim_{c \to 0} \frac{c/2}{h_{3,1} - 2} = \frac{5}{6}. \tag{2.32}$$

We denoted by b_{polymers} the indecomposability parameter as it corresponds to the theory of SAWs (dilute polymers). If instead we had considered the fusion of Kac operators $\Phi_{1,1+2j}$ living in the first row of the Kac table, we would have had to use the Kac operator $\Phi_{1,5}$ ($h_{1,5} = 2$ at $c = 0$) to cancel the divergences, leading to a different value

10. We allowed for an additive constant θ in the correlation function $\langle t(z)t(0) \rangle$, but whereas b is universal, θ will depend on the UV cutoff of the theory as the argument of the logarithm has to be dimensionless.

for the indecomposability parameter

$$b_{\text{percolation}} = -\lim_{c\to 0} \frac{c/2}{h_{1,5}-2} = -\frac{5}{8}, \tag{2.33}$$

relevant this time for the percolation theory [11]. These values of b were computed for the first time in [19], even though the correct attribution of $-\frac{5}{8}$ to percolation only came many years later [57]. We also remark in passing that for percolation and polymers, the algebraic indecomposability parameter $\beta = \langle T|t\rangle$ is equal to b

$$L_2\,|t\rangle = b\,|0\rangle\,. \tag{2.34}$$

where we have used eq. (2.29).

2.2.2 Generalization and formulas for indecomposability parameters

Actually, the results of the previous paragraph are not restricted to $c = 0$ and the same line of reasoning can be applied to other values of the central charge, and to other operators. This can be used to infer general formulas for the indecomposability parameters [71] (see also [72]). We follow here [72].

Logarithmic Ising model

As another example, let us consider the logarithmic Ising model ($p = 3$, $c = 1/2$). We deform our logarithmic theory into a generic ordinary CFT ($p = 3+\epsilon$) and consider the OPE of $\Phi_{1,3}$ with itself

$$\Phi_{1,3} \times_f \Phi_{1,3} = \Phi_{1,1} + \Phi_{1,3} + \Phi_{1,5}. \tag{2.35}$$

As before, this fusion rule means that when two primary fields $\Phi_{1,3}(z)$ are brought close to each other in a correlation function, their product can be expanded onto the fields $\Phi_{1,1}(z)$, which is the identity field I, $\Phi_{1,3}(z)$, $\Phi_{1,5}(z)$ and their descendants. At the Ising point $p = 3$, we are going to show that the fields $\Phi_{1,3}(z)$ and $\Phi_{1,5}(z)$ (and their descendants) are mixed together and we thus expect logarithms to appear.

More explicitly, the OPE of $\Phi_{1,3}(z)$ with itself in the generic case reads

$$\begin{aligned}\Phi_{1,3}(z)\Phi_{1,3}(0) \sim \frac{C^{\Phi_{1,3}}_{\Phi_{1,3},\Phi_{1,3}}}{z^{h_{1,3}}} \Big[\Phi_{1,3}(0) + \frac{1}{2}z\partial\Phi_{1,3}(0) + \alpha^{(-2)}z^2 L_{-2}\Phi_{1,3}(0) \\ +\alpha^{(-1,-1)}z^2 L_{-1}^2\Phi_{1,3}(0) + \dots\Big] + \frac{C^{\Phi_{1,5}}_{\Phi_{1,3},\Phi_{1,3}}}{z^{2h_{1,3}-h_{1,5}}}\left[\Phi_{1,5}(0) + \dots\right] + \frac{1}{z^{2h_{1,3}}}\left[1 + \dots\right],\end{aligned} \tag{2.36}$$

11. Once again, we emphasize that the precise identification of the LCFTs corresponding to percolation or dilute polymers will be discussed in the following chapters of this thesis.

$\vdots$	$\vdots$	$\vdots$	$\vdots$	$\vdots$	$\ddots$
7	5	$\frac{10}{3}$	2	1	$\dots$
$\frac{33}{8}$	$\frac{21}{8}$	$\frac{35}{24}$	$\frac{5}{8}$	$\frac{1}{8}$	$\dots$
2	1	$\frac{1}{3}$	0	0	$\dots$
$\frac{5}{8}$	$\frac{1}{8}$	$-\frac{1}{24}$	$\frac{1}{8}$	$\frac{5}{8}$	$\dots$
0	0	$\frac{1}{3}$	1	2	$\dots$

$p = 2$ $(c = 0)$

$\vdots$	$\vdots$	$\vdots$	$\vdots$	$\vdots$	$\ddots$
6	$\frac{65}{16}$	$\frac{5}{2}$	$\frac{21}{16}$	$\frac{1}{2}$	$\dots$
$\frac{7}{2}$	$\frac{33}{16}$	1	$\frac{5}{16}$	0	$\dots$
$\frac{5}{3}$	$\frac{35}{48}$	$\frac{1}{6}$	$-\frac{1}{48}$	$\frac{1}{6}$	$\dots$
$\frac{1}{2}$	$\frac{1}{16}$	0	$\frac{5}{16}$	1	$\dots$
0	$\frac{1}{16}$	$\frac{1}{2}$	$\frac{21}{16}$	$\frac{5}{2}$	$\dots$

$p = 3$ $(c = \frac{1}{2})$

Table 2.1: Extended Kac tables at $c = 0$ (percolation) and $c = \frac{1}{2}$ (Ising), showing the conformal weights $h_{r,s}$ for $r, s \geq 1$ (see eq. (2.26)). The shaded parts correspond to minimal models, whereas logarithmic CFTs typically involve operators outside this minimal part.

where the coefficients $\alpha^{(-2)} = \frac{6}{5\epsilon} + \frac{16}{25} + \mathcal{O}(\epsilon)$ and $\alpha^{(-1,-1)} = -\frac{9}{10\epsilon} - \frac{9}{50} + \mathcal{O}(\epsilon)$ are fixed by global conformal invariance and are diverging as $\epsilon \to 0$. However, if we introduce the field $\phi = (L_{-2} - \frac{3}{4}L_{-1}^2)\Phi_{1,3}$, we can get rid of one of these divergences as $\frac{3}{4}\alpha^{(-2)} + \alpha^{(-1,-1)} = \frac{3}{10} + \mathcal{O}(\epsilon)$ is well-defined:

$$\Phi_{1,3}(z)\Phi_{1,3}(0) \sim \frac{C^{\Phi_{1,3}}_{\Phi_{1,3},\Phi_{1,3}}}{z^{h_{1,3}}} \Big[\Phi_{1,3}(0) + \frac{1}{2} z \partial \Phi_{1,3}(0) + \alpha^{(-2)} z^2 \phi(0) + z^2 (\alpha^{(-1,-1)} + \frac{3}{4}\alpha^{(-2)}) \partial^2 \Phi_{1,3}(0) + \dots \Big] + \frac{C^{\Phi_{1,5}}_{\Phi_{1,3},\Phi_{1,3}}}{z^{2h_{1,3}-h_{1,5}}} [\Phi_{1,5}(0) + \dots] + \dots . \quad (2.37)$$

We dropped the identity channel as it will play no role in the following. We then define a new field $\psi(z)$ as

$$\psi(z) = \frac{C^{\Phi_{1,5}}_{\Phi_{1,3},\Phi_{1,3}}}{C^{\Phi_{1,3}}_{\Phi_{1,3},\Phi_{1,3}}} \frac{b(\epsilon)}{\alpha^{(-2)} N_\phi(\epsilon)} \Phi_{1,5}(z) + \frac{b(\epsilon)}{N_\phi(\epsilon)} \phi(z), \quad (2.38)$$

where $b = -\frac{N_\phi(\epsilon)}{h_{1,5}-h_{1,3}-2}$. The factor $N_\phi(\epsilon)$ is defined as the coefficient that appears in the two-point function $\langle \phi(z)\phi(0) \rangle = N_\phi(\epsilon) z^{-2(h_{1,3}+2)}$. This number can be computed using standard CFT techniques [72], with the result $N_\phi(\epsilon) = \frac{35}{96}\epsilon + \mathcal{O}(\epsilon)$. Since ϕ becomes a singular state at $\epsilon = 0$, we obviously have $N_\phi(0) = 0$. Because $b(\epsilon)$ has a finite limit when $\epsilon \to 0$, we can now safely take the limit $\epsilon \to 0$ so that the logarithmic

OPE reads

$$\Phi_{1,3}(z)\Phi_{1,3}(0) \sim \frac{C^{\Phi_{1,3}}_{\Phi_{1,3},\Phi_{1,3}}}{z^{1/2}}\left[\Phi_{1,3}(0)+\frac{1}{2}z\partial\Phi_{1,3}(0)+\frac{3}{10}z^2\partial^2\Phi_{1,3}(0)+\right.$$
$$\left.\frac{7}{16b}z^2(\psi(0)+\phi(0)\log z)+\dots\right]+\dots \quad (2.39)$$

where we have used that $\lim_{\epsilon\to 0} N_\phi(\epsilon)\alpha^{(-2)} = \frac{7}{16}$. One can check that the operators ψ and ϕ defined this way satisfy the usual OPEs for logarithmic operators with physical indecomposability parameter $b = \lim_{\epsilon\to 0} b(\epsilon) = -\frac{35}{24}$. In particular, it is possible to check that $L_0\,|\psi\rangle = \frac{5}{2}\,|\psi\rangle + |\phi\rangle$.

Using this approach, it is also possible to compute the associated algebraic indecomposability parameter

$$(L_2 - \frac{3}{4}L_1^2)\,|\psi\rangle = \frac{b(\epsilon)}{N_\phi(\epsilon)}(L_2 - \frac{3}{4}L_1^2)\,|\phi\rangle = \beta(\epsilon)\,|\Phi_{1,3}\rangle\,, \quad (2.40)$$

where in the limit $\epsilon \to 0$

$$\beta \equiv \langle\phi|\psi\rangle = \lim_{\epsilon\to 0}\beta(\epsilon) = -\lim_{\epsilon\to 0}\frac{\langle\phi|\phi\rangle}{h_{1,5}-h_{1,3}-2}. \quad (2.41)$$

In our case, we find $\langle\phi|\phi\rangle = \left\langle\Phi_{1,3}|(L_2 - \frac{3}{4}L_1^2)(L_{-2} - \frac{3}{4}L_{-1}^2)|\Phi_{1,3}\right\rangle = \frac{1}{4}(2c + h_{1,3}(18h_{1,3} - 11))$. Although $\langle\phi|\phi\rangle \neq N_\phi(\epsilon)$, these two expressions coincide up to order $\mathcal{O}(\epsilon^2)$, so that we find $\beta = b = -\frac{35}{24}$. Once again, these two numbers do not have to coincide in general, and it is actually quite easy to find examples for which they are different [58].

General pattern and formulas for the indecomposability parameters

In fact, this OPE construction that we presented on two specific examples is actually quite general. Indeed, the divergence of the OPE coefficients $\alpha^{(-2)}$ and $\alpha^{(-1,-1)}$ for the descendants of $\Phi_{1,3}$ is directly related to the vanishing of the Kac determinant $K^{(2)}(c,h) = 2h(16h^2 + 2h(c-5) + c)$ at level 2 for $c = \frac{1}{2}$ and $h = h_{1,3} = \frac{1}{2}$. Actually, it can be shown in general that the OPE coefficients for the descendants are inversely proportional to the Kac determinant at this level (see *e.g.* [61] for a proof of this statement, as well as a discussion of Kac determinants in general). We thus expect these divergences to be general, and they must be canceled by the (generally unique) primary operators present in the OPE with same conformal weights at $\epsilon \to 0$ as the ill-defined descendant terms. However, there might be some additional cancellations between the Kac determinant and the numerator in the descendant OPE coefficients, which are hard to control in general [12]. Let us also remark that these divergences in the OPEs correspond to fields that are quotiented out in the ordinary minimal models. Therefore, the logarithms that we obtained at $c = 0$ and $c = \frac{1}{2}$ appear in LCFTs that

12. As a simple example, the Kac determinant $K^{(1)}(c,h) = 2h$ at level 1 is canceled in the OPE coefficient $\alpha^{(-1)} = \frac{1}{2}$ in (2.36).

should be thought of as extensions of the minimal models $\mathcal{M}(2,3)$ and $\mathcal{M}(3,4)$ (Ising) (see Tab. 2.1).

This pattern being quite general, one can also infer from this construction general formulas to compute indecomposability parameters. Let us consider a more general LCFT with central charge $c = 1 - \frac{6}{x_0(x_0+1)}$ that we slightly deform $x = x_0 + \epsilon$ to make it non-logarithmic. Let $\phi = A\xi$ be a null field at $\epsilon = 0$, with ξ primary with conformal weight h_ξ; and ψ its logarithmic partner at $\epsilon = 0$ normalized such that $L_0 |\psi\rangle = h |\psi\rangle + |\phi\rangle$ at the logarithmic point. We normalize ξ so that $\langle\xi|\xi\rangle = 1$ and we choose $A = L_{-n} + \dots$ (see eq. (2.21)), so the dimension of ϕ is $h_\phi = h_\xi + n$. We call h_ψ the generic conformal weight of the primary field that will collide with ϕ at $\epsilon = 0$ (we had $h_\psi = h_{3,1}$ and $h_\psi = h_{1,5}$ in our previous example). We also define $N_\phi(\epsilon)$ as the coefficient that appears in the two-point function $\langle\phi(z)\phi(0)\rangle = N_\phi(\epsilon) z^{-2h_\phi}$. At the logarithmic point $\epsilon = 0$, we have $\langle\phi|\phi\rangle = \langle\xi|A^\dagger A|\xi\rangle = N_\phi = 0$ and $h_\psi = h_\phi = h_\xi + n$.

Then, the algebraic indecomposability parameter reads [71]

$$\beta \equiv \langle\phi|\psi\rangle = -\lim_{\epsilon\to 0} \frac{\langle\phi|\phi\rangle}{h_\psi - h_\phi}, \tag{2.42}$$

whereas the physical indecomposability parameter of the Jordan cell (ϕ, ψ) at $c = 0$ can be expressed as [72]

$$b = \lim_{z\to\infty} z^{2h} \langle\phi(z)\psi(0)\rangle = -\lim_{\epsilon\to 0} \frac{N_\phi(\epsilon)}{h_\psi - h_\phi}. \tag{2.43}$$

2.2.3 Boundary dilute polymers four-point functions

The OPE approach of the previous paragraph provides a nice and simple understanding of how logarithms can appear in correlation functions, so as to cancel divergent quantities in operator product expansions. One can check that the logarithmic operators obtained as limits such as the ones in eqs. (2.29) or (2.38) are well-behaved when inserted in correlation functions. However, this argument is rather heuristic, and it is quite reassuring to see that it is perfectly consistent with other methods that do not involve limits.

As an example, we will consider the boundary theory of self-avoiding walks, also known as dilute polymers. Because the partition function is trivial, the central charge of the corresponding CFT is $c = 0$, and we will admit for the moment that the boundary spectrum involves *watermelon* (or $2j$-leg) operators $\Phi_{2j+1,1}(z)$ that create $2j$ polymers, with $j \in \mathbb{N}/2$, with critical exponents $h_{1+2j,1}$ [23] (see also Chapter 3). We have seen in section 2.2.1 that the OPE $\Phi_{2,1}(z_1)\Phi_{2,1}(z_2)$ contains logarithmic terms at $c = 0$, with a physical indecomposability parameter $b = \frac{5}{6}$. If this is correct, the four-point function $\langle\Phi_{2,1}(z_1)\Phi_{2,1}(z_2)\Phi_{2,1}(z_3)\Phi_{2,1}(z_4)\rangle$ should show some signatures of this logarithmic dependence. Hence, we would like to analyze in details the case of the four-point function of the operator $\Phi_{2,1}(z)$ at the boundary, with its conformal dimension is $h_{2,1} = \frac{5}{8}$. This operator inserts one polymer at the boundary, and since it is a Kac

operator, it is degenerate at level 2

$$\left(L_{-2} - \frac{2}{3}L_{-1}^2\right)\Phi_{2,1} = 0. \tag{2.44}$$

This null-vector condition implies a simple differential equation for the four-point function $\langle\Phi_{2,1}(z_1)\Phi_{2,1}(z_2)\Phi_{2,1}(z_3)\Phi_{2,1}(z_4)\rangle$. We introduce the fonction $F(\eta)$ such that

$$\langle\Phi_{2,1}(z_1)\Phi_{2,1}(z_2)\Phi_{2,1}(z_3)\Phi_{2,1}(z_4)\rangle = \frac{1}{z_{12}^{5/4}z_{34}^{5/4}}\frac{F(\eta)}{(1-\eta)^{5/4}}, \tag{2.45}$$

where $\eta = \frac{z_{12}z_{34}}{z_{13}z_{24}}$ is the usual anharmonic ratio. The null-vector condition then yields the following differential equation

$$z(1-z)\frac{d^2}{dz^2}F(z) + (1-2z)\frac{d}{dz}F(z) + \frac{5}{4}F(z) = 0, \tag{2.46}$$

with solution

$$F(\eta) = A(1-\eta)^2\ {}_2F_1\left[-\frac{1}{2},\frac{3}{2},3,1-\eta\right] + B\eta^2\ {}_2F_1\left[-\frac{1}{2},\frac{3}{2},3,\eta\right]. \tag{2.47}$$

Here, ${}_2F_1(\alpha,\beta,\gamma;z)$ are the usual hypergeometric functions

$${}_2F_1(\alpha,\beta,\gamma;z) = \sum_{n=0}^{\infty}\frac{(\alpha)_n(\beta)_n}{(\gamma)_n}\frac{z^n}{n!}, \tag{2.48}$$

where $(x)_n = x(x+1)\dots(x+n-1)$ (and $(0)_n = 1$) is the Pochhammer symbol. For generic central charge, the four-point function of $\Phi_{2,1}$ satisfies a similar differential equation, with two hypergeometric functions (conformal blocks) that correspond to the two channels $\Phi_{1,1}$ and $\Phi_{3,1}$ in the fusion $\Phi_{2,1}\times_f\Phi_{2,1}$. At $c=0$ however, things are a bit more complicated as this two channels are mixed together. To see this, we first set $A = \frac{15\pi}{32}$ to respect the usual normalization of the two-point functions in the identity channel. The constant B depends on the boundary conditions and can be determined using different limits of the correlation function. Using this result, we can expand the correlation function for small anharmonic ratio

$$\begin{aligned}\langle\Phi_{2,1}(z_1)\Phi_{2,1}(z_2)\Phi_{2,1}(z_3)\Phi_{2,1}(z_4)\rangle = \frac{1}{z_{12}^{5/4}z_{34}^{5/4}}\left(1+\left(\frac{65}{64}+B-\frac{15\log 2}{8}\right)\eta^2+\right.\\ \left.\frac{15}{32}\eta^2\log\eta + \left(B-\frac{15\log 2}{8}+\frac{5}{4}+\frac{15}{32}\log\eta\right)\eta^3+\mathcal{O}(\eta^4)\right).\end{aligned} \tag{2.49}$$

As expected, we see that there are logarithms in this expansion, all coming from the function ${}_2F_1\left[-\frac{1}{2},\frac{3}{2},3,1-\eta\right]$. The coefficient $\frac{15}{32}$ is nothing but $\frac{h_{2,1}^2}{b}$, with $b=\frac{5}{6}$, so

this four-point function is consistent with the result for b for polymers. To see this, we can now use the OPE (2.30) at $c = 0$ along with equations (2.31) to find

$$\langle \Phi_{2,1}(z_1)\Phi_{2,1}(z_2)\Phi_{2,1}(z_3)\Phi_{2,1}(z_4)\rangle = \frac{1}{z_{12}^{5/4} z_{34}^{5/4}} \left(1 + \frac{9}{16}\theta\eta^2 + \frac{15}{32}\eta^2 \log\eta + \left(\frac{9}{16}\theta + \frac{15}{64}\right)\eta^3 + \frac{15}{32}\eta^3\log\eta + \mathcal{O}(\eta^4)\right). \quad (2.50)$$

This equation is perfectly consistent with eq. (2.49) provided that $\theta = \frac{65}{36} + \frac{16}{9}B - \frac{10}{3}\log 2$. Logarithmic OPEs can thus be observed directly at $c = 0$, as solutions of simple differential equations.

If we expand both hypergeometric functions, it is very tempting to interpret the A-channel (with ${}_2F_1\left[-\frac{1}{2}, \frac{3}{2}, 3, 1-\eta\right]$) as the identity, as it involves logarithms and starts with a constant term. This is consistent with the fact that the other B-channel starts with a term η^2, so it is natural to say that it corresponds to the conformal block $\Phi_{3,1}$ ($h_{3,1} = 2$). However, this observation is a bit too naive and one should really think of the two channels as mixed together at the logarithmic point. Note also that in the OPE approach, we considered $\eta \to 0$ before taking the limit $c \to 0$. This is an important point as there is no reason for these limits to commute in general. To understand what happens to the conformal blocks at the logarithmic point, it is actually very instructive to have a look at the limit $c \to 0$ of the generic four-point function of $\Phi_{2,1}(z)$. We also mention the geometrical interpretation of the different conformal blocks is a bit subtle for LCFTs [87].

2.3 Intermezzo: Indecomposable representations and $GL(1|1)$

In the introduction of this thesis, we have defined indecomposable representations as representations that cannot be decomposed into a direct sum of smaller representations [13]. Before going deeper in our analysis of LCFTs, let us pause for some time and come back to basic algebra to give some examples of indecomposable representations using the simple example of the Lie superalgebra $\mathfrak{gl}(1|1)$. Applications to field theory will be given in the next section.

2.3.1 Defining relations and irreducible representations

We first define the Lie super algebra $\mathfrak{gl}(1|1)$ and describe its irreducible representations. This paragraph has some strong overlap with Appendix A which reviews the properties of superalgebras in a rather formal and less pedagogical way. The Lie superalgebra $\mathfrak{gl}(1|1)$ is generated by two bosonic elements E, N and two fermionic generators

13. Note that strictly speaking, irreducible representations are also indecomposable – they cannot be decomposed onto smaller objects by definition. Nevertheless, in this thesis we will call *indecomposables* representations that are also reducible, that is, that contain invariant subrepresentation(s).

$\Psi^\pm$ such that E is central and the other generators obey

$$[N, \Psi^\pm] \;=\; \pm\Psi^\pm \quad \text{and} \quad \{\Psi^-, \Psi^+\} \;=\; E \;\; . \tag{2.51}$$

N is an operator that counts the number of fermions. Let us also fix the following Casimir element C

$$C \;=\; (2N-1)E + 2\Psi^-\Psi^+ \;\; . \tag{2.52}$$

The choice of C is not unique since we could add any function of the central element E.

The irreducible representations of $\mathfrak{gl}(1|1)$ are either one-dimensional (atypicals), or two-dimensional (typicals). Atypical representations are given by 1-dimensional representations $\langle n\rangle$, parametrized by the value $n \in \mathbb{R}$ of N, with vanishing other generators $\Psi^+ = \Psi^- = E = 0$. As we shall see in the following, these one-dimensional representations will appear as 'building blocks' of larger indecomposable representations. The typical representations are 2-dimensional representations $\langle e, n\rangle$ labeled by pairs e, n with $e \neq 0$ and $n \in \mathbb{R}$. In these representations, the generators take the form $E = e\mathbf{1}_2$ and

$$N \;=\; \begin{pmatrix} n-1 & 0 \\ 0 & n \end{pmatrix} \;\; , \;\; \Psi^+ \;=\; \begin{pmatrix} 0 & 0 \\ e & 0 \end{pmatrix} \;\; , \;\; \Psi^- \;=\; \begin{pmatrix} 0 & 1 \\ 0 & 0 \end{pmatrix} \;\; , \tag{2.53}$$

in a basis $\{|0\rangle, |1\rangle\}$. So far, everything is quite simple, even simpler than one would obtain for $\mathfrak{su}(2)$ for example, as there is no irreducible representation with dimension larger than two. But the Lie superalgebra $\mathfrak{gl}(1|1)$ is actually more complicated than $\mathfrak{su}(2)$, because it is *non-semisimple*[14] (it has an abelian ideal generated by E). In a nutshell, non-semisimplicity means that irreducible representations are not the end of the story, and that one also has to worry about *indecomposable* representations that are not irreducible, but that cannot be expressed as direct sums of smaller representations either.

2.3.2 A first look at indecomposability

As a first example of indecomposable representation, let us consider the case $e = 0$ of the typicals $\langle e, n\rangle$. The representations $\langle e, n\rangle$ are irreducible as long as $e \neq 0$. When $e = 0$, the generators (2.53) still provide a representation of $\mathfrak{gl}(1|1)$, but it is not irreducible. Indeed, the one-dimensional vector space with basis $\{|0\rangle\}$ provides an invariant subrepresentation, isomorphic to the atypical $\langle n-1\rangle$. It would thus be tempting to claim that $\langle 0, n\rangle$ is fully reducible (*i.e.* is *semisimple*) and that it can be decomposed onto $\langle n-1\rangle \oplus \langle n\rangle$. However, this is not the case, and $\langle 0, n\rangle$ is said to be

14. Recall that in mathematics, a semi-simple algebraic object means that it can be decomposed as a direct sum of *simple* objects. For modules (or representations), simple means irreducible, and a non-semisimple representation is also said to be indecomposable. For Lie algebras, a simple Lie algebra has no other ideal that $\{0\}$ and itself.

indecomposable, as it cannot be expressed as a direct sum of smaller representations. This is because of the form of Ψ^- in eq. (2.53). It is useful to picture the structure of indecomposable representations

$$\langle 0, n\rangle = \begin{array}{ccc} & & \langle n\rangle \\ & \overset{\Psi^-}{\swarrow} & \\ \langle n-1\rangle & & \end{array} \tag{2.54}$$

This diagram represents the structure of $\langle 0, n\rangle$ in terms of its two atypical (one-dimensional) components $\langle n-1\rangle$ and $\langle n\rangle$. The arrow represents the action of the algebra $\mathfrak{gl}(1|1)$, here, the generator Ψ^-. Acting with Ψ^-, one can go from the 'top' $\langle n\rangle$ to the 'bottom' (also called 'socle') $\langle n-1\rangle$ but not the other way around. The irreducible $\langle n-1\rangle$ is subrepresentation of $\langle 0, n\rangle$, and the quotient $\langle 0, n\rangle/\langle n-1\rangle \simeq \langle n\rangle$ is also irreducible. We will refer to the structure of indecomposable modules (representations) in terms of irreducible modules and mappings between them (arrows) as *subquotient structure*, and the irreducible components as subquotients. The diagram may appear to the reader as a quite complicated way to represent the structure of a two-dimensional representation. Nevertheless, in most examples of indecomposable representations that we shall encounter in this thesis, the subquotients will not be simply one-dimensional, the structure might become much more complicated. In these cases, diagrams such as (2.54) are a useful way to represent the 'backbone' of the indecomposable representation, even if it is infinite-dimensional for example.

2.3.3 Tensor products

To obtain more involved indecomposable representations, let us consider tensor products of typical representations $\langle e_1, n_1\rangle \otimes \langle e_2, n_2\rangle$. We emphasize that we deal here with graded tensor products, that is, when we pass a fermionic operator through a fermionic state, we generate an additional minus sign. We will take the convention that $|0\rangle$ is bosonic and $|1\rangle$ is fermionic. So for example, we have

$$\Psi^- |11\rangle = \left(\Psi_1^- + \Psi_2^-\right)|11\rangle = \Psi_1^- |1\rangle \otimes |1\rangle - |1\rangle \otimes \Psi_2^- |1\rangle = |01\rangle - |10\rangle . \tag{2.55}$$

In the basis $\{|00\rangle, |01\rangle, |10\rangle, |11\rangle\}$, we find

$$\Psi^+ = \begin{pmatrix} 0 & 0 & 0 & 0 \\ e_2 & 0 & 0 & 0 \\ e_1 & 0 & 0 & 0 \\ 0 & e_1 & -e_2 & 0 \end{pmatrix}, \ \Psi^- = \begin{pmatrix} 0 & 1 & 1 & 0 \\ 0 & 0 & 0 & 1 \\ 0 & 0 & 0 & -1 \\ 0 & 0 & 0 & 0 \end{pmatrix}, \ N = \begin{pmatrix} n-1 & 0 & 0 & 0 \\ 0 & n & 0 & 0 \\ 0 & 0 & n & 0 \\ 0 & 0 & 0 & n+1 \end{pmatrix}, \tag{2.56}$$

and $E = (e_1 + e_2)\mathbf{1}_4$. As long as $e_1 + e_2 \neq 0$, this four-dimensional representation is reducible. To see this, we define the change-of-basis matrix

$$P = \begin{pmatrix} e_1+e_2 & 0 & 0 & 0 \\ 0 & e_2 & 1 & 0 \\ 0 & e_1 & -1 & 0 \\ 0 & 0 & 0 & 1 \end{pmatrix}, \tag{2.57}$$

which is invertible only for $e_1 + e_2 \neq 0$. In the new basis, the Casimir operator is diagonal with eigenvalues $C = \mathrm{diag}\{(e_1+e_2)(2n-1), (e_1+e_2)(2n-1), (e_1+e_2)(2n+1), (e_1+e_2)(2n+1)\}$, and the fermionic generators $\Psi^{\pm}$ read

$$\Psi^+ = \begin{pmatrix} 0 & 0 & 0 & 0 \\ e_1+e_2 & 0 & 0 & 0 \\ 0 & 0 & 0 & 0 \\ 0 & 0 & e_1+e_2 & 0 \end{pmatrix}, \quad \Psi^- = \begin{pmatrix} 0 & 1 & 0 & 0 \\ 0 & 0 & 0 & 0 \\ 0 & 0 & 0 & 1 \\ 0 & 0 & 0 & 0 \end{pmatrix}. \tag{2.58}$$

The bosonic (even) generator remain unchanged. These equations show that as long as $e_1 + e_2 \neq 0$, the tensor product representation $\langle e_1, n_1\rangle \otimes \langle e_2, n_2\rangle$ is reducible with the decomposition

$$\langle e_1, n_1\rangle \otimes \langle e_2, n_2\rangle = \langle e_1+e_2, n\rangle \oplus \langle e_1+e_2, n-1\rangle, \tag{2.59}$$

where we recall that $n \equiv n_1 + n_2 - 1$.

When $e_1 + e_2 = 0$, things become more complicated. First of all, the matrix (2.57) is no longer invertible, so the decomposition (2.59) does not hold anymore. It should also be noted that the Casimir operator has 4 degenerate eigenvalues 0, so knowing them is not enough to label typical representations. After a trivial change of basis, one finds the following expressions for the generators (we take $e_1 = -e_2 = 1$)

$$\Psi^+ = \begin{pmatrix} 0 & 0 & 0 & 0 \\ 1 & 0 & 0 & 0 \\ 0 & 0 & 0 & 0 \\ 0 & 0 & 1 & 0 \end{pmatrix}, \ \Psi^- = \begin{pmatrix} 0 & 0 & 1 & 0 \\ 0 & 0 & 0 & -1 \\ 0 & 0 & 0 & 0 \\ 0 & 0 & 0 & 0 \end{pmatrix}, \ N = \begin{pmatrix} n-1 & 0 & 0 & 0 \\ 0 & n & 0 & 0 \\ 0 & 0 & n & 0 \\ 0 & 0 & 0 & n+1 \end{pmatrix}, \tag{2.60}$$

and $E = 0$. It is straightforward to see that this four-dimensional representation is indecomposable, that is, that it cannot be decomposed as a direct sum anymore. It is not irreducible, as it contains invariant subrepresentations of dimension 1 and 2. It is also convenient to represent the structure of this representation, that we shall denote by $\mathcal{P}_n$, in terms of a diagram. The form of N tells us that $\mathcal{P}_n$ is made of one-dimension irreducibles (atypical representations) $\langle n-1\rangle, 2\langle n\rangle, \langle n+1\rangle$. The action of $\Psi^{\pm}$ relates

these four representations as follows

$$\langle 1, n_1\rangle \otimes \langle -1, n_2\rangle \equiv \mathcal{P}_{n\equiv n_1+n_2-1} = \qquad (2.61)$$

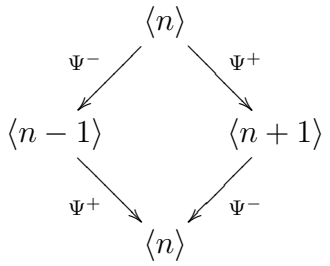

The Casimir operator

$$C = \begin{pmatrix} 0 & 0 & 0 & 0 \\ 0 & 0 & -2 & 0 \\ 0 & 0 & 0 & 0 \\ 0 & 0 & 0 & 0 \end{pmatrix} \qquad (2.62)$$

is non-diagonalizable and maps the top subquotient $\langle n\rangle$ to the bottom $\langle n\rangle$ in $\mathcal{P}_n$. Sometimes, it is also convenient to represent the structure of representations like $\mathcal{P}_n$, not in terms of irreducible atypicals, but in terms of the typicals that generically appeared as direct summands (see eq. (2.59)). For example, we have

$$\mathcal{P}_n = \qquad (2.63)$$

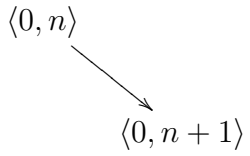

where $\langle 0, n\rangle$ is itself reducible (see eq. (2.54)). We remark in passing that the four-dimensional representation $\mathcal{P}_n$ is called *projective cover* of the atypical $\langle n\rangle$ (see Appendix A). Examples of application of these indecomposable representations to field theory will be given in the next section.

2.4 Indecomposability in field theory: the example of symplectic fermions

In order to illustrate the concepts of indecomposability and logarithmic operators on a concrete example, we discuss in this section some aspects of the *symplectic fermions* theory [51, 52]. As we shall see later on, it describes the scaling limit of the (twisted) XX spin chain, and is related to the critical behavior of dense polymers (self-avoiding walks). It is also believed to be closely related to abelian sand piles [35, 36], and it was proposed as the bulk theory for a quantum Hall state described by the Haldane-Rezayi wavefunction [88]. Much can be said about symplectic fermions, and we will focus in

this short section on a few salient ingredients relevant for our purpose. In particular, we will shall not address the relations between symplectic fermions, the $\beta\gamma$-ghosts system, and the $c = -2$ triplet model $\mathcal{W}(1,2)$; and we will also say next to nothing about the underlying $\mathcal{W}$ algebra structure of the theory. We refer the interested reader to the reviews [89, 90] (see also [66]).

2.4.1 Symplectic fermions

Let us work out in some details the continuum version of the so-called symplectic fermions theory [51, 52]. This theory has central charge $c = -2$, so it corresponds to $p = 2$ with our notations. This is a non-interacting theory, so the whole logarithmic structure can be worked out in details. Let us illustrate on this simple example how indecomposability arises. Our starting point will be the action

$$S[\theta^{\pm}] = \frac{1}{4\pi}\int \mathrm{d}^2 z J_{\alpha\beta}\partial_\mu\theta^\alpha\partial^\mu\theta^\beta = \frac{1}{\pi}\int \mathrm{d}^2 z\partial\theta^+\bar{\partial}\theta^-, \tag{2.64}$$

where $J_{\alpha\beta}$ in the inverse of the symplectic form $J^{+-} = -J^{-+} = -1$ so the model has a global $Sp(2)$ symmetry. However, the associated Noether currents of the form $\theta\partial\theta$ do not form a Kac-Moody algebra, because of the logarithmic structure of theory. In a non-unitary theory, continuous symmetry plus conformal invariance do not imply Kac-Moody symmetry in general. This is but one characteristic unpleasant features of Logarithmic CFTs. Instead, the theory admits generators of dimension 3 that form a $\mathcal{W}$-algebra [91].

This symplectic fermions theory seems quite similar to the analogous theory of a complex boson, but it has some crucial differences. A very important feature is that the partition function vanishes because of the fermionic zero modes (constant pieces) in the field $\theta^{\pm}$. More precisely, we can decompose

$$\theta^{\pm}(z,\bar{z}) = \theta_0^{\pm} + \psi^{\pm}(z,\bar{z}), \tag{2.65}$$

so that the partition function vanishes

$$Z = \int \mathcal{D}\theta^-\mathcal{D}\theta^+ \mathrm{e}^{-S[\theta^{\pm}]} = \int \mathcal{D}\psi^-\mathcal{D}\psi^+ \mathrm{d}\theta_0^+\mathrm{d}\theta_0^- \mathrm{e}^{-\frac{1}{\pi}\int \mathrm{d}^2 z\partial\psi^+\bar{\partial}\psi^-} = 0, \tag{2.66}$$

because of the Grassmannian rules of integration over the zero modes $\theta_0^{\pm}$. It is thus reasonable to define correlation functions as

$$\langle\mathcal{O}[\theta^{\pm}]\rangle \propto \int \mathcal{D}\theta^-\mathcal{D}\theta^+ \mathrm{e}^{-S[\theta^{\pm}]}\mathcal{O}[\theta^{\pm}]. \tag{2.67}$$

As a result, the expectation value of the identity field $\Omega = I$ vanishes $\langle\Omega\rangle = 0$, so that the vacuum $|\Omega\rangle$ is somewhat unusual as its norm is equal to zero $\langle\Omega|\Omega\rangle = 0$. We choose

the normalization so that the corresponding two-point function is

$$\langle \theta^+(z,\bar{z})\theta^-(w,\bar{w})\rangle = \log|z-w|^2 = \log(z-w)+\log(\bar{z}-\bar{w}). \tag{2.68}$$

In the following, we will restrict our study to the chiral sector and will forget about the antiholomorphic components. More explicitly, we rewrite eq. (2.68) as

$$\theta^+(z)\theta^-(0) \sim \omega + \log z\ \Omega, \tag{2.69}$$

where $\omega =: \theta^+\theta^- :$ is the normal ordered product of θ^+ and θ^-. We will argue shortly that ω is a logarithmic partner for the identity field Ω. We have

$$\langle\omega\rangle = \langle\theta_0^+\theta_0^-\rangle = 1. \tag{2.70}$$

Zero-modes must also be inserted explicitly in correlation functions involving derivatives of the fields $\theta^\pm$ in order to make them non-zero. The (holomorphic component of the) energy momentum tensor is also readily obtained

$$T(z) = \sum_{n\in\mathbb{Z}} \frac{L_n}{z^{n+2}} = -:\partial\theta^+\partial\theta^-:, \tag{2.71}$$

where we have used the usual fermionic normal order. The OPE of T with itself is consistent with a central charge $c=-2$

$$T(z)T(w) \sim \frac{-1}{(z-w)^4} + \frac{2T(w)}{(z-w)^2} + \frac{\partial T(w)}{z-w}. \tag{2.72}$$

The theory is obviously non-unitary as for example, $\langle T|T\rangle = -1 \leq 0$.

2.4.2 Hilbert space and zero-dimensional logarithmic operators

Following the usual quantization scheme, one expands $\theta^\pm(z) = \theta_0^\pm + \psi^\pm(z)$ in terms of fermionic modes

$$\psi^\pm(z) = -i\psi_0^\pm \log z + i\sum_{n\neq 0} \frac{\psi_n^\pm}{n} z^{-n} \tag{2.73}$$

with anti-commutators

$$\{\psi_n^+, \psi_m^-\} = n\delta_{n+m,0} \qquad \{\psi_0^\pm, \theta_0^\mp\} = \pm i, \tag{2.74}$$

the other anti-commutators vanish. Using the form of the stress-energy tensor, we can then express the Virasoro generators in terms of these modes

$$L_0 = \psi_0^+\psi_0^- + \sum_{m=1}^{\infty}(\psi_{-m}^+\psi_m^- - \psi_{-m}^-\psi_m^+), \qquad L_n = \sum_{m\in\mathbb{Z}} \psi_{n-m}^+\psi_m^-. \tag{2.75}$$

Logarithmic partner of the identity

The crucial feature here is the presence of a non-diagonalizable term in L_0. This term is responsible for the appearance of logarithms in correlation functions. Let us define the vacuum $|\Omega\rangle$ such that $\psi_m^\pm|\Omega\rangle = 0$ for $m \geq 0$ (recall that $\langle\Omega|\Omega\rangle = 0$). The creation modes are $\psi_{-m}^\pm$ $(m > 0)$ and $\theta_0^\pm$. There are thus four operators with dimension 0: $|\Omega\rangle$, $\theta_0^+|\Omega\rangle$, $\theta_0^-|\Omega\rangle$ and

$$|\omega\rangle = \theta_0^+\theta_0^-|\Omega\rangle\,. \tag{2.76}$$

The states $|\Omega\rangle$ and $|\omega\rangle$ are mixed into a Jordan cell for L_0

$$L_0|\omega\rangle = |\Omega\rangle\,. \tag{2.77}$$

There is no interesting logarithmic coupling to compute here as $|\Omega\rangle$ is already a primary and not a descendant. The coefficient that appears in front of the logarithmic term here is merely a question of convention. The corresponding OPEs are easily computed using Wick's theorem

$$\begin{aligned} T(z)\omega(0) &\sim \frac{\Omega}{z^2} + \frac{\partial\omega(0)}{z}, && (2.78a)\\ \theta^\pm(z)\omega(0) &\sim -\theta^\pm \log z, && (2.78b)\\ \omega(z)\omega(0) &\sim -2\log z\,\omega(0) - \log^2 z\,\Omega. && (2.78c) \end{aligned}$$

More explicitly, the logarithmic two-point functions read (see eq. (2.17))

$$\begin{aligned} \langle\Omega\Omega\rangle &= 0, && (2.79a)\\ \langle\omega(z)\Omega\rangle &= 1, && (2.79b)\\ \langle\omega(z)\omega(0)\rangle &= -2\log z. && (2.79c) \end{aligned}$$

All these equations are therefore consistent with the identification of ω as the logarithmic partner of the identity Ω. That said, it might be tempting to consider only derivatives such as $\partial\theta^\pm$ to get rid of the zero-modes and thus, of the logarithmic behavior. However, as was argued in [45] (see also the recent review [82]), the symplectic fermions theory at $c = -2$ must also contain another field $\mu(z)$ [15], with conformal dimension $h = -\frac{1}{8}$. Using the Kac table, one can identify μ as the Kac operator $\Phi_{1,2}$ with

15. It appears when considering antiperiodic boundary conditions for the fermions, the resulting new groundstate being then $|\mu\rangle = \lim_{z\to 0}\mu(z)|\Omega\rangle$.

dimension $h_{1,2} = -\frac{1}{8}$. The generic fusion of $\Phi_{1,2}$ contains the identity field and the primary $\Phi_{1,3}$, whose conformal dimension $h_{1,3}$ vanishes at $c = -2$. Using the appropriate differential equation for the Kac operator $\mu(z)$, one finds [45]

$$\langle \mu(z_1)\mu(z_2)\mu(z_3)\mu(z_4)\rangle = ((z_1-z_3)(z_2-z_4)\eta(1-\eta))^{1/4} \times \left(A\ {}_2F_1\left[\frac{1}{2},\frac{1}{2},1,\eta\right] + B\ {}_2F_1\left[\frac{1}{2},\frac{1}{2},1,1-\eta\right]\right), \quad (2.80)$$

where we used the same notations as in Sec.2.2.3. These hypergeometric functions contain logarithms in their Taylor expansions, and it is straightforward to check that the conformal blocks are consistent with the OPE (see Sec.2.2.3 for a similar computation at $c = 0$)

$$\mu(z)\mu(0) \sim z^{1/4}\left(\log z\ \Omega + \omega(0) + \dots\right). \quad (2.81)$$

Considering $\mu(z)$ thus forces us to include the logarithmic field ω, which should be considered as a mix of $\Phi_{1,1}$ and $\Phi_{1,3}$ at $c = -2$. In order to be consistent, it seems necessary to include ω in the theory, and there is no way around these logarithmic terms at $c = -2$.

$PSL(1|1)$ supersymmetry and indecomposability

As it turns out, the Jordan cells in the Hamiltonian L_0 are related to indecomposable representations of Lie superalgebras. To see this, let is first notice that the equations of motion state that the currents $J^{\pm} = \partial\theta^{\pm}(z,\bar{z})$ are holomorphic. They satisfy the following OPEs

$$J^+(z)J^-(0) \sim \frac{\Omega}{(z-w)^2}, \quad J^{\pm}(z)J^{\pm}(0) \sim 0, \quad (2.82)$$

where we recall that $\Omega = 1$ is the identity field. Their modes satisfy the relations $\{\psi_n^+, \psi_m^-\} = n\delta_{n+m,0}$ and $\{\psi_n^{\pm}, \psi_m^{\pm}\} = 0$ which can actually be interpreted as a realization of the affine Lie super algebra $\widehat{\mathfrak{psl}}(1|1)$. We will not go into more detail concerning the Kac-Moody $\widehat{\mathfrak{psl}}(1|1)$ algebra, but rather simply remark that the modes ψ_0^+ and ψ_0^- satisfy the anticommutation of the Lie superalgebra $\mathfrak{psl}(1|1)$

$$\{\psi_0^+, \psi_0^-\} = 0. \quad (2.83)$$

$\mathfrak{psl}(1|1)$ can be obtained from $\mathfrak{gl}(1|1)$ (see section 2.3) by considering two $\mathfrak{u}(1)$ quotients: the first one to factor out the elements with non-zero supertrace, and the other one to factor out the ideal spanned by the central generator E. Hence, it corresponds to $\mathfrak{gl}(1|1)$ with $E = N = 0$, and $\Psi^{\pm} = \psi_0^{\pm}$. We wish to emphasize here that the four fields with conformal weight $h = 0$ in the symplectic fermions theory can be organized into

a diamond-shaped indecomposable representation of $\mathfrak{psl}(1|1)$ (see section 2.3)

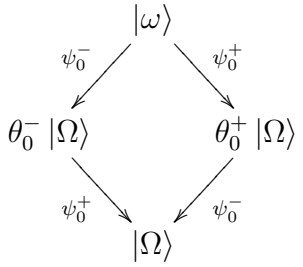

(2.84)

The Casimir operator $C = \psi_0^+ \psi_0^-$ in the basis $\{\theta_0^- |\Omega\rangle, |\omega\rangle, |\Omega\rangle, \theta_0^+ |\Omega\rangle\}$

$$C = \begin{pmatrix} 0 & 0 & 0 & 0 \\ 0 & 0 & 1 & 0 \\ 0 & 0 & 0 & 0 \\ 0 & 0 & 0 & 0 \end{pmatrix} \tag{2.85}$$

is non-diagonalizable and maps $|\omega\rangle$ onto $|\Omega\rangle$. Note that this is precisely the non-diagonalizable term that appears in L_0 (2.75), so this non-diagonalizability of the theory can thus be understood in terms of the properties of the superalgebra (2.83).

2.4.3 A first step towards Virasoro staggered modules

It is an interesting and straightforward exercise to construct the Jordan cells associated with excited states in the holomorphic sector. For example, the first fermionic excitations over the vacuum can be organized as follows [16]

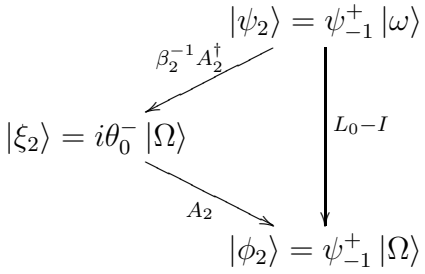

(2.86)

where the arrows now represent the action of the holomorphic Virasoro generators just as in (2.24), and $A_2 = L_{-1}$. As far as logarithmic operators and indecomposability parameters are concerned, we will use the notations of section 2.1.3. Actually, this picture is not complete but things will become more precise as we go on. This will lead us to the concept of Virasoro staggered module. At this stage, we will only consider the arrows as a schematic way to show the action of some Virasoro generators, as in eq. (2.24), and not as an accurate way to give the structure of a representation like we

16. We remind that reader we restrict our study to the holomorphic sector, that is, we do not consider the action of the antiholomorphic Virasoro generators $\bar{L}_n$.

did in section 2.3. In the basis $\{|\phi_2\rangle,|\psi_2\rangle\}$, the Hamiltonian reads

$$L_0 = \begin{pmatrix} 1 & 1 \\ 0 & 1 \end{pmatrix}, \tag{2.87}$$

this explains the vertical arrow in (2.86). A short calculation shows that

$$A_2 |\xi_2\rangle = L_{-1} i\theta_0^+ |\Omega\rangle = \psi_{-1}^+ |\Omega\rangle = |\phi_2\rangle , \tag{2.88}$$

this explains the normalization of the operator $|\xi_2\rangle = i\theta_0^+ |\omega\rangle$. We are now ready to compute the associated (algebraic) indecomposability parameter that we shall denote β_2. We find

$$L_1 |\psi_2\rangle = L_1 \psi_{-1}^+ \omega = - |\xi_2\rangle , \tag{2.89}$$

which gives, using eq. (2.23) ,

$$\beta_2 = -1. \tag{2.90}$$

This is consistent with the number that was computed [46]. Note that this coefficient can also be computed using the Virasoro bilinear form $(\psi_m^\pm)^\dagger = \psi_{-m}^\mp$.

Other indecomposability parameters can be computed in a similar fashion although the calculations are slightly more complicated. For example, the next excited states have the following structure

$$\begin{array}{ccc} & |\psi_3\rangle = \psi_{-2}^+ \psi_{-1}^+ |\omega\rangle & \\ {\scriptstyle \beta_3^{-1} A_3^\dagger} \swarrow & & \\ |\xi_3\rangle = \frac{i}{3} \psi_{-1}^+ \theta_0^- |\Omega\rangle & & \downarrow {\scriptstyle L_0 - 3I} \\ {\scriptstyle A_3} \searrow & & \\ & |\phi_3\rangle = \psi_{-2}^+ \psi_{-1}^+ |\Omega\rangle & \end{array} \tag{2.91}$$

where $A_3 = L_{-1}^2 - 2L_{-2}$ [17]. The dimension 1 operator $|\xi_3\rangle = \frac{i}{3}\psi_{-1}^+ \theta_0^+ |\Omega\rangle$ has been normalized such that $A_3 |\xi_3\rangle = |\phi_3\rangle$. $|\psi_3\rangle$ is the logarithmic partner of the null field $|\phi_3\rangle$. Finally, a straightforward calculation shows that

$$(L_1^2 - 2L_2) |\psi_3\rangle = (-18) |\xi_3\rangle , \tag{2.92}$$

which yields

$$\beta_3 = -18. \tag{2.93}$$

17. Note that we do not use the normalization given by eq. (2.21) in order to be consistent with [46].

It should seem clear that in principle, all the logarithmic couplings (indecomposability parameters) could be computed in a similar way. However, there is no clear lesson in this calculation that one could use to tackle more complicated, interacting theories.

Some indecomposable Virasoro representations at $c = -2$

Actually, the fields $|\phi_2\rangle$ and $|\psi_2\rangle$ (or $|\phi_3\rangle$ and $|\psi_3\rangle$) belong to more complicated, indecomposable, Virasoro representations that are called staggered modules. We will define more precisely how they are constructed in the next section, but for the moment, let us try to reformulate our previous results using a more accurate mathematical language. The L_0 Jordan cells constructed in the previous paragraphs correspond to infinite dimensional Virasoro modules $\mathcal{P}_j$, with a diamond structure

$$\mathcal{P}_j = \begin{array}{ccccc} & & h_{j,1} & & \\ & \swarrow & & \searrow & \\ h_{j-1,1} & & & & h_{j+1,1} \\ & \searrow & & \swarrow & \\ & & h_{j,1} & & \end{array} \quad = \quad \begin{array}{ccccc} & & \psi_j & & \\ & \swarrow & & \searrow & \\ \xi_j & & & & \rho_j \\ & \searrow & & \swarrow & \\ & & \phi_j & & \end{array} \quad . \tag{2.94}$$

This diagram now has the same meaning as that of eq. (2.61), except that the algebra under scrutiny in (2.94) is Virasoro and not $\mathfrak{gl}(1|1)$. The arrows thus represent the action of the Virasoro generators, and the nodes correspond Virasoro simple (irreducible) modules, which are themselves infinite dimensional. This contrasts with (2.61) where the subquotients were one-dimensional. Simple (irreducible) Virasoro modules in (2.94) are denoted by their conformal weights, or by the corresponding quantum fields ψ_j, ϕ_j, ξ_j and ρ_j. Only the field ρ_j is new in our discussion, its role will be discussed further in Sec. 2.5. To understand more this structure, we are going to need a few algebraic tools of Virasoro representation theory that will be given in the next section. At this point, one should really think of (2.94) as the analog of (2.61) for the Virasoro algebra.

The indecomposable modules $\mathcal{P}_j$ are completely characterized by the indecomposability parameters β_j, and each module corresponds to a Jordan cell

$$\begin{aligned} L_0 |\phi_j\rangle &= h_{j,1} |\phi_j\rangle , && \text{(2.95a)} \\ L_0 |\psi_j\rangle &= h_{j,1} |\psi_j\rangle + |\phi_j\rangle , && \text{(2.95b)} \\ |\phi_j\rangle &= A_j |\xi_j\rangle && \text{(2.95c)} \\ A_j^\dagger |\psi_j\rangle &= \beta_j |\xi^j\rangle . && \text{(2.95d)} \end{aligned}$$

We normalize the operators A_j such that $A_j = L_{-1}^{j-1} + \ldots$, unlike in our previous examples, $A_2 = L_{-1}$ and $A_3 = L_{-1}^2 - 2L_{-2}$. This normalization is convenient and customary for $c = -2$. With this convention, the associated indecomposability parameters have been conjectured to be [71]

$$\beta_j = -\frac{[(2j-3)!]^2}{4^{j-2}}(j-1), \quad j \in \mathbb{N} \setminus \{0,1\}. \tag{2.96}$$

2.5 Indecomposable Virasoro representations

Let us conclude this first introductory chapter by addressing the main feature of Logarithmic CFTs: indecomposable Virasoro representations. We have already seen in the previous sections how logarithms were related to indecomposability, but it is now time to make things more concrete and provide some examples of Virasoro representations with a non-diagonalizable action of the Virasoro zero-mode L_0. Before doing so, we first recall some well-known facts about Verma modules, and introduce some notations that shall be used extensively throughout the remainder of this manuscript. We then introduce the special class of Virasoro staggered modules and relate them to indecomposability parameters. We conclude this last section with a very short discussion of fusion algorithms for Virasoro modules.

2.5.1 Virasoro algebra and Verma modules

Our starting point will be the Virasoro algebra $\mathfrak{vir}$

$$[L_n, L_m] = (n-m)L_{n+m} + \frac{c}{12}n(n^2-1)\delta_{n+m,0}, \tag{2.97}$$

and we will take $c \in \mathbb{R}$. Strictly speaking, the central charge is rather a central element that can be taken to be a constant in a given representation, but we will take it to be a parameter of the algebra from the very beginning. We will denote by $\mathfrak{vir}^{\pm}$ the subalgebras spanned by the modes L_n with n positive or negative. The Virasoro bilinear form (also called Shapolanov form) is defined by $L_n^\dagger = L_{-n}$ and is extended antilinearly to the whole algebra.

Verma modules form an especially important class of Virasoro representations. As often in physics, they are constructed from highest-weight vectors. A highest-weight vector $|\phi_h\rangle$ is defined as an eigenstate of L_0 which is annihilated by the elements of $\mathfrak{vir}^+$ [18]. In field theory, eigenstates can be obtained by letting primary operators act on the vacuum $|\phi_h\rangle = \lim_{z\to 0}\phi_h(z)|0\rangle$. A Verma module $\mathcal{V}_h$ is then simply defined by letting the lowering part of the Virasoro algebra $\mathfrak{vir}^-$ act freely on a highest weight state $|\phi_h\rangle$. A Verma module $\mathcal{V}_h$ therefore contains all the 'descendants' of $|\phi_h\rangle$

$$\mathcal{V}_h = \{L_{-n_1}\dots L_{-n_k}|\phi_h\rangle\,,\ n_1 \geq \dots \geq n_k,\ k \in \mathbb{N}^\star\}. \tag{2.98}$$

It is also convenient to represent the conformal spectrum (operator content) of modules thanks to characters $\mathrm{Tr} q^{L_0-c/24}$. Characters will be used extensively throughout this thesis as they allow to manipulate functions instead of complicated representations. In the case of a Verma module, we have

$$\mathrm{Tr}_{\mathcal{V}_h} q^{L_0-c/24} = \frac{q^{-c/24}}{P(q)}q^h, \tag{2.99}$$

18. Actually, it is straightforward to show that $L_1|\phi_h\rangle = L_2|\phi_h\rangle = 0$ is enough to imply that $\mathfrak{vir}^+|\phi_h\rangle = 0$.

with

$$P(q) \equiv q^{-1/24}\eta(q) \equiv \prod_{n=1}^{\infty}(1-q^n). \tag{2.100}$$

2.5.2 Verma modules theory

We follow here [61] and the introduction of Ref. [59].

Singular vectors and Kac determinant

It is important to realize that Verma modules are not always irreducible. It may happen that among the descendants of $|\phi_h\rangle$, there are other eigenvectors of L_0, not proportional to $|\phi_h\rangle$, which are also annihilated by $\mathfrak{vir}^+$. These are referred to as 'singular vectors' or null vectors. If such a singular vector $|s\rangle = (L_{-n} + \dots)\,|\phi_h\rangle$ does exist at grade n (that is, with conformal weight $h+n$), then it generates a submodule isomorphic to $\mathcal{V}_{h+n}$ and $\mathcal{V}_h$ is obviously reducible. Singular vectors therefore allow to probe the rather intricate indecomposable structure of Verma modules. From a practical point of view, calculations are done by noticing that a singular vector $|s\rangle$ (and its descendants) are orthogonal to the whole Verma module as

$$\langle s|U\phi_h\rangle = \left\langle sU^\dagger|\phi_h\right\rangle = 0, \tag{2.101}$$

for any descendant $U\,|\phi_h\rangle \in \mathcal{V}_h$, where $U = L_{-n_1}\dots L_{-n_k}$ is (a bit pedantically) an element of the universal enveloping algebra of $\mathfrak{vir}^-$. In particular, $\langle s|s\rangle = 0$. The Virasoro bilinear form $\langle .|.\rangle$ is therefore non-degenerate on a Verma module $\mathcal{V}_h$ if and only if $\mathcal{V}_h$ is irreducible. Hence, it is of the utmost interest to analyze the zeros of $\langle .|.\rangle$, and in particular, its determinant $\det\langle .|.\rangle$ on a given Verma module $\mathcal{V}_h$.

General structure of Verma modules

The zeros of this so-called Kac determinant were conjectured by Kac [92], and proved by Feigen and Fuchs [93]. This analysis shows that something happens when h has the form given by the Kac formula (2.26), with r and s positive integers. The resulting structure of the Verma modules can be separated in four cases: point, link, chain and braid (see Tab. 2.2). We will restrict ourselves to $c \leq 1$ in this thesis. Let us shortly remind the reader when these cases occur:

- **Point.** If $h \neq h_{r,s}$ for every positive integers r, s, then the Verma module $\mathcal{V}_h$ is irreducible.
- **Link.** If the central charge is generic, that is if $p \notin \mathbb{Q}$, and if there exist $r, s \in \mathbb{N}^\star$ (unique) such that $h = h_{r,s}$, then the Verma module $\mathcal{V}_h$ is reducible and has a singular vector with conformal weight $h_{r,-s} = h_{r,s} + rs$. The maximal proper submodule is therefore isomorphic to $\mathcal{V}_{h_{r,-s}}$.

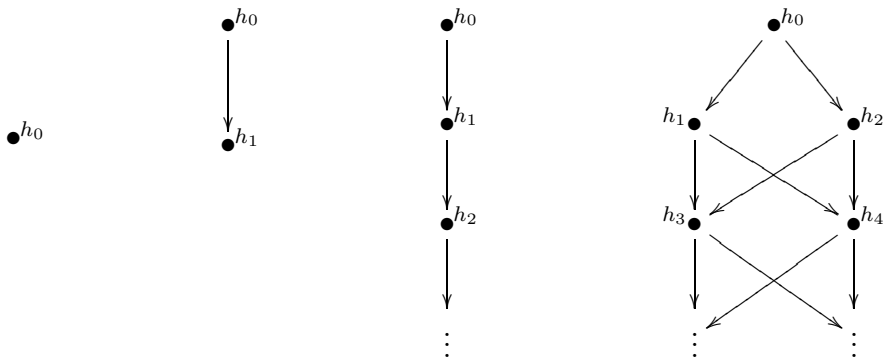

Point Link Chain Braid

Table 2.2: Subquotient structures of Verma modules for $c \leq 1$. The black dots correspond to Virasoro irreducible modules, and arrows represent (negative) Virasoro modes action. Alternatively, one can think of the black dots as representing singular vectors, each one generating a proper submodule of the original Verma modules by keeping the dots and arrows emanating from it.

- **Chain.** Suppose that $p \in \mathbb{N}^\star$ in eq. (2.25). Then [19] if there exist $r, s \in \mathbb{N}^\star$ such that $h = h_{r,s}$ and $p+1|s$ or $p|r$, $\mathcal{V}_h$ is reducible just like in the link case but the maximal proper submodule is itself reducible with a chain structure. The structure is therefore found iteratively and the singular vectors have a chain structure as in Tab. 2.2.
- **Braid.** Let $p \in \mathbb{N}^\star$. If there exist $r, s \in \mathbb{N}^\star$ such that $h = h_{r,s}$, and $p+1 \not| s$ and $p \not| r$, then $\mathcal{V}_h$ has a braid (or ladder) subquotient structure as in Tab. 2.2.

Kac modules

When $r, s \geq 1$ are positive integers, the Verma module $\mathcal{V}_{h_{r,s}}$ is reducible with a singular vector at level (grade) rs with conformal weight $h_{r,-s} = h_{r,s} + rs$. We then define a Kac module as the quotient $\mathcal{K}_{r,s} \equiv \mathcal{V}_{h_{r,s}}/\mathcal{V}_{h_{r,-s}}$. The Kac modules $\mathcal{K}_{r,s}$ are irreducible if the central charge is generic (link case for the Verma module $\mathcal{V}_{h_{r,s}}$). The character of the Kac module $\mathcal{K}_{r,s}$ reads

$$\mathrm{Tr}_{\mathcal{K}_{r,s}} q^{L_0 - c/24} = \frac{q^{-c/24}}{P(q)} \left(q^{h_{r,s}} - q^{h_{r,-s}} \right). \tag{2.102}$$

The corresponding quantum operators in field theory are what we called Kac operators in Sec. 2.2.1. Kac modules and Kac operators are in fact very natural in CFT. A well-known example is for example the identity operator I, associated with the Kac module

19. Strictly speaking, this case also arises for $p \in \mathbb{Q}$, but we will focus on the case p integer for the sake of simplicity.

$\mathcal{K}_{1,1} \equiv \mathcal{V}_{h_{1,1}=0}/\mathcal{V}_{h_{1,-1}=1}$. The quotient in that case corresponds to the invariance under translations of the vacuum $L_{-1}I = \partial I = 0$.

Simple (irreducible) modules

By quotienting proper submodules out of reducible Verma modules, one eventually ends up with irreducible representations. These are denoted by $\mathcal{X}_h$, or sometimes simply by their conformal weight h. It is important to realize that the simple (or irreducible) module $\mathcal{X}_h$ appears at the top in the subquotient structure of the corresponding Verma module $\mathcal{V}_h$. CFT Minimal models are built out of such irreducible representations, which do not contain any singular vector. Singular vectors are always quotiented out in ordinary minimal CFTs, whereas they are actually crucial in the context of LCFT. The corresponding characters for the irreducible modules $\mathcal{X}_{h_{r,s}}$ associated with minimal models ($1 \leq r \leq p-1$, $1 \leq s \leq p$) are given by the Rocha-Caridi formula [61, 94]

$$\mathrm{Tr}_{\mathcal{X}_{r,s}} q^{L_0 - c/24} = \frac{q^{-c/24}}{P(q)} \left[q^{h_{r,s}} + \sum_{k=1}^{\infty} (-1)^k \times \left(q^{h_{r+kp,(-1)^k s + (1-(-1)^k)(p+1)/2}} + q^{h_{r,k(p+1)+(-1)^k s + (1-(-1)^k)(p+1)/2}} \right) \right]. \quad (2.103)$$

This formula is obviously obtained from the braid (or ladder) structure of the corresponding Verma module $\mathcal{V}_{h_{r,s}}$.

2.5.3 Virasoro staggered modules and indecomposability parameters

Whereas for minimal models, irreducible representations are all one has to worry about, LCFTs involve much more complicated, indecomposable representations. As we have seen previously, the appearance of logarithms in correlation function is related to the non-diagonalizability of the L_0 operator. It is therefore of the utmost importance to understand more the structure of Virasoro representations with Jordan cells in the Hamiltonian L_0.

Staggered modules

The simplest class of such representations are called *staggered modules*. They were introduced in [49] and fully classified in by Ridout and Kytola [59]. These modules are especially important as they encompass all the rank-2 L_0 Jordan cells that we have encountered so far, and they will play a crucial role in the following chapters of this thesis as well. Note also that in this more algebraic language, the (algebraic) indecomposability parameters (see section 2.1.3) can be thought of as characterizing the structure of these staggered modules.

We will not give a detailed account of the theory of staggered modules here, neither will we give precise mathematical statements regarding their existence and uniqueness. We will only need the fact that staggered modules can be defined as a gluing of two

highest-weight modules (quotient of Verma modules), with a non-diagonalizable action of L_0. The precise definition requires exact sequences, but we will find it more convenient and more enlightening to give explicit examples in the following rather than going into general definitions [20]. Staggered modules are reducible but indecomposable by definition, with, in the case relevant to us, a diamond-shaped structure

$$\mathcal{P} = \begin{array}{ccccc} & & h_\psi & & \\ & \swarrow & & \searrow & \\ h_\xi & & & & h_\rho \\ & \searrow & & \swarrow & \\ & & h_\phi = h_\psi & & \end{array} \quad . \tag{2.104}$$

Conformal weights in this diagram represent Virasoro irreducible (simple) modules, whereas the arrows correspond to the action of Virasoro generators. Hence, the whole module can be induced by action of the L_n's on the state $|\psi\rangle$ while the module generated from the null vector $|\phi\rangle$ belongs to an invariant submodule. We use here the same notations as in sec. 2.1.3, so the null field ϕ is actually a descendant of the primary field ξ ($L_{n>0}\,|\xi\rangle = 0$), with conformal weight $h_\xi \leq h = h_\phi = h_\psi$. Just as in 2.1.3, we will write $|\phi\rangle = A\,|\xi\rangle$, where A is fixed (up to a global normalization) by the null vector condition $L_1\,|\phi\rangle = L_2\,|\phi\rangle = 0$. The submodule generated by the action of the Virasoro generators on ξ has a link structure, and, in the case that we will encounter, it will typically be a Kac module. The quotient of $\mathcal{P}$ by this submodule is itself a Kac module with a link structure, with proper submodule generated by $|\rho\rangle$. The staggered module (2.104) can thus be considered as a gluing of two Kac modules with a link structure, with a non-diagonalizable action $L_0\,|\psi\rangle = h\,|\psi\rangle + |\phi\rangle$. Finally, note that the staggered module $\mathcal{P}$ is uniquely characterized by the indecomposability parameter $\beta \equiv \langle\phi|\psi\rangle$.

An example of explicit construction: Logarithmic Ising model

Let us illustrate these formal considerations by a more concrete example. We revisit [21] here the Jordan cell for the Ising model discussed in Sec. 2.2.2. Instead of using field theory arguments and OPEs, we analyze the existence of this Jordan cell using only the Virasoro algebra representation theory. First recall that at $c = \frac{1}{2}$, the Verma modules $\mathcal{V}_{1/2}$ and $\mathcal{V}_{5/2}$ have a braid structure (see Tab. 2.2). We then consider

20. We refer the reader to the thorough study [59] for more precise statements.

21. The following paragraph is (strongly) inspired from notes written jointly by the author and Azat M. Gainutdinov.

the gluing

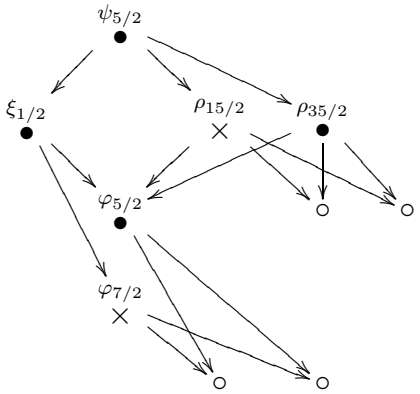

(2.105)

where the subscripts denote the conformal dimensions. In this paragraph, we will not use the Dirac BraKet notations for the states as no confusion between states and fields is possible. We note that down-right arrows correspond to the action of negative Virasoro generators while down-left arrows direction correspond to action of L_n's with positive n. Meanwhile, the crosses $\times$ denote the singular vectors that we will set to zero in order to get a staggered module [22].

We thus wish to take a quotient of this module by the submodules generated from the vectors $\rho_{15/2}$ and $\varphi_{7/2}$, denoted by crosses $\times$ in the diagram (2.105), to obtain a module that we will call $\mathcal{P}(\frac{1}{2},\frac{5}{2})$, if it is possibe, with the subquotient structure

$$\mathcal{P}(\tfrac{1}{2},\tfrac{5}{2}) \quad = \quad \begin{array}{ccc} & \psi_{5/2} & \\ \swarrow & & \searrow \\ \xi_{1/2} & & \rho_{35/2} \\ \searrow & & \swarrow \\ & \varphi_{5/2} & \end{array} \tag{2.106}$$

The associated indecomposability parameter reads

$$\beta = \langle \xi_{\frac{1}{2}} | A^\dagger \psi_{\frac{5}{2}} \rangle, \tag{2.107}$$

where $A = L_{-2} - \frac{3}{4}L_{-1}^2$ and $A\xi_{\frac{1}{2}} = \varphi_{\frac{5}{2}}$.

Following [59], we will admit that the necessary and sufficient condition for the existence of the module (2.106) is for the vector $\rho_{15/2}$ to be a singular vector, *i.e.* the arrow representing the action of the positive modes $L_{\geq 0}$ in the diagram (2.105) should actually be absent. This happens only for a particular value of the indecomposability parameter β that is a solution of the system of linear equations produced by the condition

$$L_1\rho_{15/2} = L_2\rho_{15/2} = 0. \tag{2.108}$$

22. To be more explicit, the crosses represent eigenvectors of L_0 that should be annihilated by positive Virasoro modes $L_{>0}$.

To solve the equations (2.108), we need to obtain an appropriate ansatz for the state $\rho_{15/2}$ and to express the action of positive Virasoro modes on the top vector $\psi_{5/2}$. Using the freedom in the definition of $\psi_{5/2}$ – we can add vectors from the bottom part at the same dimension $h = 5/2$ and this does not affect the value of β – we can fix the action of L_1 to be zero. Then, using the definition of β

$$A^\dagger \psi_{5/2} = \left(L_2 - \frac{3}{4} L_1^2 \right) \psi_{5/2} = \beta \xi_{1/2}, \tag{2.109}$$

we get the action of L_2

$$L_1 \psi_{5/2} = 0, \qquad L_2 \psi_{5/2} = \beta \xi_{1/2}. \tag{2.110}$$

We next choose an ansatz for the state $\rho_{15/2}$. In the Verma module $\mathcal{V}_{h_{1,5}=5/2}$, the state $\rho_{15/2}$ is a null descendant $\rho_{15/2} = B_{1,5}\psi_{5/2}$ where $B_{1,5}$ is given by the general formula (see *e.g.* [61])

$$B_{1,r} = \sum_{\substack{\{l_j \,|\, l_j \geq 1, \\ l_1 + \cdots + l_k = r\}}} (-1)^{r+k} \frac{\big((r-1)!\big)^2 \, (p/p+1)^{r-k}}{\prod_{j=1}^{k-1} (l_1 + \cdots + l_j)(r - l_1 - \cdots - l_j)} L_{-l_1} \dots L_{-l_k}, \qquad r \in \mathbb{N} \tag{2.111}$$

which generates the singular vector at level r in the Verma module corresponding to Kac labels $(1, r)$ – recall also that p parametrizes the central charge, and $p = 3$ for the Ising model. The sum in this formula is taken over all possible ordered partitions of the integer r (for example, the partitions $1 + 2$ and $2 + 1$ are different and both give a contribution to the sum).

It is important to notice that in the module (2.106), $\rho_{15/2}$ can also be a descendant of $\xi_{1/2}$, so that we choose the ansatz

$$\begin{aligned} \rho_{15/2} = B_{1,5}\psi_{5/2} + \big(& a_1 L_{-7} + a_2 L_{-6} L_{-1} + a_3 L_{-5} L_{-2} + a_4 L_{-5} L_{-1}^2 + a_5 L_{-4} L_{-3} \\ & + a_6 L_{-4} L_{-2} L_{-1} + a_7 L_{-3}^2 L_{-1} + a_8 L_{-3} L_{-2}^2 + a_9 L_{-3} L_{-2} L_{-1}^2 + a_{10} L_{-2}^3 L_{-1} \big) \xi_{1/2}, \end{aligned} \tag{2.112}$$

where we have used the constraint $L_{-1}^3 = 3L_{-2}L_{-1} - 3/4 L_{-3}$ following from the null-vector condition $\varphi_{7/2} = B_{1,3}\xi_{1/2} = 0$.

Using all this, it is now quite straightforward to calculate the unique value of β compatible with the existence of $\mathcal{P}(\frac{1}{2}, \frac{5}{2})$. In order to do so, one should solve equations (2.108) using (2.112) and (2.110). After some calculations, we find this way all the coefficients in (2.112) $a_1 = \frac{205}{8}$, $a_2 = -55$, $a_3 = 78$, $a_4 = -\frac{521}{16}$, $a_5 = -\frac{1035}{32}$, $a_6 = \frac{255}{8}$, $a_7 = \frac{525}{16}$, $a_8 = -18$, $a_9 = -\frac{21}{4}$, and $a_{10} = 0$ and we finally get $\beta = -35/24$ which coincides with the value obtained from the OPE 'limit' approach (see section 2.2.2). It is quite remarkable that these two very different approaches, yield the same result. The first one, based on OPEs and limit arguments, is probably more physical, but it is reassuring to see that indecomposability parameters are actually completely fixed [23]

23. Actually, this is not always the case. For example, at $c = -2$ the representation theory of Vira-

by Virasoro representation theory.

Logarithmic partner of $T(z)$ at $c = 0$ revisited

Let us also come back to the Jordan cell for the stress energy tensor $T(z)$ at $c = 0$ discussed in section 2.2.1. Using our notations, we have $T = \varphi_2$, and $t = \psi_2$. It is now well understood (see also 2.2.1) that there are (at least) two possibilities for the associated indecomposability parameter, which correspond to two fundamentally different theories: percolation and dilute polymers (SAWs).

The Jordan cell in percolation theory involves the field $t = \psi_2$ with conformal weight $h_{1,5} = 2$ at the top. We have to set ρ_7 (at level $rs = 5$) to zero in its Verma module in order to construct the corresponding staggered module. We have the following structure

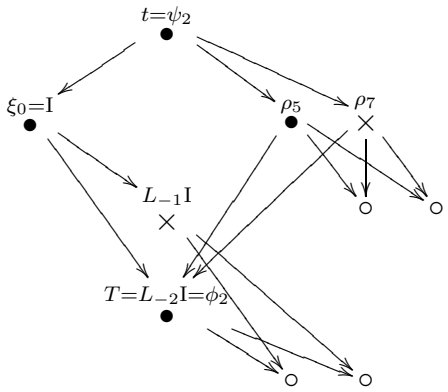

(2.113)

Using the same method as described above, we find that $\beta = -\frac{5}{8}$, in agreement with the OPE argument of Sec. 2.2.1. This calculation was done first in [57]. The calculation also yields the following expression for the null-state ρ_7:

$$\rho_7 = B_{1,5}\psi_{1,5} + \big(10L_{-7} + \frac{376}{9}L_{-5}L_{-2} - \frac{16}{3}L_{-4}L_{-3} - \frac{128}{9}L_{-3}L_{-2}^2\big)\xi_0, \qquad (2.114)$$

where $B_{1,5}$ is given by (2.111). In the polymer case, $t = \psi_2$ corresponds to the conformal

soro allows for families of staggered modules parametrized by continuous values of β. The symplectic fermions studied in the previous section are just one realization of a $c = -2$ theory, with a given set of indecomposability parameters (2.96). The Abelian sandpile model is yet another example that is believed to be characterized by different indecomposability parameters [95, 96].

weight $h_{3,1} = 2$, and the staggered module is

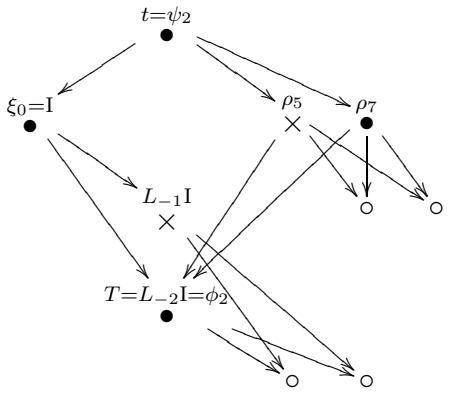

(2.115)

where this time, we factor out ρ_5 at level $rs = 3$. We find $\beta = \frac{5}{6}$, as expected, and the null-vector is

$$\rho_5 = B_{3,1}\psi_{3,1} + \big(3L_{-3}L_{-2} - 2L_{-5}\big)\xi_0, \tag{2.116}$$

where $B_{3,1}$ is again given by (2.111) but with the substitution $p/p+1 \to p+1/p$.

Remark on bulk indecomposable modules

In the case of bulk (or non-chiral) CFTs, the relevant algebra is $\mathfrak{vir}\oplus\overline{\mathfrak{vir}}$, where $\overline{\mathfrak{vir}}$ is isomorphic to $\mathfrak{vir}$, with generators $\bar{L}_n$. It is worth mentioning that despite the fact that $\big[L_n, \bar{L}_m\big] = 0$, indecomposable representations of $\mathfrak{vir}\oplus\overline{\mathfrak{vir}}$ are even more complicated as holomorphic and holomorphic sectors can be glued together, see *e.g.* [97] for examples of such modules. We will come back to this question in Sec. 4.2.

2.5.4 A word on fusion

A fundamental question about (L)CFTs is to determine the Operator Product Expansions of their quantum fields. Thanks to conformal symmetry, the OPEs are essentially determined by the fusion rules that capture their global structure. We conclude this last section by shortly mentioning the existence of fusion algorithms to compute the fusion of indecomposable Virasoro modules. It is important to realize that whereas for ordinary CFT – where representations are irreducible (or completely reducible) – one can consider fusion as an operation on primary fields, fusion for Logarithmic CFTs should rather be considered as a mathematical operation on representations. We will see how to compute fusion rules from lattice models in the next chapters, but fusion of Virasoro (indecomposable) modules can also be computed directly in the continuum (conformal) limit using the so-called Nahm–Gaberdiel-Kausch [46, 98] algorithm, a method based on the comultiplication of Virasoro generators [99]. This approach was applied to many (chiral) LCFTs like percolation with success [56–58].

Chapter 3

From the Temperley-Lieb algebra to Virasoro: indecomposability in lattice models

Much progress in the understanding of Logarithmic CFT has been obtained by studying algebraic features of their lattice regularizations. For reasons which are not entirely understood, the non semi-simple associative algebras underlying some lattice models – such as the Temperley–Lieb algebra – indeed exhibit, in finite size, properties that are in full correspondence with those of their continuum limits. This applies to the structure of indecomposable modules, but also to fusion rules, and provides an 'experimental' way of measuring couplings, such as the 'number b' quantifying the logarithmic coupling of the stress energy tensor with its partner.

In this chapter, we review the salient aspects of this approach, relying heavily on [69] and [71, 72] (see also the recent review [73]), and describe how fusion and indecomposability parameters can be extracted from lattice models. The outline is as follows. In section 3.1, we introduce the Temperley-Lieb algebra and some lattice models related to it (XXZ spin chain, dense loop models, SUSY chains). We then describe the symmetries of these models and show how to use representation theory to obtain the decomposition of the space of states ("Hilbert" space) in section 3.2. The consequences of this decomposition in the scaling limit are discussed in Sec. 3.3, and we argue that the structure of indecomposable representations can be obtained directly from the lattice. Finally, we explain how to measure indecomposability parameters and how to compute fusion rules in sections 3.4 and 3.5.

3.1 Temperley-Lieb algebra, XXZ spin chain, loop models and supersymmetry

In this first section, we introduce the Temperley-Lieb algebra and some of its physical representations, corresponding to lattice models with open boundary conditions. The spin-1/2 XXZ spin chain, the Potts model and supersymmetric vertex models are

discussed within this algebraic context. We also mention the analogous 'dilute' models (spin-1 XXZ spin chain, $O(n)$ model *etc.*). In the next sections, we will argue that all these lattice models provide regularizations of interesting boundary (chiral) LCFTs.

3.1.1 Temperley-Lieb algebra, transfer matrix and Hamiltonian

All the lattice models that we shall study throughout this section can be constructed as representations of the so-called Temperley-Lieb (TL) algebra $TL_{\mathfrak{q},L}$ defined on $L = 2N$ strands. Unless otherwise stated, we will consider $N \in \mathbb{N}$ so that L is even. The algebra $TL_{\mathfrak{q},L}$ consists of all the words written with the $L-1$ generators e_i, subject to the relations

$$\begin{aligned} [e_i, e_j] &= 0, \qquad |i-j| \geq 2, && (3.1)\\ e_i^2 &= n e_i, && (3.2)\\ e_i e_{i\pm 1} e_i &= e_i, && (3.3) \end{aligned}$$

with

$$n = \mathfrak{q} + \mathfrak{q}^{-1} = 2\cos\gamma, \tag{3.4}$$

and $\mathfrak{q} = \mathrm{e}^{i\gamma}$. For reviews on the TL algebra, see [100, 101].

The TL algebra can be thought of as an algebra of diagrams [100]. Using the notation

$e_i =$ 

the equations (3.1)-(3.3) can now be interpreted geometrically, the composition law corresponding to stacking the diagrams of the e_i's where it is assumed that every closed loop carries a weight n, henceforth called the fugacity of a loop (see Fig. 3.1). This constructs what we shall refer to as the loop or adjoint representation.

We consider two-dimensional models [1] defined by the transfer matrix

$$T = \prod_{i=1}^{N-1} \left(p_B + (1-p_B)\ e_{2i}\right) \prod_{i=1}^{N} \left((1-p_A) + p_A\ e_{2i-1}\right), \tag{3.5}$$

which acts on a given TL representation. This definition is valid for $L = 2N$ even but it can be readily adapted to an odd number of sites. We will mainly work with three different representations: geometrical (loop), XXZ, and supersymmetric. Using the geometrical representation of $TL_{2N}(q)$, we obtain a dense loop model, where each

1. See [102] for an example of study of $3D$ loop model, which should show logarithmic features as well. For simplicity, we will focus mostly on two-dimensional models in the remainder of this thesis, with the notable exception of chapter 5.

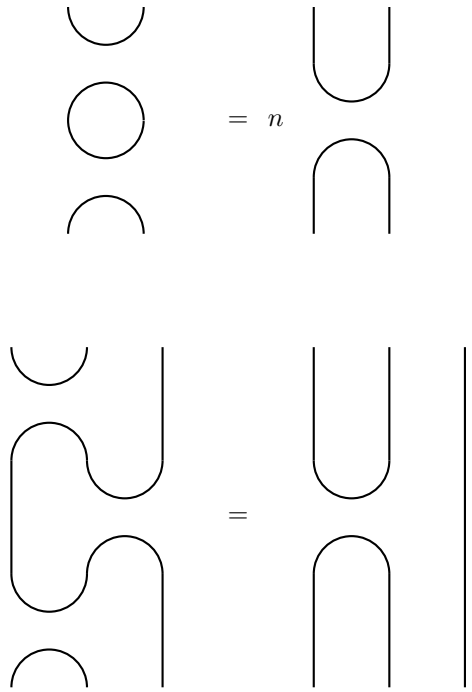

Figure 3.1: Interpretation of the Temperley-Lieb algebra defining relations in terms of diagrams.

closed loop carries a weight n (fugacity). We will discuss below how this loop model can be obtained more physically from the high-temperature expansion of the Q-state Potts model. Other representations will be introduced in the following sections. We emphasize that dense loops cannot cross in this model. For a discussion of loop models with crossings, see [103, 104].

In the strong anisotropy limit $p_A \to 0$ with $p_A/(1-p_B)$ fixed, we can extract the Hamiltonian of the equivalent one-dimensional quantum system. It reads, up to an irrelevant constant,

$$H = -\varepsilon \sum_{i=1}^{N-1} e_{2i} - \varepsilon^{-1} \sum_{i=1}^{N} e_{2i-1}, \tag{3.6}$$

where $\varepsilon = \sqrt{p_A/(1-p_B)}$. The system is isotropic when $p_A = p_B$, while a second order phase transition occurs when $p_A = 1 - p_B$. Hereafter, we will always consider the critical case $\varepsilon = 1$.

3.1.2 XXZ spin chain

A very natural representation of the Temperley-Lieb algebra is provided by the 6-vertex model. We write $n = \mathrm{e}^{i\gamma} + \mathrm{e}^{-i\gamma}$ and $\mathfrak{q} = \mathrm{e}^{i\gamma}$. The Hamiltonian limit of the 6-vertex model is the so-called XXZ chain, with Hilbert space $\mathcal{H}_{\mathrm{XXZ}} = (\mathbb{C}^2)^{\otimes L}$. We

will focus on this limit hereafter. The Temperley-Lieb generators in this representation read

$$e_i = \mathbb{I} \otimes \mathbb{I} \otimes \cdots \otimes \begin{pmatrix} 0 & 0 & 0 & 0 \\ 0 & \mathfrak{q}^{-1} & -1 & 0 \\ 0 & -1 & \mathfrak{q} & 0 \\ 0 & 0 & 0 & 0 \end{pmatrix} \otimes \cdots \otimes \mathbb{I}, \tag{3.7}$$

where we have used the basis $\{|\uparrow\uparrow\rangle, |\uparrow\downarrow\rangle, |\downarrow\uparrow\rangle, |\downarrow\downarrow\rangle\}$ of $(\mathbb{C}^2)^{\otimes 2}$, the tensor product of the Hilbert spaces of the sites i and $i+1$. In terms of Pauli matrices, we have

$$e_i = \frac{\mathfrak{q}+\mathfrak{q}^{-1}}{4} - \frac{1}{2}\left(\sigma_i^x\sigma_{i+1}^x + \sigma_i^y\sigma_{i+1}^y + \frac{\mathfrak{q}+\mathfrak{q}^{-1}}{2}\sigma_i^z\sigma_{i+1}^z\right) - \frac{\mathfrak{q}-\mathfrak{q}^{-1}}{4}\left(\sigma_i^z - \sigma_{i+1}^z\right), \tag{3.8}$$

so, up to an irrelevant constant term, the corresponding Hamiltonian $H = -\sum_i e_i$ with open boundary conditions reads

$$H = \frac{1}{2}\sum_{i=1}^{L-1}\left(\sigma_i^x\sigma_{i+1}^x + \sigma_i^y\sigma_{i+1}^y + \frac{\mathfrak{q}+\mathfrak{q}^{-1}}{2}\sigma_i^z\sigma_{i+1}^z\right) + \frac{\mathfrak{q}-\mathfrak{q}^{-1}}{4}\left(\sigma_1^z - \sigma_L^z\right). \tag{3.9}$$

This is the so-called XXZ Hamiltonian, along with some additional boundary terms that makes it symmetric under the quantum group $U_\mathfrak{q}s\ell(2)$ [67]. This symmetry will be analyzed in more detail in the following. Note also that for $\mathfrak{q} = 1$, it reduces to the celebrated antiferromagnetic Heinsenberg spin-1/2 chain.

3.1.3 Potts and dense loop models

In most of this chapter, the emphasis will be on spin chains with local (nearest-neighbor) Heinsenberg-like interactions, such as the XXZ spin chain introduced in the previous paragraph. This is because in the scaling limit, we expect these lattice spin chains to be described by well-defined, hopefully self-consistent, (Logarithmic) CFTs. Loop models on the other hand, are non-local by definition and typically fail to give self-consistent CFTs in the scaling limit (see the discussion in [74]). Geometrical observables will appear as subsectors in the spin chain models that we will mostly consider: for example, the critical exponents of geometrical percolation appears as a subset in the spectrum of the supersymmetric $\mathfrak{sl}(2|1)$ spin chain that shall be introduced in the next section. That said, loop models are interesting by themselves and have critical properties that are very well described by CFTs. Some of these geometrical properties actually show some logarithmic features, this will be studied further in chapter 5. In this paragraph, we mention the well-known relation between the Potts model and dense loops, thus giving a more physical meaning to the geometrical representation of the TL algebra.

The Q-state Potts model on a graph $G = (V, E)$ is defined through Q-component spins $\sigma_i = 1, 2, \ldots, Q$ that live on the vertices $i \in V$ and interact along the edges $(ij) \in E$ via an interaction energy $-K\delta_{\sigma_i,\sigma_j}$ proportional to the Kronecker symbol

($\delta_{x,y} = 1$ if $x = y$, and 0 otherwise). Its partition function thus reads

$$Z = \sum_{\sigma} \mathrm{e}^{K \sum_{(ij)\in E} \delta_{\sigma_i,\sigma_j}} , \tag{3.10}$$

where the sum is over all spins $\sigma = \{\sigma_i | i \in V\}$. For simplicity, we will consider that G is a square lattice in $d = 2$ dimensions.

Since $\delta_{x,y}$ can only take two values, the identity $\mathrm{e}^{K\delta_{\sigma_i,\sigma_j}} = 1 + v\delta_{\sigma_i,\sigma_j}$ holds with $v = \mathrm{e}^K - 1$. This yields

$$Z = \sum_{\sigma} \prod_{(ij)\in E} \left(1 + v\delta_{\sigma_i,\sigma_j}\right) . \tag{3.11}$$

Expanding out the product $\prod_{(ij)\in E}$ one gets a sum over subsets $A \subseteq E$ of edges for which the term $v\delta_{\sigma_i,\sigma_j}$ is taken. Each connected component (including isolated vertices) in the spanning subgraph (V, A) is called a Fortuin-Kasteleyn (FK) cluster. The factors of $\delta_{\sigma_i,\sigma_j}$ entail that the spin is constant on each FK cluster, so performing the sum $\sum_\sigma$ results in [105]

$$Z = \sum_{A\subseteq E} Q^{k(A)} v^{|A|} , \tag{3.12}$$

where $k(A)$ is the number of connected components in the spanning subgraph (V, A) with $|A|$ edges.

Spin, FK clusters and percolation

The FK representation (3.12) of the partition function is valid for any graph, thus in particular for lattices in any dimension d (see Fig. 3.2 in $d = 2$). It has the advantage over (3.10) that Q appears as a formal parameter, making it possible to approach physical (*i.e.*, integer) values via a limiting procedure. On the square lattice and for $0 \leq Q \leq 4$, the Potts model is known to have a non-trivial second order phase transition at the critical temperature $v_c = \sqrt{Q}$.

We stress that while all spins on a given FK cluster are identical, spins on different FK clusters have been independently summed over to obtain (3.12). In particular, two distinct FK clusters may or may not carry the same spin value, even when they are adjacent in G. It is possible to define 'spin clusters' as connected regions in G with constant spin, even when Q is not integer [106–108], thus leading to much more critical exponents and fractal dimensions. However, in this thesis we shall exclusively consider the better-known FK clusters.

The Potts model has several interesting limits. Among those, we have of course the Ising model ($Q = 2$), but also the percolation problem ($Q = 1$), or dense polymers or spanning tress ($Q = 0$). Let us see how percolation can be recovered from the $Q \to 1$ limit of the Potts model, the case $Q = 0$ will be discussed further in chapter 5. Let

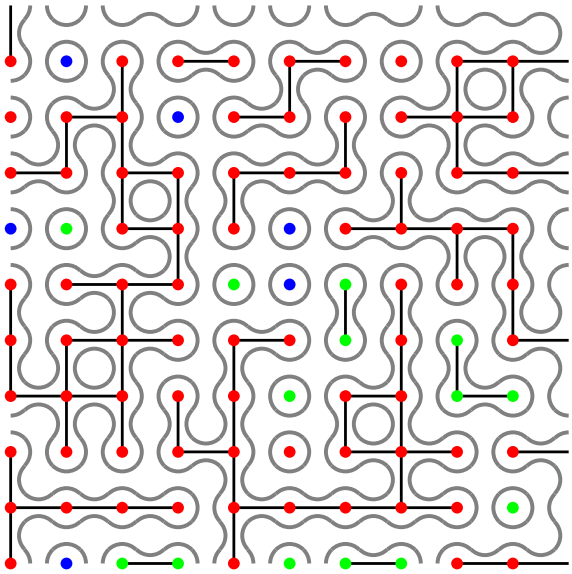

Figure 3.2: Example of spin configuration of the $Q = 3$ Potts model on the square lattice. We also show FK clusters (which can be interpreted as percolation clusters living within spin clusters) and the loops formed by their contours.

$p \in [0, 1]$ and $v = p/(1 - p)$. We then consider the rescaled partition function

$$\tilde{Z} \equiv (1-p)^{|E|} Z = \sum_{A \subseteq E} Q^{k(A)} p^{|A|} (1-p)^{|E|-|A|}. \tag{3.13}$$

For $Q = 1$, we have $\tilde{Z} = 1$, and p can be considered as the probability that each edge in E is present in A (percolation clusters). On the square lattice, the critical point corresponds to $p = \frac{1}{2}$. Let us point out that although the partition function is trivial, the correlation functions certainly are not.

Dense loop models and TL algebra

We also remark that when $d = 2$ many other representations of Z are possible. Among those, the *loop representation* consists in trading the FK clusters for their surrounding (inner and outer) contours on the medial graph $\mathcal{M}(G)$. Using topological identities this results in [109]

$$Z = Q^{|V|/2} \sum_{A \subseteq E} Q^{\ell(A)/2} \left(\frac{v}{\sqrt{Q}} \right)^{|A|}, \tag{3.14}$$

where $\ell(A)$ is the number of closed loops formed by the cluster contours. This draws dense loop configurations on the square lattice, so that the transfer matrix can be expressed in terms of Temperley-Lieb generators in the geometrical representation. For

an annulus of width N spins with free boundary conditions in the horizontal direction, the transfer matrix can indeed be expressed using elements of the TL algebra defined on $L = 2N$ strands with weight $n = \sqrt{Q}$. Using (3.14), we find

$$T = Q^{N/2} \prod_{i=1}^{N-1} (1 + x e_{2i}) \prod_{i=1}^{N} (x + e_{2i-1}) \ , \tag{3.15}$$

where $x = v/\sqrt{Q}$. We therefore recover that the Potts model is critical for $x_c = 1$ ($v_c = \mathrm{e}^{K_v} - 1 = \sqrt{Q}$). Let us drop out the term $Q^{N/2}$ and set $x = 1$. It is then convenient to represent the action of T in terms of plaquettes

$T \quad =$ 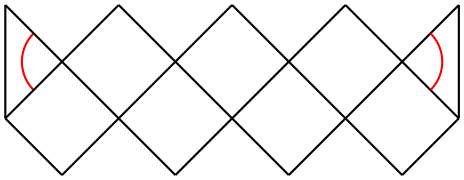

where in this example $N = 4$ ($L = 8$). The right and leftmost half plaquettes correspond to free (reflecting) boundary conditions. The bulk plaquettes carry the action of the Temperley-Lieb generators

$1 + e_i \ =$ 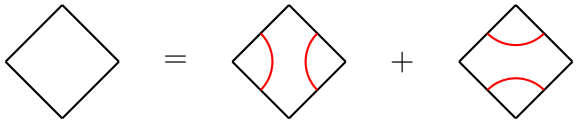

The action of this transfer matrix builds up loop configurations, and the Boltzmann weight of a configuration is computed by attributing a weight n to closed loops.

3.1.4 Supersymmetric models and sigma models

Another natural way to construct representations of $TL_{\mathfrak{q},L}$ is given by supersymmetric (SUSY) spin chains or vertex models [31, 110]. We consider a vertex model with a transfer matrix propagating vertically. Each edge of this two-dimensional lattice carries a $\mathbb{Z}_2$ graded vector space of dimension $n + m|m$, that is, a bosonic (*resp.* fermionic) space of dimension $n + m$ (*resp.* m). We choose these vector spaces to be the fundamental $\square$ of the Lie superalgebra $\mathfrak{gl}(n + m|m)$ for i odd (corresponding to down arrows of Fig. 3.3) and the dual $\bar{\square}$ for i even (up arrows). We refer the reader to Appendix A for a discussion of the superalgebras relevant to our purpose (see also section 2.3). The transfer matrix (or the Hamiltonian) then acts on the graded tensor product $\mathcal{H} = (\square \otimes \bar{\square})^{\otimes N}$. The TL generators are defined (up to a multiplicative constant) as projectors onto the singlet in the tensor products $\square \otimes \bar{\square}$ and $\bar{\square} \otimes \square$. The transfer matrix and the Hamiltonian are then defined in the usual way. The partition function can be expanded graphically, and one recovers a dense loop model with a weight $\mathrm{STr}\, \mathbb{I} = n + m - m = n$ for each closed loop as expected. An example of such

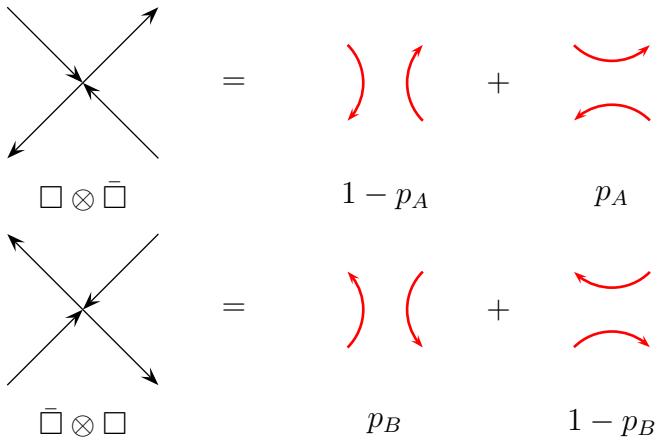

Figure 3.3: Graphical representation of the Temperley-Lieb-based supersymmetric vertex model. The lattice consists of alternating arrows going up for i even and down for i odd, where $i = 1, \ldots, L = 2N$ corresponds to the horizontal (space) coordinate. The system has free boundary conditions in the horizontal direction and periodic in the vertical (imaginary time) direction. We choose each vertex according to its probability, this draws a dense loop configuration on the lattice. Each closed loop carries a weight $n = \mathfrak{q} + \mathfrak{q}^{-1}$. In the supersymmetric language, the alternating $\square, \bar{\square}$ representations correspond to a lattice orientation, conserved along each loop. The system is isotropic when $p_A = p_B$, while the phase transition occurs when $p_A = 1 - p_B$.

dense loop configuration is shown on Fig. 3.4. Notice the alternating orientation of the arrows corresponding to the representations $\square$ and $\bar{\square}$. Let us also point out that these models are non-unitary because of the dual representations that contain negative norm states (see Appendix A).

Supersymmetric sigma models

These spin chains describe the strong coupling limit of a continuum quantum field theory [110], which turns out to be a non-linear σ-model on the complex projective superspace

$$\mathbb{CP}^{n+m-1|m} = \frac{\mathrm{U}(m+n|m)}{\mathrm{U}(1) \times \mathrm{U}(m+n-1|m)}, \tag{3.16}$$

at topological angle $\theta = \pi$. The Lagrangian of this theory involves a multiplet of fields with complex bosonic components z^a $(a = 1, \ldots, n+m)$ and fermionic components ξ^a $(a = 1, \ldots, m)$. These fields satisfy the constraint equation $z_a^\dagger z^a + \xi_a^\dagger \xi^a = 1$, modulo $U(1)$ gauge transformations, so they provide a parametrization of $\mathbb{CP}^{n+m-1|m}$. In terms

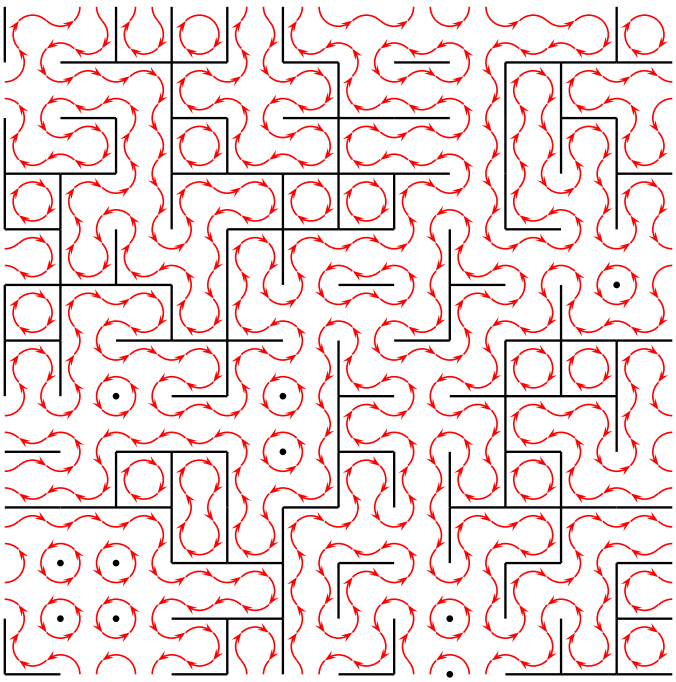

Figure 3.4: Example of dense loop configuration obtained as an expansion of the partition function of supersymmetric vertex models, in the case of a periodic model. We also show the equivalent percolating clusters. The lattice consists of alternating arrows going up for i odd and down for i even, where $i = 1, \ldots, L = 2N$ corresponds to the horizontal (space) coordinate. The alternating $\square, \bar{\square}$ representations correspond to a lattice orientation, conserved along each loop. The system has periodic boundary conditions in both spacial and imaginary time directions. Each closed loop carries a weight $\mathrm{STr}\, \mathbb{I} = n = \mathfrak{q} + \mathfrak{q}^{-1}$.

of these fields, the Euclidian Lagrangian density reads

$$\mathcal{L} = \frac{1}{2g_\sigma^2} \left[(D_\mu z_a)^\dagger D_\mu z^a + (D_\mu \xi_a)^\dagger D_\mu \xi^a \right] + \frac{i\theta}{2\pi} \varepsilon^{\mu\nu} \partial_\mu a_\nu, \tag{3.17}$$

where $a_\mu = \frac{i}{2} \left(z_a^\dagger \partial_\mu z^a + \xi_a^\dagger \partial_\mu \xi^a - \partial_\mu z_a^\dagger z^a - \partial_\mu \xi_a^\dagger \xi^a \right)$ is a gauge potential and $D_\mu = \partial_\mu + i a_\mu$ is the covariant derivative. The coefficient θ controls the topological term and is defined modulo 2π.

For $m > 0$, the beta function

$$\frac{\mathrm{d} g_\sigma}{\mathrm{d} \ln L} = m g_\sigma^4 + \ldots \tag{3.18}$$

is positive and the coupling flows to large values under the renormalization group. For $\theta \neq \pi \pmod{2\pi}$, the coupling becomes large, the $U(n+m|n)$ symmetry is restored, and the theory is massive. At $\theta = \pi$ and $m \leq 2$, a second order transition occurs, and

the system flows to a conformally invariant strong-coupling fixed point (see Fig. 3.5). The CFT description of this fixed point will be discussed further in the following. We also mention that in the presence of a boundary, the physics of the system depends crucially on the precise value of θ and not only on $\theta \pmod{2\pi}$, the corresponding critical exponents for all values of $\theta = \pi \pmod{2\pi}$ were computed in [111]. This turns out to have an interesting physical interpretation in terms of edge-states and higher-plateau transitions in quantum Hall systems [112].

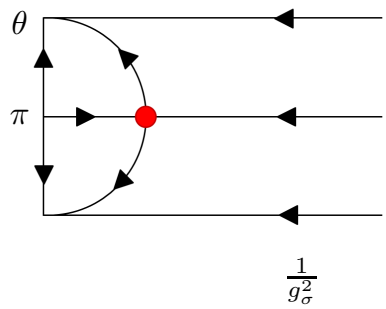

Figure 3.5: Renormalization group flow of the $\mathbb{CP}^{n+m-1|m}$ sigma model. For $0 \leq m \leq 2$, the system with $\theta = \pi \pmod{2\pi}$ flows to a conformally invariant strong-coupling fixed point.

Two interesting examples: $\mathfrak{gl}(1|1)$ and $\mathfrak{sl}(2|1)$ superspin chains

In the following, we will focus on two simple supersymmetric models based on the $\mathfrak{gl}(1|1)$ and $\mathfrak{sl}(2|1)$ superalgebras. As we shall see, the low energy limit of these lattice models is described by $c = -2$ and $c = 0$ LCFTs. For these two examples, it is helpful to be slightly more specific regarding the construction of the spin chains (see also Appendix A for algebraic details on the definition and the representation theory of $\mathfrak{gl}(1|1)$ and $\mathfrak{sl}(2|1)$).

The definition is especially simple in the case of $\mathfrak{gl}(1|1)$. The fundamental and dual representations are easily constructed from the 'fermions' $\{f_i, f_j^\dagger\} = (-1)^i \delta_{ij}$, with $i = 1, \dots L$ (see Appendix A). Notice the unusual minus sign for dual representations (i odd). The Temperley-Lieb generators then read

$$e_i = (f_i + f_{i+1})(f_i^\dagger + f_{i+1}^\dagger). \tag{3.19}$$

It is straightforward to check that this provides a representation of $TL_{\mathfrak{q},L}$ with $\mathfrak{q} = i$ ($n = 0$).

Another very important example is the $\mathfrak{sl}(2|1)$ spin chain [31, 110]. It can be considered as the supersymmetric formulation of the percolation problem, and appears naturally as an effective model describing the plateaus transition in the Spin Quantum Hall Effect [31]. The definition of the spin chain is quite simple. On each site, we

introduce two bosonic operators $[b_{i,\sigma}, b^\dagger_{j,\sigma'}] = \delta_{ij}\delta_{\sigma\sigma'}$, where $\sigma \in \{\uparrow,\downarrow\}$, and one fermion $\{f_i, f^\dagger_j\} = (-1)^{i+1}\delta_{ij}$. We further impose that there cannot be more than one particle by site, so the whole 'Hilbert' space has dimension $3^L = 9^N$. This provides a representation $\mathcal{H} = (\square \otimes \bar{\square})^{\otimes N}$ of $\mathfrak{sl}(2|1)$, so the sites with i even correspond to fundamental representations $\square$, whereas i odd sites carry a dual representation $\bar{\square}$. We refer the reader to Appendix A for more detail concerning the Lie superalgebra $\mathfrak{sl}(2|1)$. The Temperley-Lieb generator is given by the projector on the singlet in the tensor product $\square \otimes \bar{\square}$, which reads

$$e_i = (b^\dagger_{i+1,\downarrow} b^\dagger_{i,\uparrow} + b^\dagger_{i+1,\uparrow} b^\dagger_{i,\downarrow} + (-1)^{i+1} f^\dagger_{i+1} f^\dagger_i)(b_{i,\uparrow} b_{i+1,\downarrow} + b_{i,\downarrow} b_{i+1,\uparrow} + (-1)^{i+1} f_i f_{i+1}). \quad (3.20)$$

It provides a representation of $TL_{\mathfrak{q},L}$ with $\mathfrak{q} = \mathrm{e}^{i\pi/3}$ ($n = 1$). Note that although the whole Hilbert space is quite large, there are two good quantum numbers S_z and B conserved by the Hamiltonian that we can use to label the states

$$S_z = \frac{1}{2}\sum_{i=1}^{L} (b^\dagger_{i,\uparrow} b_{i,\uparrow} - b^\dagger_{i,\downarrow} b_{i,\downarrow}), \quad (3.21a)$$

$$B = \sum_{i=1}^{L} \left((-1)^{i+1} \frac{b^\dagger_{i,\uparrow} b_{i,\uparrow} + b^\dagger_{i,\downarrow} b_{i,\downarrow}}{2} + f^\dagger_i f_i \right). \quad (3.21b)$$

The dimension $g(N, S_z, B)$ of the various sectors of the Hilbert space is then given by the generating function

$$\sum_{N,S_z,B} g(N, S_z, B) x^N y^{2B} z^{2S_z} = \frac{1}{1 - x(y + z + z^{-1})(y^{-1} + z + z^{-1})}. \quad (3.22)$$

As discussed previously, this model corresponds to the fixed point of a nonlinear sigma model on $\mathbb{CP}^{1|1}$.

3.1.5 A remark on dilute models and other representations

To conclude this section, let us also mention the models built out of the 'dilute' version of the TL algebra. This denomination obviously refers to the dense or dilute nature of the underlying loop gas. Instead of the Potts model, dilute models can be obtained very naturally from the $O(n)$ model. It corresponds to a dilute loop model where closed loops carry a weight n. We shall focus here only on the dilute phase – this model also possesses a dense phase which is in the same universality class as the dense loop model. The case $n \to 0$ is relevant for the physics of polymers. In terms of spin chains, it is described by a $S = 1$ $U_\mathfrak{q} s\ell(2)$-invariant chain where the states $S_z = \pm 1$ are viewed as occupied by parts of loops and $S_z = 0$ as empty. This model also corresponds to $\mathfrak{osp}(n+2m|2m)$ (super)spin chains and to non-linear sigma models with supersphere target space $S^{2m+n-1|2m} \simeq \mathrm{OSp}(2m+n|2m)/\mathrm{OSp}(2m+n-1|2m)$ [110]. There is a dilute version of the Temperley-Lieb algebra behind all these models. We will not go

into the details of these different formulations here, as for simplicity we will focus on the dense models only. For a more thorough discussion of LCFTs associated with dilute models, we refer the reader to, *e.g.* [69].

Going back to the TL algebra, it goes without saying that there exist other representations that the ones discussed above. We just mention here RSOS models [113], that correspond in the scaling limit to minimal models [114] – note also that there has been a recent renewal of interest in RSOS models because of their connection to anyonic chains [115–117].

3.2 TL representation theory and Hilbert space decomposition

In this section, we analyze the symmetries of the lattice models introduced in the previous section, and decompose the space of states with respect to these symmetries. The point is that one can already see on the lattice the indecomposability pattern of the Virasoro algebra. This observation probably goes back to the work of Pasquier and Saleur [67], but it was fully understood and used efficiently to tackle LCFTs by Read and Saleur many years later [68, 69]. We will mostly focus on the $U_{\mathfrak{q}}s\ell(2)$-invariant XXZ spin chain for pedagogical reasons, but most of our results can also be understood in terms of supersymmetric spin chains. It is worth mentioning that the supersymmetric formulation turns out to be particularly convenient when dealing with *periodic* systems, as the $U_{\mathfrak{q}}s\ell(2)$ symmetry of the XXZ spin chain is lost in that case (see *e.g.* [69, 118–120]).

3.2.1 Reduced states and standard modules

We now come back to the geometrical representation of the TL algebra. Recall that all the elements of the TL algebra can be represented as diagrams, for instance, on $L = 4$ sites,

$e_2e_1 =$ 

We also stress that composition can be computed by stacking diagrams,

$e_2e_1e_2e_1 =$ 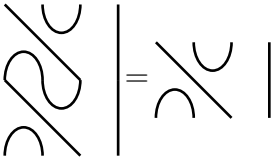 $= e_2e_1.$

An important point is that any state can be turned into a pair of reduced states by cutting all its strings and pulling apart the upper and lower parts. Conversely, a state can be obtained by adjoining two reduced states, gluing together their strings in a unique fashion. It turns out that these reduced states provide a natural basis of the (generically) irreducible representations of the TL algebra.

When q is generic, *i.e.* not a root of unity, the representation theory of $TL_{\mathsf{q},L}$ is said to be semi-simple [100, 121, 122]. This means that all reducible representations are fully reducible, so that the only indecomposable representations in that case are irreducible as well. All simple modules or irreducible representations of $TL_{\mathsf{q},L}$ can then be described geometrically; they are called standard modules. For j (half-)integer such that $0 \leq j \leq L/2$ and on L sites, we define a standard module $\mathsf{S}_j[L]$ with $2j$ through-lines (also called "strings") as the span of link diagrams – all possible nested configurations of $(\frac{L}{2} - j)$ arcs, like $\cup\,\cup\,\smile$. Through-lines are denoted by a vertical line $|$ and are not allowed to intersect any arc. The action of the generators on these modules is again interpreted as stacking the various diagrams with the additional rule that contracting any pair of strings results in zero. The dimension of these standard modules reads

$$\mathsf{d}_j \equiv \dim(\mathsf{S}_j[N]) = \binom{L}{L/2+j} - \binom{L}{L/2+j+1}, \qquad \text{and we set } \mathsf{d}_j = 0 \text{ for } 2j > L. \tag{3.23}$$

We stress that d_j does not depend on q. Note also that j must be half integer when L is odd. For $L = 4$ for instance, there are four standard modules with basis

$$\mathsf{S}_0[4] = \{\, \smile, \cup\,\cup \,\}, \tag{3.24}$$

$$\mathsf{S}_1[4] = \{\, |\cup|\,, \cup\,||\,, ||\cup \,\}, \tag{3.25}$$

$$\mathsf{S}_2[4] = \{\, |||| \,\}. \tag{3.26}$$

For example, in this basis, the action of the TL generators on $\mathsf{S}_1[4]$ is $e_2\, |\cup|\, = n\, |\cup|$, $e_2\, \cup\,|| = \,|\cup|$, and $e_3\, \cup\,|| = 0$. To give a complete example, in the basis $\mathsf{S}_0[4] = \{\, \smile, \cup\,\cup \,\}$, the full action of the TL generators is given by

$$e_1 = \begin{pmatrix} 0 & 0 \\ 1 & n \end{pmatrix}, \quad e_2 = \begin{pmatrix} n & 1 \\ 0 & 0 \end{pmatrix}, \quad e_3 = \begin{pmatrix} 0 & 0 \\ 1 & n \end{pmatrix}. \tag{3.27}$$

Because of the relation between the reduced states and the elements of the algebra, it is easy to compute the dimension of $TL_{\mathsf{q},L}$ (recall that $L = 2N$)

$$\dim(TL_{\mathsf{q},L}) = \sum_{j=0}^{N} \mathsf{d}_j^2 = \frac{1}{L+1}\binom{2L}{L}, \tag{3.28}$$

which are the celebrated Catalan numbers.

3.2.2 Generic case: decomposition of the partition function

Let us consider a dense loop model on an annulus on width N spins and length M (with, typically $M \gg N$), with free boundary conditions in the spatial direction, and periodic boundary conditions in the vertical (imaginary time) direction. The partition

function of the loop gas is then given by

$$Z(N,M) = \text{Tr } T^M, \tag{3.29}$$

where the trace operation in this expression is the so-called Markov trace. The Markov trace amounts to gluing the strands on the top and on the bottom of a state so as to get the geometry of an annulus, giving an appropriate weight $n' = t + t^{-1}$ to loop winding around the imaginary time direction.

When the fugacity of a loop $n = \mathfrak{q} + \mathfrak{q}^{-1}$ is generic, that is, when $\mathfrak{q}$ is not a root of unity, one can then argue [2] that the partition function decomposes onto different sectors with a fixed number of through lines $2j$

$$Z(N,M) = \text{Tr } T^M = \sum_{j=0}^{N} [1+2j]_t \, K_{1,1+2j}, \tag{3.30}$$

where K_{1+2j} is an ordinary trace evaluated within the standard module $\mathsf{S}_j[L]$ with $2j$ strings (reduced states)

$$K_{1,1+2j} = \text{tr}_{\mathsf{S}_j[L]} T^M, \tag{3.31}$$

and the multiplicities $D_j = [1+2j]_t$ are expressed in terms of the t-deformed numbers

$$[x]_t \equiv \frac{t^x - t^{-x}}{t - t^{-1}}. \tag{3.32}$$

By continuity of the partition function of loop models with respect to the loop weight, this formula should hold also for $\mathfrak{q}$ roots of unity. If one wants the same weight $n' = n$ to non-contractible loops winding around the annulus, the multiplicities read in that case $[1+2j]_{\mathfrak{q}}$ as $t = \mathfrak{q}$. The XXZ spin chain on the other hand, after a mapping onto the 6-vertex model, can be described by a loop gas with $n' = 2$, so that $D_j = 2j+1$ and

$$Z_{\text{XXZ}}(N,M) = \sum_{j=0}^{N} (2j+1) K_{1,1+2j}. \tag{3.33}$$

In the quantum spin chain language, $M = \beta$ is the inverse temperature. Finally, in the case of supersymmetric spin chains based on the $\mathfrak{gl}(n+m|m)$ superalgebra, the multiplicities are given by $[1+2j]_t$ [3], with $t + t^{-1} = 2m + n$ [110].

2. The proof of that statement involves the computation of the trace of the so-called Jones-Wenzl projector P_{2j} that projects onto the sector with $2j$ through lines, satisfying $P_{2j}^2 = P_{2j}$, and $e_i P_{2j} = P_{2j} e_i = 0$ if $i < 2j$ (see [100]).

3. These multiplicities correspond to the so-called *modified* partition function [110] – the generating function of the spectrum, defined as a trace instead of a supertrace.

3.2.3 Generic case: algebraic analysis of the spectrum, commutant and bimodules

Of course, these multiplicities can (and should) be interpreted in terms of the symmetries of the models under scrutiny. As it so happens, all these numbers correspond to some dimension of irreducible representations of symmetry algebras, called commutant [68].

Let us reinterpret the results of the previous section from a more algebraic perspective in the XXZ case. To understand the multiplicities in the spectrum, it is crucial to discuss the symmetries of the lattice models. Recall that the usual Heisenberg XXX spin chain ($\mathfrak{q} = 1$ in (3.9)) is defined by its Hamiltonian H acting in the vector space $\mathcal{H}_L$

$$H = \sum_i \vec{S}_i \cdot \vec{S}_{i+1}, \qquad \mathcal{H}_L = \square^{\otimes L} \tag{3.34}$$

where $\square = \mathbb{C}^2$ denotes the fundamental representation of $s\ell(2)$, and $L = 2N$ is chosen to be even for simplicity. It is an antiferromagnetic chain, and accordingly its nearest neighbor coupling $\vec{S}_i \cdot \vec{S}_{i+1}$, projects neighbor pairs of spins onto the singlet. The continuum limit is well-known to be described by the $O(3)$ sigma model at $\theta = \pi$ [123] which flows to the level-1 $SU(2)$ WZW theory at low energy [124]. So of course in that case, the continuum theory is not logarithmic but this example will be useful to illustrate our approach.

For this Heisenberg XXX spin chain, there are two natural algebras to consider. One is the symmetry algebra $s\ell(2)$ generated by $S^{\pm}$ and S^z operators satisfying the usual relations

$$[S^+, S^-] = 2S^z, \qquad [S^z, S^{\pm}] = \pm S^{\pm}. \tag{3.35}$$

The other is the algebra generated by the local hamiltonian densities $\vec{S}_i \cdot \vec{S}_{i+1}$. This algebra actually coincides with (a quotient of) the group algebra of the permutation group, which is nothing in this case but the Temperley–Lieb algebra for the value $n = 2$ of the fugacity parameter n. The actions of the two algebras commute – the symmetry generators commute not only with the Heisenberg Hamiltonian but also with all its densities. What this really means is that we can decompose the Hilbert space $\mathcal{H}_L$ in terms of $s\ell(2)$ representations of (integer, if we restrict to chains of even length) spin j. The vector space of all highest-weight states of a given spin j then provides a representation of the permutation group or of the TL algebra with $\mathfrak{q} = 1$. Its dimension is obviously the multiplicity of the spin j representation of $s\ell(2)$ in $(\mathbb{C}^2)^{\otimes 2N}$ and it is given by the numbers

$$\mathsf{d}_j = \binom{2N}{N+j} - \binom{2N}{N+j+1}, \qquad \text{and we set } \mathsf{d}_j = 0 \text{ for } j > N. \tag{3.36}$$

This representation is irreducible by construction, and it actually corresponds to the

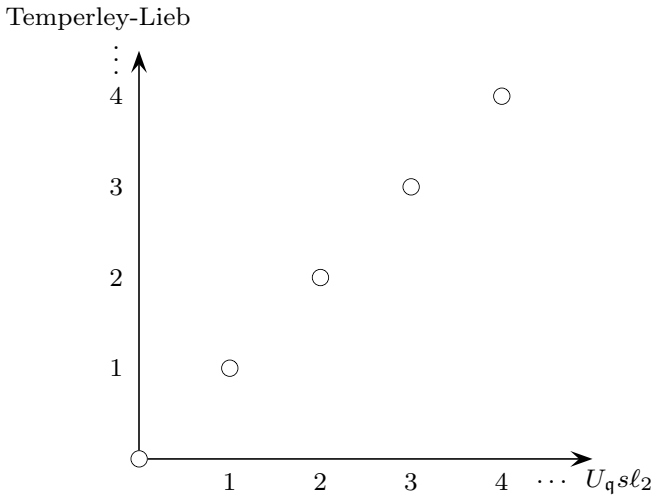

Figure 3.6: Bimodule for the antiferromagnetic Heisenberg or XXX spin chain and $L = 2N$ even. This shows the commuting action of the quantum group $U_\mathfrak{q} s\ell(2)$ and of the Temperley-Lieb algebra.

standard module $\mathsf{S}_j[L]$. The full Hilbert space of states can thus be considered not just a representation (or equivalently a module) for one of the algebras, but rather a *bi*-module for both algebras simultaneously. In other words, the space of states $\mathcal{H}_L$, as a (semi-simple) bi-module over this pair of commuting algebras, can be decomposed as

$$\mathcal{H}_L \cong \bigoplus_{j=0}^{N} \mathsf{S}_j[L] \otimes \mathcal{W}_j, \tag{3.37}$$

where the first algebra generated by the densities $\vec{S}_i \cdot \vec{S}_{i+1}$ acts on the left tensorands denoted by $\mathsf{S}_j[L]$, while the second algebra $s\ell(2)$ acts on the right components which are spin j representations denoted by $\mathcal{W}_j$ – remark that these $s\ell(2)$-representations do not depend on N. This relation between (the universal enveloping algebra of) $s\ell(2)$ and $TL_{\mathfrak{q},L}$ for $\mathfrak{q} = 1$ is an example of *Schur–Weyl duality*. Finally, the resulting bimodule can be represented graphically as in Fig. 3.6, where each open dot represents a simple (irreducible) module for both algebras.

The Hamiltonian (3.9) of the XXZ model now generalizes this usual Heisenberg (or XXX) model to a spin chain with quantum-group $U_\mathfrak{q} s\ell(2)$ symmetry. This symmetry is generated by the $S^\pm$ and S^z operators that now satisfy the quantum-group relations

$$[S^+, S^-] = \frac{\mathfrak{q}^{2S^z} - \mathfrak{q}^{-2S^z}}{\mathfrak{q} - \mathfrak{q}^{-1}}, \qquad [S^z, S^\pm] = \pm S^\pm, \tag{3.38}$$

which are just $\mathfrak{q}$-deformed versions of the usual relations (3.35).

When $\mathfrak{q}$ is generic, *i.e.* not a root of unity, the Hilbert space of the Hamiltonian densities (3.8) nicely decomposes onto the irreducible standard modules $\mathsf{S}_j[L]$ of $TL_{\mathfrak{q},L}$

again,

$$\mathcal{H}_L|_{TL_{\mathfrak{q},L}} \cong \bigoplus_{j=0}^{N} (2j+1)\mathsf{S}_j[L], \tag{3.39}$$

where the degeneracies $2j+1$ correspond to the dimension of the spin j representations (which are also generically irreducible) over the symmetry algebra for $TL_{\mathfrak{q},L}$, (a finite-dimensional image of) the quantum group $U_{\mathfrak{q}}s\ell(2)$. We can thus consider the space $\mathcal{H}_L$ again as a semi-simple bi-module over the pair of commuting algebras $TL_{\mathfrak{q},L} \otimes U_{\mathfrak{q}}s\ell(2)$ and it has the same decomposition as in (3.37).

3.2.4 Representation theory of the Temperley-Lieb algebra

Whereas the representation theory for $\mathfrak{q}$ generic is quite simple, things become more intricate when $\mathfrak{q}$ is a root of unity, which corresponds to most of the physically relevant cases. We shall denote $\mathfrak{q} = \mathrm{e}^{\frac{i\pi}{p+1}}$ in this case, and we will use the following denominations, borrowed from the Potts model terminology, for the several physically relevant cases: dense polymers ($p = 1$), percolation ($p = 2$), Ising model ($p = 3$), *etc.* In these cases, the algebra $TL_{\mathfrak{q},L}$ is non-semisimple and the decomposition (3.39) is no longer true. We will describe the structure of the XXZ spin-chain at these roots of unity cases after a short detour around the representation theory of the TL algebra.

When $\mathfrak{q} = \mathrm{e}^{\frac{i\pi}{p+1}}$ is a root of unity, the representation theory of $TL_{\mathfrak{q},L}$ becomes much more complicated. The first striking feature is that the standard modules become reducible, but indecomposable – that is, there is no way to decompose them onto irreducible representations. As an example, let us consider the standard module $\mathsf{S}_0[4]$ with basis $\mathsf{S}_0[4] = \{\cup\,\cup, \cup\!\!\cap\}$. When $\mathfrak{q} = \mathrm{e}^{i\pi/3}$ ($n = 1$), it is easy to see that the space $\mathsf{X}_2 = \{\cup\,\cup - \cup\!\!\cap\}$ is invariant under the action of $TL_{\mathfrak{q},4}$. The module $\mathsf{S}_0[4]$ is thus reducible but indecomposable, and we represent its structure by the following diagram

$$\begin{aligned} \mathsf{S}_0[4] = &\quad \mathsf{X}_0 \longrightarrow \mathsf{X}_2, \\ = &\quad \{\cup\,\cup\} \longrightarrow \{\cup\,\cup - \cup\!\!\cap\}. \end{aligned} \tag{3.40}$$

The arrow in these diagrams ("subquotient structure") should be understood as the action of TL on $\mathsf{S}_0[4]$. It means that it is possible to go from $\{\cup\,\cup\}$ to X_2 acting with TL generators, but not the other way around. To be more precise, it means that X_2 is an irreducible submodule in $\mathsf{S}_0[4]$, and the quotient $\mathsf{S}_0[4]/\mathsf{X}_2 \cong \mathsf{X}_0$ by this submodule is also irreducible. This is of course the analog of the indecomposable representations encountered in chapter 2.

This structure is quite general, and it can be shown that other standard modules have a similar indecomposable pattern for other roots of unity. These results can be found in [121, 122, 125, 126] (see also [72] for complete results using techniques similar to those developed in this chapter). We will only give the main results here and refer the reader to those references for details and proofs. It turns out that the irreducible (also called simple) modules X_j of the Temperley-Lieb algebra when $\mathfrak{q} = \mathrm{e}^{i\pi/p+1}$ is a

root of unity can still be labeled by $0 \leq j \leq N$. For simplicity, we restrict here to the case $L = 2N$ even so that the parameter j must be integer. The standard modules can then be indecomposable, with the following subquotient structure

$$\mathsf{S}_j : \quad \mathsf{X}_j \longrightarrow \tilde{\mathsf{X}}_{j+p-2(j \bmod (p+1))} \qquad \text{where} \quad \tilde{\mathsf{X}}_{j'} = \begin{cases} \mathsf{X}_{j'}, & \text{if } j' > j, \\ 0, & \text{if } j' = j, \\ \mathsf{X}_{j'+p}, & \text{if } j' < j, \end{cases} \tag{3.41}$$

and we additionally set $\mathsf{S}_j = 0$ for all $j > N$ which is crucial when the number of through lines $2j$ is close to its maximum value $j = N$. We note also that the standard modules are irreducible whenever $j \bmod (p+1) = \frac{k(p+1)-1}{2}$ with $k = 0, 1$. The subquotient structure (3.41) then allows to compute the dimension d_j^0 of the irreducible modules taking standard alternating sums

$$\dim(\mathsf{X}_j) \equiv \mathsf{d}_j^0 = \sum_{n \geq 0} \mathsf{d}_{j+n(p+1)} - \sum_{n \geq t(j)+1} \mathsf{d}_{j+n(p+1)-1-2(j \bmod (p+1))}, \tag{3.42}$$

where we recall that d_j is given by (3.23) and we also introduce the step function $t(j) \equiv t$ as

$$t = \begin{cases} 1, & \text{for} \quad j \bmod (p+1) > \frac{p}{2}, \\ 0, & \text{for} \quad j \bmod (p+1) < \frac{p}{2}. \end{cases} \tag{3.43}$$

Unfortunately, to describe the structure of spin chains when $\mathfrak{q}$ is a root of unity, the knowledge of standard modules are not enough. At special indecomposable points, standard modules may actually "collide" and get glued together. This is reminiscent of the staggered modules for the Virasoro algebra that are gluings of two Kac modules. These more complicated modules are called *tilting* modules [127], and they will be the "fundamental blocks" of the Hilbert of XXZ spin chains. The structure of these tiltings can be deduced from their properties, in particular from the fact that they are self-dual, which means that they should be invariant under the adjoint $\cdot^\dagger$ operation defined by $e_i^\dagger = e_i$ (see also [74] for a short review in the context of boundary spin chains). We give here only the structure of these fundamental representations, and refer the reader to [72] for details.

Using the diagram (3.41) and introducing T_j as the tilting module that can be mapped onto S_j, we have, for an integer or half integer j, the subquotient structure

$$\mathsf{T}_j = \mathsf{S}_j \longrightarrow \tilde{\mathsf{S}}_{j-1-2(j \bmod (p+1))}, \qquad \text{for} \quad \frac{p+1}{2} \leq j \leq N, \tag{3.44}$$

where we set

$$\tilde{\mathsf{S}}_{j'} = \begin{cases} \mathsf{S}_{j'}, & \text{if } j'+p+1 > j, \\ 0, & \text{if } j'+p+1 = j, \\ \mathsf{S}_{j'+p+1}, & \text{if } j'+p+1 < j. \end{cases} \tag{3.45}$$

and in terms of irreducible representations we get, for $j \geq (p+1)/2$ and $j \bmod (p+1) \neq \frac{k(p+1)-1}{2}$ with $k = 0, 1$,

$$\mathsf{T}_j : \quad \begin{array}{ccccc} & & \mathsf{X}_j & & \\ & \swarrow & & \searrow & \\ \mathsf{X}_{j+tp-2(j \bmod (p+1))} & & & & \mathsf{X}_{j+(1+t)p-2(j \bmod (p+1))} \\ & \searrow & & \swarrow & \\ & & \mathsf{X}_j & & \end{array} \tag{3.46}$$

where the right subquotient is absent whenever its subscript j is greater than N.

3.2.5 Hilbert space decomposition in the root of unity case

Our ultimate goal is to obtain the structure of the Hilbert space (the space of states) for the algebra $TL_{\mathfrak{q},L}$. This will be useful as, anticipating a little bit, this algebraic structure will carry over to the continuum limit, and the $TL_{\mathfrak{q},L}$ representations will become representations over the Virasoro algebra. It turns out that the representation theory of the symmetry algebra $U_{\mathfrak{q}}s\ell(2)$ is easier to study than that of the "hamiltonian densities" algebra $TL_{\mathfrak{q},L}$. Actually, because of the double centralizing structure – $TL_{\mathfrak{q},L}$ and $U_{\mathfrak{q}}s\ell(2)$ are mutually centralizing each other, it is possible to deduce the decomposition for $TL_{\mathfrak{q},L}$ from the decomposition over $U_{\mathfrak{q}}s\ell(2)$, and *vice versa*. In particular, the multiplicities in front of tilting $TL_{\mathfrak{q},L}$-modules give the dimensions of simple $U_{\mathfrak{q}}s\ell(2)$-modules, and the subquotient structure of tilting $TL_{\mathfrak{q},L}$-modules can be deduced from the one of the tilting $U_{\mathfrak{q}}s\ell(2)$-modules (and *vice versa*), see [128]. This was used to obtain the TL decomposition in [69], and generalized in [72].

Following these lines, one can obtain the decomposition of the spin-chain $\mathcal{H}_L$ over $TL_{\mathfrak{q},L}$ as [72]

$$\begin{aligned} \mathcal{H}_L|_{TL_{\mathfrak{q},L}} \cong & \bigoplus_{r=1}^{r_m-1} \bigoplus_{\substack{s=0, \\ r(p+1)+s+N=1 \bmod 2}}^{p} \dim\big(\mathcal{X}_{p+1-s,r}\big)\mathsf{T}_{\frac{r(p+1)+s-1}{2}} \oplus \bigoplus_{\substack{s=0, \\ s+s_m=1 \bmod 2}}^{s_m+1} \dim\big(\mathcal{X}_{p+1-s,r_m}\big) \\ & \mathsf{T}_{\frac{r_m(p+1)+s-1}{2}} \oplus \bigoplus_{\substack{s=1, \\ s+s_m=1 \bmod 2}}^{s_m+1} \dim\big(\mathcal{X}_{s,r_m+1}\big)\mathsf{X}_{\frac{r_m(p+1)+s-1}{2}} \oplus \bigoplus_{\substack{s=s_m+2, \\ s+s_m=1 \bmod 2}}^{p} \dim\big(\mathcal{X}_{p+1-s,r_m}\big)\mathsf{X}_{\frac{r_m(p+1)-s-1}{2}}, \end{aligned} \tag{3.47}$$

where $L = r_m(p+1)+s_m$, for $r_m \in \mathbb{N}$ and $-1 \leq s_m \leq p-1$. Here, we use the notation

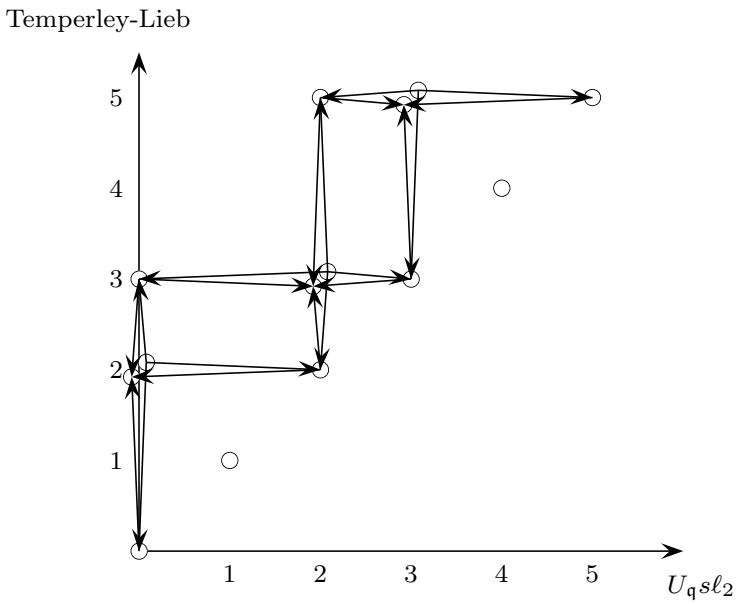

Figure 3.7: Bimodule for percolation ($\mathfrak{q} = \mathrm{e}^{i\pi/3}$) and $L = 10$ sites. Horizontal (*resp.* vertical) arrows correspond to the action of the quantum group $U_{\mathfrak{q}}s\ell(2)$ (*resp.* the Temperley-Lieb algebra). Each node with a Cartesian coordinate (n, n') corresponds to the tensor product $\mathsf{X}_{n'} \otimes \mathcal{X}_{[n]}$. Some nodes occur twice and those nodes have been separated slightly for clarity.

$\mathcal{X}_{s,r}$ for irreducible representations of the quantum group $U_{\mathfrak{q}}s\ell(2)$. They have dimension rs and they are irreducible quotients of the spin-n quantum group representations, where $n = \frac{(p+1)(r-1)+s-1}{2}$. We will also use the notation $\mathcal{X}_{[n]}$.

Just like in semisimple cases, it is convenient to represent the Hilbert space structure as a bimodule over both Temperley-Lieb and $U_{\mathfrak{q}}s\ell(2)$ [69].

As an example, we show in Fig. 3.7 the analogue of Fig. 3.6 for $\mathfrak{q} = \mathrm{e}^{i\pi/3}$ ($n = 1$, percolation) at $N = 10$ sites. The decomposition over the TL algebra is

$$\mathcal{H}_{10}|_{TL_{\mathfrak{q},10}} \cong 3\mathsf{T}_1 \oplus \mathsf{T}_2 \oplus 4\mathsf{T}_3 \oplus 9\mathsf{T}_4 \oplus 3\mathsf{T}_5 \oplus 8\mathsf{X}_5. \tag{3.48}$$

In this bimodule diagram, each node with a Cartesian coordinate (n, n') corresponds to the tensor product $\mathsf{X}_{n'} \otimes \mathcal{X}_{[n]}$ of simple modules over the TL algebra and $U_{\mathfrak{q}}s\ell(2)$, respectively, and the arrows show the action of both algebras – the Temperley–Lieb $TL_{\mathfrak{q},N}$ acts in the vertical direction (preserving the coordinate n), while $U_{\mathfrak{q}}s\ell(2)$ acts in the horizontal direction. The diamond-shape tilting $TL_{\mathfrak{q},N}$-modules $\mathsf{T}_{n'}$ described in (3.46) can be recovered by ignoring all the horizontal arrows of the bimodule diagram. These are squeezed, so that the first tilting TL module T_1 is just a node (this one is irreducible), the second tilting T_2 consists of the left-most set of four vertical arrows, etc.

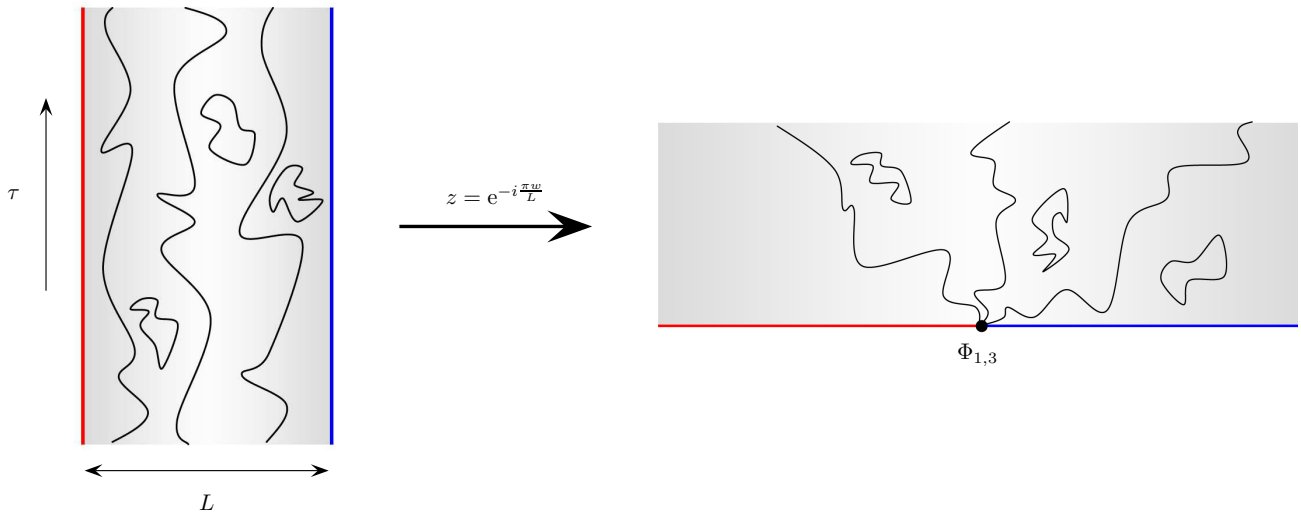

Figure 3.8: Mapping of a strip of width L onto the upper half-plane $\mathbb{H}$. In terms of dense loops, the standard module S_j with $2j$ through-lines ($2j = 3$ here) corresponds in the scaling limit to the insertion of the Kac operator $\Phi_{1,1+2j}$ (see Sec. 3.3.2).

3.3 Scaling limit and Virasoro representations

Now that we have analyzed the spin chain from an algebraic point of view, the idea is that the algebra of local energy hamiltonian densities should go over, in the continuum limit, to the Virasoro algebra, and that many of its features may be stable as the length of the chain is increased, as long as one focuses only on low energy excitations. So our general strategy will be to consider the XXZ spin chain (3.9) as a lattice regularization for (L)CFTs. The representation theory of the TL algebra when $\mathfrak{q}$ is a root of unity then mimics what happens in the scaling limit for the Virasoro algebra. One can even obtain interesting results for the Virasoro algebra representation theory, starting directly from lattice models. The idea of doing so probably goes back to [67], and was pushed forward more recently by Read and Saleur, who studied the structure of XXZ spin chains and supersymmetric models [69, 110] on the lattice.

3.3.1 Finite size scaling

The first step to understand the scaling limit of our critical lattice models is to compute the spectrum of critical exponents (the operator content) and the central charge. Conformal invariance fixes the finite size scaling form of the eigenvalues of the transfer matrix of a critical lattice model on a strip of width L – or of the energies of the Hamiltonian of a gapless quantum spin chain. Mapping the upper-half plane onto an infinite strip using the conformal transformation

$$w = \frac{iL}{\pi} \log z, \tag{3.49}$$

one finds that the two-point function of two-operators on the strip scales as $\langle\phi(w = il)\phi(0)\rangle \propto \exp\left(-\frac{\pi h}{L}l\right)$, for $l \gg L$. If we now compare this expression to what is expected from the eigenvalues of the transfer matrix, we find that there is a one-to-one mapping between the eigenstates of the transfer matrix and the operators of the underlying CFT. The subdominant eigenvalues $\lambda_\phi(L)$ of the transfer matrix are then related to the conformal dimension h_ϕ (critical exponent) of the operators in the underlying boundary conformal field theory [129]

$$\lambda_\phi(L) \simeq \lambda_0(L)\ \mathrm{e}^{-\frac{\pi}{L}h_\phi}. \tag{3.50}$$

We also have a similar formula for the finite size correction to the gap of critical quantum spin chains. The Hamiltonian of a CFT on a strip reads $H = \frac{\pi}{L}\left(L_0 - \frac{c}{24}\right)$, so the energy of the groundstate – that we assume corresponds to $h = 0$, this is not always the case for non-unitary CFTs! – scales as [29, 130]

$$E_0 = e_\infty L + e_\infty^S - \frac{\pi v_F c}{24L} + \dots \tag{3.51}$$

where e_∞ and e_∞^S are non-universal (cutoff dependent) bulk and surface energies, and v_F is the Fermi velocity – the dispersion relation of the massless excitations is $\epsilon(k) = v_F|k|$. Meanwhile, the subdominant eigenstates have energy [4]

$$E_i = e_\infty L + e_\infty^S + \frac{\pi v_F}{L}\left(h_i - \frac{c}{24}\right) + \dots \tag{3.52}$$

The central charge can thus be obtained by analyzing the finite-size corrections to the groundstate energy, while the critical exponents can be measured from the scaled energy gaps.

From the scaling form of the Hamiltonian, the partition function can be expressed as

$$Z = \lim \mathrm{Tr}\ \mathrm{e}^{-\beta H} = \mathrm{e}^{-\beta(Le_\infty + e_\infty^S)}\mathrm{Tr}\ q^{L_0 - c/24}, \tag{3.53}$$

with $q = \mathrm{e}^{-\beta v_F \pi/L}$. We therefore see that the partition function contains a universal part that takes the form of a Virasoro character $\mathrm{Tr}\ q^{L_0 - c/24}$. A similar formula holds for the partition function of a $2D$ statistical model on a strip.

3.3.2 Critical exponents, Kac modules and lattice Virasoro modes

It is not clear how the continuum limit can be taken in a mathematically rigorous way for any $\mathfrak{q}$, but roughly speaking, we take the eigenvectors of H in the spin-chain that have low-energy eigenvalues only, and we expect that the inner products among these vectors can be made to tend to some limits. Moreover, if we focus on long

4. Note also that for periodic systems, we have the scaling $H = Le_\infty + \frac{2\pi v_F}{L}\left(L_0 + \bar{L}_0 - \frac{c}{12}\right) + \dots$.

wavelength Fourier components of the set of local generators e_j, we expect their limits to exist, and their commutation relations to tend to those of the Virasoro generators L_n (this was shown explicitly for free fermion systems: for the Ising chain in [131, 132], and for the XX model in [118]). Then, the modules over the TL algebra restricted to the low-energy states become, now in the scaling limit [5], modules over the Virasoro algebra at appropriate central charge.

As an example, let us discuss how the TL standard modules become Kac modules (see Sec. 2.5) over the Virasoro algebra when the scaling limit is taken [67]. As discussed in the previous section, all our models (XXZ, SUSY) can be decomposed onto TL standard modules, only the multiplicities are different (and the logarithmic features!). As far as critical exponents are concerned, it is therefore enough to understand the spectrum of standard modules only. For $\mathfrak{q} = \mathrm{e}^{\frac{i\pi}{p+1}}$ ($p \in \mathbb{R}$ here), the low-energy excitations are described by a CFT with central charge $c = 1 - \frac{6}{p(p+1)}$. Using Bethe ansatz and keeping only low-lying excitations, it can be then shown that the spectrum generating function of the module $\mathsf{S}_j[L]$ has the following limit [67]

$$K_{1,1+2j} \equiv \lim_{L\to\infty} \sum_{\text{states } i} q^{\frac{L}{\pi v_F}\left(E_i(L) - L e_\infty - e_\infty^S\right)} = q^{-c/24}\, \frac{q^{h_{1,1+2j}} - q^{h_{1,-1-2j}}}{\prod_{n=1}^{\infty}(1-q^n)}, \tag{3.54}$$

where $v_F = \frac{\pi \sin\gamma}{\gamma}$ is the Fermi velocity, $2\cos\gamma = \mathfrak{q} + \mathfrak{q}^{-1} = n$ is the fugacity of a loop, $E_i(L)$ is the eigenvalue of the i^{th} (counted from the vacuum) eigenstate of $H = -\sum_i e_i$, e_∞^S is the non-universal surface energy, and $e_\infty = \lim_{L\to\infty} E_0(L)/L$ is the non-universal bulk energy, with $E_0(L)$ the groundstate energy. The latter can be computed by Bethe ansatz [133], and reads [6]

$$e_\infty = \sin^2\gamma \int_{-\infty}^{+\infty} \frac{\mathrm{d}x}{\cosh \pi x}\, \frac{1}{\cosh 2\gamma x - 2\cos\gamma}. \tag{3.55}$$

As the notations suggest, $K_{1,1+2j}$ corresponds to the scaling limit of (3.31) with $q = \mathrm{e}^{-\pi v_F M/L}$ and $M \gg L$.

The expression on the right-hand side of (3.54) coincides with the Virasoro character $\mathrm{Tr}\, q^{L_0 - c/24}$ of the *Kac module* $\mathcal{K}_{1,1+2j} \equiv \mathcal{V}_{h_{1,1+2j}}/\mathcal{V}_{h_{1,-1-2j}}$ with conformal weight $h_{1,1+2j}$. In other words, the scaling limit of the standard module S_j is described by the Kac operator (see 2.2.1) $\Phi_{1,1+2j}$, which is degenerate at level $h_{1,-1-2j} = h_{1,1+2j} + 1 + 2j$ (see also Fig. 3.8). These fields are called watermelon $2j$-leg operators, as they effectively create j FK clusters ($2j$ polymers/strings) in the Potts geometrical language [7]. We will study these operators in more detail in chapter 5. We also remark that these exponents can be computed within the Coulomb Gas setup, as our loop model can be mapped onto a height model which in turn renormalizes towards a free boson theory

5. The two notions – continuum and scaling limits – are essentially the same.

6. We mention this formula as it will be especially important for eq. (3.56).

7. Obviously, if we think in terms of the Potts model, j must be integer as loops correspond to the boundary of FK clusters. However, one can still consider operators creating an odd number of polymers (j half-integer) in the dense loop model even if they do not correspond to something meaningful in the Potts model.

with background charge (see *e.g.* [134, 135]). In this framework, watermelon operators correspond to magnetic excitations.

We already see at the level of generating functions and characters that we have a deep correspondence between the TL and Virasoro algebras in the scaling limit, where the (properly rescaled) Hamiltonian H becomes the L_0 generator. As mentioned above, it is even possible to construct other Fourier modes by taking appropriate combinations of TL generators on the lattice that will tend (in a sense that can be made rigorous in some cases) to other Virasoro generators L_n in the limit [118, 132]. Thanks to different techniques (numerical or analytical whenever possible) it can be shown that the lattice operators

$$L_n^{(L)} = \frac{L}{\pi}\left[-\frac{1}{v_F}\sum_{k=1}^{L-1}(e_k - e_\infty)\cos\left(\frac{nk\pi}{L}\right) + \frac{1}{v_F^2}\sum_{k=1}^{L-2}[e_k, e_{k+1}]\sin\left(\frac{nk\pi}{L}\right)\right] + \frac{c}{24}\delta_{n,0}, \tag{3.56}$$

become the Virasoro modes L_n in the continuum limit $L \to \infty$.

We note in passing that the knowledge of $K_{1,1+2j}$ is enough to compute the partition function of all our models. For instance for the XXZ spin chain, using (3.33), we obtain

$$Z_{\mathrm{XXZ}} = \lim \mathrm{Tr}\ \mathrm{e}^{-\beta(H_{\mathrm{XXZ}} - Le_\infty - e_\infty^S)} = q^{-c/24}\ \sum_{j=0}^{\infty}(2j+1)\frac{q^{h_{1,1+2j}} - q^{h_{1,-1-2j}}}{\prod_{n=1}^{\infty}(1-q^n)}, \tag{3.57}$$

with $q = \mathrm{e}^{-\beta v_F \pi/L}$, whereas for say, a dense loop gas on an annulus of width L and lenth M, the universal part of the partition function reads

$$Z_{\mathrm{loop}}^{\mathrm{CFT}} = q^{-c/24}\ \sum_{j=0}^{\infty}[2j+1]_{\mathfrak{q}}\frac{q^{h_{1,1+2j}} - q^{h_{1,-1-2j}}}{\prod_{n=1}^{\infty}(1-q^n)}, \tag{3.58}$$

where this time $q = \mathrm{e}^{-M\pi/L}$. As a highly non-trivial check, one can observe that $Z_{\mathrm{loop}}^{\mathrm{CFT}} = 1$ for percolation ($\mathfrak{q} = \mathrm{e}^{i\pi/3}$), as expected. This algebraic way to compute partition function is extremely powerful, as once the spectrum of standard modules in under control, the only things that make our various models different from the point of view of the partition function are the multiplicities.

3.3.3 Hilbert space structure and bimodules in the limit

Having now the algebraic structure of the spin-chain for finite L at hands, we can analyze its behavior in the limit $L \to \infty$. It is clear that the symmetry algebra of the Hamiltonian densities also provides a symmetry of the low-lying part of spectrum of the Hamiltonian.The symmetry algebra in the scaling limit, which commutes now with the Virasoro algebra, must thus be at least as large as that of finite-L chains. The only difference in the limit is that we now admit arbitrarily high values of the $U_{\mathfrak{q}}s\ell(2)$ spins. For example, the decomposition of the open XXZ spin-chain as a bimodule over the pair $(TL_{\mathfrak{q},L}, U_{\mathfrak{q}}s\ell(2))$ of commuting algebras, like in Fig. 3.7, goes over in the scaling

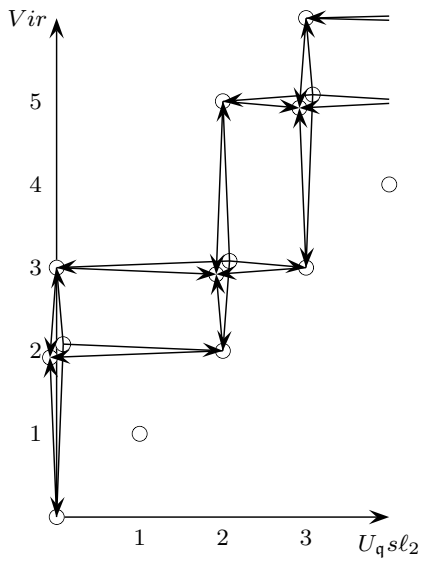

Figure 3.9: Bimodule for boundary percolation ($p = 3$ or $c = 0$) showing the commuting action of the Virasoro algebra and the quantum group $U_{\mathfrak{q}}s\ell(2)$ (see [69]).

limit to a semi-infinite ('staircase') bimodule over the Virasoro algebra with central charge $c = 1 - \frac{6}{p(p+1)}$. This is illustrated in Fig. 3.9 for the example of percolation, where the same comments as in the finite chain apply exactly, with the replacement of $TL_{\mathfrak{q},L}$ by the Virasoro algebra. Using the correspondence between the irreducible TL modules X_j and irreducible Virasoro modules with weight $h_{1,2j+1}$, which holds at least at the level of characters, we obtain complicated indecomposable Virasoro modules that turn out to coincide with Virasoro staggered modules. Note also that in some cases, it is possible to observe the quantum group symmetry directly in the continuum limit [136, 137].

While the scenario described above has not been analytically established for general models, it is confirmed *a posteriori* by the validity of the results (structure of Virasoro modules and their fusion) obtained using the bimodule structure [69, 72]. Of course, in some special cases, such as free theories, much more can be said. For instance, the symplectic fermions CFT arising in the scaling limit of the XXZ spin-chains at the free fermion point ($n = 0$ or $\mathfrak{q} = i$) can be analyzed independently of the lattice results. Recall that the symplectic fermions theory action involves two fermionic fields of dimension 0, and has Noether's currents generating a global $SU(2)$ symmetry [52]. Together with the fermionic zero modes, we obtain the full symmetry algebra of operators commuting with the Virasoro algebra. It turns out that this symmetry algebra is realized by a representation of the quantum group $U_{\mathfrak{q}}s\ell(2)$ at $\mathfrak{q} = i$, see [118]. The full Hilbert space in such chiral LCFT can then be decomposed onto indecomposable Virasoro modules and its symmetry algebra, with precisely the same result as in the $\mathfrak{q} = i$ analog of Fig. 3.9 (see [69]). As mentioned earlier, it is even possible to show [118, 138] that the lattice regularizations $L_n^{(L)}$ of the Virasoro modes indeed converge to the well-known [52] symplectic fermions representation of the L_n generators.

3.3.4 Virasoro staggered modules from the lattice

As discussed in Sec. 3.3.2, the continuum limit of the XXZ spin chain at $\mathfrak{q} = \mathrm{e}^{\frac{i\pi}{p+1}}$ is described by a CFT with central charge $c = 1 - \frac{6}{p(p+1)}$. In particular, the generating functions of energy levels on the standard modules S_j of the TL algebra at $\mathfrak{q} = \mathrm{e}^{\frac{i\pi}{p+1}}$ give in the limit the characters of the Kac modules $\mathcal{K}_{1,2j+1}$ over the Virasoro algebra. This correspondence does not end at the level of Kac modules, as the indecomposable structure (3.41) of the TL standard modules mimics exactly that of the corresponding Kac modules $\mathcal{K}_{1,2j+1}$ in the limit. In particular, the operator content of the TL irreducible modules is given by a formula similar to (3.42) that coincides with the Rocha–Caridi formula for the irreducible characters (see Sec. 2.5.2, see also the very useful appendix in [139] for Virasoro characters).

Furthermore, using our semi-infinite bimodules (see Fig. 3.9 in the example of percolation), we can extract Virasoro modules keeping only the vertical arrows. We then obtain the following diamond-shape diagram for indecomposable Virasoro modules, for $j \bmod p \neq \frac{k(p+1)-1}{2}$ with $k = 0, 1$,

$$\mathcal{P}_{1,2j+1}: \qquad \begin{array}{ccc} & h_{1,2j+1} & \\ \swarrow & & \searrow \\ h_{1,2j'-1} & & h_{1,2(j'+p+1)-1} \\ \searrow & & \swarrow \\ & h_{1,2j+1} & \end{array} \qquad \text{for} \quad j \geq \tfrac{p+1}{2}, \tag{3.59}$$

where $j' = (j+t(j)(p+1))-2(j \bmod (p+1))$ and the function $t(j)$ was defined in (3.43). Irreducible Virasoro subquotients are denoted by their conformal weights $h_{1,j}$, as usual in this thesis. This diagram (3.59) is a 'gluing' of two indecomposable Kac modules: the one in the top composed of irreducibles with $h_{1,2j+1}$ and $h_{1,2(j'+p)-1}$ is the quotient $\mathcal{K}_{1,2j+1} = \mathcal{V}_{h_{1,2j+1}}/\mathcal{V}_{h_{1,-2j-1}}$, while the second Kac module in the bottom corresponds to $\mathcal{K}_{1,2j'-1}$. To summarize, we have

$$\mathsf{S}_j \underset{L\to\infty}{\longrightarrow} \mathcal{K}_{1,2j+1} = \mathcal{V}_{h_{1,2j+1}}/\mathcal{V}_{h_{1,-2j-1}}, \tag{3.60}$$

$$\mathsf{T}_j \underset{L\to\infty}{\longrightarrow} \mathcal{P}_{1,2j+1}. \tag{3.61}$$

We therefore see that the staggered Virasoro modules for different central charges abstractly discussed in Sec. 2.5 can quickly be recovered from the lattice – at least their subquotient structure can be deduced from our spin chain analysis. If we add on top of that the conjectured Koo–Saleur formula (3.56) for the Virasoro generators, this opens the way to measuring [71, 140] indecomposability parameters characterizing these Virasoro representations completely. This will be discussed further in the following.

3.3.5 Some consequences of the bimodule structure: differential equations

It is a natural question to wonder which of the fields that appear in our (yet chiral) theories satisfy differential equations, and what physical meaning they have. We shall focus on the percolation theory ($\mathfrak{q} = \mathrm{e}^{i\pi/3}$), although the following considerations are completely general. From the geometrical point of view, the fields $\Phi_{1,1+2j}$ are degenerate at level $h_{1,-1-2j} = h_{1,1+2j} + 1 + 2j$, and they correspond to the insertion of $2j$ legs at the boundary. The correlation functions of these fields can be determined solving differential equations from the null-vector condition, and they have a clear geometrical meaning. For example, the differential equation satisfied by the four-point function of $\Phi_{1,2}$ yields Cardy's formula for percolation [25]. Note that these fields correspond to what we called Kac operators in the previous chapter (see 2.2.1).

Now where are these fields in the spectrum of our model? Let us consider the spectrum of the XXZ spin chain at $\mathfrak{q} = \mathrm{e}^{i\pi/3}$ (or of the $\mathfrak{sl}(2|1)$ spin chain) with the Hilbert space structure given by Fig. 3.9. The fields that satisfy the differential equations are on the diagonal of this diagram, they are either in simple (irreducible) modules or they correspond to the 'left' field ξ_j in the indecomposable diamond modules (2.104). For example, let us consider the first (Virasoro) Jordan cell in Fig. 3.9 at $j = 0$ for $U_\mathfrak{q} s\ell(2)$. The stress energy tensor and its logarithmic partner t live in this module, and we also impose $L_{-1}I = \partial I = 0$ which is the first example of operator in the theory satisfying a (trivial) differential equation. It is clear that we have the same kind of equations for all the fields in the diagonal of Fig. 3.9, as they correspond to the top of the left Kac module. For example, there are three different (up to multiplicities) fields with conformal weight $h = 2$ in the theory: T,t and what we would like to call $\Phi_{1,5}$. The latter corresponds to the field (2,2) in Fig. 3.9. It satisfies $B_{1,5}\Phi_{1,5} = 0$ (we recall that the operator $B_{1,r}$ was defined in (2.111)), or more explicitly

$$\left(L_{-1}^5 - \frac{40}{3}L_{-2}L_{-1}^3 + \frac{256}{9}(L_{-2}^2 L_{-1} - L_{-3}L_{-2}) + \frac{52}{3}L_{-3}L_{-1}^2 - \frac{104}{3}L_{-4}L_{-1} + \frac{208}{9}L_{-5}\right)\Phi_{1,5} = 0. \quad (3.62)$$

The correlation function $\langle\Phi_{1,5}\Phi_{1,5}\Phi_{1,5}\Phi_{1,5}\rangle$ can thus be computed – in principle! – using the corresponding differential equation.

It is worth mentioning that because of the "horizontal" $U_\mathfrak{q} s\ell(2)$ symmetry, the stress energy tensor should also satisfy $B_{1,5}T = 0$! This can indeed be checked using Virasoro commutation relations along with $L_{-1}I = 0$. This is one example of application of this bimodule structure – the observations of Ref. [141] that null-vector conditions "factorize" are thus quite natural thanks to this quantum group language. This property obviously extends to all the other Jordan cells. For example, it is quite straightforward to check that because of $B_{1,7}\Phi_{1,7} = 0$ (this corresponds to the field with coordinates (3,3) in Fig. 3.9), we have $B_{1,7}\phi_{j=3} = 0$, with $\phi_{j=3} = (L_{-3} - L_{-2}L_{-1} + \frac{1}{6}L_{-1}^3)\Phi_{1,5}$ is the null field (2,3) in Fig. 3.9. Once again, to prove this, we need the property $B_{1,5}\Phi_{1,5} = 0$.

N	b_{perco}	N	b_{poly}
10	-0.605858	4	0.021029
12	-0.606403	6	0.145101
14	-0.607775	8	0.276585
16	-0.609226	10	0.382046
18	-0.610561	12	0.463292
20	-0.611738	14	0.526436
22	-0.612764		
∞	-0.6249 $\pm$ 0.0005	∞	0.9 $\pm$ 0.1
Exact	-5/8 = -0.625	Exact	$5/6 \simeq 0.8333$

Table 3.1: Numerical measure of the b parameter in percolation and polymers with free boundary conditions.

3.4 Lattice indecomposability parameters

While the analysis of symmetries of the lattice models provides information about the general structure of the Virasoro indecomposable modules, getting more detailed information about the action of the Virasoro generators in these modules—such as the numerical values of the indecomposability parameters—is more challenging. Recall that Virasoro staggered modules are characterized by universal numbers called logarithmic couplings or indecomposability parameters (see chapter 2). Indecomposability parameters are universal, and they are believed to play an important role in physical applications of LCFTs. They can be defined rather abstractly [57, 59] as parameters crucial for characterizing the staggered modules completely, or they can be thought of as universal coefficients that appear in front of logarithmic singularities in correlation functions of fields living in such modules.

Although the method is completely general, we will focus here on the celebrated b-number that characterizes the logarithmic structure associated with the stress energy tensor at $c = 0$ (see Sec. 2.2). Recall that the parameter b can be expressed as $b = \langle T|t\rangle$, where $|t\rangle$ is normalized such that $L_0 |t\rangle = 2|t\rangle + |T\rangle$. This b parameter has attracted a lot of attention since it was introduced by Gurarie, and computing the values allowed for the parameter b in any given $c = 0$ conformal field theory, for example the LCFT describing the transition between plateaus in the IQHE, remains an interesting open problem. For simple $c = 0$ theories, namely Self-Avoiding Walks (SAWs also known as dilute polymers) or percolation, b is now known both in bulk and boundary CFTs [57, 75]. It is important to realize that despite this explicit definition, the measure of b in a concrete lattice model is quite involved. For example, even though the expectation value of t on a strip of width L satisfies

$$\langle t\rangle = \frac{\pi b}{12L^2}, \tag{3.63}$$

making it look like that the measure of b might be very similar to the measure of the central charge, measuring b is extremely difficult *a priori*: what is t actually? How to normalize it properly?

In spite of these difficulties, b can indeed be directly measured on the lattice, just like the central charge or the conformal dimensions, but using a rather intricate method. For percolation ($\mathfrak{q} = \mathrm{e}^{i\pi/3}$) for example, the logarithmic structure for the stress-energy tensor corresponds on the lattice to a Jordan cell involving the state $\left|T^{(N)}\right\rangle$ corresponding [8] to $T(z)$ in the spectrum of the Hamiltonian $H = -\sum_{i=1}^{L-1} e_i$. We normalize the states such that in the basis $(\left|T^{(L)}\right\rangle, \left|t^{(L)}\right\rangle)$, the Hamiltonian reads

$$H^{(L)} - E_0(L)\mathbb{I} = \frac{\pi v_F}{L} \begin{pmatrix} h^{(L)} & 1 \\ 0 & h^{(L)} \end{pmatrix}, \tag{3.64}$$

where $E_0(L)$ is the groundstate energy and $h^{(L)} = \frac{L}{\pi v_F}(E(L) - E_0(L))$, with $\lim_{L\to\infty} h^{(L)} = 2$. This Jordan cell appears because H is not diagonalizable on the Temperley-Lieb tilting module T_2 described by (3.46)

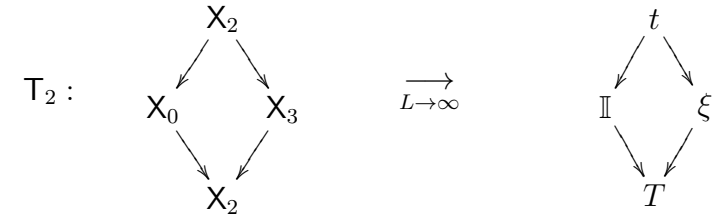

In the scaling limit, this representation goes to a Virasoro staggered module where the state t lives at the top and $T = L_{-2}\mathbb{I}$ at the bottom (we loosely denote the Virasoro simple modules by the corresponding field). Note that the field ξ has dimension $h_{1,7} = 5$. This staggered module is known to be characterized by a number $b = \langle T|t\rangle = -\frac{5}{8}$ from algebraic methods [57]. It is interesting to check this result directly on the lattice. This was first done in [140] using a beautiful trick unfortunately restricted to $c = 0$, and generalized to many other cases in [71]. The idea is to compute the inner product $\langle T|t\rangle$ on the lattice, the main issue being the proper normalization of $\left|T^{(N)}\right\rangle$ which is non-trivial because $\left\langle T^{(N)}|T^{(N)}\right\rangle = \langle T|T\rangle = 0$ exactly. As we will explain here, a proper normalization is provided by a regularization of the stress energy tensor given by the lattice versions $L_n^{(N)}$ of the Virasoro modes (3.56).

There are two crucial steps to measure indecomposability parameters on the lattice: identifying a lattice inner product that will go to the Virasoro bilinear form in the limit, and properly normalizing the null state $|\phi\rangle$ on the lattice ($|T\rangle$ in our example). The Virasoro form on the lattice can be regularized in terms of the TL inner product (non-definite positive!) defined by $e_i^\dagger = e_i$. More precisely, it is given by:

XXZ: The inner product is the usual bilinear form on $\mathbb{C}$ without complex conjugation, that is, treating $\mathfrak{q}$ as a formal parameter. For example, on $L = 4$ sites, the vector

8. $\left|T^{(L)}\right\rangle$ is the only state corresponding to the conformal weight $h = 2$ in the vacuum sector.

$|\phi\rangle = |\uparrow\uparrow\downarrow\downarrow\rangle + \mathfrak{q}\,|\uparrow\uparrow\uparrow\uparrow\rangle$ has norm $\langle\phi|\phi\rangle = 1 + \mathfrak{q}^2$. Note that if we had considered the usual inner product on $\mathbb{C}$, we would have found $1 + |\mathfrak{q}|^2$ instead.

LOOP: The correct inner product is obtained gluing the mirror image of the first state on top of the second one. Each closed loop carries a weight $n = \mathfrak{q} + \mathfrak{q}^{-1}$. This is of course the usual form used in Temperley-Lieb representation theory. For instance, the scalar product between the two states $|\alpha\rangle = |$  $\rangle$ and $|\beta\rangle = |$  $\rangle$ is $\langle\alpha|\beta\rangle =$ $\langle$  $|$  $\rangle =$ $= n$. The case with a non-zero number of strings $2j$ is treated in a similar fashion. We have not talked much about the case of dilute models, but a loop models can be defined in a similar fashion except that we now allow for empty sites. In the case of the dilute $O(n)$ model, the inner product between two states is chosen to be zero if the empty sites (marked as dots) are not the same. For example for $L = 6$, $\langle$  $|$  $\rangle = \langle$$|$$\rangle = n$, whereas $\langle$  $|$  $\rangle = 0$.

SUSY: We use the usual inner product in Fock space. There are negative norm states because of the use of the dual representation. For example, let us consider the $\mathfrak{sl}(2|1)$ case still on $L = 4$ sites. The important point here is that each site must be occupied by one particle which can be either a fermion $\{f_i, f_j^\dagger\} = (-1)^{i+1}\delta_{ij}$, or a Schwinger boson $[b_{i,\sigma}, b_{j,\sigma'}^\dagger] = \delta_{ij}\delta_{\sigma\sigma'}$, with $\sigma \in \{\uparrow, \downarrow\}$. Let us consider the state $|\phi\rangle = b_{1\uparrow}^\dagger f_2^\dagger b_{3\downarrow}^\dagger b_{4\uparrow}^\dagger\,|0\rangle$. Its norm is $\langle\phi|\phi\rangle = \langle 0|\, b_{4\uparrow} b_{3\downarrow} f_2 b_{1\uparrow} b_{1\uparrow}^\dagger f_2^\dagger b_{3\downarrow}^\dagger b_{4\uparrow}^\dagger\,|0\rangle = -1$ because of the fermionic operator $f_2^\dagger$ of the dual representation which satisfies $\{f_2, f_2^\dagger\} = -1$.

The second step is the proper normalization of $\left|T^{(L)}\right\rangle$. This is achieved using the Koo-Saleur formula (3.56). Let us define

$$b^{(L)} = \frac{\left|\left\langle t^{(L)}\right| L_{-2}^{(L)} \left|0^{(L)}\right\rangle\right|^2}{\langle t^{(L)}|T^{(L)}\rangle}, \tag{3.65}$$

where $\left|0^{(L)}\right\rangle$ is the groundstate of the system, and $L_{-2}^{(L)}$ is given by (3.56). It is easy to see that this quantity does not depend on the normalization of $\left|T^{(L)}\right\rangle$, and that it provides a lattice version of b.

The various steps to compute b can thus be summarized in the following way:

1. Using exact diagonalization methods, find a Jordan basis for the first few excitations of H on $L = 2N$ sites.
2. Identify a Jordan cell in the spectrum of H and normalize the states like in eq. (3.64).
3. Also identify the (ground)state $\left|0^{(L)}\right\rangle$ and normalize it such that $\left\langle 0^{(L)}|0^{(L)}\right\rangle = 1$ for the lattice inner product.
4. Using Virasoro generators on the lattice (3.56), construct the operator $L_{-2}^{(L)}$.
5. Compute $b^{(L)}$ using eq. (3.65).

The value of the indecomposability parameter $b = \lim_{L\to\infty} b^{(L)}$ is then computed using an extrapolation $b^{(L)} = b + A/L + B/L^2 + \ldots$ We find numerically that $b^{(L)}$ does not depend on the chosen Temperley-Lieb representation (Loop, XXZ, or SUSY).

Numerical results are given in Tab. 3.1, and are in good agreement with the expectation $b = -\frac{5}{8}$. We also show the result for the dilute polymers theory ($b = \frac{5}{6}$). Note that the method presented here is completely general and can in principle be applied to the computation of any indecomposability parameter [71].

Despite the numerical success of the approach outlined above, it unfortunately remains unclear to what extent it provides an accurate way to measure indecomposability parameters – that is, whether the numbers we measure are truly indecomposability parameters, or numbers very close numerically to indecomposability parameters. As discussed in [132] on the example of the central charge, the order of the limits when using the Koo-Saleur formula (3.56) is crucial. The formula is conjectured to hold only when the field theory scaling limit is respected: one wants to keep the number of scaling fields M fixed while taking the continuum limit $L \to \infty$, compute the matrix elements of Virasoro operators in that basis of M fields, and then, take the limit $M \to \infty$. The problem is that, for interacting theories, lattice Virasoro generators (3.56) will typically couple scaling fields to non-scaling ones on the lattice, thus maybe producing residual corrections to scaling matrix elements such as indecomposability parameters when naively taking the scaling limit. These fundamental considerations are of course almost metaphysical, as numerically one need not worry about the order of the limits to obtain a very good accuracy on indecomposability parameters.

3.5 Lattice fusion rules

To conclude this chapter on lattice regularizations of LCFTs, we now describe a procedure allowing to compute fusion rules on the lattice [68, 69, 72]. The procedure was outlined in [68], and also developed independently by Pearce, Rasmussen and Zuber in [70] and in *e.g.* [142, 143].

3.5.1 Fusion on the lattice and in the continuum

The lattice fusion that we are going to present here was introduced in [68, 69], and studied in details in [72]. The idea is that fusion corresponds to joining two spin chains, each one carrying a representation of the TL algebra, by acting with an additional TL generator at their junction. In the scaling limit, those lattice representations will eventually become representations of the group of conformal transformations in the interior of the strips. In a more mathematical language, fusion can be thought of as an induction process. Because of the additional TL generator that will join the two spin chains, or any pair of TL modules, one expects a single copy of the conformal group to emerge, which contains the tensor product of the conformal groups associated with the two initial strips. Therefore, the induction process over the Temperley-Lieb algebra corresponds, in the continuum limit, to the induction over the group of conformal transformations in the corresponding regions. Hence, fusion is related to a slit-strip geometry (see Fig. 3.10) that can be mapped by a Schwarz–Christoffel transformation [144] onto the upper half plane, where both sides and the slit of the strip are mapped onto the real line. Then, the incoming and outcoming states correspond to

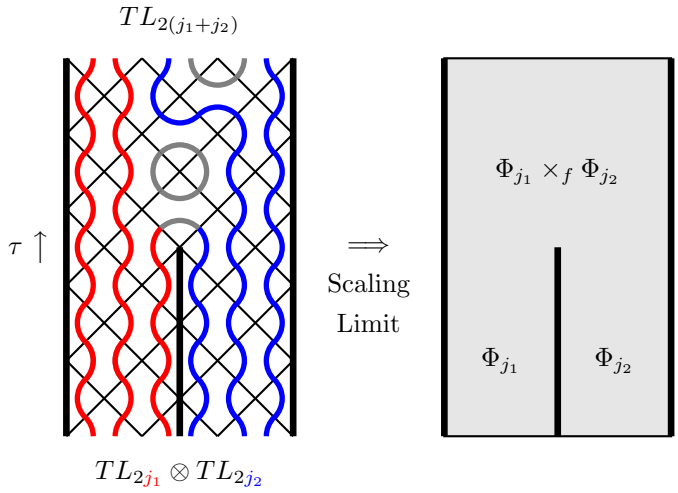

Figure 3.10: Physical interpretation of the lattice fusion of two standard TL modules $\mathsf{S}_{j_1}[L_1]$ and $\mathsf{S}_{j_2}[L_2]$ (in the picture, $L_1 = 2j_1$ and $L_2 = 2j_2$ so that both standard modules are one-dimensional). Fusion can then be seen as an event in imaginary time τ, consisting in "joining" the two standard modules by acting with an additional TL generator (induction procedure). In the scaling limit, we expect this construction to coincide with the usual fusion procedure or OPE of boundary fields, here $\Phi_{j_1} = \Phi_{1,1+2j_1}$ and $\Phi_{j_2} = \Phi_{1,1+2j_2}$, living in the corresponding Virasoro modules.

fields localized at points on the boundary of the half plane. One can then recover the usual interpretation of the fusion as OPE of the boundary fields.

Formally, the fusion associates with any pair of modules over the algebras $TL_{\mathfrak{q},L_1}$ and $TL_{\mathfrak{q},L_2}$ a module over the bigger algebra $TL_{\mathfrak{q},L_1+L_2}$. Let M_1 and M_2 be two modules over $TL_{\mathfrak{q},L_1}$ and $TL_{\mathfrak{q},L_2}$ respectively, with the same fugacity n. Then, the tensor product $M_1 \otimes M_2$ is a module over the product $TL_{\mathfrak{q},L_1} \otimes TL_{\mathfrak{q},L_2}$ of the two algebras. We note that this product of algebras is naturally a subalgebra in $TL_{\mathfrak{q},L_1+L_2}$. *The fusion* $\times_f$ of two modules M_1 and M_2 is then defined as the module induced from this subalgebra, *i.e.*

$$M_1 \times_f M_2 = TL_{\mathfrak{q},L_1+L_2} \otimes_{TL_{\mathfrak{q},L_1} \otimes TL_{\mathfrak{q},L_2}} M_1 \otimes M_2, \tag{3.66}$$

where the balanced product $\otimes_A$ (of right and left modules) over an algebra A is defined as a quotient of the usual tensor product by the relations $v_1 \triangleleft a \otimes v_2 = v_1 \otimes a \triangleright v_2$ for all $a \in A$, where the left and right actions of A are denoted by $\triangleright$ and $\triangleleft$, respectively. In simple words, we simply allow any element from A to pass through the tensor-product symbol from right to left and *vice versa*. For any pair of left modules M_1 and M_2 over $TL_{\mathfrak{q},L_1}$ and $TL_{\mathfrak{q},L_2}$ we shall call *fusion rules* the decomposition of the induced module into indecomposable direct summands.

When $\mathfrak{q}$ is not a root of unity, it is quite easy to convince oneself that the fusion

rules for the TL standard modules follow a simple $s\ell(2)$ spin addition rule

$$\mathsf{S}_{j_1}[L_1] \times_f \mathsf{S}_{j_2}[L_2] = \bigoplus_{j=|j_1-j_2|}^{j_1+j_2} \mathsf{S}_j[L_1+L_2], \tag{3.67}$$

for $2j_1 \leq L_1$ and $2j_2 \leq L_2$. This relation to $s\ell(2)$ is not a coincidence of course and is related to the centralizing property with $U_{\mathfrak{q}}s\ell(2)$ with a dual construction [68, 69, 72] – the quantum-group fusion. A direct argument for (3.67) is given by considering the geometric interpretation of the induced module $\mathsf{S}_{j_1}[L_1 = 2j_1] \times_f \mathsf{S}_{j_2}[L_2 = 2j_2]$ in terms of link diagrams. This module is composed of (or filtered by) subspaces indexed by the number j of through-lines which obviously takes integer values from $|j_1 - j_2|$ up to $j_1 + j_2$. Then, using a semi-simplicity argument we deduce the direct sum decomposition (3.67). For other values of L_1 and L_2, the decomposition can be shown in a similar way. We note that a rigorous derivation of the generic fusion (3.67) can be found in section 4 of [72].

Let us reformulate this result in a language more familiar to physicists. Using the correspondence between standard modules and Virasoro Kac modules, this generic fusion corresponds to

$$\Phi_{1,1+2j_1} \times_f \Phi_{1,1+2j_2} = \sum_{j=|j_1-j_2|}^{j_1+j_2} \Phi_{1,1+2j}, \tag{3.68}$$

where $\Phi_{1,1+2j}$ has conformal weight $h_{1,1+2j}$.

3.5.2 $c \to 0$ catastrophe on the lattice

When $\mathfrak{q}$ is a root of unity things become much more complicated and one encounters once again indecomposability. As an example, let us discuss how the $c \to 0$ catastrophe (see section 2.2) manifests itself on the lattice.

Let us consider the fusion $\mathsf{S}_1[2] \times_f \mathsf{S}_1[2]$, where $\mathsf{S}_1[2]$ has the basis $\{\,|\,|\,\}$ with $e_1\,|\,| = 0$. The induction results in a six-dimensional $TL_{\mathfrak{q},4}$-module with the basis

$$\mathsf{S}_1[2] \times_f \mathsf{S}_1[2] = \langle\, l,\, e_2l,\, e_1e_2l,\, e_3e_2l,\, e_1e_3e_2l,\, e_2e_1e_3e_2l \,\rangle, \tag{3.69}$$

with $l = |\,| \otimes |\,|$. This module is decomposed for $\mathfrak{q}$ generic as

$$\mathsf{S}_1[2] \times_f \mathsf{S}_1[2] = \mathsf{S}_0[4] \oplus \mathsf{S}_1[4] \oplus \mathsf{S}_2[4], \tag{3.70}$$

where the two-dimensional invariant subspace $\mathsf{S}_0[4]$ is spanned by $e_1e_3e_2l$ and $e_2e_1e_3e_2l$ which may be identified with the link states $\cup\,\cup$ and $\cup\!\!\cup$, respectively. The invariant one-dimensional subspace $\mathsf{S}_2[4]$ is spanned, after solving a simple system of linear

equations, by

$$\mathrm{inv}(n) = l + \frac{1}{n^2-2}\Big(e_1e_2l + e_3e_2l - ne_2l + \frac{1}{n^2-1}(e_2e_1e_3e_2l - ne_1e_3e_2l)\Big), \qquad (3.71)$$

with $e_j\mathrm{inv}(n) = 0$, for $j = 1, 2, 3$. Moreover, three remaining linearly independent states contribute to the three-dimensional irreducible direct summand isomorphic to $\mathsf{S}_1[4]$ because the algebra is semisimple for generic $\mathfrak{q}$.

We see that the submodules $\mathsf{S}_0[4]$ and $\mathsf{S}_1[4]$ (or their basis elements) have a well-defined limit $n \to 1$ ($p = 2$, percolation) while the invariant $\mathrm{inv}(n)$ spanning $\mathsf{S}_2[4]$ is not defined in this limit – the state in (3.71) has a term diverging as $n \to 1$. As it turns out, this can be thought of as the lattice analog of the $c \to 0$ catastrophe (see section 2.2). The resolution of this lattice catastrophe was discussed in details in [72]. The idea is to introduce the new state

$$t(n) = \mathrm{inv}(n) - \frac{1}{(n^2-2)(n^2-1)}\big(e_2e_1e_3e_2l + a_-e_1e_3e_2l\big), \qquad (3.72)$$

with $a_- = -h_-(n) - n$ and $h_-(n) = -\frac{3n-\sqrt{8+n^2}}{2}$. It can be easily shown that the state $t(n)$ has a finite limit as $n \to 1$. Borrowing the terminology of LCFT, we say that the state t is the "logarithmic partner" of the "stress-energy tensor" $T =$  . Indeed, we find a Jordan cell between these two states

$$Ht = \frac{2}{3}T. \qquad (3.73)$$

We will also say that T is the "descendant" of the vacuum state $|0\rangle =$ 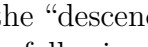 as the standard module S_0 has the following indecomposable structure at $n = 1$: $\mathsf{S}_0 = |0\rangle \to T$ where we recall that the arrow corresponds to the action of the TL algebra.

We see that the standard modules $\mathsf{S}_0[4]$ and $\mathsf{S}_2[4]$ arising in the generic fusion rules are "glued" together at $n = 1$ into a bigger indecomposable module with the TL action given by the diagram $t \to |0\rangle \to T$. The subquotient structure of this module reads $\mathsf{X}_2 \to \mathsf{X}_0 \to \mathsf{X}_2$, where each subquotient is one-dimensional and we recall that X_j denotes the irreducible top of $\mathsf{S}_j[N]$. We will denote the resulting module $\mathsf{T}_2[4]$; this is an example of tilting module (see section 3.3.4). Finally, the fusion rules at $n = 1$ reads

$$\mathsf{S}_1[2] \times_f \mathsf{S}_1[2] = \mathsf{S}_1[4] \oplus \mathsf{T}_2[4], \qquad \text{for } p = 2. \qquad (3.74)$$

In the scaling limit, the diamond T_2 module becomes a staggered module that contains T and its logarithmic partner t.

3.5.3 Systematic calculations and general results

Let us first go back to the fusion $\mathsf{S}_1[2]\times_f\mathsf{S}_1[2] = \langle\, l,\, e_2l,\, e_1e_2l,\, e_3e_2l,\, e_1e_3e_2l,\, e_2e_1e_3e_2l \,\rangle$. Note that the fusion states can be identified with link states in the following way:

$l =$  , $e_2 l =$  , $e_1 e_2 l =$  , $e_3 e_2 l =$  , $e_1 e_3 e_2 l =$  , and $e_2 e_1 e_3 e_2 l =$  . We use colors to keep track of the original algebras and their modules, red through-lines correspond to the left $\mathsf{S}_1[2]$ in $\mathsf{S}_1[2] \times_f \mathsf{S}_1[2]$ while the blue ones correspond to the right $\mathsf{S}_1[2]$. We only keep these colors for convenience but these are not really necessary as we can always split the through lines into two halves (the number of through lines is even in this case) and assign the red color to the leftmost ones while the other lines should be blue. One can then compute the action of the Temperley-Lieb generators on these states using the usual TL rules with a slight modification: when a Temperley-Lieb generator acts on two through lines with two different colors, it comes with a weight 1 instead of 0. In other words, one can fuse a red trough-line with a blue one with weight 1. For example, one has e_2  $=$  while e_1  $= 0$. With these rules in hand, the calculations become easy and can be done geometrically, we shall use these notations as they are less cumbersome. These rules also make transparent the equivalence with the approach based on integrable boundary conditions used by Pearce-Rasmussen-Zuber [70]. These two approaches actually correspond to the very same thing. It is indeed not hard to see that our construction with through-lines of two different colors, corresponds exactly to the so-called $(1, s)$ boundary conditions used in [70] (in the case we considered, to $(1, 2)$ conditions on both sides of a strip). However, the algebraic definition that we use provide a more powerful tool as it allows one to obtain exact and rigorous results for any finite size using quantum group results.

The Hamiltonian $H = -e_1 - e_2 - e_3$ in this basis reads

$$H = -\begin{pmatrix} 0 & 0 & 0 & 0 & 0 & 0 \\ 1 & n & 1 & 1 & 0 & 0 \\ 0 & 1 & n & 0 & 0 & 0 \\ 0 & 1 & 0 & n & 0 & 0 \\ 0 & 0 & 1 & 1 & 2n & 2 \\ 0 & 0 & 0 & 0 & 1 & n \end{pmatrix}. \tag{3.75}$$

It is of course also a simple matter to find the eigenvalues of H in the standard modules $\mathsf{S}_0[4]$, $\mathsf{S}_1[4]$ and $\mathsf{S}_2[4]$ on $N = 4$ sites. The Hamiltonian H applied to the one-dimensionnal module $\mathsf{S}_2[4]$ always yields 0. When $p = 3$, we find that $\mathsf{S}_0[4]$ corresponds to the eigenvalues $\{0, -3\}$ and $\mathsf{S}_1[4]$ to $\{-1, -1 - \sqrt{2}, -1 + \sqrt{2}\}$. Moreover, we find that H has the following Jordan form in the fusion basis

$$H = \begin{pmatrix} -3 & 0 & 0 & 0 & 0 & 0 \\ 0 & 0 & 1 & 0 & 0 & 0 \\ 0 & 0 & 0 & 0 & 0 & 0 \\ 0 & 0 & 0 & -1 & 0 & 0 \\ 0 & 0 & 0 & 0 & -1 - \sqrt{2} & 0 \\ 0 & 0 & 0 & 0 & 0 & -1 + \sqrt{2} \end{pmatrix}. \tag{3.76}$$

Using the subquotient structure $\mathsf{T}_2[4] = \mathsf{S}_2[4] \longrightarrow \mathsf{S}_0[4]$, we conclude that

$$\mathsf{S}_1[2] \times_f \mathsf{S}_1[2] = \mathsf{S}_1[4] \oplus \mathsf{T}_2[4], \qquad \text{for } p = 2, \tag{3.77}$$

in agreement with what we had found in the previous section.

We can repeat this easy calculation for the extended Ising model ($p = 3$), in which case we find that $\mathsf{S}_0[4]$ corresponds to the Hamiltonian eigenvalues $\{-\frac{3+\sqrt{5}}{\sqrt{2}}, \frac{1}{2}(\sqrt{10} - 3\sqrt{2})\}$ and $\mathsf{S}_1[4]$ to $\{0, -\sqrt{2}, -2\sqrt{2}\}$. We can infer the fusion rules from the Jordan form of H in the fusion basis

$$H = \begin{pmatrix} -2\sqrt{2} & 0 & 0 & 0 & 0 & 0 \\ 0 & -\sqrt{2} & 0 & 0 & 0 & 0 \\ 0 & 0 & 0 & 1 & 0 & 0 \\ 0 & 0 & 0 & 0 & 0 & 0 \\ 0 & 0 & 0 & 0 & -\frac{3+\sqrt{5}}{\sqrt{2}} & 0 \\ 0 & 0 & 0 & 0 & 0 & \frac{1}{2}(\sqrt{10} - 3\sqrt{2})\} \end{pmatrix}. \tag{3.78}$$

This is consistent with the fusion rule

$$\mathsf{S}_1[2] \times_f \mathsf{S}_1[2] = \mathsf{S}_0[4] \oplus \mathsf{T}_2[4], \qquad \text{for } p = 3, \tag{3.79}$$

where $\mathsf{T}_2[4] = \mathsf{S}_2[4] \longrightarrow \mathsf{S}_1[4]$ in this case.

These are just two examples of a lattice fusion rule, in good agreement with what is expected on the field theory side. Using the bimodule structure of the spin chains and algebra involving quantum group results (see [137]), it is actually possible to obtain rigorous, general results for the lattice fusion of most of Temperley-Lieb modules [72] for all roots of unity $\mathfrak{q}$, for any sizes L_1 and L_2. The physical consequences for the OPEs were also discussed in [72]. The general results are quite cumbersome, so we refer the reader to that reference for details.

Chapter 4

Blob algebra, braid translator and bulk LCFTs

In the previous section, we have analyzed in detail the simplest case of critical lattice models providing regularization of boundary LCFTs. These spin chains or loop models were built out of representations of the Temperley-Lieb algebra, and are described in the scaling limit by Kac and staggered Virasoro modules. However, this is not the end of the story, and one could wonder if it is possible to construct a lattice algebra, larger than TL, that would have representations that would correspond generically to Verma modules instead of Kac representations. The answer to that question is yes and is provided by the so-called blob algebra [145]. The critical exponents of the corresponding boundary dense loop models were computed in [146], and the full algebraic analysis including the relation to Virasoro was worked out slightly after in [74]. This lattice construction provides new indecomposable representations which are much more intricate than their diamond-shaped counterparts that appear as limits of TL representations. These representations were fully classified – and conjectured to exhaust the indecomposable modules relevant for physics in the case where Virasoro in the only symmetry – in [74]. This will be discussed in section 4.1.

Another very important open problem in the field is to understand the structure of non-chiral, bulk, LCFTs. While the case of boundary LCFTs is slowly getting under control, the understanding of the bulk case remains in its infancy. The main problem here, from the continuum point of view, is the expected double indecomposability of the modules over the sum of the left and right Virasoro algebras, leading to potentially very complicated modules which have proven too hard to study so far, except in some special cases [147, 148], including for instance WZW models [64, 65]. From the lattice point of view, while it is possible to define and study lattice models whose continuum limit is a (bulk) LCFT, the underlying structures are also very difficult to get: the lattice algebras have a much more complicated representation theory. This was achieved for the periodic $\mathfrak{gl}(1|1)$-symmetric (free-fermions) spin chain only [118, 119, 149], and is still in progress in the $\mathfrak{sl}(2|1)$ (percolation) case [120].

The remaining of this chapter goes as follows. We argue in section 4.3 that one can build periodic lattice models from open ones using the so-called braid translator [145].

This provides an interesting perspective on the relation between bulk and boundary CFTs from a lattice point of view, and this also makes clear the difference between logarithmic and ordinary CFTs as far as this correspondence between bulk and boundary is concerned. This will also illustrate the deep relation between the blob algebra and periodic Temperley-Lieb algebras. Genuine periodic models are also shortly addressed, mostly from the point of view of indecomposability parameters, in section 4.2.

4.1 Blob algebra and classification of Virasoro indecomposable representations

One of the difficulties of LCFTs is the absence of methods to understand and control the amount of indecomposability one might expect to encounter in the general case. While models such as WZW theories on supergroups can be (partly) tackled because they admit semi-classical limits where intuition from supergeometry can be used, the world of, say, LCFTs at $c = 0$ appears overwhelmingly hard to tame abstractly. This difficulty can in fact be given a clear mathematical formulation: for instance, it is known that the representation theory of the Virasoro algebra is *wild* which means roughly that it is as complicated as can be [62, 150]. Among the rather modest questions whose answer is not known is, for instance, the question of how large are the L_0 Jordan cells appearing in a given (chiral or non-chiral) CFT, such as the long searched for "CFT for percolation".

As is often the case however, physics provides powerful constraints which can be used to restrict the wilderness of the algebraic problem. Rather than getting into abstract considerations, it thus seems that important progress will be obtained by first studying in details concrete models. For example, we have seen in the previous chapter that the Temperley-Lieb algebra allowed us to get a handle on Virasoro staggered modules. Despite the striking resemblances between the TL algebra and Virasoro, this is not the end of the story, as there are many other lattice algebras that one can use to construct critical statistical models described in the scaling limit by Logarithmic Conformal Field Theory. An especially interesting example is provided by the so-called *blob algebra* [145] (also known as "one-boundary TL algebra").

4.1.1 Blob algebra and Verma modules

To define the blob algebra $\mathcal{B}(L = 2N, n, y)$, let us start from the Temperley-Lieb algebra and consider all the words written with the $L - 1$ generators e_i and an extra "blob" generator b, subject to the additional relations

$$b^2 = b, \tag{4.1a}$$

$$e_1 b e_1 = y e_1, \quad y \in \mathbb{R}, \tag{4.1b}$$

$$[b, e_i] = 0, \quad i > 1. \tag{4.1c}$$

The extra boundary operator b can be interpreted as decorating strands at the left boundary with a "blob", so we represent it graphically as

$b =$ 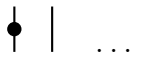 ,

It gives to the corresponding "blobbed loops" a weight y [145], different from the bulk weight n. We parametrize

$$y = \frac{\sin\left((r+1)\gamma\right)}{\sin\left(r\gamma\right)} = \frac{[r+1]_{\mathfrak{q}}}{[r]_{\mathfrak{q}}}. \tag{4.2}$$

where $r \in (0, x+1)$ and we recall that

$$[x]_{\mathfrak{q}} = \frac{\mathfrak{q}^x - \mathfrak{q}^{-x}}{\mathfrak{q} - \mathfrak{q}^{-1}}. \tag{4.3}$$

Standard modules

As for the Temperley-Lieb algebra, one can define standard modules $\mathcal{W}_j^b$ and $\mathcal{W}_j^u$ that are still parametrized by the number of through-lines $2j$ [1], but there are also two sectors *blobbed* and *unblobbed* corresponding to the two orthogonal projectors b and $u = 1 - b$, respectively [151]. We recall that within a standard module, through lines cannot be contracted by the TL generators e_i. When there are through lines in the system ($j > 0$), only the leftmost line is exposed to the boundary where b and u act. We can choose a basis so that the leftmost through line is either blobbed by the symbol '$\bullet$' or unblobbed, with symbol '$\square$', and it has to stay that way under the action of the algebra.

Following [145], the standard modules can be constructed iteratively using a Pascal triangle construction (see Fig. 4.1). The action of the algebra on states can be obtained geometrically by stacking the diagrams on top of one another, just as for the Temperley-Lieb algebra with the convention that the TL generators e_i cannot contract two through lines. This convention implies that each standard module is stable under the action of the algebra. The blobbed and unblobbed standard modules have the same dimension

$$d_j \equiv \mathrm{dim}\mathcal{W}_j^{b/u} = \begin{pmatrix} 2N \\ N-j \end{pmatrix}. \tag{4.4}$$

Indeed, the Pascal construction of the state is compatible with the standard recursion relation $\binom{2N-1}{N-j} + \binom{2N-1}{N-j-1} = \binom{2N}{N-j}$. The dimension of $\mathcal{B}(2N, n, y)$ is therefore

$$\mathrm{dim}\mathcal{B}(2N, n, y) = \sum_{j=-N}^{N} \begin{pmatrix} 2N \\ N-j \end{pmatrix}^2 = \begin{pmatrix} 4N \\ 2N \end{pmatrix}. \tag{4.5}$$

1. Recall that $2j$ has the same parity as L.

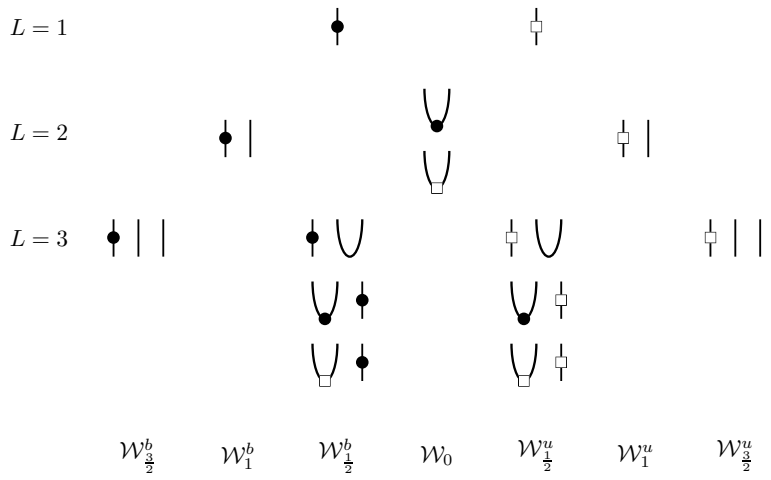

Figure 4.1: Pascal triangle construction of the standard modules of the blob algebra. The diagram is here truncated to $L = 3$. The symbols $\bullet$ and $\square$ represent the blob b and antiblob $1 - b$ operators, respectively. In the left (resp. right) part of the diagram, a step one row down and to the left (resp. right) corresponds to adding a through line on the right of the diagram; and a step one row down and to the right (resp. left) corresponds to bending the rightmost through line to the right of the diagram.

These standard modules are irreducible for any $\mathfrak{q}$ when r is not an integer (generic).

Boundary loop models and scaling limit

It is possible to define critical lattice models based on this blob algebra, and one finds that whereas the TL standard modules were related in the scaling limit to Kac modules over the Virasoro algebra, the blob standard modules tend to Verma modules [74, 146]. The blob algebra is clearly larger than TL and so are its representations, since they correspond in the limit to Verma modules without any quotient being taken. In order to see this more precisely, we start from the *transfer matrix*

$$T = (1 + \lambda b) \prod_{i=1}^{N-1} (1 + e_{2i}) \prod_{i=1}^{N} (1 + e_{2i-1}) \,, \tag{4.6}$$

As in the Temperley-Lieb case, we represent its action in terms of plaquettes

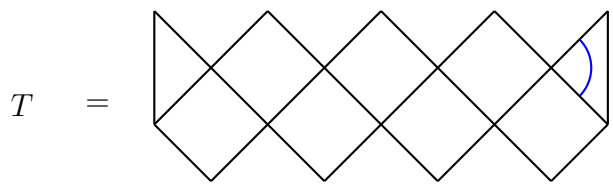

where in this example $N = 4$ ($L = 8$). The rightmost half plaquette corresponds to a free boundary condition whereas the first half plaquette may or may not carry a blob symbol. The bulk plaquettes carry the usual action of the Temperley-Lieb generators

$1 + e_i \;=$ 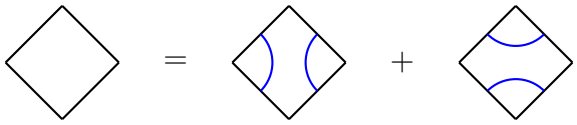 $=$

whilst the first one represents

$1 + \lambda b \;=$ 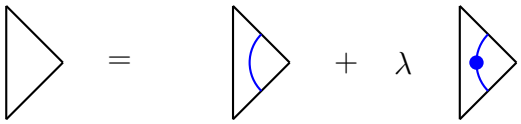 $=$

The action of this transfer matrix builds up loop configurations, where the edges touching the boundary may or may not be blobbed, depending on the parameter λ. In addition to these λ factors, the Boltzmann weight of a configuration is computed by attributing a weight y to closed loops carrying at least one blob symbol, and a weight n to the other loops. The blob algebra is completely symmetric between blob b and antiblob $1 - b$ operators, and it is convenient to introduce the diagrammatic representation

$1 - b \;=$ 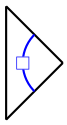

where the box represents the antiblob operator, and each loop carrying at least one box will be weighted by $n - y$. Note also that configurations with at least one loop that is blobbed and unblobbed at the same time should be excluded from the partition function, since $b(1 - b) = 0$.

Thanks to the extensive numerical study of [146] and the Bethe ansatz results of [152, 153], the phase diagram of this statistical model in terms of the boundary coupling λ is now well understood, and can be summarized by the diagram below:

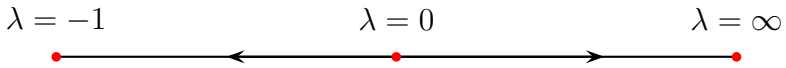

Here, the fixed point $\lambda = 0$ corresponds to free boundary conditions, and is described algebraically by the Temperley-Lieb algebra. The perturbation by the boundary cou-

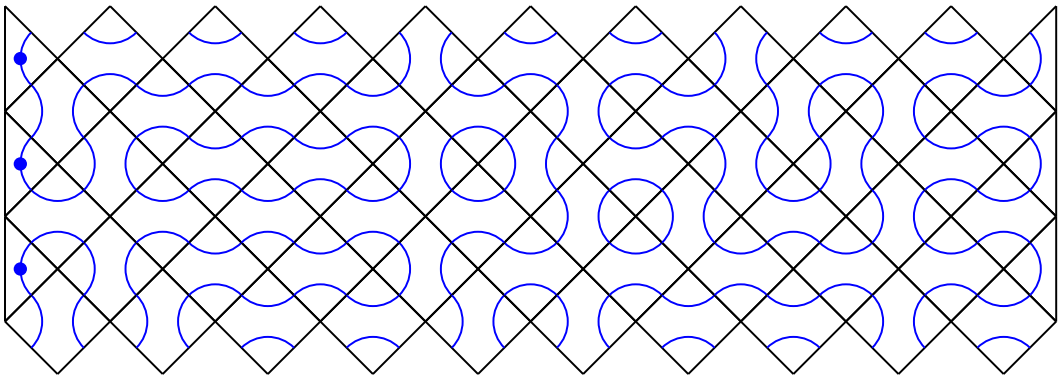

Figure 4.2: Example of loop configuration on $L = 20$ sites, after 3 iterations of the transfer matrix T in the limit $\lambda = \infty$. Every loop touching the left boundary is blobbed and hence carries a weight y. The other loops that do not carry a blob symbol get a weight n.

pling λ is relevant in the renormalization group sense, so that the system flows to one of the two conformally invariant boundary conditions where every loop touching the left boundary carries a blob or unblob symbol. These two fixed points are related by a simple switch between the weights of blobbed and unblobbed loops, and in the following we will focus only on the fixed point $\lambda = \infty$.

The limit $\lambda = \infty$ in the transfer matrix $\lambda^{-1}T$, corresponds to blobbing every loop touching the boundary; the transfer matrix reads then schematically

$\lim_{\lambda\to\infty} \lambda^{-1}T =$ 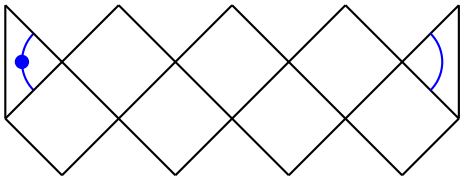

and an example of loop configuration in this case is shown in Fig. 4.2. The limit $\lim_{\lambda\to\infty}$ has the advantage of reducing the dimension of the Hilbert space while keeping the correct universality class in the continuum limit: the relevant algebra is now reduced to

$$\mathcal{B}^b(2N, n, y) \equiv b\mathcal{B}(2N, n, y)b, \tag{4.7}$$

which was dubbed "JS blob algebra" in [74].

At the renormalization group fixed point $\lambda = \infty$, we expect statistical mechanics systems with transfer matrix (4.6) to exhibit conformal invariance at low energy, and their scaling limit to be described by a conformal field theory. One finds that the scaling limit is described by a CFT with central charge $c = 1 - \frac{6}{x(x+1)}$, where we recall that x parametrizes the loop fugacity $n = 2\cos\frac{\pi}{x+1}$. One can then compute the low-energy spectrum in the scaling limit and identify all the exponents h_i occurring in the

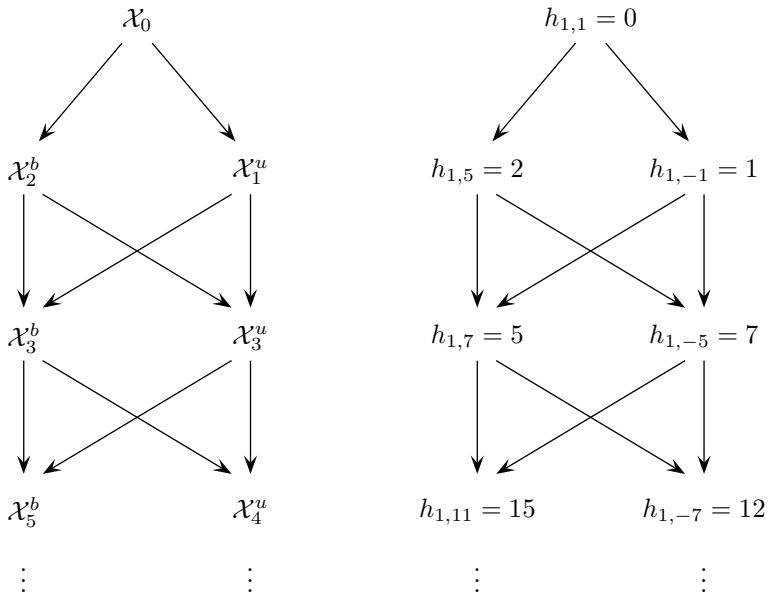

Figure 4.3: Example of standard module $\mathcal{W}_0$ for the blob algebra with $n = 1$ and $y = 1$, and corresponding $c = 0$ Verma module $\mathcal{V}_{h=0}$ in the scaling limit.

spectrum of the transfer matrix (or the hamiltonian) acting in the standard modules $\mathcal{W}_j^{b/u}$ over the blob algebra. It is convenient to gather the results into a generating function (character) $\mathrm{Tr}_{\mathcal{W}_j^{b/u}} q^{L_0 - c/24} \equiv \sum_i q^{h_i - c/24}$, where the sum is taken over all low-energy states. In the sector with no through lines, one finds [146]

$$Z_0 = \mathrm{Tr}_{\mathcal{W}_0} q^{L_0 - c/24} = \frac{q^{-c/24}}{P(q)} q^{h_{r,r}}, \tag{4.8}$$

where we recall that $P(q) = q^{-1/24}\eta(q) = \prod_{n=1}^{\infty}(1 - q^n)$. On the other hand, the generating functions [146] for the blobbed and unblobbed sectors read

$$Z_j^b = \mathrm{Tr}_{\mathcal{W}_j^b} q^{L_0 - c/24} = \frac{q^{-c/24}}{P(q)} q^{h_{r,r+2j}}, \tag{4.9a}$$

$$Z_j^u = \mathrm{Tr}_{\mathcal{W}_j^u} q^{L_0 - c/24} = \frac{q^{-c/24}}{P(q)} q^{h_{r,r-2j}}. \tag{4.9b}$$

These formulas coincide with the character of the Verma modules $\mathcal{V}_{h_{r,r\pm 2j}}$.

4.1.2 Representation theory: from the Blob algebra to Virasoro

Actually, this correspondence between standard and Verma modules go way beyond a simple equality between characters. The blob algebra representation theory is in fact

JS blob algebra $\mathcal{B}^b(2N,n,y) = b\mathcal{B}(2N,n,y)b$	Virasoro algebra
$n = \mathfrak{q} + \mathfrak{q}^{-1} = 2\cos\frac{\pi}{x+1}$	central charge $c = 1 - \frac{6}{x(x+1)}$
$y = \frac{[r+1]_\mathfrak{q}}{[r]_\mathfrak{q}}$	row of the Kac table r
Standard module $\hat{\mathcal{W}}_j^{b/u} = b\mathcal{W}_j^{b/u}$	Verma module $\mathcal{V}_{h_{r,r\pm 2j}}$
Quotient module $\hat{\mathcal{K}}_j^{b/u} = \hat{\mathcal{W}}_j^{b/u}/\hat{\mathcal{W}}_{r\pm j}^{u}$ (r integer)	Kac module $\mathcal{V}_{h_{r,r\pm 2j}}/\mathcal{V}_{h_{r,-r\mp 2j}}$
Simple module $\hat{\mathcal{X}}_j^{b/u}$	Simple module $h_{r,r\pm 2j}$
$L_n^{(2N)}$ (see [74])	Virasoro generators L_n
Inner product with $b^\dagger = b$, $e_i^\dagger = e_i$	Virasoro bilinear form $L_n^\dagger = L_{-n}$

Table 4.1: Correspondence between the JS blob algebra $\mathcal{B}^b(2N,n,y) = b\mathcal{B}(2N,n,y)b$ and Virasoro.

very rich [145, 154], and standard modules turn out to have a complicated indecomposable structure in non-generic cases (see Fig. 4.3 for an example taken from [74], where $\mathcal{X}_j^{b/u}$ are simple modules of the blob algebra). The important point is that the blob algebra somehow provides a lattice version of the Virasoro algebra [2], and that the indecomposable structure of standard modules mimics exactly that of Verma modules. In particular, the operator content of the irreducible blob representations $\mathcal{X}_j^{b/u}$ is given by the character of the Virasoro simple modules with conformal weight $h_{r,r\pm 2j}$. Note also that Kac modules can be recovered by considering quotients of standard modules – in fact, the Temperley-Lieb algebra itself can be considered as a quotient of the Blob algebra.

Though the lattice expressions $L_n^{(N)}$ for the Virasoro generators L_n were proposed [74] for the blob algebra as well, this correspondence between the blob algebra (a finite-dimensional, lattice algebra) and Virasoro (a infinite-dimensional Lie algebra) should be understood as a conjecture, since the correspondence has been established only at the level of modules so far. It is however tempting to conjecture that the standard modules, their quotients, and simple modules of the blob algebra provide lattice regularizations of their well-known Virasoro modules counterparts. This (loosely stated) correspondence between the (JS) blob algebra and (the universal enveloping algebra of) Virasoro is summarized in Tab. 4.1. This result is especially useful as one can now use the representation theory of the Blob algebra (which is well under control), to obtain new results for the Virasoro algebra.

2. To be more precise, it is the JS blob algebra $\mathcal{B}^b(2N,n,y) \equiv b\mathcal{B}(2N,n,y)b$ that provides a lattice version of Virasoro [74]. As the differences between the full blob algebra and $\mathcal{B}^b(2N,n,y) \equiv b\mathcal{B}(2N,n,y)b$ occur only for $y = 0$, we will ignore this subtlety in what follows.

4.1.3 Towards a classification of Virasoro indecomposable representations

We can now use this correspondence to obtain new results [74] for the Virasoro algebra representation theory. As mentioned above, the representation theory of the Virasoro algebra is known to be wild, which makes classification issues *a priori* extremely difficult. However, physicists are not just interested in "all" Virasoro representations. Rather, they are interested in modules which may appear in physical LCFTs – CFTs which are fixed points of interacting, non unitary, field theories with well defined actions. If such LCFTs exist, it is reasonable to expect that they must also admit some lattice regularizations, that is, that their properties can be studied by considering models defined on large, but finite, lattices, and exploring the thermodynamic and scaling limits. The point is now that the representation theory of the algebras occurring for such finite lattice models – such as the Temperley Lieb algebra or the blob algebra – is well under control. We might therefore hope to classify all physically relevant indecomposable Virasoro representations by simply defining them as scaling limit of spin-chains modules. Of course, there is a large choice of spin chains, determined not only by the degrees of freedom but also by type of interaction. Nevertheless, experience with unitary models (say, the $O(3)$ sigma model at $\theta = \pi$) has shown that, if the continuum limit admits only the Virasoro algebra as a chiral algebra, it can be fully understood by using lattice models with the simplest possible algebra compatible with the symmetries (in the case of the $O(3)$ sigma model, the spin 1/2 XXX spin chain). Given the striking correspondence between blob representations and Virasoro modules in the limit, it is tempting to conjecture that Virasoro representations of physical interest can be obtained a limits of blob representations.

This approach can be used to classify (or at the very least, obtain a large class of) indecomposable Virasoro representations relevant for LCFTs. We will not go into more detail here, but only give one example of a generalization of the diamond staggered modules encountered before in (3.59), obtained as the scaling limit of a blob algebra modules for $n = 1$ and $y = 1$ (this corresponds to $c = 0$ in the CFT language):

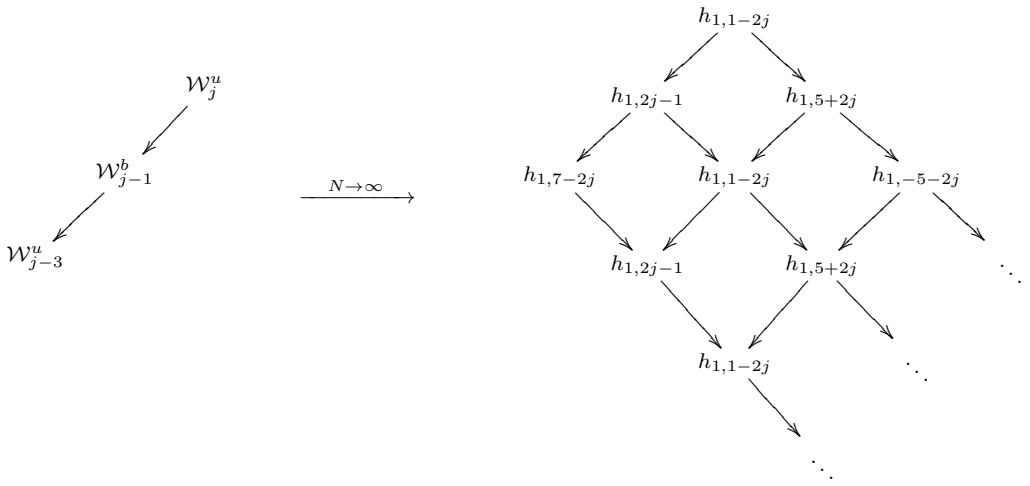

Note that this module is a gluing of three Verma modules and it should in particular

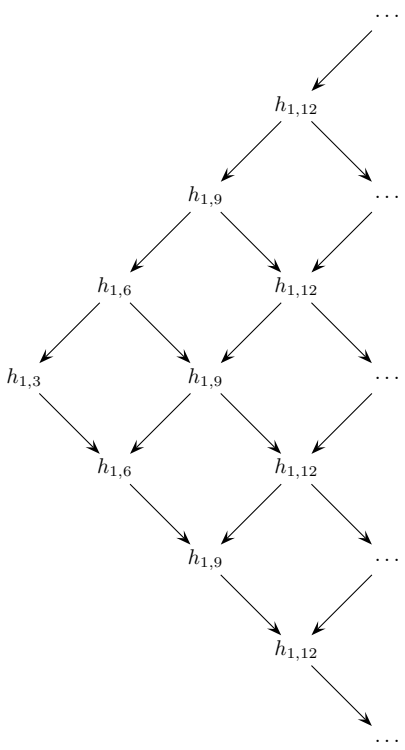

Figure 4.4: Structure in terms of simple modules of an indecomposable Virasoro module at $c = 0$ obtained from the blob algebra. All the down-left arrows in the figure represent the action of positive Virasoro modes, whereas the other arrows correspond to negative modes. There are Jordan cells for L_0 of any rank occurring in the spectrum.

admit Jordan cells of ranks up to 3 for the L_0 generator. Finally, the blob algebra admits even more complicated modules – the tilting modules – which admit now Jordan cells of any finite rank in the scaling limit. An example of such a module is shown in Fig. 4.4.

To conclude this section, let us mention that this lattice approach can obviously be generalized to CFTs with extended symmetries – *i.e.* larger than the Virasoro algebra. For instance, the spin-1 XXZ $U_{\mathfrak{q}}s\ell(2)$-symmetric spin chain is expected to be described by CFTs with super-Virasoro symmetry, and super-Virasoro indecomposable modules could also be obtained directly from the lattice. Another example is the $\mathcal{W}$-algebra symmetry, which can also be realized on the lattice [138].

4.2 Periodic lattice models and bulk LCFTs

While chiral LCFTs are thus fairly well understood, much remains to be done to understand the structure of bulk theories. Attempts to construct nonchiral theories at $c = 0$ (see, *e.g.*, [147, 148]) often exhibit unwanted features such as degenerate or non-$SL(2, \mathbb{C})$ invariant ground states which should not occur in, for instance, percolation. As we have seen so far, part of the progress in the chiral case originates from considering

lattice models with open boundary conditions, and observing that the indecomposable features of the chiral (Virasoro) algebra appearing in the scaling limit are similar to those occurring, in finite size, on the lattice. This suggests that eventually, LCFTs may be solved by a careful exercise in the representation theory of the algebras satisfied by the local energy terms, also in the non-chiral case. The non-chiral or bulk case corresponds, on the lattice, to periodic boundary conditions, which is rather difficult mathematically. One can, nevertheless, use lattice algebraic techniques to investigate aspects of the simplest representations under the full left and right Virasoro algebras present in this case (see [118, 119, 149] for recent progress).

4.2.1 Periodic version of the TL algebra, standard modules and operator content

When one tries to generalize the TL algebra to periodic models, the most natural thing to do is to simply add a last generator e_L and to define the labels modulo L so that $e_{L+1} = e_1$, $e_L e_1 e_L = e_1$ *etc* .... The resulting algebra is infinite dimensional, even for finite L, and considerably too big for our purpose. In order to define the relevant quotients, it is useful to go again to a diagram representation, which now involves an annulus instead of a rectangle. We also introduce a translation generator u that shifts the label of the e_j generators, giving rise to the relations

$$\begin{aligned}
[e_i, e_j] &= 0 \ (|i-j| \geq 2) && \text{(4.10a)}\\
e_i^2 &= n e_i && \text{(4.10b)}\\
e_i e_{i\pm 1} e_i &= e_i && \text{(4.10c)}\\
u e_i u^{-1} &= e_{i+1} && \text{(4.10d)}\\
u^2 e_{L-1} &= e_1 \dots e_{L-1} && \text{(4.10e)}\\
u^L &\text{is central.} && \text{(4.10f)}
\end{aligned}$$

The resulting algebra is again infinite dimensional, and called the affine Temperley-Lieb algebra $TL_L^a(n)$. The infinite dimensionality, can now be understood easily, since there is no way, in the algebra, to undo non contractible loops, or through lines that wind around the horizontal direction.

Note that the relation $u^2 e_{L-1} = e_1 \dots e_{L-1}$ is easily understood in terms of diagrams, for example for $L = 4$

$e_1e_2e_3 =$ 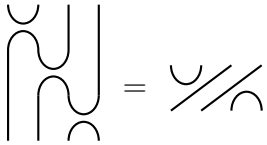 $= u^2 e_3$

The finite dimensional quotients which are relevant to us are obtained by considering the diagrams on the annulus (recall they do not involve crossings) and imposing additional relations. The simplest case corresponds to the so called Jones-Temperley-

Lieb algebra $JTL_L(n)$ and is obtained [155] by (i) replacing non contractible loops by the same weight n as contractible ones (ii) setting $u^L = 1$, which allows one to unwind through lines and (iii) identifying non-isotopic (in the annulus) diagrams connecting the same sites.

Standard modules

The generic irreducible representations of this algebra are well known [145, 156], and can be interpreted in a geometrical fashion just like for the usual TL or the blob algebra. Let $2j$ be the number of strings (through lines) that meet at the infinite past and propagate along the (vertical) imaginary time direction. In the sector with no string ($j = 0$), we can construct the modules $\hat{\mathcal{W}}_0$ that turn out to be the same as in the open TL case. In particular, dimensions are given by the celebrated Catalan numbers

$$\hat{d}_0 = \dim \hat{\mathcal{W}}_0 = \binom{2N}{N} - \binom{2N}{N+1}. \tag{4.11}$$

This is because we decided to identify non-isotopic diagrams connecting the same sites when there is no through lines propagating. When $j \neq 0$, there are more patterns allowed. For example, for $N = 3$ ($L = 6$) and $j = 1$, the state $|\curlyvee\,|\,|\curlyvee\rangle$ is allowed. If we do not distinguish between the strings, we can construct the (irreducible) representations $\hat{\mathcal{W}}_j$, with dimensions

$$\hat{d}_j = \dim \hat{\mathcal{W}}_{2N,j} = \binom{2N}{N-j}. \tag{4.12}$$

Actually, it is possible to construct $j-1$ other inequivalent irreps corresponding to cyclic permutations of the strings. To see that, let us try to distinguish one string from the others, this leads to modules $\tilde{\hat{\mathcal{W}}}_j$ with dimension $j\hat{d}_j$. Let us then introduce the operator T_N that shifts the tagged string two steps to the right. This operator commutes with the JTL algebra as it acts only on strings, and its eigenvalues are phases because $(T_N)^N = 1$. Using Schur's lemma, we can label irreps of JTL with the eigenvalues of T_N, and one introduces a pseudomomentum in the space of the strings $K = \pi q/M$ where $M|J$ and with a greatest common divisor $q \wedge M = 1$. The modules $\tilde{\hat{\mathcal{W}}}_{2N,j}$ are thus reducible

$$\tilde{\hat{\mathcal{W}}}_{2N,j} = \bigoplus_{q=0}^{j-1} \hat{\mathcal{W}}_{2N,j,\mathrm{e}^{2\pi i q/j}}. \tag{4.13}$$

In the module $\hat{\mathcal{W}}_{2N,j,\mathrm{e}^{2\pi i q/j}}$, the eigenvalue of T_N is $\mathrm{e}^{2\pi i q/j}$. $\hat{\mathcal{W}}_{2N,j,\mathrm{e}^{2\pi i q/j}}$ has dimension $\hat{d}_j$ as it is made of $\hat{d}_j$ equivalence classes for the translation in string space, which all contain j elements. Choosing $K = 0$ is equivalent not to distinguish between the strings so that $\hat{\mathcal{W}}_{2N,j,1} \simeq \hat{\mathcal{W}}_{2N,j}$. The modules we described are often referred to as standard or cell modules of the JTL algebra, their structure may be quite complicated

in non-generic cases, where they become highly reducible. In the case of the affine Temperley-Lieb algebra, the pseudomomentum K can take any complex value.

Scaling limit and operator content

Although the geometrical setup of loop models is appealing, it is instructive and useful to consider related periodic models. We define here a periodic version of the XXZ spin chain [67] (or equivalently of the 6-vertex model). We define the last generator as

$$e_L = \mathbb{I} \otimes \mathbb{I} \otimes \cdots \otimes \begin{pmatrix} 0 & 0 & 0 & 0 \\ 0 & \mathfrak{q}^{-1} & -\mathrm{e}^{i\phi} & 0 \\ 0 & -\mathrm{e}^{-i\phi} & \mathfrak{q} & 0 \\ 0 & 0 & 0 & 0 \end{pmatrix}. \tag{4.14}$$

The resulting Hamiltonian $H = -\sum_i e_i$ reads, up to an irrelevant constant

$$H = \frac{1}{2}\sum_{i=1}^{2N} \left(\sigma_i^x \sigma_{i+1}^x + \sigma_i^y \sigma_{i+1}^y + \frac{\mathfrak{q}+\mathfrak{q}^{-1}}{2} \sigma_i^z \sigma_{i+1}^z \right) + \frac{\mathrm{e}^{i\phi}}{4} \sigma_{2N}^+ \sigma_1^- + \frac{\mathrm{e}^{-i\phi}}{4} \sigma_{2N}^- \sigma_1^+. \tag{4.15}$$

We shall refer to this model as XXZ twisted spin chain. Note that it may be useful to redistribute the twist in order to restore translation invariance. The choice of the twist $\mathrm{e}^{i\phi} = \mathrm{e}^{2iK}$ allows to select specific generic irreducible representations of the JTL algebra. For $j \neq 0$, the Hilbert space of this model in the sector with spin $S_z = \pm j$ ($j > 0$) is isomorphic to the module $\hat{\mathcal{W}}_{j,\mathrm{e}^{\pm 2iK}}$. The operator content of these representations follows from the results of Ref. [67]. We use our usual parametrization

$$c = 1 - \frac{6}{p(p+1)}, \tag{4.16a}$$

$$h_{r,s} = \frac{[(p+1)r - ps]^2 - 1}{4p(p+1)}, \tag{4.16b}$$

where we recall that $\mathfrak{q} = \mathrm{e}^{i\pi/(p+1)}$. The generating function of levels in the scaling limit of the module $\hat{\mathcal{W}}_{j,\mathrm{e}^{2iK}}$ reads

$$F_{j,\mathrm{e}^{2iK}} \equiv \mathrm{Tr}_{\hat{\mathcal{W}}_{j,\mathrm{e}^{2iK}}} q^{L_0} \bar{q}^{\bar{L}_0} = \frac{1}{P(q)P(\bar{q})} \sum_{e\in\mathbb{Z}} q^{h_{e+p/M,-j}} \bar{q}^{h_{e+p/M,j}}, \tag{4.17}$$

where $K = \frac{\pi}{M} p$ and $P(q) = \prod_{n=1}^{\infty}(1-q^n)$. Note that we did not introduce the usual central charge term in the definition of this character.

The case $j = 0$ requires more care as one has to be careful about the loops that wrap around the spatial direction due to the periodic boundary conditions which would get a weight 2 with the generators of the open case. One then needs to introduce a twist $\mathrm{e}^{i\phi} = \mathfrak{q}^2$ to account for this [3]. In this case, the sector $S_z = 0$ corresponds to the sum of

3. The weight $\overline{n}$ carried by non-contractible loops can be computed using the relation

two irreps of the JTL algebra $\mathcal{H}^{2N}_{S_z=0} \simeq \hat{\mathcal{W}}_0 \oplus \hat{\mathcal{W}}_{1,1}$. The space $\mathcal{H}^{2N}_{S_z=0}$ would correspond in the geometrical language to all the diagrams with $2N$ sites on the outer and in the inner boundary of an annulus, with no through line and without the identification of non-isotopic diagrams connecting the same sites. The trace over the scaling limit of the representation $\hat{\mathcal{W}}_0$ (with identification of the non-isotopic diagrams connecting the same sites) thus reads

$$\mathrm{Tr}_{\hat{\mathcal{W}}_0} q^{L_0} \bar{q}^{\bar{L}_0} = F_{0,\mathfrak{q}^2} - F_{1,1}. \tag{4.18}$$

In general, we will use the notation $\hat{\mathcal{W}}_{j=0,\alpha^2}$ for the representation of the affine TL algebra with no through-line, without the identification of non-isotopic diagrams connecting the same sites, and with weight $\alpha + \alpha^{-1}$ for non-contractible loops. It has dimension

$$\dim \hat{\mathcal{W}}_{0,\alpha^2} = \binom{2N}{N}. \tag{4.19}$$

We thus have $\mathcal{H}^{2N}_{S_z=0} \simeq \hat{\mathcal{W}}_{0,\mathfrak{q}^2}$, and $\hat{\mathcal{W}}_0 = \hat{\mathcal{W}}_{0,\mathfrak{q}^2}/\hat{\mathcal{W}}_{1,1}$.

4.2.2 Periodic $\mathfrak{gl}(1|1)$ spin chain and lattice indecomposability parameters

We start our study of periodic models with the $\mathfrak{gl}(1|1)$ spin chain, which corresponds to symplectic fermions in the continuum limit. The full algebraic analysis can be found in [118, 119, 149], and we shall not repeat it here, but focus instead on indecomposability parameters. The non-chiral theory of symplectic fermions is closely related to the boundary theory, and actually, the indecomposability parameters are the same in both cases. This will not be the case for more complicated theories like percolation. That said, symplectic fermions provide a very concrete example where lattice indecomposability parameters can be computed analytically.

Let us first recall the expression of the periodic $\mathfrak{gl}(1|1)$ spin chain

$$H = -\sum_{j=1}^{2N} (f_j + f_{j+1})(f_j^\dagger + f_{j+1}^\dagger), \tag{4.20}$$

with the fermionic operators $\{f_i, f_j\} = 0$, $\{f_i, f_j^\dagger\} = (-1)^i \delta_{i,j}$, and $f_{2N+1} = f_1$. Note that this formulation in terms of fermions can be mapped [118] onto a XX(Z) spin chain at $\mathfrak{q} = i$ thanks to a Jordan-Wigner transformation. In this twisted XXZ formulation, we have $j = |S_z|$ and the twist reads $\mathrm{e}^{i\phi} = (-1)^{S_z+1}$. Using the operator content of JTL

$e_1 e_3 \dots e_{2N-1} e_2 e_4 \dots e_{2N} e_1 e_3 \dots e_{2N-1} = \overline{n}^2 e_1 e_3 \dots e_{2N-1}$. In the XXZ case, we find that $\bar{n}$ is related to the twist through $\overline{n} = 2\cos\frac{\phi}{2}$.

representations derived above, we hence find the (modified) CFT partition function [4]

$$Z = F_{0,-1} + 2\sum_{j=1}^{\infty} F_{j,(-1)^{j+1}} = 4\left|\prod_{n=1}^{\infty}(1+q^n)^2\right|^2 . \tag{4.21}$$

The resulting CFT is the symplectic fermion theory with $c = -2$.

Analytical expression of the lattice indecomposability parameters

We will show in this section that the lattice indecomposability parameters can be computed analytically, using the fact that the spin chain can be (almost) diagonalized in terms of fermionic modes. We follow [118] for the diagonalization of the Hamiltonian. First of all, it turns out to be convenient to introduce the canonical fermions $f_j^\dagger = i^j c_j^\dagger$ and $f_j = i^j c_j$, in terms of which we have

$$e_j = i(-1)^j\left[c_j c_{j+1}^\dagger - c_j^\dagger c_{j+1} + i\left(c_j^\dagger c_j - c_{j+1}^\dagger c_{j+1}\right)\right]. \tag{4.22}$$

We also define the Fourier transforms of the fermions c and $c^\dagger$

$$c_j^\dagger = \frac{1}{\sqrt{L}}\sum_p \mathrm{e}^{-ijp}\theta_p^\dagger, \qquad c_j = \frac{1}{\sqrt{L}}\sum_p \mathrm{e}^{ijp}\theta_p, \tag{4.23}$$

where $p = \frac{2\pi n}{L}$, with $L = 2N$, N even and $n = 0, \ldots, L-1$. They obviously satisfy $\{\theta_{p_1}, \theta_{p_2}^\dagger\} = \delta_{p_1,p_2}$ and $\{\theta_{p_1}, \theta_{p_2}\} = \{\theta_{p_1}^\dagger, \theta_{p_2}^\dagger\} = 0$. We then introduce the fermionic modes

$$\eta_p = \frac{1}{\sqrt{2}}\left(\sqrt{\cot\frac{p}{2}}\theta_{p-\frac{\pi}{2}} - \sqrt{\tan\frac{p}{2}}\theta_{p+\frac{\pi}{2}}\right), \tag{4.24a}$$

$$\eta_p^\dagger = \frac{1}{\sqrt{2}}\left(\sqrt{\tan\frac{p}{2}}\theta_{p-\frac{\pi}{2}}^\dagger - \sqrt{\cot\frac{p}{2}}\theta_{p+\frac{\pi}{2}}^\dagger\right), \tag{4.24b}$$

$$\chi_p = \frac{1}{\sqrt{2}}\left(\sqrt{\cot\frac{p}{2}}\theta_{p-\frac{\pi}{2}} + \sqrt{\tan\frac{p}{2}}\theta_{p+\frac{\pi}{2}}\right), \tag{4.24c}$$

$$\chi_p^\dagger = \frac{1}{\sqrt{2}}\left(\sqrt{\tan\frac{p}{2}}\theta_{p-\frac{\pi}{2}}^\dagger + \sqrt{\cot\frac{p}{2}}\theta_{p+\frac{\pi}{2}}^\dagger\right), \tag{4.24d}$$

$$\chi_0^\dagger = \theta_{\frac{\pi}{2}}^\dagger, \quad \chi_0 = \theta_{\frac{\pi}{2}}, \quad \eta_0^\dagger = \theta_{\frac{3\pi}{2}}, \quad \eta_0 = \theta_{\frac{3\pi}{2}}. \tag{4.24e}$$

4. Recall that this modified partition function is defined as a trace, not a supertrace. This amounts to considering anti-periodic boundary conditions for the fermions along the imaginary time direction. We emphasize that in particular, this partition function need not be modular invariant.

In terms of these modes, the Hamiltonian reads

$$H = 4\chi_0^\dagger \eta_0 + 2 \sum_{\substack{p=\epsilon \\ \text{step}=\epsilon}}^{\pi-\epsilon} \sin p \left(\chi_p^\dagger \chi_p - \eta_p^\dagger \eta_p \right). \tag{4.25}$$

where $\epsilon = \frac{\pi}{N}$. The Hamiltonian is almost diagonal in this form, except for the non-diagonalizable term $4\chi_0^\dagger \eta_0$ that mixes the zero-modes. There are four different ground-states

$$\phi^+ = \prod_{\substack{p=\epsilon \\ \text{step}=\epsilon}}^{\pi-\epsilon} \chi_p \left|\uparrow \ldots \uparrow\right\rangle, \quad \phi^- = \chi_0 \eta_0 \phi^+, \quad \Omega = \eta_0 \phi^+, \quad \omega = \chi_0 \phi^+, \tag{4.26}$$

where $|\uparrow \ldots \uparrow\rangle$ is the state with all spins up in the XX language. The corresponding energy reads

$$E_0^{(N)} = -2 \sum_{n=1}^{N-1} \sin \frac{n\pi}{N} = -2 \operatorname{cotan} \frac{\pi}{2N} = -\frac{4N}{\pi} + \frac{\pi}{3N} + \mathcal{O}(N^{-2}). \tag{4.27}$$

This is formula is consistent with the values $e_\infty = 2/\pi$, $v_F = 2$ and $c = -2$. The states $|\Omega\rangle$ and $|\omega\rangle$ are mixed into a Jordan cell by the Hamiltonian on the lattice because of the zero-mode term $\chi_0^\dagger \eta_0$.

It is also quite instructive to construct Jordan cells corresponding to excited states. For example, let $|\phi\rangle = \chi_{\pi-\epsilon}^\dagger |\Omega\rangle$ and $|\psi\rangle = -\frac{1}{2}\frac{2\pi}{N} \chi_{\pi-\epsilon}^\dagger |\omega\rangle$ where $\epsilon = \pi/N$. One can express exactly the Hamiltonian and the conformal momentum (see below for an expression of the latter in terms of the fermions $\chi - \eta$) on the lattice in this basis

$$(L_0 + \bar{L}_0)^{(N)} = \begin{pmatrix} \Delta_N & 2 \\ 0 & \Delta_N \end{pmatrix} \tag{4.28a}$$

$$(L_0 - \bar{L}_0)^{(N)} = \begin{pmatrix} -\frac{N}{2\pi} \sin \frac{2\pi}{N} & 0 \\ 0 & -\frac{N}{2\pi} \sin \frac{2\pi}{N} \end{pmatrix} \tag{4.28b}$$

where

$$\Delta_{(N)} = \frac{N}{\pi} \sin \frac{\pi}{N} + \left[\frac{2N^2}{\pi^2} - \frac{1}{6} - \frac{N}{\pi} \operatorname{cotan} \frac{\pi}{2N} \right] = 1 + \mathcal{O}\left(\frac{1}{N} \right). \tag{4.29}$$

These states belong to the antiholomorphic sector $(h, \bar{h}) = (0, 1)$. It is important to notice that the action $(L_0 - \bar{L}_0)^{(N)}$ is closed on the states $\left(\left|\psi^{(N)}\right\rangle, \left|\phi^{(N)}\right\rangle\right)$. Unfortunately, this is not the case in more complicated situations such as percolation, and the operator $(L_0 - \bar{L}_0)^{(N)}$ generally couple these two states to many others. In general, finite size eigenvectors of $(L_0 + \bar{L}_0)^{(N)}$ *are not* eigenstates of $L_0^{(N)}$ or $\bar{L}_0^{(N)}$.

This lattice Jordan cell corresponds in the limit to a Virasoro staggered module,

and the associated indecomposability parameter $\beta_2 = -1$ was computed in section 2.4. Generalizing the lattice method (see Sec. 3.4) to measure indecomposability parameters to the bulk case, let us try to recover this value directly from the lattice. Actually, because of the free fermions formulation of the model, it is even possible to obtain exact formula on the lattice.

We will need the expression of the dagger operator with respect to the Fock state scalar product which goes to the Virasoro bilinear form in the scaling limit. We denote the dagger operation with a bar, so that in terms of the original fermions $\bar{f}_i = f_i^\dagger$. For the modes diagonalizing the Hamiltonian, we have

$$\eta_p^\dagger = -\bar{\eta}_p, \quad \chi_p^\dagger = \bar{\chi}_p, \quad \eta_0^\dagger = \bar{\chi}_0, \quad \chi_0^\dagger = \bar{\eta}_0. \tag{4.30}$$

We emphasize that the dagger symbol $\dagger$ *does not* correspond to the dagger operation for this scalar product.

The main step is then to use the Koo-Saleur formula [132] to properly normalize our states

$$H_n^{(N)} = -\frac{N}{\pi v_F}\sum_{j=1}^{2N} \mathrm{e}^{inj\pi/N}\,(e_i - e_\infty) + \frac{c}{12}\delta_{n,0}, \tag{4.31a}$$

$$P_n^{(N)} = \frac{iN}{\pi v_F^2}\sum_{j=1}^{2N} \mathrm{e}^{inj\pi/N}\,[e_i, e_{i+1}]\,, \tag{4.31b}$$

where $H_n^{(N)} = L_n^{(N)} + \bar{L}_{-n}^{(N)}$ and $P_n^{(N)} = L_n^{(N)} - \bar{L}_{-n}^{(N)}$. These formulas can be expressed in terms of the fermionic modes $\chi - \eta$. The final expressions are quite cumbersome so we refer the interested reader to [118] for details. Using all these elements, we are now ready to compute exactly β_2 on the lattice.

Let us now construct $\beta_2^{(N)}$ explicitly. First, we note that $\langle\psi|\phi\rangle = -\epsilon$. Then, some algebra using the Koo-Saleur formulae (4.31) yields

$$(L_1 - \bar{L}_{-1})^{(N)}\left|\phi^+\right\rangle = -\cos\frac{\epsilon}{2}\frac{\sqrt{\sin\epsilon}}{\epsilon}\mathrm{e}^{i\epsilon}\chi^\dagger_{\pi-\epsilon}\left|\Omega\right\rangle \tag{4.32a}$$

$$(L_1 + \bar{L}_{-1})^{(N)}\left|\phi^+\right\rangle = \frac{\sqrt{\sin\epsilon}}{\epsilon}\mathrm{e}^{i\epsilon/2}\chi^\dagger_{\pi-\epsilon}\left|\Omega\right\rangle \tag{4.32b}$$

from which we deduce

$$\left\langle\psi\left|\bar{L}_{-1}^{(N)}\right|\phi^+\right\rangle = \frac{\mathrm{e}^{i\epsilon/2}}{2}\sqrt{\sin\epsilon}\left[1 + \cos\frac{\epsilon}{2}\mathrm{e}^{i\epsilon/2}\right] \tag{4.33}$$

The lattice indecomposability parameter $\beta_2^{(N)}$ can then be expressed as

$$\beta_2^{(N)} \equiv \frac{|\left\langle\psi|\bar{L}_{-1}|\phi^+\right\rangle|^2}{\langle\psi|\phi\rangle} = -\frac{\sin\epsilon}{4\epsilon}\left[(1+\cos^2\frac{\epsilon}{2})^2 + \cos^2\frac{\epsilon}{2}\sin^2\frac{\epsilon}{2}\right]. \tag{4.34}$$

Some trigonometric algebra finally yields the result

$$\begin{aligned}\beta_2^{(N)} &= -\frac{N}{8\pi}\sin\frac{\pi}{N}\left(5+3\cos\frac{\pi}{N}\right)\\ &= -1+\frac{17}{48}\left(\frac{\pi}{N}\right)^2+\mathcal{O}(N^{-4}).\end{aligned} \tag{4.35}$$

Note that it is also possible to define

$$\frac{|\left\langle\psi|L_1+\bar{L}_{-1}|\phi^+\right\rangle|^2}{\langle\psi|\phi\rangle} = -\frac{N}{\pi}\sin\frac{\pi}{N}, \tag{4.36}$$

which actually converges faster towards the continuum value. A similar calculation holds for holomorphic excitations, so we obtain the same indecomposability parameters in both sectors.

We remark that one can obtain explicit lattice formulae for other indecomposability parameters, however, the algebra becomes much more complicated. For example, we find

$$\begin{aligned}\beta_3^{(N)} = -\frac{N}{256\pi^3}\sin\frac{2\pi}{N}\Big[&16\sin^2\frac{\pi}{N}(4\pi+N(1+\cos\frac{\pi}{N})\sin\frac{\pi}{N})^2\\ &+(32\pi\cos\frac{\pi}{N}+5N\sin\frac{2\pi}{N}+2N\sin\frac{3\pi}{N})^2\Big].\end{aligned} \tag{4.37}$$

This coefficient has the following asymptotic behavior

$$\beta_3^{(N)} = -18+\frac{125}{4}\left(\frac{\pi}{N}\right)^2-\frac{29209}{1502}\left(\frac{\pi}{N}\right)^4+\mathcal{O}(N^{-6}). \tag{4.38}$$

This is consistent with the continuum expression $\beta_3 = -18$ (see Sec. 2.4). We could go on and compute lattice expressions of other logarithmic couplings in a similar fashion. In principle, all the coefficients characterizing the continuum LCFT could be obtained from the spin chain using the same method.

4.2.3 Measure of b in periodic percolation

We have seen that the case of periodic symplectic fermions is not so different from the corresponding boundary LCFT, in particular, the indecomposability parameters are the same in both cases. This is probably due to the lack of interaction, as it turns out that more complicated interacting theories like polymers or percolation have a bulk theory that seems to be be completely unrelated to the boundary case [75]. In this section, we come back to these results in more detail.

Note that we tackle in details the percolation theory in this section, but let us mention that a similar analysis can be done for the $c = -7$ theory, or for dilute polymers for example.

Percolation and supersymmetry

We now focus on the percolation problem, for which the full bulk theory is still missing. This theory has central charge $c = 0$ (which follows from the trivial partition function $Z = 1$), and as in the chiral case, we expect the stress energy tensor $T(z) = L_{-2}I$ to be mixed into a Jordan cell with its logarithmic partner $t(z, \bar{z})$ such that in the basis (T, t), the generator of the scale transformation reads [5]

$$L_0 + \bar{L}_0 = \begin{pmatrix} 2 & 2 \\ 0 & 2 \end{pmatrix}. \tag{4.39}$$

We will show later (see also [85]) that the non diagonalizable term can be decomposed as $L_0 t = 2t + T$ and $\bar{L}_0 t = T$, so that the field $t(z, \bar{z})$ has a non trivial antiholomorphic part $\bar{\partial} t \neq 0$. Just like in the chiral setup, we define $b = \langle T|t\rangle$.

The natural setup for this theory is of course geometrical, and after a slight modification similar (see [140] for a similar discussion in the open case), it is straightforward to build a transfer matrix (or a Hamiltonian) for a dense loop model with fugacity $n = 1$, which has Jordan cells in the spectrum. The different sectors of the transfer matrix can be labeled using the parameters j and K of the JTL algebra, where it is understood that we allow contractions of through lines in order to mix the sectors. As a consequence, j can only decrease under the action of the transfer matrix. We must first define what we call the stress energy tensor $|T\rangle$. It is the only state with conformal weight $(2, 0)$ in the vacuum standard module $\hat{\mathcal{W}}_0$. There are states with the same exponents in the modules $\hat{\mathcal{W}}_1$ and $\hat{\mathcal{W}}_{2,1}$, but the eigenvalues corresponding to $|T\rangle$ only appear in the module $\hat{\mathcal{W}}_{2,1}$. There are many other exact degeneracies between the module $\hat{\mathcal{W}}_0$ and $\hat{\mathcal{W}}_{2,1}$ that occur only for $n = 1$, but we will focus on the Jordan cell involving the stress energy tensor. The Jordan cell we are after should thus mix states between $\hat{\mathcal{W}}_0$ and $\hat{\mathcal{W}}_{2,1}$ – this will be discussed algebraically in Sec. 4.2.4.

Of course, this Jordan cell cannot appear in the XXZ representation as the numbers $j = 0$ and $j = 2$ correspond to different values of the spin S_z which is conserved by the Hamiltonian. To obtain another representation where this Jordan cell arises, we turn to the periodic $\mathfrak{sl}(2|1)$ spin chain (we recall that the open version of this models was defined in Chap. 3). This model corresponds to the fixed point of a nonlinear sigma model on $\mathbb{CP}^{1|1}$, the operator content is given by the partition function [110]

$$Z = F_{0,q^2} - F_{1,1} + 8F_{1,1} + 23F_{2,1} + 24F_{2,-1} + 112F_{3,1} + 105(F_{3,e^{2i\pi/3}} + F_{3,e^{4i\pi/3}}) + \dots \tag{4.40}$$

which strongly suggests that the building blocks of this spin chain are the standard modules of the JTL algebra.

First of all, we note that there are 32 fields in the continuum limit with conformal weights $(2, 0)$. We have to discard 8 of them that live in the module $\hat{\mathcal{W}}_1$ as their eigenvalues do not match those of T in finite size. This multiplet of 8 fields transforms in

5. Note that in principle, we could have expected more that one logarithmic partner of the stress energy tensor T in the bulk, but as can be confirmed numerically, the rank of the Jordan cell for T is 2, just like in the chiral case.

the adjoint of $\mathfrak{sl}(2|1)$, so they can be thought of as "descendants" of the currents. There are thus 24 degenerate eigenvalues that may correspond to $|T\rangle$ (or $|t\rangle$) in the superspin chain spectrum [6]. It turns out to be useful to analyze this multiplet of fields under the action of $\mathfrak{sl}(2|1)$. To that purpose, we use the notations gathered in appendix A. Except for the trivial representation $\{0\}$ of dimension 1,the representations that occur in the spin chain have to be *projective representations*. This means that either typical representations $\{b, j\}$ and atypical projective covers $\mathcal{P}^{\pm}(j)$ can occur. Coming back to the 24-state multiplet with the same eigenvalue as the stress energy tensor, each of these states can be labeled by the two quantum numbers (S_z, B) conserved by the Hamiltonian. From elementary representation theory considerations, one can deduce that they transform with respect to $\mathfrak{sl}(2|1)$ as $\{0, 2\} \oplus \mathcal{P}(0)$. A similar analysis shows that in the open case, the multiplet eigenvalues corresponding to $|T\rangle$ transforms as $\mathbf{56} = \{0, 1\} \oplus \{\frac{1}{2}, \frac{3}{2}\} \oplus \{-\frac{1}{2}, \frac{3}{2}\} \oplus \{0, 2\} \oplus \mathcal{P}(0)$. Notice the occurrence of the projective cover $\mathcal{P}(0)$ in both cases. Moreover, it is straightforward to check numerically that the rank 2 Jordan cell occurs only in the sector ($S_z = 0$, $B = 0$). Therefore, we conjecture that the fields t and T appear respectively at the top and at the bottom of the structure

$$\mathcal{P}(0) = \begin{array}{ccc} & \{0\} & \\ \swarrow & & \searrow \\ \{\frac{1}{2}\}_+ & & \{\frac{1}{2}\}_- \\ \searrow & & \swarrow \\ & \{0\} & \end{array} \quad , \tag{4.41}$$

both in the open and periodic cases, where the arrows represent the actions of the generators of $\mathfrak{sl}(2|1)$. Note that this idea of considering t and T at the top and at the bottom of a SUSY multiplet goes back to the work of Gurarie and Ludwig [54]. Although the indecomposable $\mathfrak{sl}(2|1)$ representations associated with t and T are the same in the chiral and non-chiral cases, the Virasoro structure seems much more intricate in the bulk and we emphasize that the symmetry algebra (commutant) of the $\mathfrak{sl}(2|1)$ spin chain is in fact much larger than $\mathfrak{sl}(2|1)$ [68], so the analysis with respect to this partial $\mathfrak{sl}(2|1)$ symmetry is not the end of the story.

Numerical results

We would like to measure directly on the lattice the indecomposability parameter for the stress energy tensor $b = \langle T|t\rangle$, using both the supersymmetric and geometrical setups. It is quite easy to identify the lattice version of the stress energy tensor T. Let us normalize the states in order to prepare the comparison with CFT; in the basis $(\left|T^{(N)}\right\rangle, \left|t^{(N)}\right\rangle\})$, we have

$$L_0^{(N)} + \bar{L}_0^{(N)} = -\frac{2N}{2\pi v_F} \sum_{j=1}^{2N} (e_i - e_\infty) = \begin{pmatrix} \Delta_T^{(N)} & 2 \\ 0 & \Delta_T^{(N)} \end{pmatrix}, \tag{4.42}$$

6. Actually there are 48 such degenerate eigenvalues in the whole spectrum, but we only focus on fields with $s = h - \bar{h} = +2$.

$L = 2N$	$b_1^{(N)}$	$b_2^{(N)}$
10	-4.33296	-3.75812
12	-4.55078	-4.12350
14	-4.68234	-4.35560
16	-4.76634	-4.50978
18	-4.82256	-4.61640
20	-4.86168	-4.69272
22	-4.88978	-4.74896
∞	-5.00 $\pm$ 0.01	-5.00 $\pm$ 0.02
Exact	-5	-5

Table 4.2: Measure of the indecomposability parameter b in periodic percolation.

where $\Delta_T^{(N)} = \frac{2N}{2\pi v_F}(E_T^{(N)} + 2Ne_\infty) = \frac{2N}{2\pi v_F}(E_T^{(N)} - E_0^{(N)}) + \mathcal{O}(N^{-1})$ and $\lim_{N\to\infty} \Delta_T^{(N)} = 2$. Percolation has $e_\infty = 1$ and $v_F = \frac{3\sqrt{3}}{2}$. Note that $\left|T^{(N)}\right\rangle$ is an eigenvector of the translation operator $Q = u^2$

$$Q\left|T^{(N)}\right\rangle = \mathrm{e}^{4\pi i/N}\left|T^{(N)}\right\rangle, \tag{4.43}$$

so that it indeed has a conformal spin $s = h - \bar{h} = 2$. We still have to deal with the normalization of the stress energy tensor, this can be done using the Koo-Saleur formula (4.31).

The lattice scalar products for the loop and supersymmetric representations are well-known, and it is now well accepted that they go to the Virasoro bilinear form in the continuum limit (see the discussion in the chiral case in the previous chapter). Gathering all the pieces, we define two different versions of b on the lattice

$$b_1^{(N)} = \frac{|\left\langle t^{(N)}|(L_{-2} + \bar{L}_{+2})^{(N)}|0^{(N)}\right\rangle|^2}{\langle t^{(N)}|T^{(N)}\rangle}, \tag{4.44a}$$

$$b_2^{(N)} = \frac{|\left\langle t^{(N)}|L_{-2}^{(N)}|0^{(N)}\right\rangle|^2}{\langle t^{(N)}|T^{(N)}\rangle}. \tag{4.44b}$$

Results are shown on Tab. 4.2, they do not depend on the chosen representation (SUSY spin chain or geometric model). Note that there are infinitely many ways to regularize the number b on the lattice. In the scaling limit, we expect $\left|T^{(N)}\right\rangle = \alpha\left|T^{CFT}\right\rangle + \ldots$ and there are various ways to get rid of the proportionality factor α. It is clear in eq. (4.44a) that the factor α cancel out of the numerator and the denominator in the scaling limit.

OPE argument

The value $b = -5$ is quite surprising, since using standard arguments, one would identify to a large extent the chiral sector of the bulk theory with the chiral theory, and thus one would expect to recover the standard values $-\frac{5}{8}$ or $\frac{5}{6}$. However, it was recently argued by D. Ridout that this special value actually emerges from non-chiral Virasoro representation theory [97]. Moreover, to derive this value analytically, it is also possible to generalize the $c \to 0$ catastrophe argument (see Sec. 2.2) to the non-chiral case [75]:

For generic $c \neq 0$, conformal invariance fixes the OPE of an operator $\Phi_{h,\bar{h}}(z,\bar{z})$ with itself to be of the form

$$\Phi_{h,\bar{h}}(z,\bar{z})\Phi_{h,\bar{h}}(0,0) \sim \frac{a_\Phi}{z^{2h}\bar{z}^{2\bar{h}}}\left[1 + \frac{2h}{c}z^2 T(0) + \frac{2\bar{h}}{c}\bar{z}^2\bar{T}(0) + \dots\right]. \tag{4.45}$$

This expression is ill-defined as $c \to 0$. Just like the chiral case, we assume that there is a field in the spectrum with conformal weights $(2,0)$ that will cancel this divergence [7]. Let us consider the $\mathfrak{sl}(2|1)$ spin chain to fix the ideas. There is an unique primary field $X(z,\bar{z})$ that has $(h,\bar{h}) = (2,0)$ in the partition function (4.40), in terms of Kac labels, it reads

$$X(z,\bar{z}) = \Phi_{1,-2}(z) \otimes \Phi_{1,2}(\bar{z}). \tag{4.46}$$

In the Coulomb Gas (loop) language, this field is the spin-2 4-leg operator. It lives in the module $\hat{\mathcal{W}}_{2,1}$ with character

$$F_{2,1} = q^2 + \bar{q}^2 + q^{5/8}\bar{q}^{5/8} + \dots \tag{4.47}$$

whereas T appears as a descendant of the identity in the module $\hat{\mathcal{W}}_0$, with character

$$F_{0,q^2} - F_{1,1} = 1 + q^2 + \bar{q}^2 + q^{5/8}\bar{q}^{5/8} + \dots \tag{4.48}$$

This is consistent with our observation that the modules $\hat{\mathcal{W}}_{2,1}$ and $\hat{\mathcal{W}}_0$ should be mixed into a Jordan cell. When c is slightly different from 0 ($x = 2 + \epsilon$), the OPE reads [8]

$$\Phi_{h,\bar{h}}(z,\bar{z})\Phi_{h,\bar{h}}(0,0) \sim \frac{a_\Phi}{z^{2h}\bar{z}^{2\bar{h}}}\left[1 + \frac{2h}{c}z^2 T(0) + z^{h_{1,-2}}\bar{z}^{h_{1,2}}X(0,0) + \dots\right]. \tag{4.49}$$

We then define a new field $t(z)$ as

$$X(z,\bar{z}) = \frac{2h\,\langle T|T\rangle}{c\beta(\epsilon)}t(z,\bar{z}) - \frac{2h}{c}T(z), \tag{4.50}$$

7. We drop the term $\frac{2\bar{h}}{c}\bar{z}^2\bar{T}(0)$ to focus on the holomorphic one. The antiholorphic divergence will be canceled by $\bar{X}$ in the same way.

8. In order to simplify the notations, we normalize the field $X(z,\bar{z})$ to absorb the structure constants.

where $\beta(\epsilon) = -\frac{\langle T|T\rangle}{h_{1,-2}-2} = -\frac{\langle T|T\rangle}{h_{1,2}}$ and $\langle T|T\rangle = \frac{c}{2}$. It is an easy exercise to check that this way, the OPE involves quantities that are perfectly defined as $c \to 0$

$$\Phi_{h,\bar{h}}(z,\bar{z})\Phi_{h,\bar{h}}(0,0) \sim \frac{a_\Phi}{z^{2h}\bar{z}^{2\bar{h}}}\left[1 + \frac{h}{b}z^2(\log|z|^2 T(0) + t(0,0)) + \frac{\bar{h}}{b}\bar{z}^2(\log|z|^2\bar{T}(0) + \bar{t}(0,0)) + \dots\right], \tag{4.51}$$

with $b = \lim_{\epsilon\to 0}\beta(\epsilon) = -5$. The fields $T(z)$ and $t(z,\bar{z})$ then satisfy the standard equations for logarithmic operators

$$\langle T(z)T(0)\rangle = 0 \tag{4.52a}$$

$$\langle T(z)t(0,0)\rangle = \frac{b}{z^4} \tag{4.52b}$$

$$\langle t(z,\bar{z})t(0,0)\rangle = \frac{\theta - 2b\log|z|^2}{z^4}, \tag{4.52c}$$

with θ a constant. The coefficient b is thus the indecomposability parameter indeed, and this whole argument predicts $b = -5$, in perfect agreement with our numerical results. The key idea in this approach is the identification $X(z,\bar{z}) = \Phi_{1,-2}(z)\otimes\Phi_{1,2}(\bar{z})$, which is natural since this is the only candidate with conformal weights $(2,0)$ in the spectrum.

Note that this argument also predicts that $\bar{\partial}t \neq 0$ so that

$$\bar{L}_0|t\rangle = |T\rangle, \tag{4.53}$$

as it should, since we expect $L_0 - \bar{L}_0$ to be diagonalizable in any reasonable bulk theory [83].

Finally, for the generic OPE to be well-defined, it is reasonable to expect $X(z,\bar{z}) = \Phi_{1,-2}(z)\otimes\Phi_{1,2}(\bar{z})$ (and its analog $\bar{X}(z,\bar{z}) = \Phi_{1,2}(z)\otimes\Phi_{1,-2}(\bar{z})$ giving rise to $\bar{t}$) to be degenerate at holomorphic (resp. anti-holomorphic) level 2. We will thus conjecture that they satisfy the differential equations

$$\left(\bar{L}_{-2} - \frac{3}{2+4h_{1,2}}\bar{\partial}^2\right)X(z,\bar{z}) = 0 \tag{4.54a}$$

$$\left(L_{-2} - \frac{3}{2+4h_{1,2}}\partial^2\right)\bar{X}(z,\bar{z}) = 0. \tag{4.54b}$$

Expressed in terms of the usual fields $T, t, \bar{T}, \bar{t}$, we find that eq. (4.54) reads

$$\frac{2}{c}T\bar{T} = \frac{1}{b}\left(\bar{L}_{-2} - \frac{3}{2+4h_{1,2}}\bar{\partial}^2\right)t \tag{4.55a}$$

$$\frac{2}{c}T\bar{T} = \frac{1}{b}\left(L_{-2} - \frac{3}{2+4h_{1,2}}\partial^2\right)\bar{t}. \tag{4.55b}$$

We thus see that at $c = 0$

$$\psi_{(2,2)} \equiv \lim_{c\to 0} \frac{2b}{c} T\bar{T} = \left(\bar{L}_{-2} - \frac{3}{2}\bar{\partial}^2\right) t = \left(L_{-2} - \frac{3}{2}\partial^2\right) \bar{t}, \tag{4.56}$$

where the '=' symbol should of course be understood in terms of correlation function. This equality is crucial as it reduces to the quotient considered by D. Ridout to obtain a bulk module compatible with $b = -5$ [97]! The field $\psi_{(2,2)}$ is a logarithmic partner of $T\bar{T}$

$$(L_0 + \bar{L}_0) \left|\psi_{(2,2)}\right\rangle = 4 \left|\psi_{(2,2)}\right\rangle + 2 \left|\bar{T}T\right\rangle . \tag{4.57}$$

In the $\mathfrak{sl}(2|1)$ chain, it turns out that $\left|\psi_{(2,2)}\right\rangle$ also has a logarithmic partner [120], so that $T\bar{T}$ lies at the bottom of a rank 3 Jordan cell.

Physical discussion

This value of b in the bulk has interesting consequences, in particular, it implies that there are many fields that do not satisfy differential equations in the bulk.

Although computing all the n-point correlation functions in the bulk may appear as a daunting task, one may hope that as in the chiral case there would be some physical fields, with a clear geometrical meaning, that would satisfy the usual correlation functions. However, if this were correct, there would be a contradiction since the differential equation approach always yields either $b = -\frac{5}{8}$ or $b = \frac{5}{6}$ for the Jordan cell of the stress energy tensor [54] (we shall come back to this shortly). This would not be consistent with our value $b = -5$.

It has been mentioned in the literature (see *e.g.* [157]) that the original assumption of Gurarie and Ludwig ($b = \frac{5}{6}$ for percolation) could be correct in the bulk. This original argument mostly relies on the calculation of the correlation function through differential equations coming from null-vector condition. Let us consider for example the correlation function $\langle \Phi_{2,1}\Phi_{2,1}\Phi_{2,1}\Phi_{2,1}\rangle$. Recall that $\epsilon = \Phi_{2,1} = \Phi_{2,1}(z) \otimes \Phi_{2,1}(\overline{z})$ is the energy operator in the Potts model, it thus has a clear physical interpretation. It is used to construct thermal perturbations of the theory $S_{\mathrm{CFT}} + \lambda \int d^2z \Phi_{2,1}$, and is generically degenerate at level 2. We can thus readily compute its four-point correlation function, and of course, it follows closely the computation of the chiral case (see 2.2.3). The solution of this calculation is consistent $b = \frac{5}{6}$ like in the open case for polymers (recall that $\Phi_{2,1}$ belongs to the polymer theory in the open case).

All this may seem a bit puzzling, and we should ask ourselves where this operator $\epsilon(z, \bar{z})$ comes into play in our $\mathfrak{sl}(2|1)$ spin chain. To be consistent with our value $b = -5$, something very singular should happen to this operator at $c = 0$. Indeed, everything seems to indicate that ϵ is a null field with a logarithmic partner (just like $T(z)$) and that all its n-point correlation functions are equal to zero! First, recall that the energy operator has conformal weight $(\frac{5}{8}, \frac{5}{8})$ at $c = 0$, it appears with degeneracy 24. One of this value lives in the module $\hat{\mathcal{W}}_0$, this is the field that corresponds to $\epsilon = \Phi_{2,1}$, it is generically degenerate at level 2. However, there are 23 other fields that arise with the

same conformal weights at $c = 0$ coming from the module $\hat{\mathcal{W}}_{2,1}$. It turns out that ϵ is mixed into a Jordan cell for $H = L_0 + \bar{L}_0$ with one of the fields of $\hat{\mathcal{W}}_{2,1}$. These 24 fields transform under $\mathfrak{sl}(2|1)$ as $\{0, 2\} + \mathcal{P}(0)$, in particular, everything seems to indicate that ϵ lies at the bottom of the projective cover $\mathcal{P}(0)$ just like the stress energy tensor.

It is also possible to check that the energy is a null field directly on the lattice. Indeed, the thermal perturbation corresponds on the lattice to the operator $\sum_i (-1)^i e_i$. If we call $|0\rangle$ the fundamental of our spin chain, the natural state corresponding to ϵ should read

$$|\epsilon\rangle = \sum_i (-1)^i e_i \, |0\rangle \, . \tag{4.58}$$

This vector satisfies $\langle\epsilon|\epsilon\rangle = 0$ exactly on the lattice as can be checked numerically. This means that the two-point function of ϵ should be equal to 0, as expected if it lives at the bottom of a Jordan cell. Supposing that the energy operator is indeed at the bottom of the Virasoro Jordan cell, we know from conformal invariance that its two-point function should be equal to zero indeed. Using a $\varepsilon \to 0$ limit on the solution of the differential equation of ϵ, it is possible to show that if $\langle\epsilon\epsilon\rangle = 0$ at $c = 0$ ($\varepsilon = 0$), then all the n-point functions vanish $\langle\epsilon\epsilon\ldots\epsilon\rangle = 0$. Therefore, the four-point function of the energy operator does make sense at $c = 0$, and is simply irrelevant in the theory.

One could then wonder if another operator Φ with conformal weights $(\frac{5}{8}, \frac{5}{8})$ satisfies the null-vector condition

$$(L_{-1}^2 - \frac{3}{2} L_{-2})\Phi = 0, \tag{4.59}$$

that would again contradict our result $b = -5$. This would imply that the corresponding states on the lattice have a null norm. We checked that the 23 other states do no have a zero norm [9], they are thus not degenerate at level 2 like $\Phi_{2,1}$, and they *do not* satisfy the corresponding differential equation. This is quite expected because these 23 other fields live in the module $\hat{\mathcal{W}}_{2,1}$ and correspond generically to the conformal weight $h_{0,2}$. Although one has $h_{0,2} = h_{2,1} = \frac{5}{8}$ at $c = 0$, these fields do not have the same continuation when $c \neq 0$. In particular, $h_{2,1} = h_{1+1/(x+1),0} = \frac{5}{8} - \frac{3}{16}\varepsilon + \mathcal{O}(\varepsilon^2)$ and $h_{0,2} = \frac{5}{8} + \frac{7}{48}\varepsilon + \mathcal{O}(\varepsilon^2)$, where we have parametrized $x = 2 + \varepsilon$. These fields $\Phi_{0,2}$ do not satisfy any differential equation, so in particular we do not know in general how to compute their correlation functions.

In general, this discussion seems to indicate that one has to be careful using differential equations to compute the correlation functions of bulk observables. Ludwig and

9. It turns out that Virasoro null-vector in the scaling limit can be easily identified on the lattice using the Koo-Saleur formula (4.31). The continuum null-vectors regularized on the lattice this way always have a very small norm, usually of the order of the numerical precision. For example, if $|0^{(N)}\rangle$ is the normalized groundstate of the percolation spin chain, it is then straightforward to check that $L_{-2}^{(N)} |0^{(N)}\rangle$ has a "very small norm" (i.e. of the order of the numerical precision) as expected from the continuum result $\langle T(z)T(0)\rangle = 0$ at $c = 0$. Note however that there is no reason for these vectors built using the Koo-Saleur formula to be exactly null on the lattice (although it may be hard to tell from a numerical point of view), as opposed to their H-eigenstate counterparts that should be exactly null for algebraic reasons.

Gurarie showed that the solution of the differential equations associated with the two first row and the first column of the Kac table always yield either $b = -\frac{5}{8}$ and $b = \frac{5}{6}$. This is consistent with the results of the chiral case but our result in the bulk tends to show that none of these operators satisfy these differential equations, and when they do, there may be some strong logarithmic structure that enforces their correlation functions to be 0, just like for the energy operator.

4.2.4 Towards a bulk $c = 0$ LCFT for percolation

Among the remaining challenges, the understanding of bulk LCFTs at $c = 0$ is of utmost interest. In the lattice approach, bulk LCFTs are tackled by considering periodic spin chains, in particular, the $\mathfrak{sl}(2|1)$ supersymmetric spin chain. Because of the "loops" then going around the space direction, the corresponding algebras defined in 4.2.1 are considerably more complicated. In particular, the quantum group symmetry is partly lost. The spectrum of conformal weights is then extremely rich, in particular, the conformal weights cannot be arranged in a finite number of families where weights differ from each other by integers. Although the conformal weights are all rational, the theory is therefore not rational [110].

Another crucial issue is that whereas in the case the TL algebra, irreducible representations go to irreducible Virasoro modules in the continuum limit, irreducible representations over the JTL algebra correspond in the scaling limit to a infinite direct sum of irreducible representations of $\mathfrak{vir} \oplus \overline{\mathfrak{vir}}$. Getting a handle on the structure of representations over the two chiral and antichiral copies of the Virasoro algebra is therefore quite intricate. This can actually be understood as the existence of a larger symmetry in the limit, whose irreducible representations decompose over an infinite direct sum of modules when restricted to the subalgebra $\mathfrak{vir} \oplus \overline{\mathfrak{vir}}$. While the Virasoro modes L_n and $\bar{L}_n$ can be extracted from the periodic Temperley–Lieb algebras [118, 132], it is interesting to remark that the scaling limit of some elements in the periodic TL can lead to other physical observables corresponding to different bulk scaling fields. A very important example of such a field is the energy operator $\Phi_{2,1} \times \overline{\Phi}_{21}$ which can be realized by the staggered perturbation $\sum(-1)^i e_i$. The introduction of such fields in the organizing algebra of a LCFT requires a discussion of objects that mix chiral and anti-chiral sectors, thus leading to the concept of interchiral algebra [149], which appears as limit of the JTL algebra. This interchiral algebra is probably the key to understand algebraically such LCFTs. Despite these difficulties, it is worth emphasizing that we are directly dealing with a physical theory, so that in particular, the $c = 0$ LCFT constructed here naturally has a unique vacuum Ω, invariant under translations $L_{-1}\Omega = 0$.

The full analysis of the bulk percolation LCFT will be described in details in [120], one of the main results being that the Hamiltonian operator $L_0 + \overline{L}_0$ admits Jordan cells of arbitrarily large rank as the corresponding conformal weight is increased. Just to give a flavor of the results, let us mention that the stress-energy tensor $T(z)$ and its logarithmic partner $t(z, \bar{z})$ (together with their antiholomorphic counterparts) are living in a very complicated (vacuum) module that consists of a gluing of many standard JTL modules. In particular, the fields with conformal weights $(2, 0)$ are living in the

standard modules $\hat{\mathcal{W}}_0$ and $\hat{\mathcal{W}}_{2,1}$, the latter being itself indecomposable with structure

$$\hat{\mathcal{W}}_0 = \hat{\mathcal{W}}_{0,\mathfrak{q}^2}/\hat{\mathcal{W}}_{1,1} = \qquad (4.60)$$

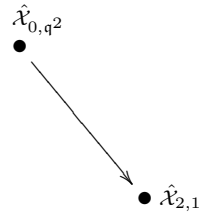

while $\hat{\mathcal{W}}_{0,\mathfrak{q}^2}$ has the following structure

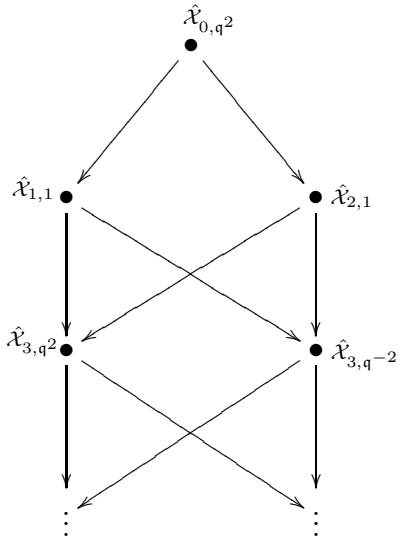

(4.61)

The operator content of JTL simple modules can then be obtained from this structure, for instance

$$F^{(0)}_{0,\mathfrak{q}^2} \equiv \mathrm{Tr}_{\hat{\mathcal{X}}_{0,\mathfrak{q}^2}} q^{L_0}\bar{q}^{L_0} = \sum_{n=0}^{\infty} \left(F_{3n,\mathfrak{q}^2} + F_{3n+3,\mathfrak{q}^{-2}} - F_{3n+1,1} - F_{3n+2,1}\right) = \chi_{1,1}\overline{\chi}_{1,1} = 1, \qquad (4.62)$$

where $\chi_{r,s}$ are the irreducible Virasoro characters (without the central charge term). The operator content of $\hat{\mathcal{X}}_{2,1}$ is much more complicated

$$F^{(0)}_{2,1} = \chi_{2,1}\overline{\chi}_{2,1} + \chi_{3,1}\overline{\chi}_{1,1} + \chi_{1,1}\overline{\chi}_{3,1} + \dots \qquad (4.63)$$

so that $\hat{\mathcal{X}}_{2,1}$ contains an infinite numbers of irreducible representations $(h, \bar{h})$ of $\mathfrak{vir}\oplus\overline{\mathfrak{vir}}$

$$\hat{\mathcal{X}}_{2,1}\Big|_{\mathfrak{vir}\oplus\overline{\mathfrak{vir}}} \longrightarrow \left(\frac{5}{8},\frac{5}{8}\right) \oplus (2,0) \oplus (0,2) \oplus 2\,(2,2) \oplus \dots \qquad (4.64)$$

The indecomposable vacuum module being a complex gluing of such simple JTL modules, we thus see that the structure over $\mathfrak{vir} \oplus \overline{\mathfrak{vir}}$ is especially intricate. Arguably,

computing bulk 4-point correlation functions in percolation remains even more complicated, and sadly out of reach as of now.

4.3 From boundary to bulk LCFTs: braid translator

The relation between bulk and boundary theories is a crucial issue in CFT. As far as ordinary CFTs are concerned, Cardy argued in his celebrated paper [158] that boundary fields can be interpreted as operators changing boundary conditions, and that they are in one-to-one correspondence with bulk fields (see also [159, 160] for related works). Unfortunately, this interplay between bulk and boundary is far more complicated for Logarithmic CFTs, see [147]. In this section, we shortly review some of the results that shall be presented in [76], and analyze how to go from boundary to bulk theories from the point of view of lattice models.

4.3.1 Braid translator

The braid translator is a tool that allows us to generate affine TL algebra representations from representations of the ordinary TL and blob algebras. Starting from (a representation of) the blob algebra $\mathcal{B}(L=2N,\mathfrak{q},y)$ one defines the braid operators

$$g_i^{\pm 1} = 1 - \mathfrak{q}^{\mp 1} e_i. \tag{4.65}$$

These operators satisfy the braid relations

$$g_i g_{i\pm 1} g_i = g_{i\pm 1} g_i g_{i\pm 1}. \tag{4.66}$$

They can be represented graphically as

$g_i =$  $\qquad g_i^{-1} =$ 

The key point observed in [145] is that the generator defined by

$$e_{2N}^{\text{braid}} = \left(\prod_{i=1}^{2N-1} g_i\right)^{-1} (\alpha b + 1)\, e_1\, (1+\beta b) \prod_{i=1}^{2N-1} g_i, \tag{4.67}$$

where $\prod_{i=1}^{n} g_i = g_1 g_2 \dots g_n$ and

$$\alpha \equiv \alpha(\mathfrak{q}) = \frac{\mathfrak{q}-\mathfrak{q}^{-1}}{\mathfrak{q}^{-1}-y}, \qquad \beta = \alpha(\mathfrak{q}^{-1}), \tag{4.68}$$

obeys the relations $e_{2N}^{\text{braid}} e_1 e_{2N}^{\text{braid}} = e_{2N}^{\text{braid}}$, $e_1 e_{2N}^{\text{braid}} e_1 = e_1$, *etc.*, and $(e_{2N}^{\text{braid}})^2 = (\mathfrak{q} + \mathfrak{q}^{-1}) e_{2N}^{\text{braid}}$ of the affine TL algebra TL_L^a.

Recall then that the TL_L^a is generated by e_j's and the translation element u together with the defining relations (4.10). We can go further and define a translation operator as

$$u = (-1)^N \mathfrak{q}^N \sqrt{\frac{y - \mathfrak{q}}{y - \mathfrak{q}^{-1}}} (1 + \beta b) \prod_{i=1}^{2N-1} g_i \tag{4.69}$$

which obeys

$$u e_i u^{-1} = e_{i+1}, \qquad 1 \leq i \leq L \mod L, \tag{4.70}$$

along with the relation

$$u^2 e_{L-1} = e_1 \dots e_{L-1}. \tag{4.71}$$

The relation $u^{-1} e_1 u = e_L$ readily follows from the expression (4.67) while the last one can be easily proven by an induction and using the braid relations (4.66).

This construction can be used to generate a representation of the affine TL algebra $TL_N^a(n)$ starting from a representation of $\mathcal{B}(L, n, y)$: in more mathematical terms, the *braid translation* is an algebra homomorphism $\mathsf{br} : TL_N^a(n) \longrightarrow \mathcal{B}(L, n, y)$. Starting from a representation of the Blob algebra $\rho : \mathcal{B}(L, n, y) \longrightarrow \text{End}(E)$ (with E a vector space, for instance $E = V^{\otimes N}$ for a spin chain), we call Braid-generated representation the representation over the $TL_N^a(n)$ algebra $\rho \circ \mathsf{br}$.

It is worth noticing that u^{2N} is central and it thus acts on irreducible representations proportionally to the identity operator. If we parametrize

$$y = \frac{\mathfrak{q}^{-1} - \mathfrak{q} \mathrm{e}^{2i\eta}}{1 - \mathrm{e}^{2i\eta}}, \tag{4.72}$$

one can show that in the standard representation with $2|j|$ through-lines (we use the convention $j > 0$ in the blobbed sector, and $j < 0$ for the unblobbed one) its action reads

$$u^{2N} = (\mathfrak{q}^{2j} \mathrm{e}^{2i\eta})^j. \tag{4.73}$$

In other words, the factor picked by $2j$ through-lines as they wind one time around the annulus is given by

$$\alpha_{2j} = (\mathfrak{q}^{2j} \mathrm{e}^{2i\eta})^j. \tag{4.74}$$

Finally for the sector with zero through-lines, $j = 0$, the braid translator generates affine TL representations where each non-contractible loop should be replaced by the

factor

$$\alpha_0 = \mathrm{e}^{i\eta} + \mathrm{e}^{-i\eta}. \tag{4.75}$$

More precisely, the action of the braid translator on blob standard modules is given by

$$\mathcal{W}_j^b \xrightarrow{\mathsf{br}} \hat{\mathcal{W}}_{j,\mathfrak{q}^{2j}e^{2i\eta}} \tag{4.76}$$

$$\mathcal{W}_j^u \xrightarrow{\mathsf{br}} \hat{\mathcal{W}}_{j,\mathfrak{q}^{2j}e^{-2i\eta}}. \tag{4.77}$$

In particular, the image of $\mathcal{W}_0$ is $\hat{\mathcal{W}}_{0,\mathrm{e}^{2i\eta}}$.

We now introduce the braid translator in the ordinary TL case, which corresponds to setting $y = \mathfrak{q} + \mathfrak{q}^{-1}$, so $\mathrm{e}^{i\eta} = \mathfrak{q}$, and the blob operator to the identity $b \to 1$. In this case, eq. (4.67) reduces to (note that $(\alpha+1)(\beta+1) = 1$)

$$e_{2N}^{\mathrm{braid}} = \left(\prod_{i=1}^{2N-1} g_i\right)^{-1} e_1 \left(\prod_{i=1}^{2N-1} g_i\right). \tag{4.78}$$

The translation operator u then reads

$$u = (-1)^N \mathfrak{q}^{N-1} \prod_{i=1}^{2N-1} g_i, \tag{4.79}$$

and the factor picked by $2j$ through-lines as they wind one time around the annulus is given by $\alpha_{2j} = (\mathfrak{q}^{2j+2})^j$. The $TL_{2N}^a(n)$ module generated from a TL standard by the braid-translator is given by

$$\mathsf{S}_j \xrightarrow{\mathsf{br}} \hat{\mathcal{W}}_{j,\mathfrak{q}^{2j+2}} / \hat{\mathcal{W}}_{j+1,\mathfrak{q}^{2j}}. \tag{4.80}$$

4.3.2 Braid translation of minimal models

We start by studying the braid translation of lattice Minimal models – open RSOS models. We shall show that a remarkable phenomenon occurs, as the periodic Minimal models can be exactly recovered as the braid translation of various sectors of the corresponding open models. In some simple cases, it is possible to work out explicitly the expression of the last braid-induced generator (4.78). For minimal models $\mathcal{M}(p, p+1)$, it turns out that this last interaction is local, and couples the first and the last sites only. In addition, we shall see that the expression is completely natural, in the sense that it has the same form as the other generators. This contrasts with logarithmic models, for which we will argue that the last generator is highly non-local, with some kind of long-range interaction.

For instance, let us consider first the minimal Ising model $\mathcal{M}(3,4)$. It corresponds to the Temperley-Lieb algebra with $\mathfrak{q} = \mathrm{e}^{i\pi/4}$, with the following quotient $e_i e_{i+1} +$

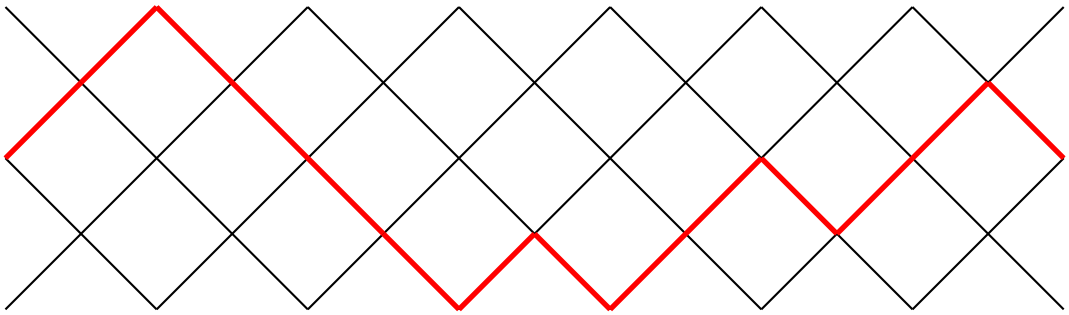

Figure 4.5: Example of RSOS path for $p = 5$ and $N = 7$ with fixed boundary conditions $(3, 3)$. The blob operator b acts on this state as the identity as $h_1 = s + 1 = 4$.

$e_{i+1}e_i - \sqrt{2}(e_i + e_{i+1}) + 1 = 0$. It can be parametrized using the Pauli matrices as

$$e_{2i-1} = \frac{1}{\sqrt{2}}\left(1 + \sigma_i^x\right) \tag{4.81a}$$

$$e_{2i} = \frac{1}{\sqrt{2}}\left(1 + \sigma_i^z\sigma_{i+1}^z\right). \tag{4.81b}$$

The corresponding Hamiltonian expressed in terms of Pauli matrices is usually called transverse field Ising chain. We consider free boundary conditions, that is, $b = 1$. Using the $\mathbb{Z}_2$-symmetry of the Ising model and the expression $\sigma^a\sigma^b = \delta_{ab} + i\epsilon_{abc}\sigma^c$, it is straightforward to show that the braid-induced generator is local

$$e_{2N}^{\text{braid}} = \frac{1}{\sqrt{2}}\left(1 - \sigma_N^z\sigma_{N+1}^z\right), \qquad \sigma_{N+1}^z = \epsilon\sigma_1^z, \tag{4.82}$$

with $\epsilon = \pm 1$. This expression is totally natural is the sense that is corresponds to the usual periodic expression. This can be generalized to other boundary conditions – for instance, $b = \frac{1+\sigma_z}{2}$ corresponds to fixed boundary condition in the Ising chain – and to other minimal models [76] (see related expressions in [161, 162]).

Braid translation of RSOS models

One can actually induce the full diagonal bulk minimal models starting from open spin chains thanks to the braid translator.

Recall first the definition of the open A_p RSOS models, which corresponds to $\mathfrak{q} = \mathrm{e}^{i\gamma}$, $\gamma = \frac{\pi}{p+1}$. We consider a height models with $h_i \in \{1, 2, \ldots, p\}$, $i = 1, \ldots, L = 2N$, subject to the relation $|h_i - h_{i\pm1}| = 1$. We define the action of the Temperley-Lieb

generators as

$$e_i \left|h_1, h_2, \ldots, h_i \ldots, h_L\right\rangle = \delta_{h_{i-1},h_{i+1}} \sum_{h_i'=h_{i-1}\pm 1} \frac{\sqrt{[h_i]_{\mathfrak{q}}\,[h_i']_q}}{[h_{i-1}]_{\mathfrak{q}}} \left|h_1, h_2, \ldots, h_i' \ldots, h_L\right\rangle, \tag{4.83}$$

where we set $h_0 = 1$. The conformal invariant boundary conditions for RSOS models have been discussed extensively in the literature [163–165], and we shall only require the fact that fixing the BCs to be $h_0 = s$ and $h_L = s$ generates the irreducible representation $\rho_{s,s} = \mathcal{X}_0$ of the blob algebra, where s parametrizes the weight of the blobbed loops

$$y = \frac{\sin(s+1)\gamma}{\sin s\gamma} = \frac{[s+1]_{\mathfrak{q}}}{[s]_{\mathfrak{q}}}, \qquad s = 1, \ldots, p. \tag{4.84}$$

The action of the blob generator in these RSOS representations is given by

$$b \left|h_0 = s, h_1, \ldots, h_L = s\right\rangle = \delta_{h_1,s+1} \left|h_0 = s, h_1, \ldots, h_L = s\right\rangle. \tag{4.85}$$

The image space of b corresponds to all the states with $h_1 = s+1$. An example of such state for $j = 0$ is given on Fig. 4.5.

The RSOS models in periodic geometry do not, *a priori*, require such a discussion of boundary conditions: we simply take the Temperley Lieb matrix elements defined in (4.83) and let them act on RSOS configurations which are periodic, that is, $h_{L+1} \equiv h_0$. This produces a finite dimensional representation ρ_{period} of the periodic Temperley–Lieb algebra, which obviously must be some particular quotient. Note that we can choose h_0 to be odd or even from the beginning, and it remains this way upon acting with the Hamiltonian/Transfer matrix. We define the periodic RSOS models without this kind of restriction, *i.e.*, the height h_0 takes all values from 1 to p. It is, in fact, known [67] that such defined representation ρ_{period} decomposes as a direct sum of irreducible representations of the periodic TL algebra, where there are no through lines, and where non-contractible loops are given the weight $2\cos\frac{s\pi}{p+1}$, with $s = 1, \ldots, p$. These representations are $\hat{\mathcal{X}}_{0,\mathfrak{q}^{2s}}$ in our standard notations. The operator content of these irreps is [67]

$$\sum_{r=1}^{p-1} \chi_{rs}\bar{\chi}_{rs}, \tag{4.86}$$

where we use the standard notations for the character of Virasoro simple modules.

The point is now that each of these irreducible representations $\hat{\mathcal{X}}_{0,\mathfrak{q}^{2s}}$ can be obtained by the braid translation br defined in (4.67)

$$\rho_{s,s} = \mathcal{X}_0 \xrightarrow{\ \mathsf{br}\ } \hat{\mathcal{X}}_{0,\mathfrak{q}^{2s}}, \tag{4.87}$$

where we have used the identification (4.75) and $e^{i\eta} = \mathfrak{q}^s$ for $y = \frac{[s+1]_{\mathfrak{q}}}{[s]_{\mathfrak{q}}}$. After summing

of all values of s, we finally obtain

$$\bigoplus_{s=1}^{p} \rho_{s,s} \xrightarrow{\text{br}} \rho_{\text{period}}, \tag{4.88}$$

so the overall partition function reads

$$Z = \sum_{s=1}^{p} \sum_{r=1}^{p-1} \chi_{rs} \bar{\chi}_{rs}. \tag{4.89}$$

Therefore, after a sum over the braid translation of the p sectors of the open model with boundary conditions (s, s), we end up with the partition function of the periodic A_p models.

4.3.3 Braid translation of Logarithmic CFTs

Braid translation of the $\mathfrak{gl}(1|1)$ spin chain

Whereas for minimal models, one can obtain the full bulk theory starting for open spin chains, this approach unfortunately does not work for Logarithmic CFTs. Starting from the $\mathfrak{gl}(1|1)$ spin chain for example, one finds that the last generator is highly non-local in terms of the fermions

$$e^{\text{braid}}_{L=2N} = \left(f_1 + (1-i) \sum_{j=2}^{L-1} f_j + f_L \right) \left(f_1^\dagger + (1+i) \sum_{j=2}^{L-1} f_j^\dagger + f_L^\dagger \right). \tag{4.90}$$

This is fundamentally different from the case of the minimal models, since the braid-induced last generator does not reduce to the usual periodic expression $e_{2N} = (f_1 + f_{2N})(f_1^\dagger + f_{2N}^\dagger)$. However, the spectrum of this spin chain is actually the same as in the original periodic case. In the continuum limit, this can be easily seen as the operator content of the braid translation of the TL standard module with $2j$ through lines reads

$$F_{j,(-1)^{j+1}} - F_{j+1,(-1)^j}, \tag{4.91}$$

so that the partition function reduces to that of the usual periodic $\mathfrak{gl}(1|1)$ chain

$$Z = \sum_{j=0}^{\infty} (2j+1) \left(F_{j,(-1)^{j+1}} - F_{j+1,(-1)^j} \right) = F_{0,-1} + 2 \sum_{j=1}^{\infty} F_{j,(-1)^{j+1}}. \tag{4.92}$$

Even though the spectrum is the same, the logarithmic structure is completely different. The full analysis is too long to be given here, and we refer the reader to [76] for details. The outcome of this lattice analysis is that all the indecomposability is concentrated in the holomorphic sector, while the antiholomorphic one is fully reducible. For example,

we find

$$L_0 = \psi_0^+\psi_0^- + \sum_{m\in\mathbb{Z}^\star} :\psi_{-m}^+\psi_m^-:, \tag{4.93}$$

$$\bar{L}_0 = \sum_{m\in\mathbb{Z}^\star} :\bar{\psi}_{-m}^+\bar{\psi}_m^-:, \tag{4.94}$$

so the zero-modes (the non-diagonalizable part) are only in L_0. Unfortunately, the fact that $L_0 - \bar{L}_0$ is non-diagonalizable makes the theory highly non physical, and the non-locality of the last generator has drastic consequences on the field theory. In particular, correlation functions are not invariant under translations, the fields are not local *etc.* Therefore, enforcing the bulk LCFT to be obtained from a chiral sector makes the theory non-physical, with indecomposability only in the chiral sector, and some 'artificial' fully reducible anti-holomorphic sector on top of that.

Braid translation of Percolation

$L = 2N$	$b^{(N)}$
10	-0.598912
12	-0.607285
14	-0.612164
16	-0.615264
18	-0.617357
20	-0.618839
22	-0.619927
∞	-0.62500 $\pm$ 0.00001
Conjecture	$-5/8$

Table 4.3: Measure of the indecomposability parameter b in the braid translation of the open percolation problem with $\mathfrak{q} = \mathrm{e}^{i\pi/3}$.

The study of the braid translation of the $\mathfrak{gl}(1|1)$ spin chain taught us that the braid translation operation may yield some bizarre (and most likely non-physical) bulk theories, as opposed to the case of unitary minimal models. The braid induced theories have an algebraic structure that mimics the chiral case, and are therefore much simpler than what is expected for "physical" bulk LCFTs. To conclude this section, we mention some results obtained for the braid translation of the percolation problem, for which the parallel with the algebraic structure of the chiral theory should be clearer. We focus on the $\mathfrak{sl}(2|1)$ supersymmetric formulation of the theory.

Using our knowledge of the representation theory of the TL algebra at $\mathfrak{q} = \mathrm{e}^{i\pi/3}$ [69, 100], we can deduce the subquotient structure of the JTL representations induced from

the TL standard modules

$$\mathsf{br}(\mathsf{S}_j) = \hat{\mathcal{W}}_{j,\mathfrak{q}^{2j+2}}/\hat{\mathcal{W}}_{j+1,\mathfrak{q}^{2j}} = \begin{cases} \hat{\mathcal{X}}_{j,\mathfrak{q}^2} & \\ \quad \searrow & j \equiv 0 \ (\mathrm{mod}3) \\ \quad\quad \hat{\mathcal{X}}_{j+2,1} & \\ \quad \hat{\mathcal{X}}_{j,1} & j \equiv 1 \ (\mathrm{mod}3) \\ \hat{\mathcal{X}}_{j,1} & \\ \quad \searrow & j \equiv 2 \ (\mathrm{mod}3) \\ \quad\quad \hat{\mathcal{X}}_{j+1,\mathfrak{q}^2} & \end{cases}$$

In terms of generating function, this implies for example that

$$F_{3n,\mathfrak{q}^2} - F_{3n+1,1} = F^{(0)}_{3n,\mathfrak{q}^2} + F^{(0)}_{3n+2,1}, \tag{4.95a}$$

$$F_{3n+2,1} - F_{3n+3,q^4} = F^{(0)}_{3n+2,1} + F^{(0)}_{3n+3,\mathfrak{q}^2}. \tag{4.95b}$$

We see that the induced modules have a structure that mimics exactly the standard modules of the TL algebra. For instance, the Jordan cell of the stress energy tensor corresponds to the diamond module

$$\begin{array}{ccccc} & & \hat{\mathcal{X}}_{2,1} & & \\ & \swarrow & & \searrow & \\ \hat{\mathcal{X}}_{0,\mathfrak{q}^2} & & & & \hat{\mathcal{X}}_{3,\mathfrak{q}^2} \\ & \searrow & & \swarrow & \\ & & \hat{\mathcal{X}}_{2,1} & & \end{array} \quad , \tag{4.96}$$

which is a cousin of the Jordan cell that arises in open chains [69]. Note that this JTL module is in fact much simpler that the one that contains the stress energy tensor in the "physical" $\mathfrak{sl}(2|1)$ spin chain.

We have measured numerically the indecomposability parameter b associated with the stress energy tensor of the theory, we recover $b = -\frac{5}{8}$ (Tab. 4.3) which is the value of the open case, which seems reasonable given the construction of the theory, with again a normalization with a factor 1 off-diagonal in the Hamiltonian. Just like for $\mathfrak{gl}(1|1)$, this suggests that the braid-induced theory is non-pysical as $L_0 - \bar{L}_0$ is not diagonalizable in this theory, and one has $\bar{L}_0 t = 0$ even though $L_0 t = 2t + T$. As a conclusion, the braid translator works well only to construct bulk theories where chiral and anti-chiral parts are fully decoupled, so this construction unfortunately fails for logarithmic CFTs. This will be discussed in more detail in [76].

Chapter 5

Logarithmic structure of geometrical models and disordered systems in dimension $d \geq 2$

To this point we have extensively exposed ideas and tools that are proper to two dimensions. However, the fundamental mechanism for producing Jordan cells of the dilatation operator remains operative in higher dimensions, $d > 2$, provided that two (or more) suitably related operators possess coinciding scaling dimensions. The algebraic tools that would permit to compute the ensuing logarithmic structure directly within such an LCFT are however missing. Instead, insight can be gained by accessing that theory as a limit, by tuning a suitable continuous (or formally continuous) parameter. For a recent review describing this point of view, see [77].

One of the main advantages of this approach is that it allows one to obtain concrete results (*e.g.* probabilities, averaged correlation functions) in situations that are of direct physical relevance – namely, disordered systems or geometrical problems. Among those are:

1. Disordered systems described by n-fold replication, in the replica limit $n \to 0$ [18, 53];
2. The O(n) model, in the limit $n \to$ a non-positive integer (including the polymer limit $n \to 0$) [18];
3. The Q-state Potts model, in the limit $Q \to$ a non-negative integer (including the bond-percolation limit $Q \to 1$) [18, 78, 79].

In all cases the key assumption is that physical operators can be fully described as irreducibles of the corresponding symmetry group (S_n, O(n) or S_Q, as the case may be). Obviously, this approach will fail to give exhaustive results if the actual symmetry turns out to be larger (*e.g.*, when specializing the results for the Potts model in general dimension to $d = 2$).

In this last chapter, we briefly review the ideas of Cardy [18, 53] to tackle critical disordered systems using a replica approach. We show how this is consistent with the $c \to 0$ catastrophe described in chapter 2, and we also mention the alternative SUSY approach which is closely related to the more algebraic framework developed in the previous chapters. We then turn to geometrical problems and argue that this 'replica'

method can be applied to obtain geometrical observables that behave logarithmically at the critical point, in any dimension below the upper critical dimension.

5.1 Critical disordered systems: supersymmetry, replicas and $c = 0$ LCFTs

5.1.1 Disordered systems and replicas

Perturbation theory and Harris criterion.

Let us consider a ferromagnet with quenched disorder, or to be more concrete, a spin model with Hamiltonian $H = -\sum_{i,j} J_{i,j} S_i S_j$ in d dimensions, where $J_{i,j}$ are quenched random variables, with short-range correlations only. Near the critical point of the pure system, the continuum limit of the system can be represented as

$$\mathcal{S} = \mathcal{S}^* + \int \mathrm{d}^d r J(r)\epsilon(r) + \dots \tag{5.1}$$

where $\mathcal{S}^*$ the action of the pure system at the critical point, $\epsilon(r)$ is the energy operator, and $J(r)$ is a random field with $\overline{J(r)} = 0$ and $\overline{J(r)J(r')} = \lambda\delta(r - r')$. Obviously, the disordered theory is not conformally invariant, since it is not even invariant under translations; however, once averaged over, the disorder may be a relevant perturbation that will drive the system to a new RG fixed point, with conformal invariance restored (in the averaged system). To see this, we need a clear field theory description of averaged observables. The typical problem when dealing with disordered systems is to compute averaged correlation functions, of the spin operator for example

$$\overline{\langle\sigma(r_1)\sigma(r_2)\rangle} = \overline{\frac{1}{Z}\mathrm{Tr}_{\sigma(r)}\ \mathrm{e}^{-\mathcal{S}[\sigma(r)]}\sigma(r_1)\sigma(r_2)}. \tag{5.2}$$

The main issue here is the partition function in the denominator. A very convenient (and standard) way around this is to introduce replicas $a = 1, \dots, n$, and to take the formal limit $n \to 0$ in the end. This amounts to computing the free energy as $\overline{\log Z} = \lim_{n\to 0} \frac{\overline{Z^n - 1}}{n}$. Doing so, we find

$$\overline{Z^n} = \mathrm{Tr}_{\sigma_a(r)} \mathrm{e}^{-\sum_a \mathcal{S}_a + \frac{\lambda}{2}\int \mathrm{d}^d r \sum_{a\neq b}\epsilon_a(r)\epsilon_b(r) + \dots}, \tag{5.3}$$

where we have dropped less relevant terms. The dimension of the perturbation is $2(d - \nu^{-1})$ where ν is the thermal exponent at the pure critical point, hence the disorder is relevant if (Harris criterion)

$$d\nu < 2. \tag{5.4}$$

When the disorder is relevant, the system will typically flow to a new random fixed point, for which we expect conformal invariance to be restored. This new fixed point is what we will study in the following, and we will argue that we expect it to be a good candidate for a LCFT. Random fixed points may be accessed perturbatively in the dimension of the perturbation, this can be done for example for the Ising model in $d = 2 + \varepsilon$ dimensions, or for the $2D$ Potts model with $Q = 2 + \varepsilon$ states (see *e.g.* [166]), or the disordered $O(n = 1 - \varepsilon)$ model [167, 168]. For a discussion of the effects of quench disorder on first-order phase transitions, see [169].

$n \to 0$ limit and logarithmic correlations.

Following Cardy [18, 53], we now argue that random fixed points in disordered systems must contain logarithmic observables. To do so, let us consider an operator ϕ_a ($a = 1, \dots, n$) in the replicated theory that transforms as a 'vector' under permutations of the replicas. Typically, one can think of ϕ as the energy operator in a spin model. More formally, $\{\phi_a\}_{a=1,\dots,n}$ is a representation of the permutation group S_n, where n is the number of replica. This representation is reducible as the linear combination $\Phi = \sum_a \phi_a$ is clearly invariant under permutations. The $n-1$ remaining fields $\tilde{\phi}_a = \phi_a - \frac{1}{n}\Phi$ (satisfying $\sum \tilde{\phi}_a = 0$) then transform irreducibly under S_n. Because S_n is a global symmetry of the replicated theory, we expect the scaling fields of the theory to transform irreducibly under the symmetric group S_n. We thus expect Φ and $\tilde{\phi}_a$ to have different scaling dimensions $\Delta_\Phi(n)$ and $\Delta_{\tilde{\phi}}(n)$. More precisely, because of the S_n symmetry, their two-point functions must take the form

$$\langle \Phi(r)\Phi(0)\rangle = \frac{nA(n)}{r^{2\Delta_\Phi(n)}}, \tag{5.5}$$

$$\langle \tilde{\phi}_a(r)\tilde{\phi}_b(0)\rangle = \frac{\tilde{A}(n)\left(\delta_{ab} - \frac{1}{n}\right)}{r^{2\Delta_{\tilde{\phi}}(n)}}, \tag{5.6}$$

where $A(n)$ and $\tilde{A}(n)$ are regular functions of n, with $A(0) \neq 0$ and $\tilde{A}(0) \neq 0$. Since we ultimately want to take the limit $n \to 0$ to obtain the physical properties of the disordered model, we see that $\tilde{\phi}_a$ is ill-defined in that limit. The $1/n$ pole in the correlation function of $\tilde{\phi}$ is actually the reason why logarithms appear when $n = 0$, this is obviously reminiscent of the $c \to 0$ catastrophe described in chapter 2. As argued by Cardy [18], averaged physical quantities are well-defined if and only if $A(0) = \tilde{A}(0)$ and $\Delta = \Delta_\Phi(0) = \Delta_{\tilde{\phi}}(0)$. Getting back to the original system, one finds that

$$\overline{\langle\phi(r)\rangle\langle\phi(0)\rangle} = \lim_{n\to 0}\langle\phi_1(r)\phi_2(0)\rangle = -\frac{2A(0)}{\mu(0)}\frac{\log r + \mathrm{Cst}}{r^{2\Delta}}, \tag{5.7}$$

$$\overline{\langle\phi(r)\phi(0)\rangle - \langle\phi(r)\rangle\langle\phi(0)\rangle} = \lim_{n\to 0}\left(\langle\phi_1(r)\phi_1(0)\rangle - \langle\phi_1(r)\phi_2(0)\rangle\right) = \frac{A(0)}{r^{2\Delta}}, \tag{5.8}$$

where $\mu = -\lim_{n\to 0}\frac{n}{\Delta_{\tilde{\phi}}(n) - \Delta_\Phi(n)}$. To reformulate these results in a more familiar language, let $\Psi = \mu(n)\phi_1$, with $\mu(n) = -\frac{n}{\Delta_{\tilde{\phi}}(n) - \Delta_\Phi(n)}$. Under a scale transformation

$r \longrightarrow \Lambda r$, one can readily check that it transforms as

$$\Psi(\Lambda r) = \Lambda^{-\Delta} \left(\Psi(r) - \log \Lambda \Phi(r) \right), \tag{5.9}$$

which means that the dilatation operator $\mathcal{D}$ acts on Ψ as $\mathcal{D}\Psi = \Delta\Psi + \Phi$. The two-point functions of these fields then read

$$\langle \Phi(z)\Phi(0) \rangle = 0, \tag{5.10a}$$

$$\langle \Phi(z)\Psi(0) \rangle = \frac{b}{r^{2\Delta}}, \tag{5.10b}$$

$$\langle \Phi(z)\Psi(0) \rangle = \frac{\theta - 2b \log r}{r^{2\Delta}}, \tag{5.10c}$$

with the b number

$$b = A(0)\mu = -\lim_{n \to 0} \frac{nA(n)}{\Delta_{\tilde{\phi}}(n) - \Delta_{\Phi}(n)}. \tag{5.11}$$

Some remarks: other operators and Replica-Symmetry-Breaking.

It is important to notice that the argument above works only if the operator ϕ transforms trivially under some eventual extended symmetry. For example [18], because of the $\mathbb{Z}_2$ spin-field symmetry of the Ising model, the spin operators $\{\sigma_a\}_{a=1,\dots,n}$ in the replicated theory transform irreducibly under the symmetry group $\mathbb{Z}_2 \times S_n$, so that the argument above does not apply in that case. However, because of the $c \to 0$ argument, we still expect logarithms to occur in higher-rank correlation functions. For instance, one can easily argue that the expected Jordan cell for the stress-energy tensor in the disordered theory implies that

$$\overline{\langle \sigma(r_1)\sigma(r_2) \rangle \langle \sigma(r_3)\sigma(r_4) \rangle} \sim \frac{1}{r_{12}^{2\Delta_\sigma} r_{34}^{2\Delta_\sigma}} \left(1 + \left(\frac{r_{12} r_{34}}{r_{13} r_{24}} \right)^2 \left(A + B \log \frac{r_{12} r_{34}}{r_{13} r_{24}} \right) + \dots \right). \tag{5.12}$$

Another important point is that the above argument holds only if the S_n symmetry is not broken. This seems to be the case for example for the disordered two-dimensional Potts model for $Q > 2$ [170]. However, there is no reason for this to be true in general, and it would be very interesting to generalize the argument above to the case of replica symmetry breaking. The representation theory is more involved in that case, but it remains manageable at least for the one-step replica symmetry breaking (1RSB). In a nutshell, instead of n replica, one has l groups of k elements each, with $n = l \times k$. The symmetry group then becomes a so-called wreath product of permutation groups [171]. Labeling the fields $\phi_a^{(i)}$, with $i = 1, \dots, l$ and $a = 1, \dots, k$, $\Phi = \sum_{a,i} \phi_a^{(i)}$ is still an invariant, but the $(n-1)$-dimensional representation $\tilde{\phi}_a^{(i)} \equiv \phi_a^{(i)} - \frac{1}{n}\Phi$ becomes reducible and is broken into two representations with dimension $l - 1$ and $n - l$. These representations are spanned by the fields $\theta_i = \sum_a \tilde{\phi}_a^{(i)}$ and $\hat{\phi}_a^{(i)} = \tilde{\phi}_a^{(i)} - \frac{1}{k}\theta_i$. Constructing correlation functions as before and taking the limit $k \to 0$ while keeping l fixed, one

obtains logarithmic correlation functions as in the replica-symmetric case.

5.1.2 Disordered systems and SUSY

In this last chapter, we shall mostly focus on replica-like approaches similar to the $n \to 0$ argument introduced in the previous sections. However, as mentioned in the introduction, there is another convenient way to deal with disordered systems in the case where there are no interactions. Let us imagine that one wants to compute the average of

$$\langle \mathcal{O} \rangle = \frac{1}{Z[\{h(\vec{r})\}]} \mathrm{Tr}_\phi \left(\mathcal{O} \mathrm{e}^{-H[\phi,\{h(r)\}]} \right), \tag{5.13}$$

where $h(r)$ are quenched disordered variables, ϕ are bosonic degrees of freedom and $H[\phi]$ is Gaussian – *i.e.* non-interacting. Using the properties of Grassmanian Gaussian integrals, one can write the denominator as $Z^{-1} = \mathrm{Tr}_\psi \mathrm{e}^{-H[\psi]}$ when ψ are fermionic variables, and then average over disorder configurations. This is the so-called supersymmetry approach [28]. As a concrete example, suppose we start with a $d+1$ dimensional random quantum problem with Hamiltonian $H = -\nabla^2 + V$, describing a single particle in a disordered potential V with $\overline{V} = 0$ and $\overline{V(r)V(r')} = \lambda\delta(r-r')$. The one-particle Green functions at fixed energy $G^\pm(E)(r,r') = \left\langle r' \right| \left(E - H \pm i\epsilon\right)^{-1} \left| r \right\rangle$ can be written as

$$\pm i G^\pm(E)(r,r') = \frac{1}{Z} \int \mathcal{D}\overline{\phi}\mathcal{D}\phi \; \overline{\phi}(r')\phi(r) \mathrm{e}^{\mp i \int \mathrm{d}r \overline{\phi}\left(-\nabla^2 + V - E \mp i\epsilon\right)\phi}. \tag{5.14}$$

Using supersymmetry and averaging over the disorder, one ends up with

$$\pm i \overline{G^\pm(E)(r,r')} = \int \mathcal{D}\overline{\phi}\mathcal{D}\phi\mathcal{D}\overline{\psi}\mathcal{D}\psi \; \overline{\phi}(r')\phi(r) \mathrm{e}^{-S_{\mathrm{SUSY}}}, \tag{5.15}$$

where

$$S_{\mathrm{SUSY}} = \pm i \int \mathrm{d}r \left[\overline{\phi} \left(-\nabla^2 + V - E \mp i\epsilon\right) \phi + \overline{\psi} \left(-\nabla^2 + V - E \mp i\epsilon\right) \psi \pm i \frac{\lambda}{2} \left(\overline{\phi}\phi + \overline{\psi}\psi\right) \right]. \tag{5.16}$$

We see that the averaged Green function can be computed from a pure field theory where bosonic and fermionic degrees of freedom are effectively interacting because of the disorder. If the SUSY problem is conformal, it must have central charge $c = 0$ since $Z_{\mathrm{SUSY}} = 1$, and so this means that averaged quantities in the original disordered system will behave algebraically with critical exponents given by a $c = 0$ theory.

We therefore see that disorder systems must correspond to $c = 0$ CFTs [1], and thus must be described by Logarithmic CFTs [18, 19]. Examples of problems described by $c = 0$ LCFT after mapping onto a SUSY model include the transition between plateaus

1. In the replica approach, this corresponds to the fact that the central charge of the replicated theory $c(n)$ goes to $c = 0$ as $n \to 0$.

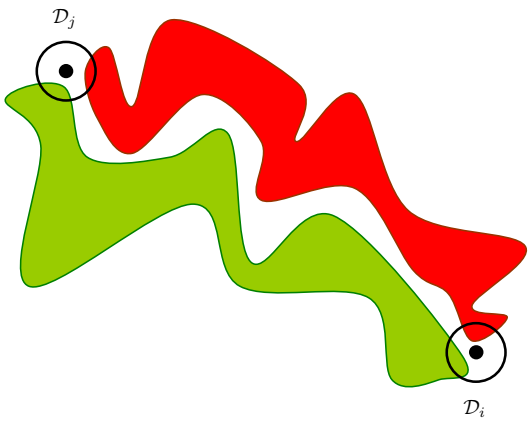

Figure 5.1: $2N$-leg watermelon operators in the Potts model correspond to the insertion of N FK clusters that will persist until they are taken out by another watermelon operator.

in the IQHE, or for instance, the so-called Nishimori point in the two-dimensional random-bond Ising model [30]. In the following, we will not use this supersymmetry approach which corresponds more to the algebraic framework developed in the previous chapters, but instead we shall argue that the replica approach can be used to study geometrical problems as well.

5.2 Operator content of the Potts model in d dimensions

Disordered systems and geometrical problems are very closely related. The transition in the Spin Quantum Hall Effect can be mapped onto classical percolation [31], the Chalker-Coddington model for the Integer Quantum Hall Transition can also be transformed in a loop model, which can be in turn truncated to make it solvable [172]; the supersymmetric formulation of the Nishimori point [30] in the disordered 2D Ising model can be expanded in a complicated loop model as well *etc.* While disordered systems are arguably more interesting physically, it is therefore worth analyzing the simpler geometrical models to try to understand further the logarithmic structure of random fixed points.

Considering critical disordered systems or geometrical problems as limits can be very fruitful, as it allows one to obtain interesting results in arbitrary dimension, using mainly simple ideas and non-technical tools. This line of research has been pushed the furthest for the Potts model [78, 79] and we review here some of the results obtained.

5.2.1 S_Q representation theory

The operator content of the Potts model in arbitrary dimension is given by the so-called watermelon operators, that will provide natural geometrical observables, which

may or may not behave logarithmically at the critical point.

As a first step in constructing the N-cluster watermelon operators in arbitrary dimension, we need some representation theoretical preliminaries. The intuitive idea is that we must construct a certain operator acting on N spins (that will eventually be taken to be adjacent, or belong to a small neighborhood) and satisfying some symmetry requirement. If we require the N spins to take different values they will obviously belong to distinct FK clusters, but this is not enough, since we must also ensure that the N FK clusters inserted by the watermelon operator persist until they are taken out by another watermelon operator (and not just "end in the middle of nowhere"), see Fig. 5.1.

To make this idea precise, and to attain our objectives, we now set out to classify N-spin operators from the point of view of irreducible representations (irreps) of the symmetric group S_Q.

Let $L_Q^{(1)}$ be the span of all Q-component vectors $\mathcal{O}(\sigma)$, where $\sigma = 1, \dots, Q$. This space obviously has dimension Q. Letting the symmetric group S_Q acting on the index σ, this defines a reducible representation of this group. It is indeed straightforward to form the invariant quantity $\sum_{\sigma=1}^{Q} \mathcal{O}(\sigma)$ which transforms as the trivial, one-dimensional irrep $[Q]$. The decomposition with respect to S_Q thus yields

$$L_Q^{(1)} = [Q] \oplus [Q-1, 1]\,, \tag{5.17}$$

where $[Q-1,1]$ is the space of vectors $\mathcal{O}(\sigma)$ that satisfy $\sum_\sigma \mathcal{O}(\sigma) = 0$, with dimension $Q-1$.

Here, and in the sequel, an irrep λ of S_Q is denoted by its Young diagram $[\lambda_1, \lambda_2, \dots, \lambda_k]$, where λ_i is the length of row i. It is a remarkable fact that we shall only need representations with at most $k = 2$ rows; the same property is well known to hold in $d = 2$ dimensions [173].

Let us now consider a slightly more involved example. Let $L_Q^{(2)}$ be the span of all symmetric $Q \times Q$ matrices $\mathcal{O}(\sigma_1, \sigma_2)$ with zero elements on the diagonal. We have $\dim L_Q^{(2)} = \frac{Q(Q-1)}{2}$. Once again, acting with S_Q on the indices σ_1 and σ_2, this defines a representation which turns out to be reducible. Indeed, the subspace of matrices that satisfy $\sum_{\sigma_1=1}^{Q} \mathcal{O}(\sigma_1, \sigma_2) = 0$ provides an irreducible representation $[Q-2, 2]$ of dimension $\frac{Q(Q-1)}{2} - Q = \frac{Q(Q-3)}{2}$. The quotient of $L_Q^{(2)}$ by this invariant subspace is a representation of dimension Q, isomorphic to $L_Q^{(1)}$, which is spanned by the vector $\tilde{\mathcal{O}}(\sigma_2) = \sum_{\sigma_1} \mathcal{O}(\sigma_1, \sigma_2)$. We therefore write

$$L_Q^{(2)} = \underbrace{[Q] \oplus [Q-1,1]}_{\tilde{\mathcal{O}}(\sigma_2) = \sum_{\sigma_1} \mathcal{O}(\sigma_1, \sigma_2)} \oplus \underbrace{[Q-2,2]}_{\sum_{\sigma_1} \mathcal{O}(\sigma_1, \sigma_2) = 0}\,. \tag{5.18}$$

The generalization of this decomposition is straightforward. For example, the space $L_Q^{(3)}$ of $Q \times Q \times Q$ symmetric tensors $\mathcal{O}(\sigma_1, \sigma_2, \sigma_3)$ which vanish when two indices coincide is decomposed as $L_Q^{(2)} \oplus [Q-3, 3]$, where the subspace $[Q-3,3]$ corresponds to the tensors that satisfy the $Q(Q-1)/2$ constraints $\sum_{\sigma_1} \mathcal{O}(\sigma_1, \sigma_2, \sigma_3) = 0$. The remaining

space $L_Q^{(2)}$ then corresponds to the decomposition of $\tilde{\mathcal{O}}(\sigma_2,\sigma_3)=\sum_{\sigma_1}\mathcal{O}(\sigma_1,\sigma_2,\sigma_3)$. In general, we will denote by $L_Q^{(N)}$ the space of $Q\times Q\times\cdots\times Q$ symmetric tensors of rank N that vanish whenever two indices coincide. The dimension of $L_Q^{(N)}$ is $\frac{Q(Q-1)\ldots(Q-N+1)}{N!}$. We then have the decomposition

$$L_Q^{(N)}=\underbrace{[Q]\oplus[Q-1,1]\oplus\cdots\oplus[Q-N+1,N-1]}_{\tilde{\mathcal{O}}(\sigma_2,\ldots,\sigma_N)=\sum_{\sigma_1}\mathcal{O}(\sigma_1,\sigma_2,\ldots,\sigma_N)}\oplus\underbrace{[Q-N,N]}_{\sum_{\sigma_1}\mathcal{O}(\sigma_1,\sigma_2,\ldots,\sigma_N)=0}\quad. \tag{5.19}$$

5.2.2 Watermelon operators $t^{(k,N)}_{a_1,\ldots,a_k}$

We consider a symmetric operator $\mathcal{O}(\sigma_1,\ldots,\sigma_N)$, defined on N distinct Potts spins, and we impose that it vanishes if any of the N spins coincide. We would like to understand how to decompose this operator in terms of irreps of the symmetric group. According to the results of the previous section, this means that we want to construct each of the representations in the decomposition

$$[Q]\oplus[Q-1,1]\oplus[Q-2,2]\oplus\ldots\oplus[Q-N,N]. \tag{5.20}$$

By the hook formula the dimensions of the representations are

$$d_k\equiv\dim([Q-k,k])=\frac{Q!}{(Q-k+1)!}\,\frac{Q-2k+1}{k!}\,, \tag{5.21}$$

and in terms of dimensions the decomposition (5.20) reads

$$D_N\equiv\sum_{k=0}^{N}d_k=(1)+(Q-1)+\left(\frac{Q(Q-3)}{2}\right)+\ldots+\left(\frac{Q!}{(Q-N+1)!}\,\frac{Q-2N+1}{N!}\right)=\frac{Q!}{(Q-N)!\,N!}\,. \tag{5.22}$$

This is indeed the number of symmetric tensors that vanish if any two spins coincide.

Constructing the invariant tensors

To construct an explicit basis for these representations, we proceed as follows. Let us consider first the case $N=1$. The invariant $[Q]$ is just a constant $t^{(0,1)}\equiv 1=\sum_a\delta_{a,\sigma_1}$ in that case. Meanwhile, the $Q-1$ generators of the irrep $[Q-1,1]$ read

$$t_a^{(1,1)}(\sigma_1)=\delta_{a,\sigma_1}-\frac{1}{Q}t^{(0,1)}\,. \tag{5.23}$$

These operators satisfy $\sum_a t_a^{(1,1)}=0$ so we indeed have only $Q-1$ of them, and note that we also have $\sum_{\sigma_1}t_a^{(1,1)}(\sigma_1)=0$ which is expected by the definition of the representation $[Q-1,1]$.

We next consider the case $N=2$. The invariant $[Q]$ is nothing but $t^{(0,2)}\equiv\delta_{\sigma_1\neq\sigma_2}=1-\delta_{\sigma_1,\sigma_2}$. Note that since we already decided that our operators vanish whenever two

spins coincide, we can set $t^{(0,2)} = 1$ in that space. The representation $[Q-1,1]$ is trivially obtained from the case $N = 1$ as

$$t_a^{(1,2)}(\sigma_1,\sigma_2) = t_a^{(1,1)}(\sigma_1) + t_a^{(1,1)}(\sigma_2) = \delta_{\sigma_1,a} + \delta_{\sigma_2,a} - \frac{2}{Q}. \tag{5.24}$$

The only new non-trivial case is the basis of $[Q-2,2]$. We are looking for a basis of $Q(Q-3)/2$ operators $t^{(2,2)}(\sigma_1,\sigma_2)$ that satisfy

$$\sum_{\sigma_1} t_{ab}^{(2,2)}(\sigma_1,\sigma_2) = 0\,, \tag{5.25}$$

as explained in section 5.2.1. We label them using two symmetric indices a, b that run from 1 to Q. It is clear that $t^{(2,2)}(\sigma_1,\sigma_2)$ must contain the two terms $\delta_{\sigma_1,a}\delta_{\sigma_2,b}+\delta_{\sigma_2,a}\delta_{\sigma_1,b}$. However, just as in (5.24) we need to subtract multiples of the lower-order tensors in order the fulfill the constraint (5.25). Solving the resulting linear system we easily find

$$t_{ab}^{(2,2)}(\sigma_1,\sigma_2) = \delta_{\sigma_1,a}\delta_{\sigma_2,b}+\delta_{\sigma_2,a}\delta_{\sigma_1,b} - \frac{1}{Q-2}\left(t_a^{(1,2)}(\sigma_1,\sigma_2) + t_b^{(1,2)}(\sigma_1,\sigma_2)\right) - \frac{2}{Q(Q-1)}t^{(0,2)}, \tag{5.26}$$

for $a \neq b$; when $a = b$ we have $t_{ab}^{(2,2)}(\sigma_i,\sigma_j) = 0$ by definition. One can check that the constraint holds also for the tensor indices, namely $\sum_a t_{ab}^{(2,2)} = 0$, so that there are $Q(Q-1)/2 - Q = Q(Q-3)/2$ generators indeed.

General procedure and physical interpretation

The general pattern should already be clear at this point, the general results will be given in [79].

We now claim that for a given number of spins N, the most symmetric tensor $t^{(N,N)}$ is the N-cluster watermelon operator in arbitrary dimension d. This statement will be corroborated in the next section where we show that the corresponding two-point functions are proportional to the probability that N distinct FK clusters connect each of the two groups of N points. We defer the precise interpretation of the tensors of lower rank, $t^{(k,N)}$ with $k < N$, to [79] – they correspond, once properly arranged, to subleading operators.

5.2.3 Correlation functions: discrete results

We next show that one can obtain useful structural results on correlation functions of the tensors $t^{(k,N)}$ constructed in section 5.2.2, by combining the representation theoretical tools of section 5.2.1 with elementary combinatorial considerations. These results account in particular for the dependence of correlation functions on the tensorial indices. Moreover, the correlation functions of watermelon operators will be related to linear combinations of the probabilities that the spins acted on by one operator is connected by FK clusters to spins acted on by other operators in various ways.

This geometrical content is essential for unraveling the physical interpretation of the correlation functions.

The structural results found in this section involve various coefficients that have poles when Q tends to a non-negative integer. The cancellation of these singularities is at the heart of the mechanism that will eventually produce the logarithm behavior of correlation functions in the continuum limit.

Throughout this section we only apply combinatorial considerations to the finite number of spins that enter explicitly in the watermelon operators. The results are therefore completely general and do not, in particular, depend on the graph (or d-dimensional lattice) on which the Potts model is defined.

Two-point functions: $N = 1$ spin

We recall from section 5.2.2 that the two operators acting on one spin read, in our notation, $t^{(0,1)}(\sigma_1) = 1$ and $t_a^{(1,1)}(\sigma_1) = \delta_{a,\sigma_1} - \frac{1}{Q}$. The two-point functions of these operators are the following:

$$\left\langle t^{(0,1)}(r_1) t^{(0,1)}(r_2) \right\rangle = 1 \,, \tag{5.27}$$

$$\left\langle t_a^{(1,1)}(r_1) t_b^{(1,1)}(r_2) \right\rangle = \frac{1}{Q} \left(\delta_{a,b} - \frac{1}{Q} \right) \mathbb{P}\left(\begin{array}{c} \bullet \\ | \\ \bullet \end{array} \right) \,. \tag{5.28}$$

where $\mathbb{P}\left(\begin{array}{c} \bullet \\ | \\ \bullet \end{array} \right)$ is the probability that r_1 and r_2 are in the same FK cluster. While the former result is of course trivial, we wish to spend a moment discussing the latter result in order to carefully fix some ideas and notations to be used throughout this section.

First, we imagine that the two groups of $N = 1$ spins are situated at (or later, when $N > 1$, in small neighborhoods around) the points r_1 and r_2 respectively. Obviously we cannot specify how the correlation function depends on these coordinates, since we have not yet assumed anything about the lattice on which the Potts model is defined, nor whether the coordinates are widely separated. We shall come back to that issue later on, as we start exploiting the consequences of scale and conformal invariance. However, we can still denote by $\mathbb{P}\left(\begin{array}{c} \bullet \\ \bullet \end{array} \right)$ the probability that the two spins belong to two different FK clusters, and by $\mathbb{P}\left(\begin{array}{c} \bullet \\ | \\ \bullet \end{array} \right)$ the probability that they belong to the same FK cluster. In the former case, the two spins are summed over independently, and the coefficient of $\mathbb{P}\left(\begin{array}{c} \bullet \\ \bullet \end{array} \right)$ is

$$\frac{1}{Q^2} \sum_{\sigma_1, \sigma_2} \left(\delta_{a,\sigma_1} - \frac{1}{Q} \right) \left(\delta_{b,\sigma_2} - \frac{1}{Q} \right) = 0 \,. \tag{5.29}$$

In the latter case, the two spins are constrained to take the same value, and the coefficient of $\mathbb{P}\left(\begin{array}{c} \bullet \\ | \\ \bullet \end{array} \right)$ is therefore

$$\frac{1}{Q} \sum_{\sigma_1} \left(\delta_{a,\sigma_1} - \frac{1}{Q} \right) \left(\delta_{b,\sigma_1} - \frac{1}{Q} \right) = \frac{1}{Q} \left(\delta_{a,b} - \frac{1}{Q} \right) \,. \tag{5.30}$$

Combining (5.29)–(5.30) we arrive at (5.28).

We also note that the mixed correlation function is identically zero:

$$\left\langle t^{(0,1)}(r_1) t_a^{(1,1)}(r_2) \right\rangle = 0\,. \tag{5.31}$$

This is a general feature that will carry over to higher N for symmetry reasons.

Two-point functions: $N = 2$ spins

We now move to the slightly more involved case of $N = 2$ spins. Our results read as follows:

$$\left\langle t^{(0,2)}(r_1) t^{(0,2)}(r_2) \right\rangle = \left(\frac{Q-1}{Q}\right)^2 \left(\mathbb{P}\left(\begin{smallmatrix}\bullet & \bullet\\ \bullet & \bullet\end{smallmatrix}\right) + \mathbb{P}\left(\begin{smallmatrix}\bullet & \bullet\\ \vert & \vert\\ \bullet & \bullet\end{smallmatrix}\right)\right) + \frac{Q-1}{Q}\mathbb{P}\left(\begin{smallmatrix}\bullet & \bullet\\ \vert & \vert\\ \vert & \vert\\ \bullet & \bullet\end{smallmatrix}\right), \tag{5.32}$$

$$\left\langle t_a^{(1,2)}(r_1) t_b^{(1,2)}(r_2) \right\rangle = \frac{Q-2}{Q^2}\left(\delta_{a,b} - \frac{1}{Q}\right)\left(\frac{Q-2}{Q}\mathbb{P}\left(\begin{smallmatrix}\bullet & \bullet\\ \vert & \vert\\ \bullet & \bullet\end{smallmatrix}\right) + 2\mathbb{P}\left(\begin{smallmatrix}\bullet & \bullet\\ \vert & \vert\\ \vert & \vert\\ \bullet & \bullet\end{smallmatrix}\right)\right), \tag{5.33}$$

$$\left\langle t_{ab}^{(2,2)}(r_1) t_{cd}^{(2,2)}(r_2) \right\rangle = \frac{2}{Q^2}\left(\delta_{ac}\delta_{bd} + \delta_{ad}\delta_{bc} - \frac{1}{Q-2}(\delta_{ac}+\delta_{bd}+\delta_{ad}+\delta_{bc}) + \frac{2}{(Q-2)(Q-1)}\right)\mathbb{P}\left(\begin{smallmatrix}\bullet & \bullet\\ \vert & \vert\\ \vert & \vert\\ \bullet & \bullet\end{smallmatrix}\right). \tag{5.34}$$

In the corresponding diagrams, the spins corresponding to the leftmost operator (and that we imagine situated in a neighborhood around r_1) are shown on the bottom, and those corresponding to the rightmost operator are depicted on the top. We denote by $\mathbb{P}\left(\begin{smallmatrix}\vert & \vert\\ \bullet & \bullet\end{smallmatrix}\right)$ (resp. $\mathbb{P}\left(\begin{smallmatrix}\vert & \bullet\\ \bullet & \bullet\end{smallmatrix}\right)$, or $\mathbb{P}\left(\begin{smallmatrix}\bullet & \bullet\\ \bullet & \bullet\end{smallmatrix}\right)$) the probability that there are zero (resp. one, or two) FK clusters connecting an r_1 point to an r_2 point. Notice that the different points belonging to the same operator cannot be connected among themselves, because of the constraint that the watermelon operators vanish in the case of coinciding spins. We also stress that $\mathbb{P}\left(\begin{smallmatrix}\vert & \bullet\\ \bullet & \bullet\end{smallmatrix}\right)$ is the probability that any one of the two r_1 points is in the same FK cluster as any one of the two r_2 points, so even though the connected pair of points is shown on the left, the diagram actually stands for a sum of four distinct contributions. This is consistent with the fact that the watermelon operators are symmetric in their spin indices.

To fix the coefficients appearing in front of the three probabilities in (5.32) one simply needs to average the product of $t^{(0,2)}(r_1) = 1 - \delta_{\sigma_1,\sigma_2}$ and $t^{(0,2)}(r_2) = 1 - \delta_{\sigma_3,\sigma_4}$ over the spins $\sigma_1, \sigma_2, \sigma_3, \sigma_4$, upon inserting an extra factor of 1 in the case of $\mathbb{P}\left(\begin{smallmatrix}\bullet & \bullet\\ \bullet & \bullet\end{smallmatrix}\right)$, a factor $\delta_{\sigma_1,\sigma_3}$ in the case of $\mathbb{P}\left(\begin{smallmatrix}\vert & \bullet\\ \bullet & \bullet\end{smallmatrix}\right)$, and a factor $\delta_{\sigma_1,\sigma_3}\delta_{\sigma_2,\sigma_4}$ in the case of $\mathbb{P}\left(\begin{smallmatrix}\vert & \vert\\ \bullet & \bullet\end{smallmatrix}\right)$. Doing this leads to the result shown in (5.32).

To establish (5.33)–(5.34) one further needs to take account of the tensor indices. It is useful to write first an Ansatz for the possible dependence on the tensor indices. In the case of (5.33) this is obvious provided by $c_{1,1}\delta_{a,b} - c_{0,1}$, where $c_{1,1}$ and $c_{0,1}$ are some constants. We then apply the calculational scheme just explained for the $t^{(0,2)}$ correlator to the case at hand where $t_a^{(1,2)}$ is given by (5.24); the two cases $a = b$ and $a \neq b$ must be examined in turn to fix both constants $c_{1,1}$ and $c_{0,1}$. In the case of (5.34) the Ansatz for the dependence on the tensor indices should obviously take into account

that $t^{(2,2)}_{ab}$ is zero when $a = b$. Therefore we have an Ansatz of the type

$$c_{2,2}(\delta_{ac}\delta_{bd} + \text{perm}) + c_{1,2}(\delta_{ac} + \text{perm}) + c_{0,2}\,, \tag{5.35}$$

where perm denotes all internal permutations among the indices in the r_1 operator, and among those in the r_2 operator. To fix the three constants, the calculation must be done in the cases where the values of the indices a, b coincide with zero, one or two of the indices c, d. Obviously the structure of Kronecker deltas acting on the tensor indices is very reminiscent of the one appearing in the spin variable probabilities $\mathbb{P}$(:: ::), $\mathbb{P}$(:: .:) and $\mathbb{P}$(.: .:).

The results (5.32)–(5.34) display a remarkable feature that will carry over to higher N as well. Namely, the two-point function of the watermelon operator $t^{(p,N)}$ couples only to probabilities that there are *at least p distinct FK clusters* connecting the set of points in the first and the second operator. In particular, $\langle t^{(N,N)}(r_1)t^{(N,N)}(r_2)\rangle$ is proportional to the probability of having N propagating FK clusters. This establishes our claim that $t^{(N,N)}$ is the N-cluster watermelon operator. The precise interpretation of $t^{(p,N)}$ for $p < N$ is more tricky and will be deferred to [79]; suffice it here to say that loosely speaking this operator inserts "at least" p propagating FK clusters.

We have checked that just like in the $N = 1$ case all mixed correlation functions vanish:

$$\left\langle t^{(0,2)}(r_1)t^{(1,2)}_a(r_2)\right\rangle = \left\langle t^{(0,2)}(r_1)t^{(2,2)}_{ab}(r_2)\right\rangle = \left\langle t^{(1,2)}_a(r_1)t^{(2,2)}_{bc}(r_2)\right\rangle = 0\,. \tag{5.36}$$

This result could in fact be established without resorting to explicit calculations, since $t^{(0,2)}$, $t^{(1,2)}$ and $t^{(2,2)}$ have been constructed as different irreps of S_Q; the vanishing of mixed correlations then follows from representation theoretical reasons. But (5.36) is of course also consistent with the features mentioned in the preceding paragraph. Namely the vanishing correlator of the product between $t^{(0,2)}$ and either $t^{(1,2)}$ or $t^{(2,2)}$ is due to the fact that $t^{(0,2)}$ cannot "take out" the FK clusters "inserted" by either of the two latter operators. However the vanishing of $\langle t^{(1,2)}t^{(2,2)}\rangle$ cannot be explained from this simple reasoning.

This type of reasoning (or explicit calculations) also imply that the one-point functions of $t^{(p,N)}$ vanish for $p > 0$; in particular $\langle t^{(1,2)}_a(r)\rangle = \langle t^{(2,2)}_{ab}(r)\rangle = 0$. However, $\langle t^{(0,2)}\rangle = \langle 1 - \delta_{\sigma_1,\sigma_2}\rangle$ is non-zero and is proportional to the probability $\mathbb{P}$(..) that the spins σ_1, σ_2 belong to two different FK clusters. It is convenient to define an operator with this mean value subtracted:

$$\epsilon(r) \equiv t^{(0,2)}(r) - \frac{Q-1}{Q}\mathbb{P}(\bullet\bullet)\,, \tag{5.37}$$

so that now $\langle\epsilon(r)\rangle = 0$. We shall see below that in the continuum limit $\epsilon(r)$ is proportional to the energy operator, as indicated by the chosen notation. Using again the

same methods as above, we then find that

$$\langle \epsilon(r_1)\epsilon(r_2)\rangle = \frac{Q-1}{Q}\left(\mathbb{P}\left(\right) + \left(1-\frac{1}{Q}\right)\left(\mathbb{P}\left(\right) + \mathbb{P}\left(\right) - \mathbb{P}\left(\right)^2\right)\right). \quad (5.38)$$

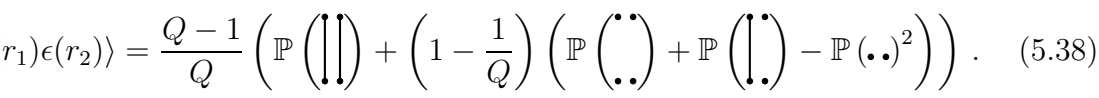

Once again these results can be generalized to higher number of spins N, or to 3-point correlation functions *etc.* We shall not need these generalizations here, and we refer the reader to [79] for details.

5.3 Logarithmic correlations: spanning trees and forests, percolation and subleading operators

5.3.1 $Q \to 0$: spanning trees and spanning forests

In this section, we discuss the limit $Q \to 0$ limit of the Potts model in relation with spanning trees and forests. We show how our lattice correlation functions give a direct geometrical interpretation of many CFT correlators, and we comment on the appearance of logarithms in the limit $Q \to 0$. In $d = 2$, we reinterpret using our framework the well known logarithmic partner of the identity operator, in relation with symplectic fermions and resistor networks. Despite the fact that we will mostly deal with free (non-interacting) theories in this section, we shall see in the following that the general ideas will work in non-trivial, interacting cases as well.

Spanning trees and lattice correlation functions

Let us first discuss the case $d = 2$. Recall the FK expansion of partition function of the Potts model defined on a graph G with N sites (3.12). Using the Euler relation $|A| + k(A) = N + \omega(A)$, where $\omega(A)$ is the number of loop in A, one can consider the limit $Q \to 0$, $v \to 0$ with $w = \frac{Q}{v}$ fixed

$$\lim \frac{1}{v^N} Z = \sum_F w^{k(F)}, \quad (5.39)$$

where F is a spanning forest of G, characterized by $\omega(F) = 0$ (no loop). In the limit $w \to 0$, only the so-called spanning trees T of the graph G survive up to a factor w, which are forests with only one connected component ($k(T) = 1$) [174]. This model is critical, as the critical line of the Potts model has a vertical tangent at the point $(Q, v) = (0, 0)$. We will further consider the case of a square lattice in the following, for which the critical line is $v = \sqrt{Q}$. To be more explicit, at the critical point, we have $v = w = \sqrt{Q}$, so that

$$Z \underset{Q\to 0}{\sim} v^N w \mathcal{T}(G) = (\sqrt{Q})^{N+1} \mathcal{T}(G), \quad (5.40)$$

where $\mathcal{T}(G)$ is the number of spanning trees of the graph G. This expression alternatively follows from the dense loop expansion of the Potts model at its critical point (see eq. (3.14))

$$Z = Q^{N/2} \sum_{\text{loops}} (\sqrt{Q})^{\text{number of loops}}, \tag{5.41}$$

where the loops are dual to the FK clusters. The limit $Q \to 0$ yields dense polymers (or dense self-avoiding walks), that are in one-to-one correspondence with spanning tree configurations.

In particular, we see that the partition function of the Potts model vanishes as $Q \to 0$. In order to obtain non-trivial results, it is convenient to define the new correlators

$$\langle \dots \rangle_0 = \frac{Z}{v^N} \langle \dots \rangle, \tag{5.42}$$

so that the new critical partition function of the model is now $Z_0 \equiv \langle 1 \rangle_0 = \sqrt{Q}\mathcal{T}(G)$. Actually, because this limit $Q \to 0$ is a bit peculiar, we will also have to rescale the observables in order to find non-trivial results[2]. For example, we will define $\phi_a = \sqrt{Q} t_a^{(1,1)} = \sqrt{Q}\delta_{\sigma_i,a} - \frac{1}{\sqrt{Q}}$. When $Q \to 0$, ϕ_a becomes (formally) singular because of the factor $\frac{1}{\sqrt{Q}}$, this will yield logarithms in the limit [18, 78].

Setting $\varphi_a = \sqrt{Q}\delta_{\sigma_i,a}$, it is not hard to check that all the correlation functions of this operator correspond to meaningful quantities. For example, since $\langle \varphi_a \rangle = \frac{1}{\sqrt{Q}}$,we immediately find $\langle \varphi_a \rangle_0 = \mathcal{T}(G)$. It is also straightforward to show that

$$\langle \varphi_a(r_i)\varphi_b(r_j) \rangle_0 \underset{Q\to 0}{\sim} \frac{Z}{Qv^N} \left(1 - \mathbb{P}\left(\right) \right) \sim \sum_F{}' (\sqrt{Q})^{k(F)-2} \underset{Q\to 0}{\longrightarrow} \mathcal{T}(G\backslash\{ij\}), \tag{5.43}$$

where $\mathcal{T}(G\backslash\{ij\})$ counts the number of spanning 2-tree forests, with one tree containing the site i while the other contains j. The symbol $\sum'$ in the intermediate expression corresponds to a sum over forests configurations where i and j can belong to different trees.

Continuum limit and logarithms

In the field theory limit, we will denote $Z_0 = \sqrt{Q}A(Q)$, where $A(Q)$ is a regular function of Q with a finite limit as $Q \to 0$. Obviously, in the scaling limit, we expect ϕ_a to become the magnetization operator, with critical exponent $\Delta_\sigma(Q) = 2h_{\frac{1}{2},0}$ where we used the standard Kac parametrization. The exponent for the corresponding boundary operator would be $h_{1,3}$. Notice that $\Delta_\sigma(Q = 0) = 0$, so this operator will be mixed

2. Of course, the global normalization factor of the operators defined in the previous sections *is not* fixed by representation theory considerations.

with the identity field at $Q = 0$. Therefore, we expect [3]

$$\langle \phi_a(r_i)\phi_b(r_j)\rangle_0 = \left(\delta_{a,b}\sqrt{Q} - \frac{1}{\sqrt{Q}}\right) \tilde{A}(Q) r^{-2\Delta_\sigma(Q)}, \tag{5.44}$$

where $\tilde{A}(Q)$ is another regular function of Q with a finite $Q \to 0$ limit. The $Q \to 0$ limit of this equation is ill-defined, however, the correlation functions of $\varphi_a = \phi_a + 1/\sqrt{Q}$ have a finite limit if one assumes that $A(0) = \tilde{A}(0)$

$$\langle \varphi_a(r)\varphi_b(0)\rangle = 4A(0) \left.\frac{\partial h_{\frac{1}{2},0}}{\partial\sqrt{Q}}\right|_{Q=0} \log r, \tag{5.45a}$$

$$\langle \varphi_a(r)\rangle = \langle \varphi_a(r)\mathbb{I}(0)\rangle = A(0), \tag{5.45b}$$

where we used $\mathbb{I} = 1$ to denote the identity operator of the theory. Using the expansion $h_{\frac{1}{2},0} = \frac{\sqrt{Q}}{4\pi} + \ldots$, we find that the ratio

$$\frac{\langle \varphi_a(r)\varphi_b(0)\rangle}{\langle \varphi_a(0)\rangle} = \frac{1}{\pi}\log r, \tag{5.46}$$

takes an universal form. This is probably the most simple correlation function showing a logarithm, and as we shall see, it is in this case strongly related to the logarithmic form of the Green function of the Laplacian in 2D. Close to a boundary, we find

$$\left.\frac{\langle \varphi_a(r)\varphi_b(0)\rangle}{\langle \varphi_a(0)\rangle}\right|_{\text{boundary}} = \frac{2}{\pi}\log r, \tag{5.47}$$

where we have used $h_{1,3} = \frac{\sqrt{Q}}{\pi} + \ldots$

Let us come back to the bulk case to see that this logarithmic singularity in the correlation function $\langle \varphi_a(r)\varphi_b(0)\rangle$ should indeed be thought of as a logarithmic CFT feature. In order to do so, we analyze how all these fields transform under a scale transformation. When Q is generic, we have

$$\mathbb{I}(\Lambda r) = \mathbb{I}(r) = 1, \tag{5.48a}$$

$$\phi_a(\Lambda r) = \Lambda^{-\Delta_\sigma(Q)}\phi_a(r). \tag{5.48b}$$

We can deduce from this the transformation law of $\varphi_a(r)$ when $Q = 0$. We find

$$\varphi_a(\Lambda r) = 2 \left.\frac{\partial h_{\frac{1}{2},0}}{\partial\sqrt{Q}}\right|_{Q=0} \log \Lambda\mathbb{I}. \tag{5.49}$$

3. In the following, we will ignore the renormalization of the fields $\phi_{\text{CFT}} = a^{-\Delta}\phi_{\text{lattice+...}}$ where a is the UV cutoff. For simplicity, we will use the same notations for lattice and CFT fields, and ignore subleading corrections corresponding to operators with the same symmetry *etc.*

We see that the scale transformations generator is non-diagonalizable as it maps φ_a onto the identity $\mathbb{I} = 1$. Using states instead of fields and Virasoro generators, this amounts to state that

$$(L_0 + \bar{L}_0)\,|\varphi_a\rangle = -2\,\frac{\partial h_{\frac{1}{2},0}}{\partial\sqrt{Q}}\bigg|_{Q=0}\,|\Omega\rangle\,. \tag{5.50}$$

where $|\Omega\rangle$ is the vacuum of the theory and L_0 and $\bar{L}_0$ are the usual Virasoro zero modes.

These universal logarithmic ratios have a very nice interpretation in terms of spanning trees (or equivalently, in terms of the dual dense polymers). Comparing our lattice expressions with eqs. (5.45), we find

$$\frac{\mathcal{T}(G\backslash\{ij\})}{\mathcal{T}(G)} \sim \frac{1}{\pi}\log r_{ij}, \tag{5.51}$$

which has a clear geometrical meaning. Note that the existence of logarithmic correlation functions for spanning trees is obviously not new (see *e.g.* [174–176]), but all the methods employed previously rely heavily on the free-fermionic/Laplacian property of the problem (see below), whereas our approach only used a simple limit argument, that will turn out to apply also to non-trivial, interacting problems. It is also worth pointing out that these correlation functions *do not* appear directly in the abelian sand pile model, as the latter only involves derivatives or differences of Green functions.

Symplectic fermions

To see how all this is related to a Laplacian problem, let us introduce Grassman variables $(\psi,\,\bar{\psi})$ on each site, with the usual integration rules

$$\int \mathrm{d}\psi\ 1 = 0, \qquad \int \mathrm{d}\psi\ \psi = 1, \qquad \int \mathrm{d}\bar{\psi}\ 1 = 0, \qquad \int \mathrm{d}\bar{\psi}\ \bar{\psi} = 1. \tag{5.52}$$

Let us introduce the measure $\mathcal{D}\left[\psi,\bar{\psi}\right] = \prod_i \mathrm{d}\psi_i \mathrm{d}\bar{\psi}_i$. In terms of these fermionic variables, one can show that [177]

$$\mathcal{T}(G) = \int \mathcal{D}\left[\psi,\bar{\psi}\right]\,\bar{\psi}_i\psi_i \mathrm{e}^{-S\left[\psi,\bar{\psi}\right]}, \tag{5.53a}$$

$$\mathcal{T}(G\backslash\{ij\}) = \int \mathcal{D}\left[\psi,\bar{\psi}\right]\,\bar{\psi}_i\psi_i\bar{\psi}_j\psi_j \mathrm{e}^{-S\left[\psi,\bar{\psi}\right]}, \tag{5.53b}$$

where the action reads

$$S\left[\psi,\bar{\psi}\right] = -\sum_{i,j}\bar{\psi}_i L_{ij}\psi_j. \tag{5.54}$$

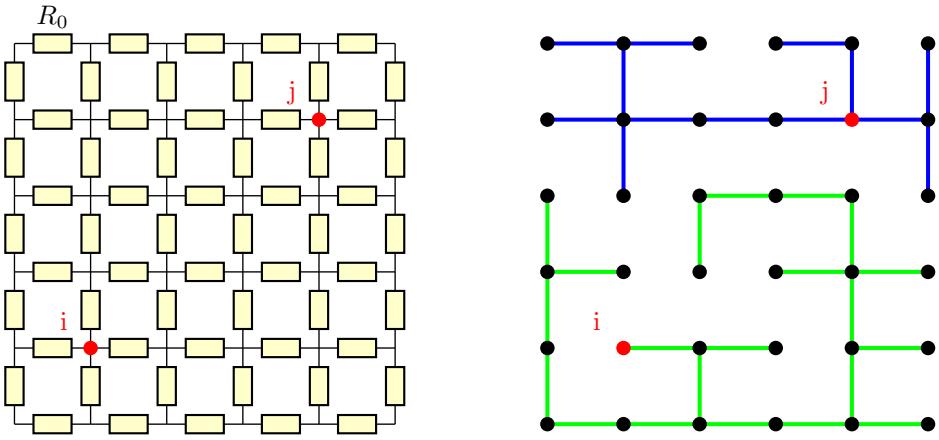

Figure 5.2: The equivalent resistance $R_{\text{eq}}(n,m)$ between the points i and j is given by $R_0\mathcal{T}(G)/\mathcal{T}(G\backslash\{ij\})$, where $\mathcal{T}(G\backslash\{ij\})$ counts the number of spanning 2-tree forests, with one tree containing the site i while the other covers j.

In this last equation, L_{ij} are the matrix elements of the discrete Laplacian, with for the square lattice $L_{i,i} = 4$ and $L_{i,j} = -1$ if i and j are neighbors. In the continuum limit, we expect this system to be described by a quantum field theory with Lagrangian density

$$\mathcal{L} = \frac{1}{4\pi}\partial_\mu\bar{\psi}\partial^\mu\psi. \tag{5.55}$$

This is of course the symplectic fermions theory encounter in chapter 2. The relation between the $2D$ Potts model at $Q = 0$ and this $c = -2$ (L)CFT is well-known, and the logarithmic operator described above is nothing but the logarithmic partner of the identity in symplectic fermions.

Applications to resistor networks

To conclude this section about spanning trees, let us discuss our result in the context of resistor networks. The problem is very simple: let us define an infinite square network of resistors, where each bond carries a resistance R_0. One would like to compute the equivalent resistance between two arbitrary points i and j of the network. The answer to this question is very simple and uses the Green's function of the Laplacian $\Delta(\log r) = 2\pi\delta(r)$. It is actually straightforward to perform the calculation directly on the square lattice. To measure the equivalent resistance between n and m, let us consider a current I flowing from n to m. Using Kirchhoff's laws, one finds that the electric potential satisfies the following Laplace equation

$$\Delta_{\text{discrete}}V_r \equiv \sum_{r' \text{ n.n. } r} V_{r'} - 4V_r = R_0 I(\delta_{r,m} - \delta_{r,n}). \tag{5.56}$$

The equivalent resistance $R_{\rm eq}(n,m)$ between n and m is then simply given by $R_{\rm eq}(n,m) = (V_n - V_m)/I$. Using the lattice Green function of the Laplacian, it is straightforward to show that (see *e.g.* [178, 179])

$$R_{\rm eq}(n,m) = R_0 \int_{-\pi}^{\pi} \frac{\mathrm{d}x}{2\pi} \int_{-\pi}^{\pi} \frac{\mathrm{d}y}{2\pi} \frac{1-\cos(nx+my)}{2-\cos x - \cos y}. \tag{5.57}$$

The asymptotic behavior of this function yields the resistance between two arbitrary points separated by a distance r

$$\frac{R_{\rm eq}(r)}{R_0} = \frac{2\gamma + 3\log 2}{2\pi} + \frac{1}{\pi}\log\frac{r}{a} + \mathcal{O}(r^{-2}), \tag{5.58}$$

where a is a UV cutoff. The first term of this equation is a non-universal constant that depends on the square lattice structure, however, the following behavior is universal

$$R_{\rm eq}(r) \sim \frac{R_0}{\pi}\log r, \tag{5.59}$$

and can be found directly from the continuum Green function $G_0(r) = \frac{1}{2\pi}\log r$. This result is directly related to eq. (5.46) and eq. (5.51) using Kirchhoff theorem: the conductance $G(i,j)$ between two arbitrary points i and j of a network G of resistors $R_0 = 1$ is given in terms of spanning trees by the ratio $\mathcal{T}(G)/\mathcal{T}(G\backslash\{ij\})$ (see Fig. 5.2). The logarithmic divergence of eq. (5.46) is thus directly related to the simple conductance calculation of an infinite resistor network. What is more interesting, though, is the interpretation of the prefactor $1/\pi$ as a derivative of a critical exponent of the Potts model. Moreover, this approach using a limit of the Potts model is quite general and not restricted to Laplacian problems, and we shall see several non-trivial examples in the following. To conclude, let us also mention that the boundary result (5.47) has also a nice interpretation in terms of resistor networks. Indeed, let us consider a resistor network covering the upper half-plane $y \geq 0$, and let us compute the resistance $R_{\rm eq}(r)$ between two points lying at the boundary $y = 0$. The Green function $G_0(x_0, y_0, x, y)$ of the Laplacian must satisfy in this case Neumann boundary conditions $\partial_y G_0(x_0, y_0, x, y = 0) = 0$. We find $G_0(x_0, y_0 = 0, x, y = 0) = \frac{1}{\pi}\log(x - x_0)$, so there is an additional factor 2 as compared to the bulk case. Therefore, the boundary resistance reads

$$R_{\rm eq}(r)|_{\rm boundary} \sim \frac{2R_0}{\pi}\log r, \tag{5.60}$$

in agreement with eq. (5.47).

Spanning forests in $d = 3$

We conclude this section on $Q = 0$ by discussing how our results can be generalized to higher dimensions d smaller than the upper critical dimension $d_c = 6$.

Equation (5.39) remains valid in that case, the only difference being that the model is believed to be critical for a finite non zero value w_c of w [180], meaning that $v \propto Q$ as $Q \to 0$, instead of $v \propto \sqrt{Q}$ for $d = 2$. One ends up with spanning forests with a non-zero fugacity w, which can be described in terms of an *interacting* fermionic field theory [177]

$$S = \int \mathrm{d}^d x \left(\partial_\mu \bar{\psi} \partial^\mu \psi + \frac{g}{2} \left[\partial_\mu (\bar{\psi}\psi) \right]^2 - g \bar{\psi}\psi \right), \tag{5.61}$$

with bare coupling $g \propto w$. To all orders of perturbation theory, this interacting fermionic field theory can be mapped onto a σ model with OSp(1|2) supersymmetry [177], or equivalently, to an O(n)-invariant σ model analytically continued to $n = -1$. In two dimensions, these models are (perturbatively) asymptotically free, with β function

$$\frac{\mathrm{d}g}{\mathrm{d}\log L} = \frac{3}{2\pi} g^2 + \dots \tag{5.62}$$

The $g = 0$ ($w = 0$) fixed point then corresponds to the free symplectic fermion (spanning trees) theory (5.55).

It is easy to see that because $v \propto Q$, the Jordan cell for the identity operator that we found for $d = 2$ does not appear in higher dimensions. This is because we have to normalize our operators with a factor v in order to find non-trivial results, so that the fact that $v \propto Q$ instead of $v \propto \sqrt{Q}$ will actually give way to a cancellation of the divergences that we encountered for $d = 2$. One can also notice that the scaling dimension of the magnetization vanishes only for $d = 2$. At one-loop for example, it reads [181]

$$\Delta_\phi = \frac{\eta + d - 2}{2} = 2 - \frac{5Q - 16}{9Q - 30}\epsilon + \mathcal{O}(\epsilon^2), \tag{5.63}$$

with $\epsilon = 6 - d$. For $Q = 0$, Δ_ϕ decreases as a function of ϵ and reaches 0 *only* for $d = 2$. However, we have considered only the simplest Jordan cell at $Q = 0$, and we do not exclude the possibility of a logarithmic structure for more complicated observables in $d = 3$. We leave the study of such observables at $Q = 0$ for future work.

5.3.2 Percolation ($Q \to 1$ limit)

CFT analysis

Let us first study the operators acting on two spins from a quantum field theory point of view. The energy operator is given by $\varepsilon(r_i) \equiv t^{(0,2)}(r_i) - \langle t^{(0,2)} \rangle$, where we subtracted the bulk expectation value of ε so as to obtain a well-defined scaling field. Its two-point function is given by

$$\langle \varepsilon(r)\varepsilon(0) \rangle = \tilde{A}(Q)(Q-1) r^{-2\Delta_\varepsilon(Q)}, \tag{5.64}$$

where $\tilde{A}(Q)$ is a regular function of Q, with a finite non-zero limit $\tilde{A}(1)$ for $Q \to 1$. The reasons why $\langle \varepsilon(r)\varepsilon(0)\rangle$ should vanish at $Q = 1$ is very natural from a lattice point of view. On the other hand, one can quite easily argue that $t^{(2,2)}$ corresponds to the 4-leg watermelon operator (the two propagating clusters correspond to four propagating hulls). We thus deduce the form of the two-point function

$$\langle t^{(2,2)}_{ab}(r) t^{(2,2)}_{cd}(0)\rangle = \frac{2A(Q)}{Q^2}\left(\delta_{ac}\delta_{bd} + \delta_{ad}\delta_{bc} - \frac{1}{Q-2}\left(\delta_{ac} + \delta_{ad} + \delta_{bc} + \delta_{bd}\right) + \frac{2}{(Q-1)(Q-2)}\right) \times r^{-2\Delta_4(Q)}, \quad (5.65)$$

where $A(Q)$ is again a regular function of Q when $Q \to 1$, and the factor $2/Q^2$ is purely conventional. The rest of the correlation function is fixed by representation theory.

In the formal limit $Q \to 1$ the two-point function (5.65) diverges. To cure this, we introduce a new field

$$\psi_{ab}(r) = t^{(2,2)}_{ab}(r) + \frac{2}{Q(Q-1)}\varepsilon(r)\,. \quad (5.66)$$

Its two-point function is easily computed and in order to have a finite $Q \to 1$ limit, we must require $A(1) = \tilde{A}(1)$, and that $\Delta_\varepsilon = \Delta_4$ at $Q = 1$. This implies that the fractal dimension d_{RB} of the so-called "red bonds" (also called "cutting bonds") is related to the thermal exponent ν via $d_{\mathrm{RB}} = \nu^{-1}$. This is indeed a well-known percolation result [182], valid in any dimension. We find

$$\langle \psi_{ab}(r)\psi_{cd}(0)\rangle = 2A(1) r^{-2\Delta_4}\left[(\delta_{ac} + \delta_{ad} + \delta_{bc} + \delta_{bd} + \delta_{ac}\delta_{bd} + \delta_{ad}\delta_{bc}) + 2\delta \log r\right], \quad (5.67)$$

where we have defined

$$\delta \equiv\ 2 \times \lim_{Q\to 1} \frac{\Delta_4 - \Delta_\varepsilon}{Q-1}\,. \quad (5.68)$$

Lattice analysis and geometrical interpretation

To understand what this logarithmic correlation means on the lattice, we define $\psi_{ab}(r_i) \equiv t^{(2,2)}(r_i) + \frac{2}{Q(Q-1)}\varepsilon(r_i)$, where $\varepsilon(r_i)$ is defined as in the continuum limit, that is, subtracting from $t^{(0,2)}$ its expectation value

$$\epsilon(r) \equiv t^{(0,2)}(r) - \frac{Q-1}{Q}\mathbb{P}\left(\bullet\bullet\right)\,. \quad (5.69)$$

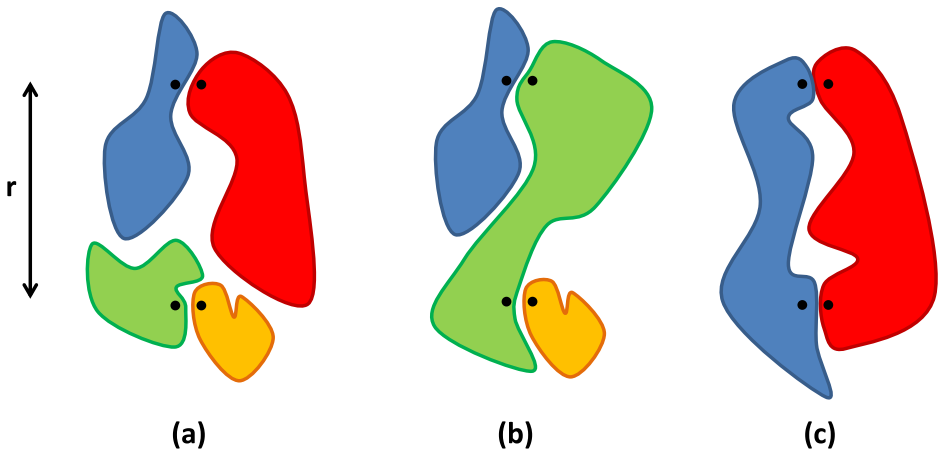

Figure 5.3: Percolation configurations contributing to the logarithmic observable $F(r)$.

A careful analysis of the limit $Q \to 1$ allows us to compute exactly the two-point function of ψ_{ab} on the lattice, we find [78]

$$\langle \psi_{ab}(r_1)\psi_{cd}(r_2)\rangle = 2\left(\delta_{ac}+\delta_{ad}+\delta_{bc}+\delta_{bd}+\delta_{ac}\delta_{bd}+\delta_{ad}\delta_{bc}\right)\mathbb{P}\left(\begin{array}{c}\bullet\\\bullet\\\bullet\\\bullet\end{array}\right) + 4\left[\mathbb{P}\left(\begin{array}{cc}\bullet&\bullet\\\bullet&\bullet\end{array}\right)+\mathbb{P}\left(\begin{array}{cc}\bullet&\bullet\\\bullet&\bullet\end{array}\right)-2\mathbb{P}\left(\begin{array}{c}\bullet\\\bullet\\\bullet\\\bullet\end{array}\right)-\mathbb{P}\left(\begin{array}{cc}\bullet&\bullet\\\bullet&\bullet\end{array}\right)^2\right]. \quad (5.70)$$

Comparing with (5.67) we deduce that

$$\mathbb{P}\left(\begin{array}{c}\bullet\\\bullet\\\bullet\\\bullet\end{array}\right) \sim A^{(2)}(1) r^{-2\Delta_4}, \quad (5.71)$$

as was of course expected from its relation to the 4-leg operator. Meanwhile, the logarithmic term in (5.67) can be identified with

$$F(r) = \mathbb{P}\left(\begin{array}{cc}\bullet&\bullet\\\bullet&\bullet\end{array}\right)+\mathbb{P}\left(\begin{array}{cc}\bullet&\bullet\\\bullet&\bullet\end{array}\right)-\mathbb{P}\left(\begin{array}{cc}\bullet&\bullet\\\bullet&\bullet\end{array}\right)^2 \sim A^{(2)}(1) r^{-2\Delta_4} \times \delta \log r. \quad (5.72)$$

Restricting now to two dimensions, the following combination [78]

$$F(r) \equiv \frac{\mathbb{P}\left(\begin{array}{cc}\bullet&\bullet\\\bullet&\bullet\end{array}\right)+\mathbb{P}\left(\begin{array}{cc}\bullet&\bullet\\\bullet&\bullet\end{array}\right)-\mathbb{P}\left(\begin{array}{cc}\bullet&\bullet\\\bullet&\bullet\end{array}\right)^2}{\mathbb{P}\left(\begin{array}{c}\bullet\\\bullet\\\bullet\\\bullet\end{array}\right)} \sim \theta + \frac{2\sqrt{3}}{\pi}\log r, \quad (5.73)$$

cancels out the dominant power law (see Fig. 5.3), leaving a pure logarithmic scaling which should be observable in numerical simulations (see below). The number $\delta =$

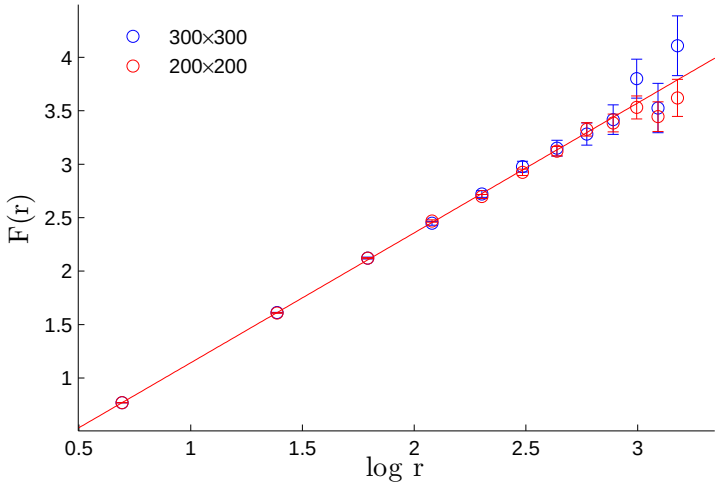

Figure 5.4: Monte Carlo estimation of the function $F(r)$ defined in eq. (5.73). Results are shown for 200×200 and 300×300 square lattices, with no significant difference.

$\frac{2\sqrt{3}}{\pi} \simeq 1.1026$ is a universal constant. Although the combination (5.73) may look slightly complicated, it is important to keep in mind that the logarithmic term we are after resides in the first *disconnected* term.

We have checked the validity of (5.73) by performing naive Monte Carlo simulations on square lattices of various sizes ranging from 150×150 to 300×300, with doubly periodic boundary conditions. Statistics were obtained on $\sim 10^3$ independent runs of 10^7 percolation configurations each. Results are shown in Fig. 5.4, and are in good agreement with (5.73). Careful extrapolations removing successively the first few short-distance points yields a slope 1.15 ± 0.05 in good agreement with our prediction $\frac{2\sqrt{3}}{\pi} \simeq 1.1026$.

5.3.3 An example of logarithm in the Ising model ($Q \to 2$ limit)

As can be seen from (5.65), the limit $Q \to 2$ (FK formulation of the Ising model) is also ill-defined. This is because the 4-leg watermelon operator $t_{ab}^{(2,2)}(r)$ is mixed with the 'vector' operator $t_a^{(1,2)}(r)$ at $Q = 2$. From the point of view of critical exponents in two dimensions, one has $h_{0,2} = h_{3/2,0}$ at $Q = 2$, where $h_{3/2,0}$ is the dimension of the first subleading magnetization operator. Unfortunately, although the mixing is clear in the continuum (it involves the 4-leg and the subleading magnetization operators), the situation is more intricate on the lattice as the magnetization and the subleading magnetization operators have the same symmetry, so it is hard to construct a precise lattice version of the subleading spin field. In practical terms, the two-point function of $t_a^{(1,2)}(r)$ defined in (5.26) has a dominant contribution given by the magnetization operator: this is because all the scaling operators with the same symmetry are mixed (not in the same sense as in indecomposability of course) on the lattice. To reformulate

this issue, ignoring for the moment the constraint $\sigma_1 \neq \sigma_2$, we can define

$$\tilde{t}_{ab}^{(1,2)}(\sigma_1, \sigma_2) = (\delta_{\sigma_1 \neq \sigma_2} - K) \left(\delta_{\sigma_1, a} + \delta_{\sigma_2, a} - \frac{2}{Q} \right), \tag{5.74}$$

where the term proportional to K involves operators acting on a single spin. In order to obtain the subleading magnetization operator, K must be fined tuned so as to cancel the leading magnetization contribution. Calling Δ_φ (resp. $\Delta_\varphi^{(1)}$) the (resp. subleading) magnetization exponent (so we have $\Delta_\varphi^{(1)} = \Delta_4$ at $Q = 2$), we define $\delta = 2 \lim_{Q \to 2} \frac{\Delta_\varphi^{(1)} - \Delta_4}{Q-2}$. In terms of probabilities, the mixing at $Q \to 2$ implies that

$$\mathbb{P}\left(\begin{array}{c} \bullet \\ | \\ | \\ \bullet \end{array} \right) \sim A r^{-\Delta_4}, \tag{5.75}$$

$$\mathbb{P}\left(\begin{array}{c} \bullet \\ | \\ \bullet \end{array} \right) \sim B r^{-\Delta_\varphi} + 4\delta \times A r^{-\Delta_\varphi^{(1)}} \log \frac{r}{a}. \tag{5.76}$$

We thus see that the logarithmic corrections arises only in the subleading term, for the reason explained above. Unfortunately, there is *a priori* no simple way using symmetry to form a linear combination of probabilities to get rid of the term $B r^{-\Delta_\varphi}$.

We emphasize that this issue arises only on the lattice, when one wants to identify geometrically the logarithmic observable. Once again, in the continuum limit, there is no ambiguity and our result indicates that the 4-leg operator is mixed into a Jordan cell with the subleading magnetization operator in the (logarithmic) Ising model ($Q = 2$).

5.4 A short overview of the generalization to the $\mathcal{O}(n)$ model

To conclude this chapter, we explain how our analysis of the Potts model could be generalized to the case of $O(n)$ model in d dimensions with action

$$S = \int \mathrm{d}^d x \left(\frac{1}{2} \sum_{a=1}^{n} (\partial_\mu \phi_a)^2 + \frac{m^2}{2} \sum_{a=1}^{n} \phi_a^2 + g \sum_{a,b} \phi_a^2 \phi_b^2 \right). \tag{5.77}$$

We will focus on the field theory although a similar analysis could be made at the level of a lattice Heisenberg Hamiltonian of n-component spins $H = -J \sum_{\langle i,j \rangle} \vec{S}_i . \vec{S}_j$. Using the representation theory of the $O(n)$ group, one can classify the scaling operators of the model. For instance, it was argued by Cardy [18] that the energy operator and the

generalization of the 2-leg operator in d dimensions could be expressed as

$$\varepsilon(r) = \sum_a :\phi_a^2:, \tag{5.78a}$$

$$\varphi_{ab}^{(2)}(r) = :\phi_a\phi_b: -\frac{1}{n}\sum_c :\phi_c^2:. \tag{5.78b}$$

The normal order means here that bulk expectation values are subtracted. Using once again the global $O(n)$ symmetry of the field theory, one can write down the general expression of the two-point functions of these fields at the critical point [18]

$$\langle\varepsilon(r)\varepsilon(0)\rangle = 2nA(n)r^{-2\Delta_\epsilon}, \tag{5.79a}$$

$$\langle\varphi_{ab}^{(2)}(r)\varphi_{cd}^{(2)}(0)\rangle = \tilde{A}(n)\left(\delta_{ac}\delta_{bd}+\delta_{ad}\delta_{bc}-\frac{2}{n}\delta_{ab}\delta_{cd}\right)r^{-2\Delta_{(2)}}, \tag{5.79b}$$

where $A(n)$ and $\tilde{A}(n)$ are regular function of n with a finite non-zero limit at $n=0$. The $n\to 0$ limit of these equations is singular and this yields logarithms as discussed in the context of the Potts model. This was argued to have a nice geometrical interpretation in terms of intersecting self-avoiding walks in Ref. [18]. More precisely, taking properly the $n\to 0$ limit, one finds the following logarithmic correlation

$$\langle :\phi^2(r)::\phi^2(0):\rangle \sim \log r \times r^{-2\Delta_{(2)}} \times f\left(\frac{r}{\xi}\right), \tag{5.80}$$

where we have allowed for the system to be off-criticality, with correlation length $\xi\sim|T-T_c|^{-\nu}$, e^{-T} being the monomer fugacity. Restricting for now to the boundary case, a more physical expression is obtained, as usual when dealing with polymers, by considering the Laplace transform so as to deal with polymers of fixed length

$$\int_{\text{boundary}}(\mathrm{d}r)\langle :\phi^2(r)::\phi^2(0):\rangle = \int_0^\infty \mathrm{d}S\mathrm{e}^{-TS}Z(S). \tag{5.81}$$

In this equation, $Z(S)$ counts the configurations with two self-avoiding loops attached to the boundary, with a total number of monomers S, with the constraints that the first loop is attached to the origin, and that both loop must intersect at least once [4]. Inverting the Laplace transform, one finds the following asymptotic behavior at the critical point $T=T_c$ [18]

$$Z(S)\sim \mathrm{e}^{T_cS}S^{\gamma-1}\log S, \tag{5.82}$$

with $\gamma=\nu\left(1-2\Delta_{(2)}\right)$. The important point in that equation is the $\log S$ term, which differs from the counting of 2-leg watermelon configurations that would scale as $Z_0(S)\sim \mathrm{e}^{T_cS}S^{\gamma-1}$ [23] (see Fig. 5.5). It would be interesting to check this formula

4. This last constraint comes from the normal order.

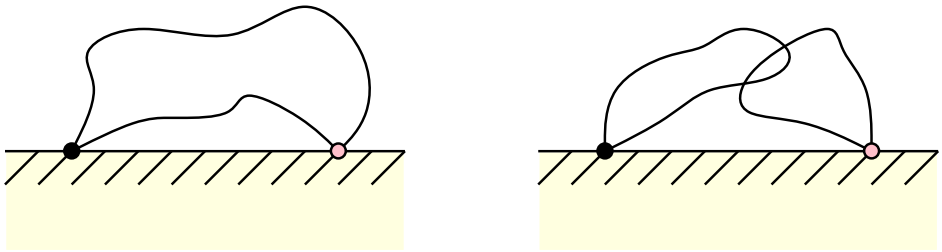

Figure 5.5: Left: The number of 2-leg watermelon configurations (two self-avoiding walks) starting from a fixed point on the boundary and coming back to another point (not fixed) on the boundary, with a total number of monomers S, scales as $Z_0(S) \sim \mathrm{e}^{T_c S} S^{\gamma-1}$ [23]. Right: Configurations with two self-avoiding loops attached to the boundary, with a total number of monomers S, with the constraints that the first loop is attached to the origin, and that both loop must intersect at least once. This scales as $Z(S) \sim \mathrm{e}^{T_c S} S^{\gamma-1} \log S$ [18]. The ratio of these two quantities thus behaves as $Z(S)/Z_0(S) \sim \log S$.

using exact enumerations.

This mixing can also be interpreted as critical exponents coinciding at $n = 0$. At one-loop, the scaling dimension of the energy is well-known

$$\Delta_\varepsilon = 2\left(\frac{d}{2} - 1\right) + \frac{n+2}{n+8}\epsilon + \mathcal{O}(\epsilon^2), \tag{5.83}$$

with $\epsilon = 4 - d$, whereas the dimension of p-leg watermelon operator can be obtained readily computing Gaussian operator product expansions (see *e.g.* [183])

$$\Delta_p = p\left(\frac{d}{2} - 1\right) + \frac{p(p-1)}{n+8}\epsilon + \mathcal{O}(\epsilon^2). \tag{5.84}$$

For $n = 0$, one has $\Delta_2 = \Delta_\varepsilon$ as expected. Note that in $d = 2$ dimensions, one has $\Delta_2 = 2h_{0,1} = \frac{2}{3}$ and $\Delta_\varepsilon = 2h_{1,2} = \frac{2}{3}$.

This line of thought can be generalized to more complicated cases. For example, we find that the 3-leg operator reads

$$\varphi^{(3)}_{abc} = \phi_a\phi_b\phi_c - \frac{1}{n+2}\sum_d \phi_d^2\left(\delta_{ab}\phi_c + \delta_{ac}\phi_b + \delta_{bc}\phi_a\right). \tag{5.85}$$

One can see that some mixing should be expected at $n = -2$ between $\varphi^{(3)}_{abc}$ and the operator $\sum_b :\phi_b^2\phi_a:$. The latter has a form energy $\times$ magnetization so we expect it to be the first subleading magnetization operator. Its scaling dimension can be easily computed at one loop order

$$\Delta^{(1)}_\phi = 3\left(\frac{d}{2} - 1\right) + \epsilon + \mathcal{O}(\epsilon^2), \tag{5.86}$$

and we indeed find that $\Delta_\phi^{(1)} = \Delta_3$ for $n = -2$. It would be very interesting to study extensively the $O(n)$ model along those lines, as we did for the Potts model above. A closer look at the lattice model would then be necessary in order to interpret these correlation functions geometrically.

Conclusion

In this thesis, we have discussed how to tackle logarithmic CFTs using lattice regularizations whose continuum limit is described by such theories.

The main idea underlying this lattice approach is to analyze thoroughly the representation theory of the symmetry algebras on the lattice, study how this Hilbert space structure carries over in the continuum limit, and deduce from this the indecomposable structure of Virasoro representations in the corresponding CFT. The point is that lattice models contain not only information about the central charge or critical exponents, but also fine structure details like representations structure, fusion rules, or Virasoro matrix elements (indecomposability parameters). We have argued that such indecomposability parameters can be measured directly on the lattice, thus providing an unambiguous way to determine them numerically for a given theory. Another major achievement of this work is the classification of a very large class of indecomposable Virasoro representations from the blob algebra. Most of the results have been obtained for chiral LCFTs, but lattice models will definitely be helpful to shed some light on bulk LCFTs, mixing holomorphic and anti-holomorphic sectors, and their relation to boundary CFTs.

Another approach discussed in this thesis is the limit or "replica" approach that consists in considering logarithmic CFTs as limits of ordinary CFTs. Here, the logarithms can be understood as power-laws "colliding" at the indecomposable point [5]. Although not new and definitely heuristic, this idea was used successfully in this thesis to obtain general formulas for indecomposability parameters, and to uncover geometrical logarithmic observables in the Potts model. In particular, we have found an observable in critical percolation which behaves exactly logarithmically, without any power-law prefactor, and checked this result numerically. Despite its simplicity, this method allows us to obtain very general results that are not restricted to two dimensions.

To conclude this thesis, we mention several interesting directions for future research, some of which corresponding to projects that I have pursued during the last year of my PhD:

- *Bulk LCFTs at $c = 0$.* Despite the recent progress in that direction, there remains a lot to be done to compute, say, four-point functions in bulk percolation.

5. In the theory of differential equations, this phenomenon is called confluence of singularities.

Although technically very difficult, the lattice approach provides us with a rather clear program: understand fully the representation theory on the lattice, analyze how this algebraic structure of the Hilbert space carries over to the continuum limit, deduce the structure for Virasoro $\times$ $\overline{\text{Virasoro}}$, and in principle, try to compute correlation functions from there. The main issue is that the algebra obtained in the scaling limit of periodic lattice models is actually larger that $\mathfrak{vir} \oplus \overline{\mathfrak{vir}}$, thus suggesting that this new object, called interchiral algebra in [149], might be the key to understanding the structure of percolation. This is a project in progress with A.M. Gainutdinov, J. Jacobsen, N. Read and H. Saleur.

- *Extended symmetries, higher dimensions, non-critical theories etc.* A rather obvious generalization of the lattice approach presented in this thesis would be to explore lattice algebras related to higher values of the quantum group spin. The simplest case would be the Birman–Wenzl–Murakami algebra, which appears in the spin-one case, and should be related to the non semi-simple $\mathcal{N} = 1$ super Virasoro algebra. Of course, logarithmic CFTs are not restricted to two dimensions, and they have actually nothing to do with the integrability of most of the models considered here. It would be of great interest to understand these higher-dimensional CFTs, as well as, for instance, non-critical deformations *etc.*
- *General analysis of logarithmic observables in geometrical models.* A deeper understanding of why and how logarithmic correlations appear in geometrical models is also definitely one of the remaining challenges of the field. Although we do know several specific examples that can be accessed and checked numerically, we are still far from understanding extensively the logarithmic structure of, say, the Potts model (let alone more complicated models!) in terms of geometrical observables. Relating the "replica" approach discussed in the last chapter of this thesis to the algebraic approach based on indecomposable representations would also be very interesting – in the end, this amounts to conciliating the replica and supersymmetry approach to disordered and geometrical models. Finally, getting a hold on logarithms from the point of view of SLE (see [184, 185] for reviews for theoretical physicists) remains a fully open question – for a recent step in that direction, see [186].
- *Logarithmic observables in disordered systems and sigma models.* Coming back to the replica approach, the only models "under control" are the Potts and $O(n)$ models, *via* limits such as $Q \to 1$ for Potts (percolation) or $n \to 0$ for $O(n)$ (SAWs). Though interesting, these examples are probably too simple to uncover a general pattern. Analyzing how logarithms arise in *e.g.* the $n \to 0$ limit of Pruisken's sigma model formulation [187] on $U(2n)/U(n) \times U(n)$ of the Integer Quantum Hall transition would definitely be something worth looking into, even though there is only very little hope that the corresponding observables will be physically interesting, let alone experimentally accessible.
- *Logarithmic structure of truncated models for the IQHE transition.* Another possibility in that direction is to analyze the logarithmic structure of truncated geometrical formulations of the IQHE transition [172]. This is possible since the truncated Hilbert space is finite-dimensional. The hope is of course that some of the logarithmic features will be unaffected by the truncation, even if

there is no reason to hope for this *a priori* since the truncated models are in a different universality class. This is one of the projects under investigation by E. Vernier. Another hope would be to find a finite-dimensional spin chain that would describe the strong-coupling limit of the non-compact sigma model underlying the IQHE. Despite the non-compact nature of the continuum limit, this is not totally hopeless, as an example of finite dimensional regularization of a non-compact sigma model has been uncovered recently [188, 189].

Appendix A

The Lie superalgebras $\mathfrak{gl}(1|1)$ and $\mathfrak{sl}(2|1)$ and some of their representations

In this appendix, we gather some well-known results concerning the Lie superalgebras $\mathfrak{gl}(1|1)$ and $\mathfrak{sl}(2|1)$, and we also recall some properties of several of their finite-dimensional representations that are used throughout this thesis. In particular, we give an explicit Fock space formulation of the fundamental and dual representations used to construct Temperley-Lieb spin chains. Note that we shall not give a formal definition of Lie superalgebras in general, but focus instead on the explicit examples relevant to our discussion. We will simply consider superalgebras as $\mathbb{Z}_2$-graded Lie algebra that contain both fermionic and bosonic generators, characterized by their (anti)commutation relations. We follow here Ref. [190] (see also [191]).

Recall also that when dealing with the irreducible representations of a superalgebra, one has to distinguish between typical (long multiplets) or atypical representations (short multiplets). Superalgebras also allows for more complicated indecomposable representations (indecomposable modules, or indecomposables) that may be considered as composites, or gluings, of the latters. An especially important class of representations is given by the so-called projective covers of atypicals, which can be thought of in this context as 'maximally indecomposable representations', containing atypical representations as building blocks [1]. Projective modules satisfy very nice properties that make them relevant for physics, for example, the tensor product of two projective modules can only yield projective modules.

1. Maximal means that it cannot occur as a subrepresentation in a yet bigger indecomposable representation. Note that this definition of projective modules is a bit misleading, especially in the context of the TL algebra for example, but it is enough as far as the superalgebras of this appendix are concerned. For a more mathematically precise and more general definition of a projective module, see [74] section 4.1.

A.1 The Lie superalgebra $\mathfrak{gl}(1|1)$ and its representations

A.1.1 Defining relations

The Lie superalgebra $\mathfrak{g} = \mathfrak{gl}(1|1)$ is generated by two bosonic elements E, N and two fermionic generators $\Psi^{\pm}$ such that E is central and the other generators obey

$$[N, \Psi^{\pm}] \;=\; \pm\Psi^{\pm} \quad \text{and} \quad \{\Psi^{-}, \Psi^{+}\} \;=\; E \;\; . \tag{1.1}$$

The even (bosonic) subalgebra is thus given by $\mathfrak{g}^0 = \mathfrak{u}(1) \oplus \mathfrak{u}(1)$, and N counts the number of fermions. Let us also fix the following Casimir element C

$$C \;=\; (2N-1)E + 2\Psi^{-}\Psi^{+} \;\; . \tag{1.2}$$

The choice of C is not unique since we could add any function of the central element E. Finally we recall the definition of the supertrace $\mathrm{STr}(.) = \mathrm{Tr}((-1)^F .)$. The superdimension is the supertrace of the identity, *ie* the number of bosons minus the number of fermions. The superdimension of $\mathfrak{gl}(1|1)$ is zero.

A.1.2 Fundamental and Dual representations in Fock space

To construct what we will refer to as fundamental representation $\square$, we introduce a fermionic generator $\{f, f^{\dagger}\} = 1$. The $\mathfrak{gl}(1|1)$ generators in the representation $\square$ read [2]

$$N = f^{\dagger}f, \quad \Psi^{+} = f^{\dagger}, \quad \Psi^{-} = f, \quad E = 1. \tag{1.3}$$

It is easy to check that these generators furnish a representation of $\mathfrak{gl}(1|1)$ in the space $\square \equiv \mathrm{Span}\{|0\rangle, |1\rangle = f^{\dagger}|0\rangle\}$. One can also construct the so-called dual representation $\overline{\square} \equiv \mathrm{Span}\{|\overline{0}\rangle, |\overline{1}\rangle = -\overline{f}^{\dagger}|\overline{0}\rangle\}$, where $\{\overline{f}, \overline{f}^{\dagger}\} = -1$. The generators act as

$$N = -\overline{f}^{\dagger}\overline{f}, \quad \Psi^{+} = \overline{f}^{\dagger}, \quad \Psi^{-} = \overline{f}, \quad E = 1. \tag{1.4}$$

To generate a $\mathfrak{gl}(1|1)$-invariant spin chain, we shall need an invariant interaction in the tensor product representation $\square \otimes \overline{\square}$. It is given by the Casimir (1.2) in $\square \otimes \overline{\square}$

$$e \equiv -\frac{1}{2}C = -\Psi^{-}\Psi^{+} = (f^{\dagger} + \overline{f}^{\dagger})(f + \overline{f}), \tag{1.5}$$

with $e^2 = 0$.

2. We use the same notation for the generators and their representation in the Fock space.

A.1.3 Finite dimensional representations of $\mathfrak{gl}(1|1)$

The irreducible representations of $\mathfrak{gl}(1|1)$ fall into two different series, typical and atypical. The typical representations are 2-dimensional representations $\langle e, n\rangle$ labeled by pairs e, n with $e \neq 0$ and $n \in \mathbb{R}$. In these representations, the generators take the form $E = e\mathbf{1}_2$ and

$$N = \begin{pmatrix} n-1 & 0 \\ 0 & n \end{pmatrix} \quad , \quad \Psi^+ = \begin{pmatrix} 0 & 0 \\ e & 0 \end{pmatrix} \quad , \quad \Psi^- = \begin{pmatrix} 0 & 1 \\ 0 & 0 \end{pmatrix} \quad . \tag{1.6}$$

Using these notations, one has $\square = \langle 1, 1\rangle$ and $\overline{\square} = \langle -1, 1\rangle$. Atypical representations are given by 1-dimensional representations $\langle n\rangle$, parametrized by the value $n \in \mathbb{R}$ of N, with vanishing other generators $\Psi^+ = \Psi^- = E = 0$.

Other finite dimensional representations are more complicated, indecomposable representations. In particular, the projective covers $\mathcal{P}_n$ of the atypical representations $\langle n\rangle$ have the following structure

$$\mathcal{P}_n = \begin{array}{ccccc} & & \langle n\rangle & & \\ & \swarrow & & \searrow & \\ \langle n-1\rangle & & & & \langle n+1\rangle \\ & \searrow & & \swarrow & \\ & & \langle n\rangle & & \end{array} \quad , \tag{1.7}$$

where the arrows represent the action of the generators $\Psi^\pm$ (see Sec. (2.3) for more details). The Casimir (1.2) is not diagonalizable on $\mathcal{P}_n$ and maps the top $\langle n\rangle$ to the bottom $\langle n\rangle$ in (1.7). We refer the reader to [190] for tensor products of these representations.

A.2 The Lie superalgebra $\mathfrak{sl}(2|1)$ and its representations

A.2.1 Defining relations

We define the Lie superalgebra $\mathfrak{g} = \mathfrak{sl}(2|1)$ by the commutation relations of its 8 generators. Its bosonic part is $\mathfrak{g}^0 = \mathfrak{u}(1) \oplus \mathfrak{sl}(2)$, that is

$$[B, Q^\pm] = [B, Q^z] = 0, \tag{1.8}$$

$$[Q^+, Q^-] = 2Q^z, \quad [Q^z, Q^\pm] = \pm Q^\pm. \tag{1.9}$$

The fermionic generators obey the simple relations

$$\{F^\pm, F^\mp\} = \{\overline{F}^\pm, \overline{F}^\mp\} = 0, \tag{1.10}$$

$$\{F^\pm, \overline{F}^\pm\} = Q^\pm, \quad \{F^\pm, \overline{F}^\mp\} = B \mp Q^\pm. \tag{1.11}$$

Finally, we have

$$[Q^z, F^\pm] = \pm\frac{1}{2}F^\pm, \quad [Q^z, \overline{F}^\pm] = \pm\frac{1}{2}\overline{F}^\pm, \tag{1.12}$$

$$[B, F^\pm] = \frac{1}{2}F^\pm, \quad [B, \overline{F}^\pm] = -\frac{1}{2}\overline{F}^\pm, \tag{1.13}$$

$$[Q^\pm, F^\pm] = [Q^\pm, \overline{F}^\pm] = 0, [Q^\pm, F^\mp] = -F^\pm, [Q^\pm, \overline{F}^\mp] = \overline{F}^\pm. \tag{1.14}$$

Note that there is a subalgebra $\mathfrak{gl}(1|1)$ spanned by the generators $\Psi^+ = F^+, \Psi^- = F^-, E = B - Q_z$ and $N = B + Q_z$.

A.2.2 Fundamental and Dual representations in Fock space

Three-dimensional representations of this superalgebra are readily obtained using creation and annihilation operators. To construct what we will refer to as fundamental representation $\square$, we introduce two bosonic operators $[b_\sigma, b^\dagger_{\sigma'}] = \delta_{\sigma,\sigma'}$, where $\sigma \in \{\uparrow, \downarrow\}$, and one fermion $\{f, f^\dagger\} = 1$. The generators read

$$B = f^\dagger f + \frac{1}{2}(b^\dagger_\uparrow b_\uparrow + b^\dagger_\downarrow b_\downarrow), Q_z = \frac{1}{2}(b^\dagger_\uparrow b_\uparrow - b^\dagger_\downarrow b_\downarrow), Q^+ = b^\dagger_\uparrow b_\downarrow, \tag{1.15}$$

$$Q^- = b^\dagger_\downarrow b_\uparrow, F^+ = f^\dagger b_\uparrow, F^- = f^\dagger b_\downarrow, \overline{F}^+ = b^\dagger_\uparrow f, \overline{F}^- = b^\dagger_\downarrow f. \tag{1.16}$$

These generators furnish a representation of $\mathfrak{sl}(2|1)$ in the space $\square \equiv \mathrm{Span}\{f^\dagger |0\rangle, b^\dagger_\uparrow |0\rangle, b^\dagger_\downarrow |0\rangle\}$. One can also construct the so-called dual representation $\overline{\square} \equiv \mathrm{Span}\{\overline{f}^\dagger |0\rangle, \overline{b}^\dagger_\uparrow |0\rangle, \overline{b}^\dagger_\downarrow |0\rangle\}$, where $[\overline{b}_\sigma, \overline{b}^\dagger_{\sigma'}] = \delta_{\sigma,\sigma'}$ and $\{\overline{f}, \overline{f}^\dagger\} = -1$. The generators act as

$$B = \overline{f}^\dagger \overline{f} - \frac{1}{2}(\overline{b}^\dagger_\uparrow \overline{b}_\uparrow + \overline{b}^\dagger_\downarrow \overline{b}_\downarrow), Q_z = \frac{1}{2}(\overline{b}^\dagger_\uparrow \overline{b}_\uparrow - \overline{b}^\dagger_\downarrow \overline{b}_\downarrow), Q^+ = -\overline{b}^\dagger_\uparrow \overline{b}_\downarrow, Q^- = -\overline{b}^\dagger_\downarrow \overline{b}_\uparrow, \tag{1.17}$$

$$F^+ = \overline{b}^\dagger_\uparrow \overline{f}, F^- = \overline{b}^\dagger_\downarrow \overline{f}, \overline{F}^+ = \overline{f}^\dagger \overline{b}_\downarrow, \overline{F}^- = \overline{f}^\dagger \overline{b}_\uparrow. \tag{1.18}$$

Note also that the operator

$$e = (\overline{b}^\dagger_\uparrow b^\dagger_\downarrow + \overline{b}^\dagger_\downarrow b^\dagger_\uparrow + \overline{f}^\dagger f^\dagger)(b_\uparrow \overline{b}_\downarrow + b_\downarrow \overline{b}_\uparrow + f\overline{f}) \tag{1.19}$$

is the projector onto the singlet in the tensor product representation $\square \otimes \overline{\square}$. This expression will be used for the definition of the Temperley-Lieb generator for our $\mathfrak{sl}(2|1)$ spin chain.

A.2.3 Finite dimensional representations

We also recall some usual notations for the finite dimensional representations of $\mathfrak{sl}(2|1)$. We begin with the irreducible representations. Except for the trivial representation $\{0\}$ of dimension 1, the irreducible atypical representations $\{j\}_\pm$ are labeled by the half-integer $j = \frac{1}{2}, 1, \ldots$; they have dimension $4j + 1$. There are also the typical

representations $\{b, j\}$ (with dimension $8j$ and $b \neq \pm j$) where b is a $U(1)$ charge, these are also projective. When $b = \pm j$, the modules $\{\pm j, j\}$ become indecomposable. Using these notations, the fundamental and dual representations are $\square = \{\frac{1}{2}\}_+$, $\overline{\square} = \{\frac{1}{2}\}_-$, and the adjoint representation is $\{0, 1\}$.

We will also be interested in atypical projective covers $\mathcal{P}^{\pm}(j)$ (with dimension $16j+4$ for $j \neq 0$ and dimension 8 if $j = 0$). The projective covers for $j \neq 0$ have the subquotient structure

$$\mathcal{P}^{\pm}(j) = \begin{array}{ccccc} & & \{j\}_{\pm} & & \\ & \swarrow & & \searrow & \\ \{j-\frac{1}{2}\}_{\pm} & & & & \{j+\frac{1}{2}\}_{\pm} \\ & \searrow & & \swarrow & \\ & & \{j\}_{\pm} & & \end{array} \quad , \tag{1.20}$$

whereas for $j = 0$, one has

$$\mathcal{P}(0) = \begin{array}{ccccc} & & \{0\} & & \\ & \swarrow & & \searrow & \\ \{\frac{1}{2}\}_{+} & & & & \{\frac{1}{2}\}_{-} \\ & \searrow & & \swarrow & \\ & & \{0\} & & \end{array} \quad . \tag{1.21}$$

The arrows represent the action of the generators of $\mathfrak{sl}(2|1)$, as usual. We shall not describe the tensor product of all these representations here, are refer the interested reader to [190]. Using those results, one can decompose the Hilbert space $\mathcal{H} = (\square \otimes \overline{\square})^{\otimes N}$ onto projective representations only (except for the fundamental). In particular, we have $\square \otimes \overline{\square} = \{0\} \oplus \{0, 1\}$.

Bibliography

[1] T. T. Wu. *Theory of Toeplitz determinants and the spin correlations of the two-dimensional Ising model. I.* Phys. Rev. **149**, 380–401 (1966).

[2] H. Cheng and T. T. Wu. *Theory of Toeplitz determinants and the spin correlations of the two-dimensional Ising model. III.* Phys. Rev. **164**, 719–735 (1967).

[3] L. Onsager. *Crystal statistics. i. a two-dimensional model with an order-disorder transition.* Phys. Rev. **65**, 117–149 (1944).

[4] A. Belavin, A. Polyakov and A. Zamolodchikov. *Infinite conformal symmetry in two-dimensional quantum field theory.* Nuclear Physics B **241(2)**, 333 – 380 (1984).

[5] D. Friedan, Z. Qiu and S. Shenker. *Conformal invariance, unitarity, and critical exponents in two dimensions.* Phys. Rev. Lett. **52**, 1575–1578 (1984).

[6] J. L. Cardy. *Operator content of two-dimensional conformally invariant theories.* Nuclear Physics B **270(0)**, 186 – 204 (1986).

[7] J. L. Cardy. *Conformal invariance and surface critical behavior.* Nuclear Physics B **240(4)**, 514 – 532 (1984).

[8] I. Affleck and A. W. Ludwig. *The Kondo effect, conformal field theory and fusion rules.* Nuclear Physics B **352(3)**, 849 – 862 (1991).

[9] I. Affleck and A. W. W. Ludwig. *The Fermi edge singularity and boundary condition changing operators.* Journal of Physics A: Mathematical and General **27(16)**, 5375 (1994).

[10] G. Moore and N. Read. *Nonabelions in the fractional quantum Hall effect.* Nuclear Physics B **360(2–3)**, 362 – 396 (1991).

[11] P. Calabrese and J. Cardy. *Entanglement entropy and quantum field theory.* Journal of Statistical Mechanics: Theory and Experiment **2004(06)**, P06002 (2004).

[12] P. Calabrese and J. Cardy. *Time dependence of correlation functions following a quantum quench.* Phys. Rev. Lett. **96**, 136801 (2006).

[13] P. Calabrese and J. Cardy. *Entanglement and correlation functions following a local quench: a conformal field theory approach.* Journal of Statistical Mechanics: Theory and Experiment **2007(10)**, P10004 (2007).

[14] D. Bernard and B. Doyon. *Energy flow in non-equilibrium conformal field theory.* Journal of Physics A: Mathematical and Theoretical **45(36)**, 362001 (2012).

[15] K. v. Klitzing, G. Dorda and M. Pepper. *New method for high-accuracy determination of the fine-structure constant based on quantized Hall resistance.* Phys. Rev. Lett. **45**, 494–497 (1980).

[16] M. R. Zirnbauer. *Conformal field theory of the integer quantum Hall plateau transition.* unpublished, `arXiv:hep-th/9905054` (1999).

[17] H. Saleur. *Conformal invariance for polymers and percolation.* Journal of Physics A: Mathematical and General **20(2)**, 455 (1987).

[18] J. Cardy. *Logarithmic correlations in quenched random magnets and polymers.* unpublished, `arXiv:cond-mat/9911024` (1999).

[19] V. Gurarie and A. W. W. Ludwig. *Conformal algebras of two-dimensional disordered systems.* Journal of Physics A: Mathematical and General **35(27)**, L377 (2002).

[20] J. Zinn-Justin. *Quantum Field Theory and Critical Phenomena* (International Series of Monographs on Physics, Claredon Press, Oxford, 4^{th} edition, 2002).

[21] S. Eggert. *Numerical evidence for multiplicative logarithmic corrections from marginal operators.* Phys. Rev. B **54**, R9612–R9615 (1996).

[22] B. Nienhuis. *Critical behavior of two-dimensional spin models and charge asymmetry in the coulomb gas.* Journal of Statistical Physics **34**, 731–761 (1984).

[23] B. Duplantier and H. Saleur. *Exact surface and wedge exponents for polymers in two dimensions.* Phys. Rev. Lett. **57**, 3179–3182 (1986).

[24] H. Saleur and B. Duplantier. *Exact determination of the percolation hull exponent in two dimensions.* Phys. Rev. Lett. **58**, 2325–2328 (1987).

[25] J. L. Cardy. *Critical percolation in finite geometries.* Journal of Physics A: Mathematical and General **25(4)**, L201 (1992).

[26] H. Saleur. *Polymers and percolation in two dimensions and twisted n = 2 supersymmetry.* Nuclear Physics B **382(3)**, 486 – 531 (1992).

[27] J. L. Cardy. *Conformal invariance and the yang-lee edge singularity in two dimensions.* Phys. Rev. Lett. **54**, 1354–1356 (1985).

[28] K. Efetov. *Supersymmetry and theory of disordered metals.* Advances in Physics **32(1)**, 53–127 (1983).

[29] H. W. J. Blöte, J. L. Cardy and M. P. Nightingale. *Conformal invariance, the central charge, and universal finite-size amplitudes at criticality.* Phys. Rev. Lett. **56**, 742–745 (1986).

[30] I. A. Gruzberg, N. Read and A. W. W. Ludwig. *Random-bond Ising model in two dimensions: The nishimori line and supersymmetry.* Phys. Rev. B **63**, 104422 (2001).

[31] I. A. Gruzberg, A. W. W. Ludwig and N. Read. *Exact exponents for the spin quantum Hall transition.* Phys. Rev. Lett. **82**, 4524–4527 (1999).

[32] J.-S. Caux, I. Kogan and A. Tsvelik. *Logarithmic operators and hidden continuous symmetry in critical disordered models.* Nuclear Physics B **466(3)**, 444 – 462 (1996).

[33] Z. Maassarani and D. Serban. *Non-unitary conformal field theory and logarithmic operators for disordered systems.* Nuclear Physics B **489(3)**, 603 – 625 (1997).

[34] J.-S. Caux, N. Taniguchi and A. Tsvelik. *Disordered Dirac fermions: Multifractality termination and logarithmic conformal field theories.* Nuclear Physics B **525(3)**, 671 – 696 (1998).

[35] G. Piroux and P. Ruelle. *Pre-logarithmic and logarithmic fields in a sandpile model.* Journal of Statistical Mechanics: Theory and Experiment **2004(10)**, P10005 (2004).

[36] G. Piroux and P. Ruelle. *Logarithmic scaling for height variables in the abelian sandpile model.* Physics Letters B **607(1–2)**, 188 – 196 (2005).

[37] M. A. Flohr. *Two-dimensional turbulence: A novel approach via logarithmic conformal field theory.* Nuclear Physics B **482(3)**, 567 – 578 (1996).

[38] M. R. Tabar and S. Rouhani. *Logarithmic correlation functions in two-dimensional turbulence.* Physics Letters A **224(6)**, 331 – 336 (1997).

[39] N. J. Berkovits, C. Vafa and E. Witten. *Conformal field theory of ads background with ramond-ramond flux.* Journal of High Energy Physics **1999(03)**, 018 (1999).

[40] G. Götz, T. Quella and V. Schomerus. *The WZNW model on PSU*$(1,1|2)$. Journal of High Energy Physics **2007(03)**, 003 (2007).

[41] A. M. Ghezelbash, M. Khorrami and A. Aghamohammadi. *Logarithmic conformal field theories and ads correspondence.* International Journal of Modern Physics A **14(16)**, 2581–2591 (1999).

[42] D. Grumiller and N. Johansson. *Instability in cosmological topologically massive gravity at the chiral point.* Journal of High Energy Physics **2008(07)**, 134 (2008).

[43] N. N. E. Frenkel, A. Losev. *Instantons beyond topological theory ii.* `arXiv:0803.3302` (2008).

[44] L. Rozansky and H. Saleur. *Quantum field theory for the multi-variable alexander-conway polynomial.* Nuclear Physics B **376(3)**, 461 – 509 (1992).

[45] V. Gurarie. *Logarithmic operators in conformal field theory.* Nuclear Physics B **410(3)**, 535 – 549 (1993).

[46] M. R. Gaberdiel and H. G. Kausch. *Indecomposable fusion products.* Nuclear Physics B **477(1)**, 293 – 318 (1996).

[47] M. R. Gaberdiel and H. G. Kausch. *A rational logarithmic conformal field theory.* Physics Letters B **386(1–4)**, 131 – 137 (1996).

[48] M. A. Flohr. *On modular invariant partition functions of conformal field theories with logarithmic operators.* International Journal of Modern Physics A **11(22)**, 4147–4172 (1996).

[49] F. Rohsiepe. *On reducible but indecomposable representations of the Virasoro algebra.* unpublished, `arXiv:hep-th/9611160` (1996).

[50] V. Gurarie. *c-theorem for disordered systems.* Nuclear Physics B **546(3)**, 765 – 778 (1999).

[51] H. G. Kausch. *Curiosities at $c = -2$.* unpublished, `arXiv:hep-th/9510149` (1995).

[52] H. G. Kausch. *Symplectic fermions.* Nuclear Physics B **583(3)**, 513 – 541 (2000).

[53] J. Cardy. *The stress tensor in quenched random systems.* Statistical Field Theories (Proceedings of a NATO workshop, Como, June 2001) eds A. Cappelli and G. Mussardo, `cond-mat/0111031` (2001).

[54] V. Gurarie and A. W. W. Ludwig. *Conformal field theory at central charge $c = 0$ and two-dimensional critical systems with quenched disorder.* In M. Shifman, A. Vainstein, and J. Wheater, editors, Ian Kogan Memorial Collection: From Fields To Strings: Circumnavigating Theoretical Physics, page 1384. World Scientific Publishing Co. Pte. Ltd., `arXiv:hep-th/0409105` (2005).

[55] M. Flohr and A. Müller-Lohmann. *Notes on non-trivial and logarithmic conformal field theories with $c = 0$.* Journal of Statistical Mechanics: Theory and Experiment **2006(04)**, P04002 (2006).

[56] H. Eberle and M. Flohr. *Virasoro representations and fusion for general augmented minimal models.* Journal of Physics A: Mathematical and General **39(49)**, 15245 (2006).

[57] P. Mathieu and D. Ridout. *From percolation to logarithmic conformal field theory.* Physics Letters B **657(1–3)**, 120 – 129 (2007).

[58] P. Mathieu and D. Ridout. *Logarithmic minimal models $\mathcal{M}(2, p)$, their logarithmic couplings, and duality.* Nuclear Physics B **801(3)**, 268 – 295 (2008).

[59] K. Kytola and D. Ridout. *On staggered indecomposable Virasoro modules.* Journal of Mathematical Physics **50(12)**, 123503 (2009).

[60] M. R. Gaberdiel, I. Runkel and S. Wood. *Fusion rules and boundary conditions in the c = 0 triplet model.* Journal of Physics A: Mathematical and Theoretical **42(32)**, 325403 (2009).

[61] P. Di Francesco, P. Mathieu and D. Sénéchal. *Conformal field theory.* Graduate texts in contemporary physics (Springer, New York, NY, 1997).

[62] J. Germoni. *On the classification of admissible representations of the Virasoro algebra.* Letters in Mathematical Physics **55**, 169–177 (2001).

[63] F. Lesage, P. Mathieu, J. Rasmussen and H. Saleur. *The $su(2)_{-\frac{1}{2}}$ WZW model and the $\beta\gamma$ system.* Nuclear Physics B **647(3)**, 363 – 403 (2002).

[64] V. Schomerus and H. Saleur. *The GL(1|1) WZW-model: From supergeometry to logarithmic CFT.* Nuclear Physics B **734(3)**, 221 – 245 (2006).

[65] H. Saleur and V. Schomerus. *On the SU(2|1) WZNW model and its statistical mechanics applications.* Nuclear Physics B **775(3)**, 312 – 340 (2007).

[66] T. Creutzig and D. Ridout. *Relating the archetypes of logarithmic conformal field theory.* `arXiv:1107.2135` (2011).

[67] V. Pasquier and H. Saleur. *Common structures between finite systems and conformal field theories through quantum groups.* Nuclear Physics B **330(2–3)**, 523 – 556 (1990).

[68] N. Read and H. Saleur. *Enlarged symmetry algebras of spin chains, loop models, and s-matrices.* Nuclear Physics B **777(3)**, 263 – 315 (2007).

[69] N. Read and H. Saleur. *Associative-algebraic approach to logarithmic conformal field theories.* Nuclear Physics B **777(3)**, 316 – 351 (2007).

[70] P. A. Pearce, J. Rasmussen and J.-B. Zuber. *Logarithmic minimal models.* Journal of Statistical Mechanics: Theory and Experiment **2006(11)**, P11017 (2006).

[71] R. Vasseur, J. L. Jacobsen and H. Saleur. *Indecomposability parameters in chiral logarithmic conformal field theory.* Nuclear Physics B **851(2)**, 314 – 345 (2011).

[72] A. Gainutdinov and R. Vasseur. *Lattice fusion rules and logarithmic operator product expansions.* Nuclear Physics B **868(1)**, 223 – 270 (2013).

[73] A. Gainutdinov, J. Jacobsen, N. Read, H. Saleur and R. Vasseur. *Logarithmic conformal field theory: a lattice approach.* `arXiv:1303.2082` (2013).

[74] A. M. Gainutdinov, J. L. Jacobsen, H. Saleur and R. Vasseur. *A physical approach to the classification of indecomposable Virasoro representations from the blob algebra.* Nuclear Physics B **873(3)**, 614 – 681 (2013).

[75] R. Vasseur, A. Gainutdinov, J. L. Jacobsen and H. Saleur. *The puzzle of bulk conformal field theories at central charge $c = 0$.* Phys. Rev. Lett. **108**, 161602 (2012).

[76] A. Gainutdinov, N. Read, H. Saleur and R. Vasseur. *On the correspondence between boundary and bulk lattice models and (logarithmic) conformal field theories.* To appear (2013).

[77] J. Cardy. *Logarithmic conformal field theories as limits of ordinary CFTs and some physical applications.* `arXiv:1302.4279` (2013).

[78] R. Vasseur, J. L. Jacobsen and H. Saleur. *Logarithmic observables in critical percolation.* Journal of Statistical Mechanics: Theory and Experiment **2012(07)**, L07001 (2012).

[79] R. Vasseur, H. Saleur and J. Jacobsen. *Watermelon operators and logarithmic correlations in the critical Potts model in d dimensions.* To appear (2013).

[80] A. Polyakov. *Conformal symmetry of critical fluctuations.* JETP Lett. **12(12)**, 381 – 383 (1970).

[81] G. Mussardo. *Statistical Field Theory: An Introduction to Exactly Solved Models in Statistical Physics.* Oxford Graduate Texts (OUP Oxford, 2010). ISBN 9780199547586.

[82] V. Gurarie. *Logarithmic operators and logarithmic conformal field theories.* `arXiv:1303.1113` (2013).

[83] M. R. Gaberdiel and H. G. Kausch. *A local logarithmic conformal field theory.* Nuclear Physics B **538(3)**, 631 – 658 (1999).

[84] M. R. R. Tabar. *Disordered systems and logarithmic conformal field theory.* International Journal of Modern Physics A **18(25)**, 4703–4745 (2003).

[85] A. N. I. I. Kogan. *Stress energy tensor in $c = 0$ logarithmic conformal field theory.* `arXiv:hep-th/0203207` (2002).

[86] I. I. Kogan and A. Nichols. *Stress energy tensor in LCFT and logarithmic Sugawara construction.* International Journal of Modern Physics A **18(25)**, 4771–4788 (2003).

[87] R. Bondesan, J. L. Jacobsen and H. Saleur. *Rectangular amplitudes, conformal blocks, and applications to loop models.* Nuclear Physics B **867(3)**, 913 – 949 (2013).

[88] V. Gurarie, M. Flohr and C. Nayak. *The Haldane-Rezayi quantum Hall state and conformal field theory.* Nuclear Physics B **498(3)**, 513 – 538 (1997).

[89] M. A. I. Florh. *Bits and pieces in Logarithmic Conformal Field Theory.* International Journal of Modern Physics A **18(25)**, 4497–4591 (2003).

[90] M. R. Gaberdiel. *An algebraic approach to Logarithmic Conformal Field Theory.* International Journal of Modern Physics A **18(25)**, 4593–4638 (2003).

[91] H. G. Kausch. *Extended conformal algebras generated by a multiplet of primary fields.* Physics Letters B **259**, 448–455 (1991).

[92] V. Kac. *Contravariant form for infinite-dimensional lie algebras and superalgebras.* W. Beiglböck, A. Böhm and E. Takasugi (Eds.), *Group Theoretical Methods in Physics*, vol. 94 of *Lecture Notes in Physics*, pp. 441–445 (Springer Berlin Heidelberg, 1979). ISBN 978-3-540-09238-4.

[93] B. Feigin and D. Fuks. *Invariant skew-symmetric differential operators on the line and verma modules over the Virasoro algebra.* Functional Analysis and Its Applications **16**, 114–126 (1982).

[94] A. Rocha-Caridi. *Vacuum vector representations of the Virasoro algebra.* Kac-Moody and Virasoro Algebras: A Reprint Volume for Physicists **3**, 353 (1988).

[95] M. Jeng, G. Piroux and P. Ruelle. *Height variables in the abelian sandpile model: scaling fields and correlations.* Journal of Statistical Mechanics: Theory and Experiment **2006(10)**, P10015 (2006).

[96] P. Ruelle. *Logarithmic conformal invariance in the abelian sandpile model*. `arXiv:1303.4310` (2013).

[97] D. Ridout. *Non-chiral logarithmic couplings for the Virasoro algebra*. Journal of Physics A: Mathematical and Theoretical **45(25)**, 255203 (2012).

[98] W. Nahm. *Quasi-rational fusion modules*. International Journal of Modern Physics B **08(25n26)**, 3693–3702 (1994).

[99] G. Moore and N. Seiberg. *Classical and quantum conformal field theory*. Communications in Mathematical Physics **123(2)**, 177–254 (1989).

[100] P. Martin. *Potts models and related problems in statistical mechanics*. Series on advances in statistical mechanics (World Scientific Publishing Company, Incorporated, 1991). ISBN 9789810200756.

[101] D. Ridout and Y. Saint-Aubin. *Standard modules, induction and the Temperley-Lieb algebra*. `arXiv:1204.4505` (2012).

[102] A. Nahum, J. T. Chalker, P. Serna, M. Ortuño and A. M. Somoza. *3D Loop Models and the CP^{n-1} Sigma Model*. Phys. Rev. Lett. **107**, 110601 (2011).

[103] J. L. Jacobsen, N. Read and H. Saleur. *Dense loops, supersymmetry, and Goldstone phases in two dimensions*. Phys. Rev. Lett. **90**, 090601 (2003).

[104] A. Nahum, P. Serna, A. M. Somoza and M. Ortuño. *Loop models with crossings*. Phys. Rev. B **87**, 184204 (2013).

[105] C. Fortuin and P. Kasteleyn. *On the random-cluster model: I. Introduction and relation to other models*. Physica **57(4)**, 536 – 564 (1972).

[106] J. Dubail, J. L. Jacobsen and H. Saleur. *Critical exponents of domain walls in the two-dimensional Potts model*. Journal of Physics A: Mathematical and Theoretical **43(48)**, 482002 (2010).

[107] J. Dubail, J. L. Jacobsen and H. Saleur. *Bulk and boundary critical behaviour of thin and thick domain walls in the two-dimensional Potts model*. Journal of Statistical Mechanics: Theory and Experiment **2010(12)**, P12026 (2010).

[108] R. Vasseur and J. L. Jacobsen. *Critical properties of joint spin and Fortuin–Kasteleyn observables in the two-dimensional Potts model*. Journal of Physics A: Mathematical and Theoretical **45(16)**, 165001 (2012).

[109] R. J. Baxter, S. B. Kelland and F. Y. Wu. *Equivalence of the Potts model or Whitney polynomial with an ice-type model*. Journal of Physics A: Mathematical and General **9(3)**, 397 (1976).

[110] N. Read and H. Saleur. *Exact spectra of conformal supersymmetric nonlinear sigma models in two dimensions*. Nuclear Physics B **613(3)**, 409 – 444 (2001).

[111] R. Bondesan, J. L. Jacobsen and H. Saleur. *Edge states and conformal boundary conditions in super spin chains and super sigma models*. Nuclear Physics B **849(2)**, 461 – 502 (2011).

[112] R. Bondesan, I. A. Gruzberg, J. L. Jacobsen, H. Obuse and H. Saleur. *Exact Exponents for the Spin Quantum Hall Transition in the Presence of Multiple Edge Channels*. Phys. Rev. Lett. **108**, 126801 (2012).

[113] G. Andrews, R. Baxter and P. Forrester. *Eight-vertex SOS model and generalized Rogers-Ramanujan-type identities*. Journal of Statistical Physics **35(3-4)**, 193–266 (1984).

[114] V. Pasquier. *Two-dimensional critical systems labelled by Dynkin diagrams*. Nuclear Physics B **285(0)**, 162 – 172 (1987).

[115] A. Feiguin, S. Trebst, A. W. W. Ludwig, M. Troyer, A. Kitaev, Z. Wang and M. H. Freedman. *Interacting anyons in topological quantum liquids: The golden chain*. Phys. Rev. Lett. **98**, 160409 (2007).

[116] Y. Ikhlef, J. L. Jacobsen and H. Saleur. *A Temperley–Lieb quantum chain with two- and three-site interactions*. Journal of Physics A: Mathematical and Theoretical **42(29)**, 292002 (2009).

[117] Y. Ikhlef, J. L. Jacobsen and H. Saleur. *The $\mathbb{Z}_2$ staggered vertex model and its applications*. Journal of Physics A: Mathematical and Theoretical **43(22)**, 225201 (2010).

[118] A. Gainutdinov, N. Read and H. Saleur. *Continuum limit and symmetries of the periodic $\mathfrak{gl}(1|1)$ spin chain*. Nuclear Physics B **871(2)**, 245 – 288 (2013).

[119] A. Gainutdinov, N. Read and H. Saleur. *Bimodule structure in the periodic $\mathfrak{gl}(1|1)$ spin chain*. Nuclear Physics B **871(2)**, 289 – 329 (2013).

[120] A. Gainutdinov, N. Read, H. Saleur and R. Vasseur. *Logarithmic CFT at $c = 0$: percolation and the continuum limit of the $\mathfrak{sl}(2|1)$ alternating spin chain*. To appear (2013).

[121] P. P. Martin and D. S. McAnally. *On commutants, dual pairs and non-semisimple algebras from statistical mechanics*. International Journal of Modern Physics A **07(supp01b)**, 675–705 (1992).

[122] P. P. Martin. *On Schur–Weyl duality, a_n Hecke algebras and quantum $sl(n)$ on $\otimes^{n+1} C^n$*. International Journal of Modern Physics A **07(supp01b)**, 645–673 (1992).

[123] F. D. M. Haldane. *Nonlinear field theory of large-spin Heisenberg antiferromagnets: Semiclassically quantized solitons of the one-dimensional easy-axis Néel state*. Phys. Rev. Lett. **50**, 1153–1156 (1983).

[124] I. Affleck and F. D. M. Haldane. *Critical theory of quantum spin chains*. Phys. Rev. B **36**, 5291–5300 (1987).

[125] B. Westbury. *The representation theory of the temperley-lieb algebras*. Mathematische Zeitschrift **219(1)**, 539–565 (1995).

[126] P. P. Martin and D. Woodcock. *On quantum spin-chain spectra and the structure of Hecke algebras and q-groups at roots of unity*. Journal of Physics A: Mathematical and General **31(50)**, 10131 (1998).

[127] S. Donkin (Cambridge University Press, 1998).

[128] F. Anderson and K. Fuller. *Rings and Categories of Modules*. Graduate Texts in Mathematics (Springer, 1992). ISBN 9780387978451.

[129] J. L. Cardy. *Conformal invariance and universality in finite-size scaling*. Journal of Physics A: Mathematical and General **17(7)**, L385 (1984).

[130] I. Affleck. *Universal term in the free energy at a critical point and the conformal anomaly*. Phys. Rev. Lett. **56**, 746–748 (1986).

[131] L. P. Kadanoff and H. Ceva. *Determination of an operator algebra for the two-dimensional Ising model*. Phys. Rev. B **3**, 3918–3939 (1971).

[132] W. Koo and H. Saleur. *Representations of the Virasoro algebra from lattice models*. Nuclear Physics B **426(3)**, 459 – 504 (1994).

[133] C. J. Hamer, G. R. W. Quispel and M. T. Batchelor. *Conformal anomaly and surface energy for Potts and Ashkin-Teller quantum chains*. Journal of Physics A: Mathematical and General **20(16)**, 5677 (1987).

[134] B. Nienhuis. *Loop models*. J. Jacobsen, S. Ouvry, V. Pasquier, D. Serban and L. Cugliandolo (Eds.), *Exact Methods in Low-dimensional Statistical Physics and Quantum Computing*, vol. 89 of *Lecture Notes of the Les Houches Summer School*, pp. 347–424 (Oxford University Press, 2008). ISBN 978-0-19-957461-2.

[135] J. L. Jacobsen. *Conformal field theory applied to loop models*. A. J. Guttman (Ed.), *Polygons, Polyominoes and Polycubes*, vol. 775 of *Lecture Notes in Physics*, pp. 347–424 (Springer Netherlands, 2009). ISBN 978-1-4020-9926-7.

[136] P. Bushlanov, B. Feigin, A. Gainutdinov and I. Tipunin. *Lusztig limit of quantum at root of unity and fusion of Virasoro logarithmic minimal models*. Nuclear Physics B **818(3)**, 179 – 195 (2009).

[137] P. Bushlanov, A. Gainutdinov and I. Tipunin. *Kazhdan–Lusztig equivalence and fusion of Kac modules in Virasoro logarithmic models*. Nuclear Physics B **862(1)**, 232 – 269 (2012).

[138] A. Gainutdinov, H. Saleur and I. Tipunin. *$\mathcal{W}$-algebras in XXZ spin chains at roots of unity*. `arXiv:1212.1378` (2012).

[139] P. Di Francesco, H. Saleur and J.-B. Zuber. *Modular invariance in non-minimal two-dimensional conformal theories*. Nuclear Physics B **285(0)**, 454 – 480 (1987).

[140] J. Dubail, J. L. Jacobsen and H. Saleur. *Conformal field theory at central charge $c = 0$: A measure of the indecomposability (b) parameters*. Nuclear Physics B **834(3)**, 399 – 422 (2010).

[141] J. J. H. Simmons, P. Kleban and R. M. Ziff. *Percolation crossing formulae and conformal field theory*. Journal of Physics A: Mathematical and Theoretical **40(31)**, F771 (2007).

[142] J. Rasmussen and P. A. Pearce. *Fusion algebra of critical percolation.* Journal of Statistical Mechanics: Theory and Experiment **2007(09)**, P09002 (2007).

[143] J. Rasmussen and P. A. Pearce. *Fusion algebras of logarithmic minimal models.* Journal of Physics A: Mathematical and Theoretical **40(45)**, 13711 (2007).

[144] M. Green, J. Schwarz and E. Witten. *Superstring Theory: Volume 2, Loop Amplitudes, Anomalies and Phenomenology.* Cambridge Monographs on Mathematical Physics (Cambridge University Press, 1987). ISBN 9780521357531.

[145] P. Martin and H. Saleur. *The blob algebra and the periodic Temperley-Lieb algebra.* Letters in Mathematical Physics **30(3)**, 189–206 (1994).

[146] J. L. Jacobsen and H. Saleur. *Conformal boundary loop models.* Nuclear Physics B **788(3)**, 137 – 166 (2008).

[147] M. R. Gaberdiel and I. Runkel. *From boundary to bulk in logarithmic CFT.* Journal of Physics A: Mathematical and Theoretical **41(7)**, 075402 (2008).

[148] M. R. Gaberdiel, I. Runkel and S. Wood. *A modular invariant bulk theory for the $c = 0$ triplet model.* Journal of Physics A: Mathematical and Theoretical **44(1)**, 015204 (2011).

[149] A. Gainutdinov, N. Read and H. Saleur. *Associative algebraic approach to logarithmic CFT in the bulk: the continuum limit of the $\mathfrak{gl}(1|1)$ periodic spin chain, Howe duality and the interchiral algebra.* `arXiv:1207.6334` (2012).

[150] P. Gabriel. *Représentations indécomposables. Séminaire Bourbaki vol. 1973/74 Exposés 436–452*, vol. 431 of *Lecture Notes in Mathematics*, pp. 143–169 (Springer Berlin Heidelberg, 1975). ISBN 978-3-540-07023-8.

[151] J. L. Jacobsen and H. Saleur. *Combinatorial aspects of boundary loop models.* Journal of Statistical Mechanics: Theory and Experiment **2008(01)**, P01021 (2008).

[152] A. Nichols, V. Rittenberg and J. de Gier. *One-boundary Temperley–Lieb algebras in the XXZ and loop models.* Journal of Statistical Mechanics: Theory and Experiment **2005(03)**, P03003 (2005).

[153] A. Nichols. *The Temperley–Lieb algebra and its generalizations in the Potts and XXZ models.* Journal of Statistical Mechanics: Theory and Experiment **2006(01)**, P01003 (2006).

[154] P. Martin and D. Woodcock. *On the structure of the blob algebra.* Journal of Algebra **225(2)**, 957–988 (2000).

[155] V. F. Jones. *A quotient of the affine Hecke algebra in the Brauer algebra.* Enseignement mathématiques **40**, 313–313 (1994).

[156] J. J. Graham and G. I. Lehrer. *The representation theory of affine Temperley-Lieb algebras.* Research report: mathematics research report/Centre for mathematics and its applications (Canberra) (1997).

[157] J. J. H. Simmons and J. Cardy. *Twist operator correlation functions in $O(n)$ loop models*. Journal of Physics A: Mathematical and Theoretical **42(23)**, 235001 (2009).

[158] J. L. Cardy. *Boundary conditions, fusion rules and the verlinde formula*. Nuclear Physics B **324(3)**, 581 – 596 (1989).

[159] R. E. Behrend, P. A. Pearce, V. B. Petkova and J.-B. Zuber. *On the classification of bulk and boundary conformal field theories*. Physics Letters B **444(1–2)**, 163 – 166 (1998).

[160] J.-B. Z. V.B. Petkova. *BCFT: from the boundary to the bulk*. `arXiv:hep-th/0009219` (2000).

[161] D. Levy. *Algebraic structure of translation-invariant spin-1/2 XXZ and q-Potts quantum chains*. Phys. Rev. Lett. **67**, 1971–1974 (1991).

[162] H. Grosse, S. Pallua, P. Prester and E. Raschhofer. *On a quantum group invariant spin chain with non-local boundary conditions*. Journal of Physics A: Mathematical and General **27(14)**, 4761 (1994).

[163] H. Saleur and M. Bauer. *On some relations between local height probabilities and conformal invariance*. Nuclear Physics B **320(3)**, 591 – 624 (1989).

[164] R. E. Behrend, P. A. Pearce and J.-B. Zuber. *Integrable boundaries, conformal boundary conditions and A-D-E fusion rules*. Journal of Physics A: Mathematical and General **31(50)**, L763 (1998).

[165] R. E. Behrend, P. A. Pearce, V. B. Petkova and J.-B. Zuber. *Boundary conditions in rational conformal field theories*. Nuclear Physics B **570(3)**, 525 – 589 (2000).

[166] J. L. Jacobsen, P. Le Doussal, M. Picco, R. Santachiara and K. J. Wiese. *Critical interfaces in the random-bond Potts model*. Phys. Rev. Lett. **102**, 070601 (2009).

[167] H. Shimada. *Disordered loop model and coupled conformal field theories*. Nuclear Physics B **820(3)**, 707 – 752 (2009).

[168] H. Shimada. *Coulomb gas partition function of a layered loop model*. Journal of Physics A: Mathematical and Theoretical **43(48)**, 485002 (2010).

[169] J. Cardy and J. L. Jacobsen. *Critical behavior of random-bond Potts models*. Phys. Rev. Lett. **79**, 4063–4066 (1997).

[170] V. Dotsenko, V. Dotsenko and M. Picco. *Random bond Potts model: The test of the replica symmetry breaking*. Nuclear Physics B **520(3)**, 633 – 674 (1998).

[171] P. Bantay and G. Zala. *Ultrametric matrices and representation theory*. Journal of Physics A: Mathematical and General **30(19)**, 6811 (1997).

[172] Y. Ikhlef, P. Fendley and J. Cardy. *Integrable modification of the critical Chalker-Coddington network model*. Phys. Rev. B **84**, 144201 (2011).

[173] A. Moore. *Representations of the Temperley-Lieb algebra*. Honors Projects p. 11 (2008).

[174] E. V. Ivashkevich. *Correlation functions of dense polymers and c=-2 conformal field theory*. Journal of Physics A: Mathematical and General **32(9)**, 1691 (1999).

[175] E. V. Ivashkevich and C.-K. Hu. *Exact multileg correlation functions for the dense phase of branching polymers in two dimensions*. Phys. Rev. E **71**, 015104 (2005).

[176] S. Y. Grigorev, V. S. Poghosyan and V. B. Priezzhev. *Three-leg correlations in the two-component spanning tree on the upper half-plane*. Journal of Statistical Mechanics: Theory and Experiment **2009(09)**, P09008 (2009).

[177] S. Caracciolo, J. L. Jacobsen, H. Saleur, A. D. Sokal and A. Sportiello. *Fermionic field theory for trees and forests*. Phys. Rev. Lett. **93**, 080601 (2004).

[178] F. Y. Wu. *Theory of resistor networks: the two-point resistance*. Journal of Physics A: Mathematical and General **37(26)**, 6653 (2004).

[179] J. Cserti. *Application of the lattice Green's function for calculating the resistance of an infinite network of resistors*. American Journal of Physics **68**, 896 (2000).

[180] Y. Deng, T. M. Garoni and A. D. Sokal. *Ferromagnetic phase transition for the spanning-forest model ($q \to 0$ limit of the Potts model) in three or more dimensions*. Phys. Rev. Lett. **98**, 030602 (2007).

[181] D. J. Amit. *Renormalization of the Potts model*. Journal of Physics A: Mathematical and General **9(9)**, 1441 (1976).

[182] A. Coniglio. *Cluster structure near the percolation threshold*. Journal of Physics A: Mathematical and General **15(12)**, 3829 (1982).

[183] J. Cardy. *Scaling and Renormalization in Statistical Physics*. Cambridge Lecture Notes in Physics (Cambridge University Press, 1996). ISBN 9780521499590.

[184] M. Bauer and D. Bernard. *Loewner chains*. `arXiv:cond-mat/0412372` (2004).

[185] J. Cardy. *SLE for theoretical physicists*. Annals of Physics **318(1)**, 81 – 118 (2005).

[186] K. Kytölä. *SLE local martingales in logarithmic representations*. Journal of Statistical Mechanics: Theory and Experiment **2009(08)**, P08005 (2009).

[187] A. Pruisken. *On localization in the theory of the quantized Hall effect: A two-dimensional realization of the θ-vacuum*. Nuclear Physics B **235(2)**, 277 – 298 (1984).

[188] Y. Ikhlef, J. L. Jacobsen and H. Saleur. *Integrable spin chain for the* $\mathrm{SL}(2,\mathbb{R})/\mathbf{U}(1)$ *black hole sigma model*. Phys. Rev. Lett. **108**, 081601 (2012).

[189] C. Candu and Y. Ikhlef. *Non-linear integral equations for the* $\mathrm{SL}(2,\mathbb{R})/\mathbf{U}(1)$ *black hole sigma model*. `arXiv:1306.2646` (2013).

[190] G. Götz, T. Quella and V. Schomerus. *Representation theory of sl*(2|1). Journal of Algebra **312(2)**, 829 – 848 (2007).

[191] M. Marcu. *The representations of* $\mathfrak{spl}$*(2,1) – an example of representations of basic superalgebras*. Journal of Mathematical Physics **21(6)**, 1277–1283 (1980).